

University of Louisville

## ThinkIR: The University of Louisville's Institutional Repository

---

Electronic Theses and Dissertations

---

5-2021

### Biomechanical Characterization of Video-Recorded Short-Distance Falls Involving Children Equipped with a Biometric Device in a Childcare Setting: A Pilot Study.

Danielle K. Cory  
*University of Louisville*

Follow this and additional works at: <https://ir.library.louisville.edu/etd>



Part of the [Biomedical Engineering and Bioengineering Commons](#)

---

#### Recommended Citation

Cory, Danielle K., "Biomechanical Characterization of Video-Recorded Short-Distance Falls Involving Children Equipped with a Biometric Device in a Childcare Setting: A Pilot Study." (2021). *Electronic Theses and Dissertations*. Paper 3439.

<https://doi.org/10.18297/etd/3439>

This Master's Thesis is brought to you for free and open access by ThinkIR: The University of Louisville's Institutional Repository. It has been accepted for inclusion in Electronic Theses and Dissertations by an authorized administrator of ThinkIR: The University of Louisville's Institutional Repository. This title appears here courtesy of the author, who has retained all other copyrights. For more information, please contact [thinkir@louisville.edu](mailto:thinkir@louisville.edu).

BIOMECHANICAL CHARACTERIZATION OF VIDEO-RECORDED SHORT-DISTANCE FALLS INVOLVING CHILDREN EQUIPPED WITH A BIOMETRIC DEVICE IN A CHILDCARE SETTING: A PILOT STUDY

By

Danielle Kristine Cory  
B.S., University of Louisville, May 2017

A Thesis  
Submitted to the Faculty of the  
University of Louisville  
J.B. Speed School of Engineering  
as Partial Fulfillment of the Requirements  
for the Professional Degree

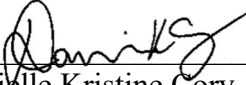
MASTER OF ENGINEERING

Department of Bioengineering

April 2021



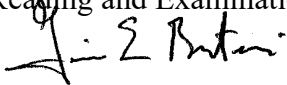
BIOMECHANICAL CHARACTERIZATION OF VIDEO-RECORDED SHORT-DISTANCE FALLS INVOLVING CHILDREN EQUIPPED WITH A BIOMETRIC DEVICE IN A CHILDCARE SETTING: A PILOT STUDY

Submitted by:   
Danielle Kristine Cory

A Thesis Submitted On

April 29, 2021  
(Date)

to the Following Reading and Examination Committee:

  
Gina E. Bertocci, Thesis Co-Director

  
Angela K. Thompson, Thesis Co-Director

  
Karen L. Bertocci



## ACKNOWLEDGEMENTS

This research was funded by the National Institute of Justice (Award No. 2017-DN-BX-0158; Office of Justice Programs, U.S. Department of Justice) for research and development in forensic science for criminal justice purposes. The opinions, findings, and conclusions or recommendations expressed in this publication are those of the authors and do not necessarily reflect those of the Department of Justice. Subjects included in this study were recruited from Bluegrass Academy Childcare Center location in Louisville, Kentucky. This project was supported by the University of Louisville Institutional Review Board (IRB # 16.1030).

I would like to express my sincere gratitude to my co-chairs, Dr. Gina Bertocci and Dr. Angela Thompson, who provided guidance and supported me throughout the entire process. Their insight, encouragement, and patience allowed me to grow both scholastically and as an engineer. I would also like to thank my committee member, Dr. Karen Bertocci, for her valuable input and patience with me as well as I navigated through my thesis. Additionally, the faculty and students at the University of Louisville's Injury Risk Assessment and Prevention Laboratory, including Craig Smalley, Dr. Raymond DSouza, Dr. Nathan Brown, Keyonna McKinsey, and Bret Hilt, all had key roles in project planning, facility installations, and data collection. Without their dedication, I could not have completed my research. Finally, I would like to express sincere gratitude to my friends and family. Their support, patience, and encouragement throughout this process helped me overcome some of the hardest challenges life has presented to me, and I could not have completed this without them.

## ABSTRACT

**Background:** A fall is the most common falsely reported injury scenario when a young child presents for medical care and the caregiver is concealing abuse. There is a lack of reliably witnessed falls with known outcomes to aid in the distinction between accidental and abusive injuries.

**Objectives:** The objectives of this study were to characterize video-recorded short distance falls involving young children in a childcare setting, to identify body regions most commonly impacted in these short distance falls, to characterize the head biomechanics of these falls, and describe fall characteristics. Additionally, physics-based models were used to predict fall biomechanics in a subset of these falls.

**Methods:** This study included children aged 12-25 months. Two childcare classrooms and a playground were each equipped with 3 digital video cameras. Video recordings involving falls were extracted for analysis. Falls were characterized by various factors (such as fall type; initial condition; fall dynamics; etc.), and these were analyzed for frequency. Descriptive statistics were performed on outcome measures. The distribution of impacted/contacted body regions was described and projected onto a child body map. Falls with biomechanical data from wearable devices were characterized by head impact and analyzed. It was hypothesized that head accelerations and velocities will be greater in falls with head impact than in falls without head impact. To analyze the accuracy and usefulness of physics-based biomechanical models, lumped mass, single rod, and inverted pendulum physics-based models were developed for previously conducted ATD

falls and falls involving head impact from the childcare center. It was hypothesized that these models could accurately predict head biomechanical measures.

Results: 100 video-recorded falls involving 8 children, age 17-25 months (mean  $\pm$  SD: 20  $\pm$  2 months) were characterized. 65% of falls involved boys, and 64% of falls occurred indoors in a classroom. No injuries occurred in any fall. The most common first contact body regions were the soles of the feet. The most common primary impact body region was the palms of the hands; bilateral shins, bilateral knees, and buttocks were also commonly impacted. Replicated ATD falls and select childcare center falls with SIM G outputs were mathematically modelled, and it was determined that mathematical physics-based models could reasonably predict biomechanical outcomes from short-distance falls.

Conclusions: This study resulted in a dataset of 100 reliably witnessed video-recorded falls involving young children in a childcare center setting. Body region contact/impact maps for first contact, primary impact, and secondary impact of these common short-distance falls were developed. This study found that head biomechanical measures were not significantly different in falls with head impact versus without head impact. This study also found that the methodology used to evaluate lumped mass, single rod, and inverted pendulum models was an important factor in predicting head biomechanical outcomes. The most accurate physics-based models were the lumped mass and inverted pendulum models. No falls in this study resulted in injury. The outcomes from this study may aid in the investigation of injury histories of a short-distance fall, further increasing the understanding and differentiation of accidental versus abusive injuries.

## TABLE OF CONTENTS

ACKNOWLEDGEMENTS.....	iv
ABSTRACT.....	v
LIST OF TABLES.....	xvi
LIST OF FIGURES .....	xxiii
I. INTRODUCTION.....	1
II. BACKGROUND .....	4
A. The head of a young infant and its increased susceptibility to injury .....	4
B. Difficulties in differentiating child abuse from accidental head injuries .....	6
C. Clinical studies pertaining to injuries resulting from short-distance falls.....	8
1. Clinical information on injuries resulting from household short distance falls .	10
D. Injury mechanisms associated with pediatric head injuries .....	16
E. Biomechanical application in the investigation of pediatric short distance falls...	19
1. Physical Models of Pediatric Falls.....	19
2. Anthropomorphic test devices and short fall studies .....	24
F. Development and application of injury thresholds from biomechanical fall data .	29
1. Thresholds based on linear acceleration and linear velocity.....	30
2. Thresholds based on rotational acceleration and rotational velocity .....	33

G.	Wearable accelerometers and the assessment of head impact biomechanics ....	36
1.	Importance of reviewing video footage when subjects are equipped with biometric sensors .....	36
2.	Wearable accelerometers and fall studies .....	36
3.	Wearable accelerometers in other applications.....	38
H.	Pediatric short distance fall assessment in childcare setting and/or on a playground.....	39
1.	Previous study involving video-recorded falls in a childcare setting.....	39
2.	Injuries resulting from falls involving playground equipment.....	42
I.	Current takeaways and gaps in the literature .....	45
III.	SPECIFIC AIMS .....	46
IV.	STUDY DESIGN AND METHODS.....	48
A.	Overview of study design and methodology.....	48
B.	Study design.....	48
1.	Inclusion/exclusion criteria .....	49
2.	Fall monitoring duration and sample size .....	49
C.	Data collection.....	50
1.	Anthropometrics.....	50
2.	Video monitoring .....	50

3.	Impact surfaces and coefficients of restitution.....	51
4.	SIM G/SKYi System and biomechanical measure recordings.....	52
D.	Childcare center procedures .....	63
1.	Observation periods.....	63
2.	SIM G and SKYi system data collection .....	64
3.	Video recording.....	64
4.	Data collection log .....	65
5.	Video review and data post-processing.....	66
E.	Specific aim 1: Characterize video-recorded short distance falls involving young children in a childcare setting.....	67
1.	Fall database and operationalization of data fields .....	67
2.	Equipment/object involvement operationalization.....	73
3.	Another person(s) (not including the fall subject) involvement operationalization	74
4.	Specific aim 1 data analysis .....	74
F.	Specific aim 2: Identify body regions most commonly contacted/impacted during falls involving young children in a childcare setting. ....	75
1.	Contact/impact operationalization.....	75
2.	Determining body regions contacted/impacted.....	76

3.	Specific aim 2 data analysis .....	78
4.	Body region contact/impact map.....	78
G.	Specific aim 3: Characterize the biomechanics of falls involving young children in a childcare setting.....	79
1.	Falls with SIM G activation .....	80
2.	Falls with SIM G activation data analysis.....	81
3.	SIM G data analysis for head impacts.....	82
4.	Development of physics-based models for ATD feet-first falls and human subject childcare center falls with SIM G activation and primary head impact.....	83
5.	Compare biomechanical outcomes from physics-based models to replicated ATD feet-first fall experiments using SIM G to measure head velocity and acceleration .....	112
6.	Compare biomechanical outcomes from physics-based models to SIM G biomechanical data from select childcare center falls .....	113
V.	RESULTS .....	114
A.	Video monitoring/video recorded falls .....	114
B.	Subject demographics .....	114
C.	Anthropometric measurements of the subjects .....	115
D.	Impact surfaces/object COR.....	116
E.	SIM G/SKYi Verification .....	118

F.	Specific Aim 1: Characterize the video-recorded short distance falls involving young children in a childcare setting.....	118
1.	Fall distribution by age.....	118
2.	Fall characterization by fall location.....	119
3.	Fall characterization by fall type.....	120
4.	Fall characterization by initial condition.....	122
5.	Fall characterization by fall initiation .....	122
6.	Fall characterization by fall dynamic(s).....	123
7.	Fall characterization by equipment/object involvement .....	126
8.	Fall characterization by another person(s) involvement .....	132
9.	Fall characterization by head impact.....	136
10.	Fall characterization by impact surface .....	138
11.	Fall characterization by plane(s) impacted during primary impact.....	139
12.	Fall characterization by final position .....	141
13.	Fall characterization by injury outcomes.....	142
G.	Specific Aim 2: Identify body regions most commonly impacted during falls involving young children in a childcare setting. ....	142
1.	First contact body map .....	143
2.	Primary impact body map .....	144



3.	Secondary impact body map .....	145
H.	Specific aim 3: Characterize the biomechanics of falls involving young children in a childcare setting by fall characteristics. ....	146
1.	Falls with SIM G activation .....	146
2.	SIM G and Head Impacts .....	152
3.	Development of physics-based models for ATD feet-first falls and human subject childcare center falls with SIM G activation and primary head impact.....	160
VI.	DISCUSSION .....	196
A.	Injury outcomes and injury risk .....	196
1.	Mean peak resultant linear head acceleration across all falls.....	196
2.	Mean peak resultant rotational head acceleration and velocity across all falls	196
3.	Mean HIC <sub>15</sub> value across all falls.....	197
4.	Mean impact duration across all falls.....	197
B.	Specific aim 1 discussion .....	198
1.	Fall type.....	198
2.	Initial condition and fall initiation.....	199
3.	Fall dynamics .....	199
4.	Equipment/Object involvement.....	201
5.	Another person(s) involvement, not including the subject .....	202

6.	Head impact during any phase of the fall.....	202
7.	Impact surface and planes impacted.....	202
8.	Final landing position.....	204
C.	Specific aim 2 discussion .....	204
1.	Body region impact maps from ATD falls.....	206
2.	Body region bruising maps from prospective cross-sectional clinical study ...	211
D.	Specific aim 3 discussion .....	213
9.	SIM G Falls with Head Impact vs No Head Impact .....	213
10.	Development of physics-based models for replicated ATD feet-first falls and human subject childcare center falls with SIM G activation and primary head impact	215
E.	Clinical and judicial relevance.....	222
1.	Clinical relevance .....	222
2.	Judicial relevance .....	223
F.	Limitations .....	224
G.	Future work and recommendations .....	226
VII.	Conclusions.....	229
VIII.	REFERENCES CITED .....	231
IX.	APPENDIX I .....	237

A.	Example from fall database.....	237
B.	Screen grabs from the clipped fall 14 video.....	243
X.	APPENDIX II.....	245
A.	SIM G/SKYi Verification .....	245
1.	Fall dynamics .....	245
2.	Comparison of results.....	247
XI.	APPENDIX III.....	253
A.	Physics-based model results for replicated ATD feet-first falls .....	254
1.	Physics-based model results for ATD feet-first falls onto carpet .....	254
2.	Physics-based model results for ATD feet-first falls onto linoleum.....	261
3.	Comparison of replicated ATD feet-first fall outcomes by fall dynamics .....	267
B.	Physics-based model results for childcare center falls with SIM G activation and primary head impact.....	278
1.	Childcare center fall 146 .....	279
2.	Childcare center fall 238 .....	282
3.	Childcare center fall 241 .....	285
4.	Childcare center fall 321 .....	288
5.	Childcare center fall 516 .....	291
6.	Childcare center fall 545 .....	294

7. Childcare center fall 676 (1).....	297
8. Childcare center fall 676 (2).....	300
XII. VITA .....	304

LIST OF TABLES

TABLE OF CONTENTS.....	VII
MEAN BIOMECHICAL MEASURES OBTAINED IN HILT, 2018.....	40
FALL CHARACTERISTICS AND THEIR EFFECT ON BIOMECHANICAL MEASURES FROM HILT, 2018.....	41
CHILDCARE CENTER OBSERVATION LOG.....	66
OPERATIONALIZATION OF DATA FIELDS.....	68
TERMS OPERATIONALIZED FOR EQUIPMENT/OBJECT INVOLVEMENT IN THE FALLS.....	73
TERMS OPERATIONALIZED FOR ANOTHER PERSON(S)' INVOLVEMENT IN THE FALLS.....	74
OPERATIONALIZED DEFINITIONS FOR BODY REGION CONTACTED/IMPACTED.....	76
ALL BODY REGIONS INVOLVED IN THE FIRST CONTACT, PRIMARY IMPACT, AND SECONDARY IMPACT .....	77
DESCRIPTIONS OF ATD FALL DYNAMICS AND PREVIOUS FALL FREQUENCIES (THOMPSON, 2018).....	85
METHODS USED TO EVALUATE THE PHYSICS-BASED MODELS.....	87
RADIUS OF ROTATION LENGTHS FOR PARAMETER SENSITIVITY ANALYSIS .....	92
PERCENT ERROR CATEGORIES FOR PHYSICS-BASED MODEL OUTCOMES	112
ANTHROPOMETRICS OF ENROLLED SUBJECTS.....	115
COEFFICIENT OF RESTITUTION MEANSUREMENT FOR IMPACT SURFACE/OBJECTS.....	117
MEAN HEAD BIOMECHANICAL MEASURES ACROSS ALL VERIFIED SIM G ACTIVATIONS (N=14 ACTIVATIONS).....	150
MEAN HEAD BIOMECHANICAL MEASURES ACROSS ALL VERIFIED SIM G ACTIVATION (N=14 FALLS).....	154
METHODS USED TO EVALUATE THE PHYSICS-BASED MODELS.....	161

REPLICATED ATD FEET-FIRST FALLS ONTO CARPET METHODS A AND B PERCENT ERROR OUTCOMES FOR PHYSICS-BASED MODELS AS COMPARED TO MEAN PEAK SIM G OUTCOMES (N=7) .....	162
REPLICATED ATD FEET-FIRST FALLS ONTO LINOLEUM METHODS A AND B PERCENT ERROR OUTCOMES FOR PHYSICS-BASED MODELS AS COMPARED TO MEAN PEAK SIM G OUTCOMES (N=7) .....	163
REPLICATE FALL DYNAMICS AND FREQUENCIES .....	164
ATD FALLS ONTO LINOLEUM WITH DYNAMIC A METHODS A AND B PERCENT ERROR OUTCOMES FOR PHYSICS-BASED MODELS AS COMPARED TO MEAN PEAK SIM G OUTCOMES (N=5) .....	165
ATD FALLS ONTO LINOLEUM WITH DYNAMIC C METHODS A AND B PERCENT ERROR OUTCOMES FOR PHYSICS-BASED MODELS AS COMPARED TO MEAN PEAK SIM G OUTCOMES (N=2) .....	166
RADIUS OF ROTATION LENGTHS FOR PARAMETER SENSITIVITY ANALYSIS .....	167
ATD MEASUREMENTS USED FOR PARAMETER SENSITIVITY ANALYSIS ...	168
MEAN PEAK SIM G VALUES FROM REPLICATED ATD FEET-FIRST FALLS ONTO CARPET (N=7) .....	168
PARAMETER SENSITIVITY ANALYSIS RESULTS (METHOD A) REPLICATED ATD FEET-FIRST FALLS ONTO CARPET, AS COMPARED TO SIM G (N=7) ....	169
MEAN PEAK SIM G VALUES FROM REPLICATED ATD FEET-FIRST FALLS ONTO LINOLEUM (N=7).....	170
PARAMETER SENSITIVITY ANALYSIS RESULTS (METHOD A) REPLICATED ATD FEET-FIRST FALLS ONTO LINOLEUM, AS COMPARED TO SIM G (N=7)	170
MEAN PEAK SIM G VALUES FROM REPLICATED ATD FEET-FIRST FALLS ONTO LINOLEUM WITH DYNAMIC A (N=5) .....	171
PARAMETER SENSITIVITY ANALYSIS RESULTS (METHOD A) REPLICATED ATD FEET-FIRST FALLS ONTO LINOLEUM WITH DYNAMIC A (N=5), AS COMPARED TO SIM G .....	171

MEAN PEAK SIM G VALUES FROM REPLICATED ATD FEET-FIRST FALLS ONTO LINOLEUM WITH DYNAMIC C (N=2) .....	172
PARAMETER SENSITIVITY ANALYSIS RESULTS FOR REPLICATED ATD FEET-FIRST FALLS ONTO LINOLEUM WITH DYNAMIC C (N=2), AS COMPARED TO SIM G .....	172
METHODS USED TO EVALUATE THE PHYSICS-BASED MODELS .....	174
OVERALL PERCENT ERROR OUTCOMES FOR METHOD A ANALYSIS OF SIMULATED CHILDCARE CENTER FALLS FOR LUMPED MASS, SINGLE ROD, AND INVERTED PENDULUM PHYSICS-BASED MODELS AS COMPARED TO MEAN PEAK SIM G OUTCOMES (N=8) .....	175
OVERALL PERCENT ERROR OUTCOMES FOR METHOD B ANALYSIS OF SIMULATED CHILDCARE CENTER FALLS FOR LUMPED MASS, SINGLE ROD, AND INVERTED PENDULUM PHYSICS-BASED MODELS AS COMPARED TO MEAN PEAK SIM G OUTCOMES (N=8) .....	176
RADIUS OF ROTATION LENGTHS FOR PARAMETER SENSITIVITY ANALYSIS .....	177
SUBJECT 11 PARAMETER SENSITIVITY ANALYSIS MEASUREMENTS AND FALL 146 SIM G OUTCOMES.....	178
OVERALL PARAMETER SENSITIVITY ANALYSIS OUTCOMES FOR SIMULATED CHILDCARE CENTER FALL 146.....	179
SUBJECT 11 PARAMETER SENSITIVITY ANALYSIS MEASUREMENTS AND FALL 238 SIM G OUTCOMES.....	180
OVERALL PARAMETER SENSITIVITY ANALYSIS OUTCOMES FOR SIMULATED CHILDCARE CENTER FALL 238.....	180
SUBJECT 5 PARAMETER SENSITIVITY ANALYSIS MEASUREMENTS AND FALL 241 SIM G OUTCOMES.....	181
OVERALL PARAMETER SENSITIVITY ANALYSIS OUTCOMES FOR SIMULATED CHILDCARE CENTER FALL 241 .....	181

SUBJECT 4 PARAMETER SENSITIVITY ANALYSIS MEASUREMENTS AND FALL 321 SIM G OUTCOMES.....	182
OVERALL PARAMETER SENSITIVITY ANALYSIS OUTCOMES FOR SIMULATED CHILDCARE CENTER FALL 321 .....	183
SUBJECT 15 PARAMETER SENSITIVITY ANALYSIS MEASUREMENTS AND FALL 516 SIM G OUTCOMES.....	184
OVERALL PARAMETER SENSITIVITY ANALYSIS OUTCOMES FOR SIMULATED CHILDCARE CENTER FALL 516.....	184
SUBJECT 21 PARAMETER SENSITIVITY ANALYSIS MEASUREMENTS AND FALL 545 SIM G OUTCOMES.....	185
OVERALL PARAMETER SENSITIVITY ANALYSIS OUTCOMES FOR SIMULATED CHILDCARE CENTER FALL 545 .....	186
SUBJECT 21 PARAMETER SENSITIVITY ANALYSIS MEASUREMENTS AND FALL 676 (1) SIM G OUTCOMES.....	187
OVERALL PARAMETER SENSITIVITY ANALYSIS OUTCOMES FOR SIMULATED CHILDCARE CENTER FALL 676 (1) .....	187
SUBJECT 21 PARAMETER SENSITIVITY ANALYSIS MEASUREMENTS AND FALL 676 (2) SIM G OUTCOMES.....	188
OVERALL PARAMETER SENSITIVITY ANALYSIS OUTCOMES FOR SIMULATED CHILDCARE CENTER FALL 676 (2) .....	189
MOST COMMON IMPACT SURFACES (FROM THIS STUDY) AND THEIR RESPECTIVE COEFFICIENT OF RESTITUTION MEASUREMENT AND CLASSIFICATION (FROM HILT (2018)) .....	203
PEAK HEAD BIOMECHANICAL MEASURES FOR HEAD IMPACT VS. NO HEAD IMPACT FROM HILT (2018) (N=102 FALLS) .....	214
EXAMPLE OF FALL ANALYSIS.....	237
DESCRIPTIONS OF ATD FALL DYNAMICS AND PREVIOUS FALL FREQUENCIES (THOMPSON, 2018).....	246
REPLICATE FALL DYNAMICS AND FREQUENCIES.....	246



ATD ONBOARD INSTRUMENTATION AND SIM G COMPARISON .....	247
METHODS USED TO EVALUATE THE PHYSICS-BASED MODELS .....	253
PERCENT ERROR CATEGORIES FOR PHYSICS-BASED MODEL OUTCOMES	254
LUMPED MASS PHYSICS-BASED MODEL OUTCOMES VS. SIM G OUTCOMES (N=7) FOR FEET-FIRST ATD FALLS ONTO CARPET .....	255
SINGLE ROD PHYSICS-BASED MODEL OUTCOMES VS. SIM G OUTCOMES (N=7) FOR FEET-FIRST ATD FALLS ONTO CARPET .....	255
INVERTED PENDULUM PHYSICS-BASED MODEL OUTCOMES VS. SIM G OUTCOMES (N=7) FOR FEET-FIRST ATD FALLS ONTO CARPET .....	256
LUMPED MASS PHYSICS-BASED MODEL OUTCOMES VS. SIM G OUTCOMES (N=7) FOR FEET-FIRST ATD FALLS ONTO LINOLEUM.....	261
SINGLE ROD PHYSICS-BASED MODEL OUTCOMES VS. SIM G OUTCOMES (N=7) FOR FEET-FIRST ATD FALLS ONTO LINOLEUM.....	262
INVERTED PENDULUM PHYSICS-BASED MODEL OUTCOMES VS. SIM G OUTCOMES (N=7) FOR FEET-FIRST ATD FALLS ONTO LINOLEUM.....	262
DESCRIPTIONS OF ATD FALL DYNAMICS AND PREVIOUS FALL FREQUENCIES (THOMPSON, 2018).....	268
REPLICATED ATD FEET-FIRST FALLS ONTO LINOLEUM WITH DYNAMIC A LUMPED MASS OUTCOMES .....	269
REPLICATED ATD FEET-FIRST FALLS ONTO LINOLEUM WITH DYNAMIC A SINGLE ROD OUTCOMES.....	269
REPLICATED ATD FEET-FIRST FALLS ONTO LINOLEUM WITH DYNAMIC A INVERTED PENDULUM OUTCOMES .....	270
REPLICATED ATD FEET-FIRST FALLS ONTO LINOLEUM WITH DYNAMIC C LUMPED MASS OUTCOMES .....	274
REPLICATED ATD FEET-FIRST FALLS ONTO LINOLEUM WITH DYNAMIC C SINGLE ROD OUTCOMES.....	274
REPLICATED ATD FEET-FIRST FALLS ONTO LINOLEUM WITH DYNAMIC C INVERTED PENDULUM OUTCOMES .....	275

RESULTS FOR FALL 146 LUMPED MASS PHYSICS-BASED MODEL .....	281
RESULTS FOR FALL 146 SINGLE ROD PHYSICS-BASED MODEL.....	281
RESULTS FOR FALL 146 INVERTED PENDULUM PHYSICS-BASED MODEL .	282
RESULTS FOR FALL 238 LUMPED MASS PHYSICS-BASED MODEL .....	284
RESULTS FOR FALL 238 SINGLE ROD PHYSICS-BASED MODEL.....	284
RESULTS FOR FALL 238 INVERTED PENDULUM PHYSICS-BASED MODEL .	285
RESULTS FOR FALL 241 LUMPED MASS PHYSICS-BASED MODEL .....	287
RESULTS FOR FALL 241 SINGLE ROD PHYSICS-BASED MODEL.....	288
RESULTS FOR FALL 241 INVERTED PENDULUM PHYSICS-BASED MODEL .	288
RESULTS FOR FALL 321 LUMPED MASS PHYSICS-BASED MODEL .....	290
RESULTS FOR FALL 321 SINGLE ROD PHYSICS-BASED MODEL.....	291
RESULTS FOR FALL 321 INVERTED PENDULUM PHYSICS-BASED MODEL .	291
RESULTS FOR FALL 516 LUMPED MASS PHYSICS-BASED MODEL .....	293
RESULTS FOR FALL 516 SINGLE ROD PHYSICS-BASED MODEL.....	293
RESULTS FOR FALL 516 INVERTED PENDULUM PHYSICS-BASED MODEL .	294
RESULTS FOR FALL 545 LUMPED MASS PHYSICS-BASED MODEL .....	296
RESULTS FOR FALL 545 SINGLE ROD PHYSICS-BASED MODEL.....	297
RESULTS FOR FALL 545 INVERTED PENDULUM PHYSICS-BASED MODEL .	297
RESULTS FOR FALL 676 (1) LUMPED MASS PHYSICS-BASED MODEL .....	299
RESULTS FOR FALL 676 (1) SINGLE ROD PHYSICS-BASED MODEL .....	300
RESULTS FOR FALL 676 (1) INVERTED PENDULUM PHYSICS-BASED MODEL .....	300
RESULTS FOR FALL 676 (2) LUMPED MASS PHYSICS-BASED MODEL .....	302
RESULTS FOR FALL 676 (2) SINGLE ROD PHYSICS-BASED MODEL.....	303
RESULTS FOR FALL 676 (2) INVERTED PENDULUM PHYSICS-BASED MODEL .....	303



## LIST OF FIGURES

FIGURE 1 – Frequency distribution of falls for each injury severity category based upon furniture type (n=79) (A. K. Thompson et al., 2011). .....	12
FIGURE 2 – Free fall of an infant from an initial fall position to a point of impact (Cory et al., 2001) .....	20
FIGURE 3 – A fall involving a horizontal velocity component on an elevated surface (Cory et al., 2001) .....	21
FIGURE 4 – A fall involving a horizontal velocity immediately before impact from a low fall height (Cory et al., 2001).....	21
FIGURE 5 – Fall involving no horizontal component (Cory et al., 2001) .....	22
FIGURE 6 – Energy dissipation of soft versus hard surfaces (Cory et al., 2001) .....	23
FIGURE 7 – Angular acceleration of the head due to whiplash (Cory et al., 2001) .....	24
FIGURE 8 – Peak resultant linear head acceleration for falls onto various surfaces. error bars represent 95% confidence intervals (A. Thompson et al., 2013) .....	27
FIGURE 9 – Peak medial-lateral angular head accelerations and peak change in angular velocity; experimental data compared to thresholds for moderate to severe diffuse axonal injury (DAI) (Margulies & Thibault, 1992). Thresholds shown are for an infant and adult with 500g and 1067g brain mass, respectively (A. Thompson et al., 2013).....	28
FIGURE 10 – Head impact durations for falls onto various surfaces. error bars represent 95% confidence intervals (A. Thompson et al., 2013) .....	29
FIGURE 11 – Tolerance curve for human head (acceleration in gravity units, time in milliseconds) (Gurdjian et al., 1966) .....	31
FIGURE 12 – Brain injury tolerance scaling in the adult, young child, and neonate (Ommaya et al., 2002) .....	35
FIGURE 13 – DAI threshold developed from scaled brain mass; regions to the upper right of each curve represent injury Margulies (Margulies & Thibault, 1992). Thresholds shown are for an infant brain mass of 500 g (heavy solid line), adult brain mass of 1067 g (solid line), and primate brain mass of 1400 g (dashed line).....	35
FIGURE 14 – Study design and methodology schematic .....	48

FIGURE 15 – COR Resiliency tester .....	51
FIGURE 16 – (A) SIM G sensor; (B) Soft elastic headband; (C) SIM G inserted into posterior pouch on headband; (D) Child wearing headband with SIM G centered on occipital region of head.....	53
FIGURE 17 – Example of 3D head model showing a head impact at the right base of the chin.....	54
FIGURE 18 – (A) SKYI aggregator receiver with power cord; (B) SIM G; (C) Headband .....	55
FIGURE 19 – Representative linear acceleration time history from ATD feet-first falls for determination of initial and final times associated with impact (where $\Delta t$ is the full impact phase); orange shaded region is the impact of the head and green shaded region is the rebound of the head.....	57
FIGURE 20 – Experimental test set-up for 0.69 m fall to verify SIM G .....	60
FIGURE 21 –SIM G placement on 12-month-old CRABI ATD .....	61
FIGURE 22 – (A) Top-down right anterolateral view of ATD; (B) Left lateral view of ATD from the ground .....	62
FIGURE 23 – SIM G placement on child subject’s head.....	64
FIGURE 24– Four views of child human body used in designing body region contact/impact maps.....	79
FIGURE 25 – Initial conditions for lumped mass physics-based model.....	88
FIGURE 26 – Lumped mass just prior to impact .....	88
FIGURE 27 – (A) Lumped mass just prior to impact. (B) Lumped mass impacting the surface, where $\delta$ is the surface deformation. (C) Lumped mass rebounding after the impact, where $V_1$ is the rebound velocity of the mass before coming to rest.....	89
FIGURE 28 – Initial conditions of single rod.....	97
FIGURE 29 – Falling conditions of single rod.....	98
FIGURE 30 – (A) Single rod just prior to impact. (B) Single rod impacting the surface, where $\delta$ is the surface deformation. (C) Single rod rebounding after the impact, where $V_{\text{Rebound}}$ is the rebound velocity of the rod before coming to rest ( $V_{\text{final}}$ is 0 m/s).....	99

FIGURE 31 – Initial conditions of the inverted pendulum.....	105
FIGURE 32 – Falling conditions of the inverted pendulum. (A) motion of the inverted pendulum and (B) angle of the inverted pendulum as it falls. ....	106
FIGURE 33 – (A) Inverted pendulum just prior to impact. (B) Inverted pendulum impacting the surface, where $\delta$ is the surface deformation. (C) Inverted pendulum rebounding after the impact, where $V_{\text{Rebound}}$ is the rebound velocity of the mass before coming to rest ( $V_{\text{final}}$ is 0 m/s).....	106
FIGURE 34 – Percent of falls (n=100) experienced by each gender .....	114
FIGURE 35 –Fall frequency by age distribution.....	119
FIGURE 36 – Location where falls occurred .....	119
FIGURE 37 – Fall type.....	121
FIGURE 38 – Tall Mushroom (left; 45.7 cm) on playground next to short mushroom (right; 33.0 cm) .....	121
FIGURE 39 –Initial condition .....	122
FIGURE 40 – Fall initiation .....	123
FIGURE 41 –Frequency of falls with each type of fall dynamics.....	124
FIGURE 42 – Subject 4 fell rearward and head-first out of the playground panel structure, impacting his occiput and upper back on the playground surface (indicated by white arrow).....	125
FIGURE 43 – Subject 4 falling from a height and impacting his head on the playground surface.....	126
FIGURE 44 – Linear head acceleration magnitude (g) and linear head velocity magnitude (m/s) from SIM G output for fall 54 .....	126
FIGURE 45 – Frequency of falls involving an object(s).....	127
FIGURE 46 – Objects involved during the fall .....	128
FIGURE 47 – Butterfly slide in classroom 2.....	128
FIGURE 48 – Carpeted stair play equipment in classroom 2.....	129
FIGURE 49 – Locations of falls that involved an object(s) .....	130
FIGURE 50 – Frequency of falls involving an object(s) by number of phases.....	131

FIGURE 51 – Frequency of falls involving an object(s) in each phase .....	132
FIGURE 52 – Frequency of falls that involved another person(s), not including the fall subject .....	133
FIGURE 53 – Frequency of another person(s) involved in the falls .....	134
FIGURE 54 – Location of falls that involved another person(s).....	134
FIGURE 55 – Frequency of falls that involved another person(s) by number of phases	135
FIGURE 56 – Frequency of falls involving another person(s) by fall phases.....	136
FIGURE 57 – Frequency of head impact .....	137
FIGURE 58 – Percentage of falls involving an object(s) or person(s) that resulted in head impact.....	138
FIGURE 59 – Impact surfaces involved in the primary impact .....	139
FIGURE 60 – Plane(s) impacted during the primary impact of a fall .....	140
FIGURE 61 – (A) Anterior plane; (B) Posterior plane; (C) Right lateral plane; (D) Left lateral plane.....	140
FIGURE 62 – Final position of the subject .....	141
FIGURE 63 – Scale for percent of falls involving contact/impact to body region (n=100 falls) .....	142
FIGURE 64 – First contact body contact map; legend represents percentage of falls involving contact to body region .....	143
FIGURE 65 – Primary impact body impact map; Legend represents percentage of falls involving impact to body region.....	144
FIGURE 66 – Secondary impact body impact map; legend represent percentage of falls involving impact to body region.....	145
FIGURE 67 – Male vs. female subjects for falls with verified SIM G activation (n=14 falls) .....	147
FIGURE 68 – Peak resultant linear head acceleration (g) vs. peak resultant linear head velocity (m/s) across all falls with SIM G activation. ....	148
FIGURE 69 – Peak resultant linear head acceleration (g) vs. peak resultant rotational head acceleration (rad/s <sup>2</sup> ) across all falls with SIM G activation. ....	149

FIGURE 70 – Peak resultant rotational head acceleration ( $\text{rad/s}^2$ ) vs. peak resultant rotational head velocity ( $\text{rad/s}$ ) across all falls with SIM G activation.....	149
FIGURE 71 – $\text{HIC}_{15}$ vs. impact duration (ms) across all falls with SIM G activation..	150
FIGURE 72 – Fall 72, the fall with the largest peak resultant linear head acceleration (28.2 g) from this sample .....	151
FIGURE 73 – Male vs. female subjects for falls with verified SIM G activations and head impact.....	152
FIGURE 74 – Male vs. female subjects for falls with verified SIM G activations and no head impact. ....	153
FIGURE 75 – Mean peak linear head acceleration (g) for falls with SIM G activation and head impact (n=7) vs. no head impact (n=7). Error bars represent 95% confidence interval. ....	155
FIGURE 76 – Mean peak linear head velocity (m/s) for falls with SIM G activation and head impact (n=7) vs. no head impact (n=7). Error bars represent 95% confidence interval. ....	156
FIGURE 77 – Mean peak rotational head acceleration ( $\text{rad/s}^2$ ) for falls with SIM G activation and head impact (n=7) vs. no head impact (n=7). Error bars represent 95% confidence interval.....	157
FIGURE 78 – Mean peak rotational head velocity ( $\text{rad/s}$ ) for falls with SIM G activation and head impact (n=7) vs. no head impact (n=7). Error bars represent 95% confidence interval. ....	158
FIGURE 79 – Mean $\text{HIC}_{15}$ for falls with SIM G activation and head impact (n=7) vs. no head impact (n=7). Error bars represent 95% confidence interval. ....	159
FIGURE 80 – Mean impact duration (ms) for falls with SIM G activation and head impact (n=7) vs. no head impact (n=7). Error bars represent 95% confidence interval.	160
FIGURE 81 – The posterior ATD body maps from Dsouza and Bertocci (2015) for each initial position scenario for rearward fall impacts onto linoleum; colors and intensities varied depending on the level of impact force (N) .....	208



FIGURE 82 – The posterior ATD body maps from Dsouza and Bertocci (2015) for each initial position scenario for rearward fall impacts onto carpet; colors and intensities varied depending on the level of impact force (N) .....	208
FIGURE 83 – Cumulative body impact maps for forward bed falls at 61 cm (n=5); impact body regions included anterior, some posterior, left lateral, and very few right lateral regions (note: these are cumulative contact region maps across all trials; in individual trials, it was observed that if more than one body plane was impacted, only 2 adjoining planes were involved, such as anterior and left lateral). (Dsouza and Bertocci, 2018). Colors and intensities varied depending on the level of impact force (N) .....	210
FIGURE 84 – Cumulative body impact maps for rearward bed falls at 61 cm (n=5); impact body regions included anterior, some posterior, right lateral, and very few left lateral regions (note: these are cumulative contact region maps across all trials; in individual trials, it was observed that if more than one body plane was impacted, only 2 adjoining planes were involved, such as anterior and right lateral) (Dsouza and Bertocci, 2018). Colors and intensities varied depending on the level of impact force (N) .....	210
FIGURE 85 – Composite anterior and posterior bruising locations for abuse (top) and non-abuse (bottom) cases from Pierce et al. (2021) .....	212
FIGURE 86 – Composite lateral left and lateral right bruising locations for abuse (top) and non-abuse (bottom) cases from Pierce et al. (2021).....	213
FIGURE 122 – Linear acceleration magnitude (g) and linear velocity magnitude (m/s) from SIM G output for fall 516.....	219
FIGURE 87 – Captured screen shots of fall 14 dynamics from the video recording .....	244
FIGURE 88 – SIM G verification with mean peak resultant linear .....	248
FIGURE 89 – SIM G verification with mean peak resultant linear .....	249
FIGURE 90 – SIM G verification with mean peak resultant rotational .....	250
FIGURE 91 – SIM G verification with mean peak resultant rotational .....	251
FIGURE 92 – SIM G verification with mean impact duration (ms) from replicated ATD feet-first falls onto linoleum.....	252

FIGURE 93 – Number line for comparison of linear acceleration (g) measured in ATD feet-first falls (SIM G range) onto carpet (n=7) to physics-based model predictions ....	257
FIGURE 94 –Number line for comparison of linear velocity (m/s) measured in ATD feet-first falls (SIM G range) onto carpet (n=7) to physics-based model predictions .....	258
FIGURE 95 –Number line for comparison of rotational acceleration (rad/s <sup>2</sup> ) measured in ATD feet-first falls (SIM G range) onto carpet (n=7) to physics-based model predictions .....	259
FIGURE 96 –Number line for comparison of rotational velocity (rad/s) measured in ATD feet-first falls (SIM G range) onto carpet (n=7) to physics-based model predictions ....	260
FIGURE 97 – Number line for comparison of linear acceleration (g) measured in ATD feet-first falls (SIM G range) onto linoleum (n=7) to physics-based model predictions	264
FIGURE 98 – Number line for comparison of linear velocity (m/s) measured in ATD feet-first falls (SIM G range) onto linoleum (n=7) to physics-based model predictions	265
FIGURE 99 – Number line for comparison of rotational acceleration (rad/s <sup>2</sup> ) measured in ATD feet-first falls (SIM G range) onto linoleum (n=7) to physics-based model predictions.....	266
FIGURE 100 – Number line for comparison of rotational velocity (rad/s) measured in ATD feet-first falls (SIM G range) onto linoleum (n=7) to physics-based model predictions.....	267
FIGURE 101 – Number line for comparison of linear acceleration (g) measured in ATD feet-first falls (SIM G range) onto linoleum with dynamic A (n=5) to physics-based model predictions.....	271
FIGURE 102 – Number line for comparison of linear velocity (m/s) measured in ATD feet-first falls (SIM G range) onto linoleum with dynamic A (n=5) to physics-based model predictions.....	272
FIGURE 103 – Number line for comparison of rotational acceleration (rad/s <sup>2</sup> ) measured in ATD feet-first falls (SIM G range) onto linoleum with dynamic A (n=5) to physics-based model predictions.....	273

FIGURE 104 – Number line for comparison of rotational velocity (rad/s) measured in ATD feet-first falls (SIM G range) onto linoleum with dynamic A (n=5) to physics-based model predictions.....	273
FIGURE 105 – Number line for comparison of linear acceleration (g) measured in ATD feet-first falls (SIM G range) onto linoleum with dynamic C (n=2) to physics-based model predictions.....	276
FIGURE 106 – Number line for comparison of linear velocity (m/s) measured in ATD feet-first falls (SIM G range) onto linoleum with dynamic C (n=2) to physics-based model predictions.....	277
FIGURE 107 – Number line for comparison of rotational acceleration (rad/s <sup>2</sup> ) measured in ATD feet-first falls (SIM G range) onto linoleum with dynamic C (n=2) to physics-based model predictions.....	278
FIGURE 108 – Number line for comparison of rotational velocity (rad/s) measured in ATD feet-first falls (SIM G range) onto linoleum with dynamic C (n=2) to physics-based model predictions.....	278
FIGURE 109 – The yellow arrow indicates subject 11, who was initially sitting on her buttocks (A) when she lost balance and fell rearward (B). She impacted her head occiput on the bulletin board and impacted her upper posterior torso on the carpeted flooring (C/D). Her final position was supine on the carpeted flooring (D). .....	279
FIGURE 110 – Linear acceleration magnitude (g) and linear velocity magnitude (m/s) from SIM G output for fall 146.....	280
FIGURE 111 – Head impact location image generated from SIM G activation.....	280
FIGURE 112 – The yellow arrow indicates subject 11, who was initially standing upright on the base of the slide when she stepped off the base with her left foot (A). Her left foot contacted the playground surface, and she lost her balance and fell forward (B). She impacted her anterior torso and bilateral anterior legs, as well as her face on the playground surface (C). Her final position was prone on the playground surface (D)...	282
FIGURE 113 – Linear acceleration magnitude (g) and linear velocity magnitude (m/s) from SIM G output for fall 238.....	283

FIGURE 114 – Head impact location image generated from SIM G activation .....	283
FIGURE 115 – Subject 5 was bending at the knees on the bottom step of the butterfly ramp (A). She projected forward (as if to jump) and fell forward (B). She contacted the palms of both hands on the carpeted flooring (C), and paused before falling straight to the carpeted flooring, where she impacted her face (D). She was in a supine final position at the end of the fall (E). .....	286
FIGURE 116 – Linear acceleration magnitude (g) and linear velocity magnitude (m/s) from SIM G output for fall 241.....	286
FIGURE 117 – Head impact location image generated from SIM G activation .....	287
FIGURE 118 – The yellow arrow indicates subject 4, who was initially walking in the classroom on the carpeted surface (A). He tripped and fell forward (B/C). He contacted his righthand palm on the carpeted floor; he then continued to fall forward, and he impacted his face on the wall/edge of the bulletin board on the wall (D). His final position was on his hands and bilateral knees on the carpeted flooring (E). .....	289
FIGURE 119 – Linear acceleration magnitude (g) and linear velocity magnitude (m/s) from SIM G output for fall 321.....	289
FIGURE 120 – Head impact location image generated from SIM G activation.....	290
FIGURE 121 – Subject 15 was initially walking and stepped with his left foot onto a toy ball, which caused him to slip rearward (A). He fell rearward and impacted his buttocks on the carpeted flooring with his torso approximately 45° to the horizontal (B/C). He then fell rearward and impacted his posterior torso and occiput on the carpeted flooring (D). He was in a final supine position at the end of the fall. ....	292
FIGURE 122 – Linear acceleration magnitude (g) and linear velocity magnitude (m/s) from SIM G output for fall 516.....	292
FIGURE 123 – The yellow arrow indicates subject 21, who was initially walking on the carpeted flooring (A). He tripped over an object and fell forward (B). He impacted his bilateral knees and the palms of both hands on the floor, and impacted his superior head/face on the side of a wooden bookshelf (C/D). He then dropped to his anterior torso, and he was in a final prone position at the end of the fall (E). .....	295

FIGURE 124 – Linear acceleration magnitude (g) and linear velocity magnitude (m/s) from SIM G output for fall 545.....	295
FIGURE 125 – Head impact location image generated from SIM G activation.....	296
FIGURE 126 – In fall 676 (1), subject 21 was initially standing upright at the base of the tall mushroom on the playground surface (A). Subject 21 was leaning to his right and lost his balance, and he fell straight down [feet-first dynamics] (B). He impacted his inferior (caudal) chin on the top of the tall mushroom surface (C). He landed on his buttocks with his torso about 90° to the horizontal (D), which completed the first part of this two-part fall. ....	298
FIGURE 127 – Linear acceleration magnitude (g) and linear velocity magnitude (m/s) from SIM G output for fall 676 (1).....	298
FIGURE 128 – Head impact location image generated from SIM G activation.....	299
FIGURE 129 – Subject 21 was on his buttocks on the playground surface after his first fall (A). He continued to fall, rotating about his torso and falling rearward (B). He impacted his occiput on the playground surface (B). His final position was supine on the playground surface (C). ....	301
FIGURE 130 – Linear acceleration magnitude (g) and linear velocity magnitude (m/s) from SIM G output for fall 676 (2).....	301
FIGURE 131 – Head impact location image generated from SIM G activation.....	302

## I. INTRODUCTION

A fall is the most common false history in cases of abuse when a child presents an injury at a medical care center (Coats & Margulies, 2008). The risk of head injury from a short-distance fall involving a young child remains ill-defined, and there is a need to differentiate between accidental injuries and abusive injuries (Burrows et al., 2015).

Adverse childhood experiences (ACEs) are defined by the Centers for Disease Control and Prevention as “potentially traumatic events that occur in childhood (0-17 years)” (Centers for Disease Control and Prevention, 2020). ACEs are a broad subject, ranging from experiencing violence, abuse, and/or neglect to witnessing violence in the home or community and can also include having a family member attempt or die by suicide. This is a significant health issue, as ACEs are linked to chronic health problems, mental illness, and substance misuse in adulthood. 61% of adults surveyed across 25 US states reported that they had experienced at least one type of ACE, and 1 in 6 reported they had experienced 4 or more types of ACEs. The CDC also estimated that the prevention of ACEs could potentially reduce later-in-life health issues, including heart disease and depression (Centers for Disease Control and Prevention, 2020). The CDC also estimated that the economic and social costs to families, communities, and society total hundreds of billions of dollars each year (Centers for Disease Control and Prevention, 2020).

In 2012, the CDC estimated that U.S. state and local Child Protective Services (CPS) received 3.4 million referrals of children being abused or neglected, and an estimated 1,640 children died from child maltreatment (National Center for Injury Prevention and Control – Division of Violence Prevention, 2014). This corresponded to a rate of 2.2

deaths per 100,000 children. Of those deaths, 70% occurred among children younger than 3 years old. The state of Kentucky in particular has an alarming rate of child abuse – according to the US Department of Health and Human Services, from 2014 to 2018, Kentucky had an overall 17.1% increase in number of children who received an investigation for child abuse from CPS – from 70.6 per 1000 children to 83.2 per 1000 children (Children’s Bureau, 2020). This is five percent higher than the national average (12%).

Trauma is the most common cause of death in children, and abusive head trauma is the primary cause of traumatic death and morbidity in infancy (<1 year age) (Girard, Brunel, Dory-Lautrec, & Chabrol, 2016). A head injury can be defined as a “clinically important external injury to the face, scalp, or calvarium and may include lacerations, contusions, abrasions, and/or fractures; they are often associated with traumatic brain injuries” (Aghakhani, Heidari, Ameri, Mehrpisheh, & Memarian, 2015).

The general school of thought associated with short-distance falls is they rarely cause fatal head injuries, but they still have the potential to do so (Burrows et al., 2015; Duhaime et al., 1992; Williams, 1991). The mortality rate from short-distance falls involving young children and infants is estimated to be <0.48 deaths per one million (Chadwick et al., 2008). It is generally accepted that most household falls can be considered neurologically benign (Duhaime et al., 1992).

Differentiation between accident and abuse is very important when reviewing a child’s injuries, and it can be particularly difficult when a child is non-verbal. The distinction between the two remains blurred. The ability to distinguish between accidental fall outcomes and abusive injury is a critical skill for medical evaluators and forensic

investigators. Unfortunately, there is a lack of published information regarding *witnessed* short-distance falls. Furthermore, there are uncertainties with injury prediction or even knowledge of incidences of severe head injury from witnessed falls. By collecting data regarding short-distance fall characteristics and their associated biomechanical measures, a better understanding of short-distance-fall consequences can be generated, which may lead to a better overall differentiation of accidental and abusive injuries.

The overall objective of this project was to video-record pediatric falls, analyze their characteristics and dynamics, and determine their associated biomechanical measures. Young children between 1-3 years old were observed in a childcare setting. Each room was equipped with digital video cameras to record observation periods. The children were equipped with a sensor embedded in a headband, and this sensor measured head biomechanical data.

This study examined biomechanical measures for pediatric falls in a video monitored setting, where the possibility of child abuse was excluded. The findings were data-based evidence for a topic that has a paucity of information and data. It generated a collection of reliably witnessed short-distance falls. These outcomes were expected to play a critical role in forensic investigations where child abuse is alleged, as they provide a better overall understanding of short-distance falls.



## II. BACKGROUND

Injury biomechanics is currently applied in three large research fields – the first is the study and understanding of the mechanism by which an injury to body tissues is produced. The second field is the study of the human body response to forces. The third major field is the determination of a force threshold that is required to produce an injury (Arregui-Dalmases, Teijeira, Forman, & Geneva, 2010). This field is often applied to forensic investigations involving cases where a child’s presenting injuries may be accidental or abusive. The following literature review pertains to the field of injury biomechanics and the current research into pediatric injuries, particularly those where the provided history is a short-distance fall.

### A. The head of a young infant and its increased susceptibility to injury

Injuries during the brain growth period of infants and young children differ from those that occur later in life (Case, 2014). Additionally, the skull and brain have much different biomechanical properties than those in adults. The skull of a young child is thin and pliable, and the sutures of the skull have not joined (differing from adults, where the cranial bones are more ossified, offering greater protection to impact). Furthermore, infant brains have very high-water content, the neural axons have not fully myelinated, and the subarachnoid space is relatively thin but occupies a large surface area. These anatomical features have led to the theory that younger brain tissue may have a lower threshold for injury than older children and adults (Case, 2014). The very soft consistency of a young brain makes it less likely to contuse, as compared to tearing, when significant force is applied to the brain (M. E. Case, 2008). The brain’s connective tissue

is neither well-developed nor supportive enough for high forces, and the veins are thin, including the bridging veins (Bagnato & Feldman, 1989).

The brain tissue bulk modulus is approximately 5 to 6 times larger than the shear modulus, so for a given impact the brain tends to deform predominately in shear (Kleiven, 2013). This means that the brain is more sensitive to rotational loading more than translational, and therefore rotational kinematics are just as important in biomechanical analyses as linear kinematics. As previously stated, young brain tissue is more susceptible to injuries, particularly shearing injuries, especially when the head is subjected to acceleration-deceleration forces, which distribute around the skull and subarachnoid spaces (M. E. Case, 2008; Case, 2014). Static head injuries occur over longer time durations (>200 ms), while dynamic injuries are associated with shorter time periods with a contact impact or an inertial load, leading to focal (scalp lacerations, contusions, skull fracture, epidural/subdural hemorrhage) and/or diffuse injuries (traumatic diffuse axonal injury, concussion, shearing of the axons) (Mary E. Case, 2008; Case, 2014; Pierce, Bertocci, Berger, & Vogeley, 2002). Duhaime et al. postulated that rotational, rather than translational, forces may cause more serious head injuries, and that epidural hematomas are signs of more acute injury (Duhaime et al., 1992).

Loyd et al. (2015) performed a study to measure the sub-injurious skull stiffness of 12 pediatric cadavers between 20 weeks of gestation period and 16 years old. They used viscoelastic compression tests in both lateral and anterior-posterior directions at deformation rates of 0.0005/s, 0.01/s, 0.1/s, and 0.3/s. Their results led them to the conclusion that structural stiffness does vary with age – a large and statistically significant stiffness increase in both the toe and elastic region of the force-deformation

curves existed as age increased. The stiffness in the elastic region was measured from 5N/mm for the neonate to 44600N/mm in the 16-year-old. This supports the idea that the skull thickens with age.

#### B. Difficulties in differentiating child abuse from accidental head injuries

In general, it is estimated that there are around 220 head injuries per 100,000 children per year, and 200,000 of those require hospitalization (Bagnato & Feldman, 1989). Short-distance falls are extremely common in children, and they are commonly reported in hospitals as the mechanism responsible for an injury (Bagnato & Feldman, 1989; G. E. Bertocci et al., 2003; Burrows et al., 2015; Mary E. Case, 2008; Coats & Margulies, 2008). While it is possible that short falls may be able to cause minor injuries (simple linear fractures, scalp lacerations, scalp contusions), it is rare that they cause serious injuries (concussion, subdural hematomas, retinal hemorrhages, etc.) or death (Bagnato & Feldman, 1989; G. E. Bertocci et al., 2003; Gina E. Bertocci et al., 2004; Chadwick et al., 2008). Chadwick et al. (1991) performed a retrospective clinical review of children who were admitted to a children's hospital trauma center between 1984 and 1988 for whom a mechanism of injury of "fall" had been recorded. They reviewed these records to determine fall height, impact surface, the nature of the fall (free or interrupted), fall witness, the patient's injury diagnosis and their outcome. This study resulted in 283 cases where the fall height was categorized into 3 categories: 1-4 feet; 5-9 feet; and 10-45 feet. 7 children were reported to have died in the 1-4 feet category; no children were reported to have died in the 5-9 feet category; 1 child was reported to have died in the 10-45 feet category. However, it was noted that all 7 deaths had "other factors in their cases that suggested false histories [from caretakers]" (Chadwick, Chin, Salerno, Landsverk, &

Kitchen, 1991)). This study concluded that falls where a witness reports the height to be from 4 feet or less may be a false history.

According to Case (2008), 2 to 3% of falls result in simple linear skull fracture, and the vast majority of these are “uneventful in terms of neurological deficit or intracranial bleeding”, and in about 1% of these fractures epidural or subdural hemorrhages occur. However, it is difficult to determine whether an injury was caused by a fall because caregivers guilty of abusive head trauma often provide a false scenario. In general, though, it is believed that short falls in the home (less than 6 ft) are associated primarily with minor focal contact injuries, such as scalp laceration or contusion, and the great majority of falls demonstrate no injury at all (Duhaime et al., 1992).

When considering a fall history that was provided by a caretaker where the injury outcomes are questionable, various factors of the provided history must be considered to determine the compatibility of the fall scenario to probability of the presented injuries. Particularly, impact surface has been found to be a significant factor in falls for assessing injury outcome. Jones, 2011 found that the risk of an infant sustaining a significant head injury could vary considerably, even across the surface of a flooring. Impact surface material properties and the location of impact must be considered when reviewing a fall history (Jones & Theobald, 2011).

The overall risk of serious head injury from a fall in a young child is still ill-defined. Because of this, physicians face a great difficulty when trying to differentiate children with head injuries as accidental or as a product of abuse (G. E. Bertocci et al., 2003; Gina E. Bertocci et al., 2004; Burrows et al., 2015). To diagnose abusive head trauma, physicians typically rely on the presence of specific injuries and trauma. These

include: subdural hemorrhage, retinal hemorrhage, fractures in various states of healing (particularly rib fractures), and fractures of the metaphysis (Girard et al., 2016).

### C. Clinical studies pertaining to injuries resulting from short-distance falls

Since the 1960s, there has been an increase in abusive head trauma studies, especially those related to infants. This section attempts to highlight some of those related to biomechanics and their impact on the overall understanding of how clinicians, physicians, and law experts may utilize biomechanical data in the assessment of an injury. A fall is defined as “an unexpected event in which the participant comes to rest on the ground, floor, or lower level” (Bagala et al., 2012; Dufek, Ryan-Wenger, Eggleston, & Mefferd, 2018). Falls are responsible for 20-30% of head injuries across all age groups, and they are more common in children and the elderly (Bagnato & Feldman, 1989; Duhaime et al., 1992). Younger children tend to sustain more severe injuries than older children, and falls are a common false explanation for head injuries in children admitted to hospitals (when a caregiver is concealing abuse). The main school of thought associated with short distance falls is that they rarely cause fatal head injuries; however, they do have the *potential* to do so, depending on the events surrounding the fall (Burrows et al., 2015).

Chadwick et al. (2008) performed a retrospective review of published materials (5 book chapters, 2 medical society statements, 7 major literature reviews, 3 public injury databases, and 177 peer reviewed, published articles indexed in the National Library of Medicine) to develop an estimate of fatality risk from short (<1.5m) falls in children between 0 and 5 years old. In all the studies, the “best” mortality estimate was <0.48 deaths per 1 million young children per year.

Mulligan et al. (2017) performed a retrospective pediatric trauma center emergency department (ED) clinical study in Australia of short distance falls in young children. They reviewed both ED presentations and admissions from January 1, 2011 to December 31, 2013. They included patients who were aged under 1 year of age and whose primary cause for presentation was an injury(s) due to a fall; their overall sample size was 916 patients. Injuries were categorized by the abbreviated injury scale (AIS) levels; details from the presentation were also categorized into mechanism of injury (such as dropped by another person, fall from a cot/bed/couch, etc.), injury type (skull fracture, skull fracture plus intracranial bleed, non-head injury, etc.), and whether an intracranial injury such as subdural hematoma resulted from the short distant fall. The most common short distance fall scenario was a fall from a cot, bed, or couch at 27%, followed by a fall from a baby seat, pram, or bouncer at 21%. Of all presentations, 12% were admitted to the hospital, and 8% were admitted to the intensive care unit. The study found that infants who were dropped by a parent or caregiver were three times more likely to be admitted than other fall mechanisms. However, infants who fell from a bed or couch were significantly less likely to be admitted. Furthermore, patients who were admitted were younger (mean age of 5.3 months) than those who were outpatient. The reason for most (85%) hospital admissions was cited as head injury, the most common being isolated skull fracture (46.2%) or skull fracture with an intracranial bleed (29.2%). 9.4% of head injuries was an intracranial bleed with no skull fracture. Other reported injuries included long bone fractures, soft tissue injuries, and lacerations. Out of these patients with injuries, 94% were managed non-operatively. All neurosurgical procedures performed (including craniotomies for evacuation of hematomas and one operation to elevate a

depressed parietal skull fracture) involved infants admitted after being dropped (n=1) or after a fall from a bed or couch (n=4). There was one reported death from all admitted children; this was a 5-month-old infant who fall from a cot onto hard floor and sustained a combined skull fracture with epidural hematoma. This infant died 5 days after injury presentation. Mulligan et al. determined that more severe injuries were often seen in cases where the child was dropped from the caretaker's arms, as well as bed falls and falls from unrestrained child equipment (i.e. prams and highchairs).

Ibrahim et al. (2012) performed a retrospective cohort study of 285 children between 0-48 months (between 2000 and 2006) with accidental head injury from a fall. They found that head falls may be both age and mechanism dependent, and that fall height and injuries can differ significantly between infants (0-12 months) and toddlers (12-48 months). They found that infants who were hospitalized with head injuries were more likely to have fallen from 3 feet or less, while toddlers who were hospitalized with head injuries were more likely to have fallen from less than 10 feet. The researchers found a higher incidence of head soft tissue injury and skull fractures in infants, as compared to toddlers, for both falls from low ( $\leq 3$  feet) and intermediate ( $>3$  feet and  $<10$  feet) heights. They also found that the incidence of primary brain injury did not significantly differ between infants and toddlers at low or intermediate heights, but were more common for infants who fell down stairs (Nicole G. Ibrahim, Wood, Margulies, & Christian, 2012).

#### 1. Clinical information on injuries resulting from household short distance falls

Thompson et al. (2011) performed a clinical study on children aged 0-4 years who presented to the Emergency Department (ED) with a history of a short distance household fall. They collected medical records, interviews, and fall scene investigations;

they rated injuries using the Abbreviated Injury Scale (AIS). This study resulted in 79 enrolled subjects, where 15 had no injuries, 45 had minor (AIS 1) injuries, 17 had moderate (AIS 2) injuries, and 2 had serious (AIS 3) injuries. No subjects had injuries classified as AIS 4 or higher, and there were no fatalities. Subjects with moderate and serious injuries were reported to have fallen from greater heights, had greater impact velocities, and had a lower body mass index than subjects with minor or no injuries. The “worst case” fall involved a 42-month-old female child (11.8 kg mass) who fell rearward from approximately 1 meter off the back of a sofa. She landed laterally left and impacted her head on hardwood flooring, and this fall resulted in a 3 mm left posterior subdural hematoma. Another fall with a serious injury involved a 1-month-old male; this child was asleep on his mother’s chest. The mother was lying supine in a bed, fell asleep, and rolled over. This caused the child to fall off the side of the bed (approx. 86 cm), and he struck his anterior head on a humidifier that was adjacent to the bed. His final position was supine on carpeted flooring. This fall resulted in a thin right frontoparietal subdural hematoma with skull fracture. Fall heights were estimated from approximately 25 cm to 90 cm. The distribution of falls for each injury severity category based upon furniture type was determined (FIGURE 1). They concluded that biomechanical measures (impact velocity, potential energy, and change in impact momentum) are associated with injury severity outcomes in short-distance household falls (A. K. Thompson, Bertocci, Rice, & Pierce, 2011).



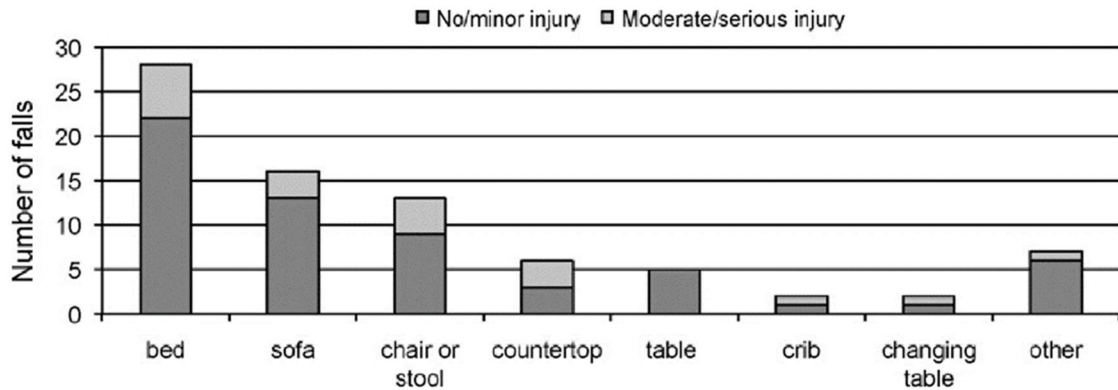


FIGURE 1 – Frequency distribution of falls for each injury severity category based upon furniture type (n=79) (A. K. Thompson et al., 2011).

Morrison et al. (2002) performed a clinical study in New Zealand based on furniture-related hospitalizations from children between 0 and 4 years old between the years of 1987-1996. Of the 1679 furniture-related injuries reported, there were 43 fatalities (average 4 deaths/year). 51% were related due to cots; 30% were related to beds; 19% were related to prams, push chairs, highchairs, car seats, portable cots, and walkers. They determined that most hospitalizations resulted from falls, specifically out of bed and cots. In a similar study, Powell et al. (2002) performed a retrospective review of data for children 3 years of age or younger from the National Electronic Injury Surveillance System (NEISS; USA) from 1994 to 1998 to determine the number of highchair-related injuries. They found 40,650 highchair-related injuries, with an annual average of 5.3 injuries per 10,000. 94% of injuries resulted from a fall, and most involved the head or face. The reported injuries included contusions/abrasions, lacerations, closed head injury, and fractures. Meanwhile, the admission rate was only 0.1 per 10,000. 94% of injuries resulted from a fall from the highchair: 4% where the chair tipped and fell; in 1% an

extremity was caught in the chair; and in 1% the chair malfunctioned. The admitted hospital injuries included closed head injury, extremity fractures, head lacerations, contusions/hematomas, skull fractures, and extremity injuries. No deaths were reported (Powell, Jovtis, & Tanz, 2002).

Helfer et al. (1977) performed a clinical study of 246 children under 5 years of age who fell from a height of 90 cm or less (about the height of a child falling out of a bed). They collected information from parents who presented their children to their primary pediatrician. They were asked to indicate incidences of falls and what, if any, injury occurred – these incidences were recorded from memory, a limitation on this study. So, the study also collected retrospective clinical reports from a children's hospital over a 6-year period. These included falls from a crib, bed, or examination table. There was a total of 161 incidences collected from the parents, and 43 injuries were reported from the parental questionnaire. These included 37 nonserious injuries (“bumps, lumps, bruises, scratches, etc.”); 3 fractured clavicles; 2 skull fractures; 1 fractured humerus. The bone fracture injuries all resulted from falls of 90 cm or less, and none of those falls resulted in serious injury sequelae and the two skull fractures did not result in serious head injury. The two skull fractures and the humeral fracture were in children younger than 6 months of age. None of the 161 children suffered any life-threatening injuries from these falls. From the hospital incidence reports, 85 incidents were obtained; some had more than one injury. 57 incidents resulted in no apparent injury; 17 incidents resulted in small cuts, scratches, and/or bloody noses; 20 children had a bump and/or bruise; 1 resulted in a child having a skull fracture, but they had no serious or apparent sequelae (the child had fallen from an emergency department cart). None had any signs of soft tissue injury. It

was concluded that, in most cases where a child falls from a short height, a trivial injury may occur; however, serious head injury or central nervous system injuries are extremely rare (Helfer, Slovis, & Black, 1977).

A large retrospective clinical study of short-distance pediatric falls related to beds was performed by Lyons and Oates (1993). The purpose of the study was to determine the likelihood of injuries occurring to infants and children who “fall out of bed.” The study design was a retrospective clinical study where injury reports and records from a children’s hospital between January 1983 and August 1992 were reviewed. The researchers estimated the height of the fall and they obtained the weight of the child from records. They calculated the momentum on impact using equation 1.

$$N = M * v \tag{1}$$

where N is the momentum in newtons, M is the mass in kilograms, v is the velocity in m/s, and the velocity on impact was calculated using equation 2.

$$v^2 = u^2 + 2 * A * S \tag{2}$$

where u is the initial velocity in m/s, A is the acceleration in m/s<sup>2</sup>, and S is the height of the fall in m. They compared the momentum on impact for children who were injured to the children in the non-injured group. This study resulted in 217 documented falls from a bed, where the children were 6 years or younger and where records contained adequate data for review. Falls more often occurred in the 1- to 2-year-old group than children

younger than one year of age or children older than two years of age. There were 31 documented injuries; 29 were considered trivial (contusions/small lacerations). There was 1 clavicle fracture and 1 skull fracture. No loss of consciousness was reported in any case. The mean momentum of children with no injury ranged from 36 N (<12 months old) to 78 N (60-71 months old). The mean momentum of injured children ranged from 41 N (<12 months old) to 72 N (48-59 months old). There was no significant difference between the injured and non-injured groups. The authors concluded that falls from short distances do not produce multiple or visceral injuries and that clinically significant injuries are uncommon (Lyons & Oates, 1993).

Nimityongskul and Anderson (1987) stated that “contact surfaces and heights of falls are the variables determining severity of injury.” They then performed retrospective clinical study to determine the likelihood and severity of injuries when children fall out of a bed, crib, chair, wagon, etc. while hospitalized for other medical reasons. Inclusion criteria were records from a medical center between January 1980 and December 1985 where a child  $\leq 16$  years of age was reported to have fallen out of a bed, crib, couch, chair, wagon, off a rocking horse in a playroom, or slipped and fell to the floor while walking or running. The child had to have been examined by a physician either right after or within a few hours of the incident. Injury and/or consequences of these incidents were reviewed. This study resulted in 76 children (31 girls, 45 boys) reported to have fallen out of a bed, crib, chair, wagon, etc. while in the hospital during the 5-year survey period. The fall height ranged from 1 to 3 feet in most cases. Most sustained injuries were minor – 2/3 of the children sustained minor bruises or were noted to have no discernable injury. 1/3 sustained lumps about the scalp and face, bumps, and minor lacerations. There was

one reportedly questionable occipital skull fracture in a 1-year-old girl with no identified intracranial injury, and she did not require treatment. One child had a nondisplaced tibial fracture when a patient with osteogenesis imperfecta fell in the physical therapy department. No upper/lower extremity injuries and no spinal injuries were documented. Most injuries occurred in the head and face region, specifically in instances where a child climbs out of a bed/crib and subsequently falls “headfirst” to the impact surface. Overall, this study concluded that severe head, neck, extremity, and spine injuries are extremely rare when children  $\leq 16$  years of age fall out of a bed, crib, chair, etc. while in the hospital. They recommended that a child being seen in an emergency room with a significant head, neck, extremity, or spine injury from a reported “fall out of bed” or “fall at home” be investigated for potential child abuse (Nimityongskul & Anderson, 1987).

#### D. Injury mechanisms associated with pediatric head injuries

It has been shown experimentally and clinically that diffuse brain injuries result from significant angular accelerations (Dufek et al., 2018). These induce brain deformation and shear strain. Bandak (2005) proposed that mechanical forces that injure the brain from contact or direct impact to the head are caused from sudden acceleration or deceleration of the movable head, and the brain does not move (due to inertial forces) until the front of the skull collides with it. Then, the brain advances until it contacts the back wall of the skull; this sequence may repeat for several oscillations. Bandak also proposed that rotational forces from shaking cause additional shearing strain, which is responsible for superficial cortical injury and deep lesions within the brain (Bandak, 2005).

Secondary injuries can include subdural hematomas, which result from “massive cortical damage and lacerations of bridging blood vessels” (Bagnato & Feldman, 1989).

Other secondary injuries include brain edema; as the tissue swells, the skull impedes the tissue expanding. This also blocks blood flow, which can lead to compound ischemic injury and hypoxic tissue death (Bagnato & Feldman, 1989).

Current research uses animal, human cadaver, and computational models which have resulted in an understanding of 4 brain injury mechanisms. These include contusions resulting from skull deformation and brain motion; intracranial pressure gradients produced from impact; rotation causing relative motion between the skull and the brain; combined linear and rotational acceleration from impact. A fifth mechanism was proposed for head injury that occurs through a combination of skull deformation, positive and negative pressures, and brain lag, which all result from linear and/or angular accelerations (Dufek, 2018).

It remains unknown and debated which forces cause the most serious injuries. Duhaime et al. (1992) proposed that the presence of more serious injuries may be due to the predominance of rotational, rather than translational, forces acting on the head. Kleiven (2013) also proposed that the human brain is more sensitive to rotational motion. However, both Burrows, et al. and Hughes, et al. report that falls from a caretaker's arms onto hardwood floors result in the most severe injuries (Burrows et al., 2015; Hughes, Maguire, Jones, Theobald, & Kemp, 2016).

Burrows et al. (2015) performed a cross-sectional study of 1775 fall cases from children younger than 6 years old who were admitted to UK Hospitals between September 2009 and February 2010. 87% of the cases had a Glasgow Coma Scale (GCS) equal to 15, which is the best outcome. Of those cases with the best GCS, 12% had intracranial injury. The types of injuries seen in children who were dropped from

caretaker's arms or fell from a building were significantly more severe than those from children who fell from standing alone (Burrows et al., 2015).

Stürtz (1980) discussed the hypothesis that the “child [skull] lies in a zone neutral to vibrations” and therefore, contrary to adults, is more protected from impact trauma (Stürtz, 1980). He proposed that when a skull suffers a blow, there is a summation of effects. These include osseous vibration mechanisms that propagate to the dura and subdural region, then to the brain. They also include mass shifts of the child's brain, which result in an intracranial drop in pressure and are decisive for the “effect of the respective impact force” (Stürtz, 1980). This is also known as the “contre-coup” center, or the opposite site of the impact and the “spatial extension” (or distance) of this center correlates to the “seriousness of the damage” (Stürtz, 1980).

Hu (2017) utilized witnessed fall cases to investigate the relationship between fall height (less than 10 feet/3 meters) and head injury severity. He reviewed cases for 463 children less than 48 months of age – 47 had skull fracture or intracranial injury (ICI), and 416 had minor head injury(s). He found that skull fracture/ICI was significantly associated with a fall height, where the head center of gravity was greater than 0.6 m (approximately 2 feet), the age was younger than 12 months, and head impacts were to the parietal/temporal region or occipital region. They were also more likely to occur from a fall from the caregiver's arms and were more likely to occur when the impact surface was wood. He found no skull fracture/ICI from falls that were from less than 0.6 meters; however, he did find that a fall height of 1.54 meters resulted in a 50% probability of skull fracture/ICI (Hu, 2017).

#### E. Biomechanical application in the investigation of pediatric short distance falls

Limitations of studies using Anthropometric Test Devices (ATDs) include the lack of biofidelity (or similarity to real biomechanics of human tissue); furthermore, ATDs typically only represent certain portions of a whole population, and many studies only test a small sample size, which prevents generalization of the results (Burrows et al., 2015). Computational models may be a better form of fall analysis, but there is a need for more biomechanically-accurate data from actual falls in order for computer models to become more robust (Kakara et al., 2013). Physics-based models help provide a means of analyzing simple forces predicted from falls and can be used to compare to outcomes from ATD test falls and computer simulations.

##### 1. Physical Models of Pediatric Falls

When investigating falls, several parameters of the fall should be reviewed, as they can affect the severity and injury type that is possibly sustained in a fall (Cory, Jones, James, Leadbeatter, & Nokes, 2001). The parameters include acceleration due to gravity, air resistance, height of the fall, impact velocity, fall and impact mechanics, impact surface, child age, etc. Cory et al. first modeled a simple free fall under the force of gravity (FIGURE 2).



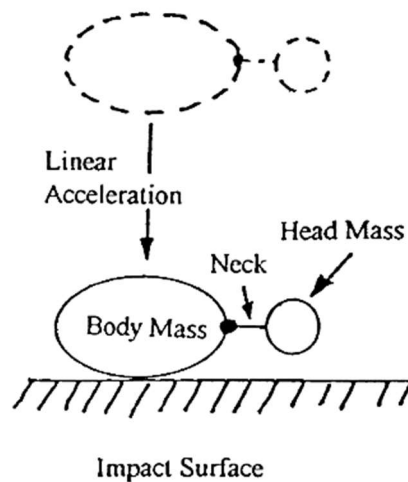


FIGURE 2 – Free fall of an infant from an initial fall position to a point of impact  
(Cory et al., 2001)

Cory also discussed the mechanics of a pediatric fall, such as a baby rolling off a changing table, a baby rolling off a bed, or a fall from a caretaker’s arms (Cory et al., 2001). These falls involve vertical linear acceleration, and it is assumed that any horizontal component is negligible. However, pediatric falls may involve an initial increase in height from an elevated surface, such as a jump before a fall or a child thrown into the air – this increases the height of the fall and the subsequent impact velocity. When falls involve a child who is running before the fall, there is a horizontal component and horizontal displacement is increased (FIGURE 3). Cory also modeled falls where the horizontal velocity immediately before the impact was involved but the initial height is from a low surface (FIGURE 4). Finally, Cory also modeled falls with no skidding on impact (no horizontal component) (FIGURE 5).

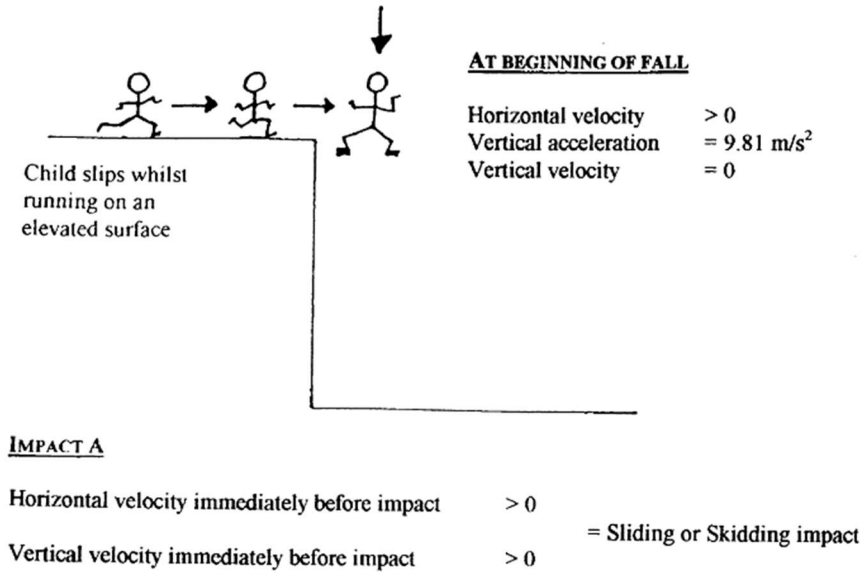


FIGURE 3 – A fall involving a horizontal velocity component on an elevated surface (Cory et al., 2001)

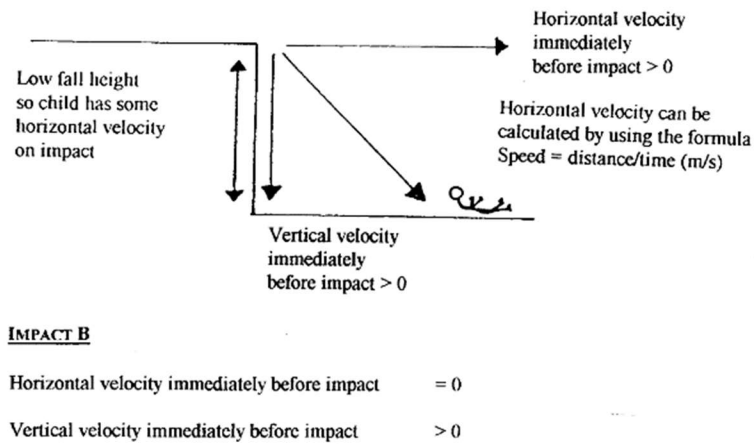


FIGURE 4 – A fall involving a horizontal velocity immediately before impact from a low fall height (Cory et al., 2001)

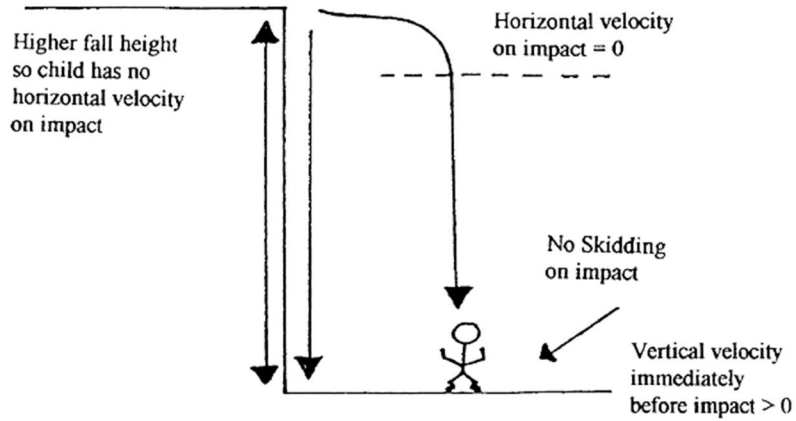


FIGURE 5 – Fall involving no horizontal component (Cory et al., 2001)

Cory also discussed the parameter of surface type and its effect on falls. Surface material properties influence the force per unit area from the child impacting the surface (stress), which in turn can affect injury severity. When the child impacts a surface, the surface itself will deform and energy is absorbed by work being done to deform the material. A deformable surface will increase the impact/contact area between the body and the surface due to curving around an object, and the energy dissipation due to the deformation of the surface reduces the stress of the impact (Cory et al., 2001). Soft versus hard surfaces were visually demonstrated by Cory (FIGURE 6).

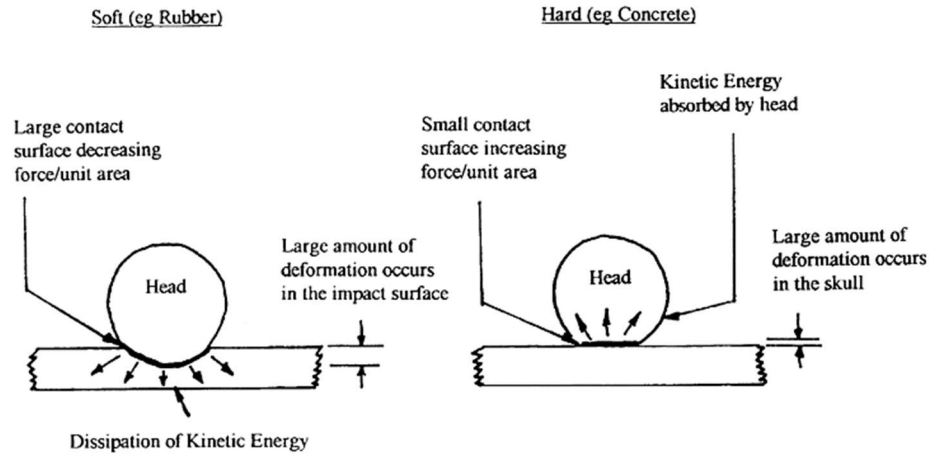


FIGURE 6 – Energy dissipation of soft versus hard surfaces (Cory et al., 2001)

Impact duration was also an important component of the fall event, as an increase in impact duration reduces injury severity (Cory et al., 2001). This is related to the impact surface and the resiliency of the material – materials that deform over a relatively long time period have been shown to effectively decelerate a body with minimal or no injury (Cory et al., 2001; Snyder & Civil Aeromedical Research, 1963).

Cory (2001) also investigated the effect of body orientation in a fall – “the amount of energy absorbed by an impact surface and other areas of the body dictate the amount of energy absorbed by the head” (Cory et al., 2001). Feet-first fall impacts with secondary impacts to the upper extremities and then the head absorb the impact energy differently than a fall with head-first impact. Head-first impacts are more likely to cause life-threatening brain injury than a feet-first fall. Body orientation can also affect the rotational acceleration of the head (i.e., whiplash; FIGURE 7).

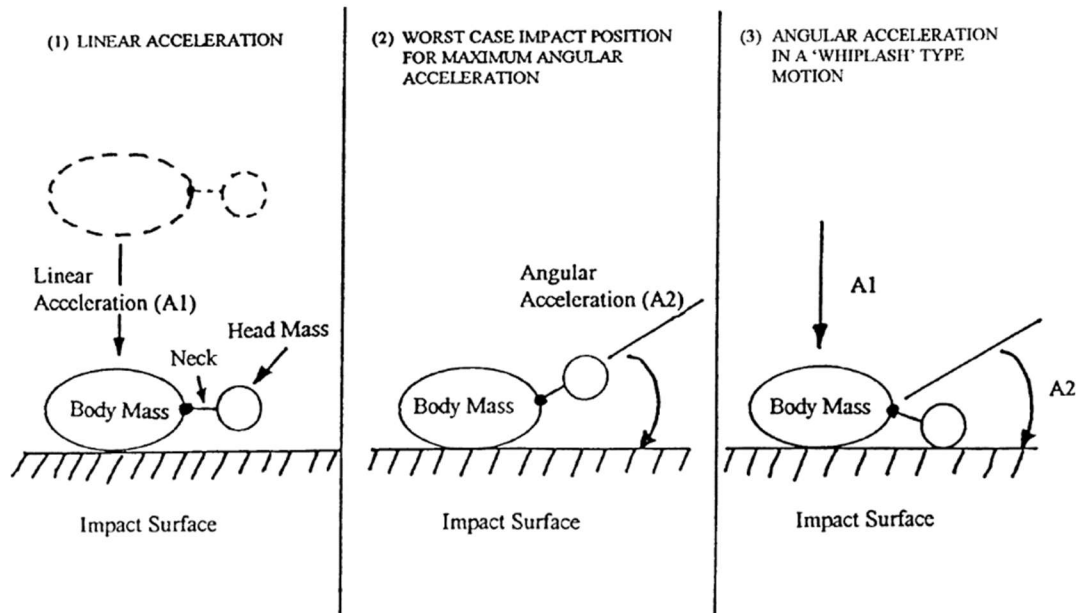


FIGURE 7 – Angular acceleration of the head due to whiplash (Cory et al., 2001)

## 2. Anthropomorphic test devices and short fall studies

According to Pierce et al. (2002), fall heights and impact surface material properties are the primary factors influencing free-fall injury severity. Impact surface has a role in the stopping distance of a falling mass. The fall victim's weight and impact landing position are also key to predicting free-fall outcome, which is why biofidelic ATDs are so important in event simulations: "Impact force, which is a function of body mass, fall height, and stopping distance, also is a critical factor in resultant free-fall injuries" (Pierce et al., 2002). Larger decelerations are correlated with greater injury severity, and the distribution of this force plays a key role in injury probability.

Hajiaghamemar et al. (2015) performed ATD standing falls onto hard surfaces to evaluate the kinematics of head impact. They used a 5<sup>th</sup> percentile female and 50<sup>th</sup> percentile male adult Hybrid III ATDs, which were dropped from a standing position (in

different postures). 107 trials of five fall scenarios were tested (backward falls with/without hip flexion, forward falls with/without knee flexion and lateral falls). The results were as follows: 95% prediction interval across all (n=107) falls for the peak translational acceleration, peak angular acceleration, peak force, impact translational velocity and peak angular velocity are 146–502 g, 8.8–43.3 krad/s<sup>2</sup>, 3.9–24.5 kN, 2.02–7.41 m/s, and 12.9–70.3 rad/s, respectively (Hajiaghmemar, Seidi, Ferguson, & Caccese, 2015). They determined that fall impact parameters depended on fall direction and type.

Bertocci et al. (2003) proposed that ATD testing of short distance falls in an isolated, controlled environment could be beneficial in the determination of the injury risk associated with them. They performed the tests by having the accelerometer-instrumented Hybrid II 3-year-old ATD fall out of a “bed” (elevated, horizontal surface) 3 times on four surface types (playground foam, carpet, linoleum, wood). They compared the calculated HIC<sub>15</sub> and HIC<sub>36</sub> values from linear acceleration data to the proposed National Highway Traffic Safety Administration (NHTSA) HIC value thresholds for Hybrid II 3-year-olds, and found that none of the test scenarios produced HIC values exceeding the injury thresholds (G. E. Bertocci et al., 2003). This study supported the hypothesis that short falls, even after a child has rolled out of a bed, are not enough to cause injury.

Bertocci et al. (2004) also studied feet-first models in a similar study, this time dropping the ATD from an elevated position onto the feet. Again, none of the test scenarios produced HIC values exceeding thresholds defined by the NHTSA. It was once again suggested that short falls would not cause significant injury to an infant or young child (Gina E. Bertocci et al., 2004). Because these studies used an ATD modeled after a

3-year-old, it is important to get biomechanical data for children younger than toddler age, as there is a paucity of these in the literature.

Coats et al. (2008) performed low-height falls using an instrumented anthropomorphic infant surrogate studies; they collected peak angular acceleration, change in peak-to-peak angular velocity, time duration associated with the change in velocity, and peak impact force for head-first drops onto a carpet pad or concrete. The drop heights ranged from 0.3 to 0.9m onto a mattress pad, carpet pad, and concrete. Drop height was found to not have a significant effect on head acceleration, but the stiffness of the surface was significant. They hypothesized that larger impact forces do have a higher likelihood of producing skull fracture (Coats & Margulies, 2008). They also noted the paucity of injury data related to angular acceleration, and that previous primate studies have noted that severity of concussion and diffuse axonal injury may be influenced by rotational direction.

Thompson et al. (2013) used an instrumented 12-month-old Child Restraint Air Bag Interaction (CRABI) ATD to evaluate injury potential in pediatric bed falls. The ATD was placed in an initial side-laying position on the edge of a 61 cm wooden platform representing a piece of furniture (bed, couch, etc.). A pneumatic actuator pushed the ATD off the platform, and five impact surfaces were tested – playground foam, padded carpet, wood, and two types of linoleum flooring (linoleum A and linoleum B). Peak resultant linear head accelerations were determined. This study resulted in a mean peak resultant linear head acceleration across all surfaces of 135.6 g (FIGURE 8) (A. Thompson, Bertocci, & Pierce, 2013).

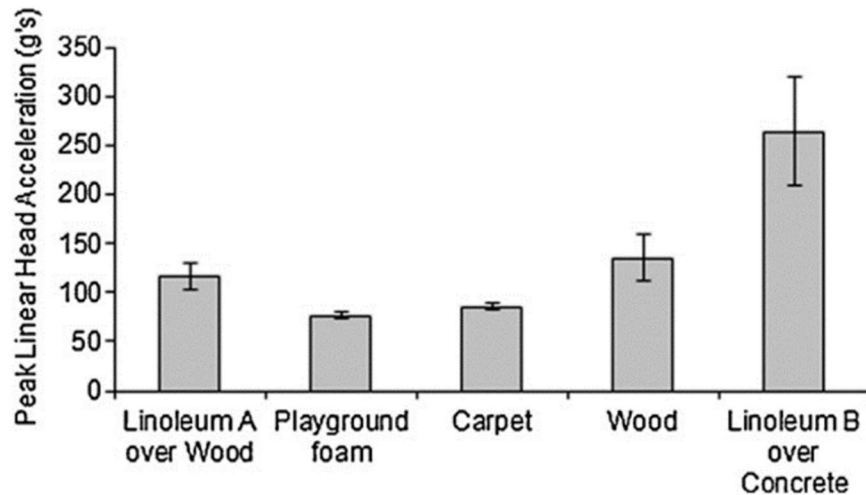


FIGURE 8 – Peak resultant linear head acceleration for falls onto various surfaces. error bars represent 95% confidence intervals (A. Thompson et al., 2013)

Thompson et al. (2013) also evaluated angular head accelerations by “differentiating the measured angular head velocities from the angular rate sensors” in the ATD (A. Thompson et al., 2013). Peak angular accelerations, peak change in angular velocity, and impact durations were determined for each fall trial (FIGURE 9). This study resulted in a mean peak angular head acceleration of  $3675 \text{ rad/s}^2$  in the anterior-posterior (AP) direction and  $6172 \text{ rad/s}^2$  in the medial-lateral (ML) direction, across all surfaces (A. Thompson et al., 2013). The greatest peak ML angular head acceleration was  $11,730 \text{ rad/s}^2$  where the impact surface was linoleum B over concrete. Head impact durations were reported to range from 2.7 to 19.1 ms with an average of 11.5 ms (FIGURE 10). Thompson et al. compared the results to published injury thresholds and concluded that the risk of severe head injury in these fall types onto most surfaces was low, but commented that there is the potential for concussion and possibly contact subdural



hematoma, particularly from falls onto surfaces such as linoleum tile over concrete (Thompson, 2013 (A. Thompson et al., 2013)).

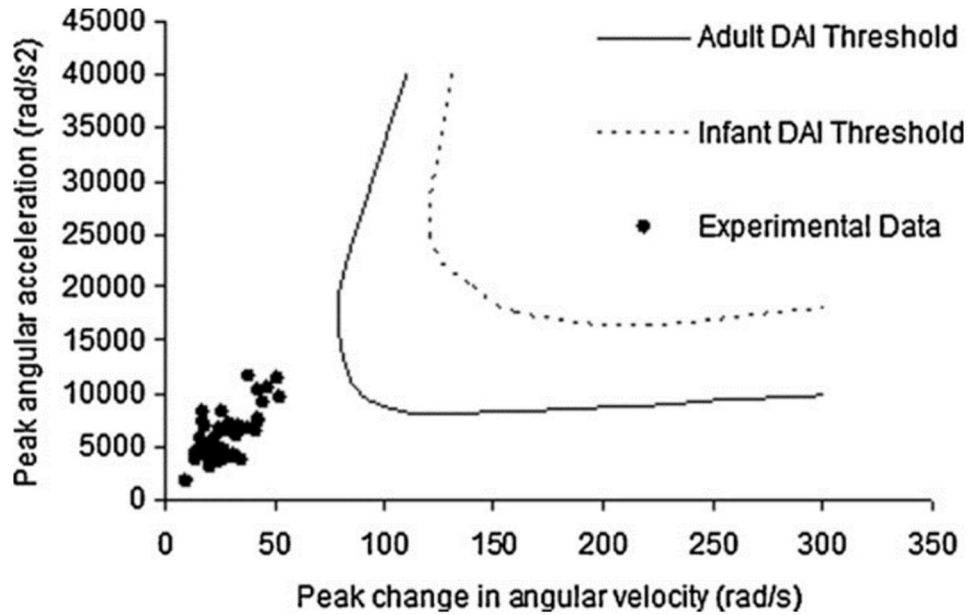


FIGURE 9 – Peak medial-lateral angular head accelerations and peak change in angular velocity; experimental data compared to thresholds for moderate to severe diffuse axonal injury (DAI) (Margulies & Thibault, 1992). Thresholds shown are for an infant and adult with 500g and 1067g brain mass, respectively (A. Thompson et al., 2013)

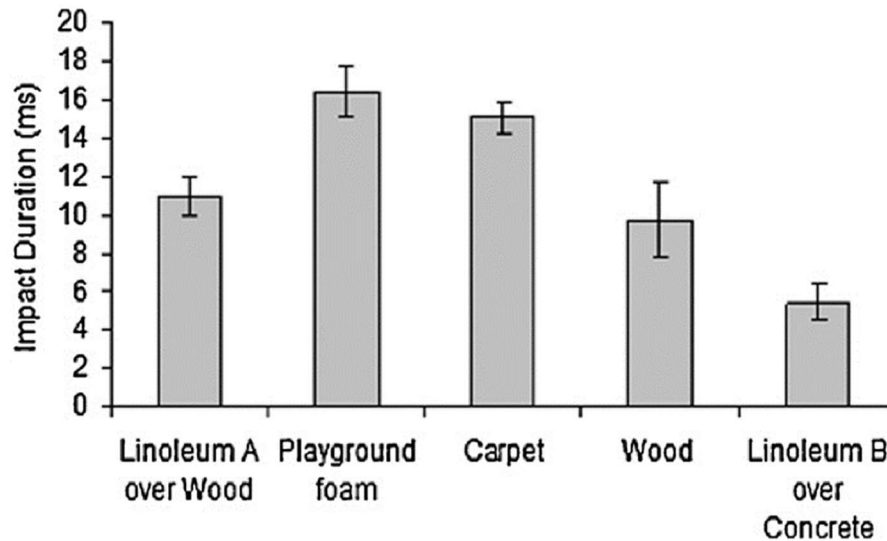


FIGURE 10 – Head impact durations for falls onto various surfaces. error bars represent 95% confidence intervals (A. Thompson et al., 2013)

Jenny et al. (2017) characterized head-neck kinematics associated with violent shaking of a child by simulating shaking events with an instrumented (triaxial accelerometers) ATD representing a 5<sup>th</sup> percentile Japanese newborn baby (Jenny, 2017). The shaking tests were performed in 3 to 4 second intervals. The study resulted in a mean peak angular accelerations in the sagittal plane within a range of 7035 rad/sec<sup>2</sup> to 10,379 rad/sec<sup>2</sup>; the maximum angular head acceleration across all shaking events was 13,260 rad/sec<sup>2</sup> (Jenny, Bertocci, Fukuda, Rangarajan, & Shams, 2017). These results were limited by surrogate biofidelity and highlighted the importance of improving ATDs to better represent real kinematics. This study addressed how experimental values have notably increased from previous studies with surrogates.

F. Development and application of injury thresholds from biomechanical fall data

Biomechanical data has been used to develop injury predictions and thresholds, and

to estimate head injury severity. The data types include linear head acceleration, rotational head acceleration, linear head velocity, rotational head velocity, and head injury criterion (HIC).

1. Thresholds based on linear acceleration and linear velocity

Focal type (direct impact) injuries are attributed to linear motion (acceleration/velocity). Often, the peak resultant linear head acceleration and peak resultant linear head velocity are evaluated to assess head injury tolerance limits for young children.

Gurdjian, Roberts, and Thomas (1966) used adult cadaveric heads to develop an acceleration-time-based tolerance curve for the human head (FIGURE 11). They found linear skull fracture occurred with an average linear acceleration of 112 g, with a peak of 200 g. Their tolerance curve indicated that “42g can be tolerated by a human head for many milliseconds to several seconds without serious injury” (Gurdjian, Roberts, & Thomas, 1966). The curve is interpreted as the values above the curve suggest a “danger to life” while values below the curve are “tolerable” (Cory, Jones, James, Leadbeatter, & Nokes, 2002). This tolerance curve would become known as the Wayne State Tolerance Curve (WSTC). The WSTC is limited, though, in that it was based on repeated post-mortem human subject drop tests where the impact site was only the forehead (Yoganandan, Stemper, Pintar, & Maiman, 2011).

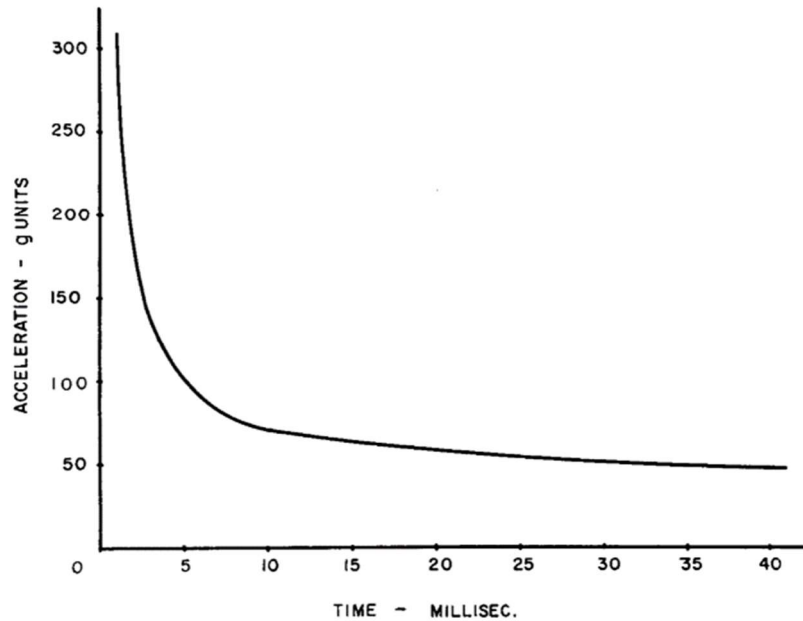


FIGURE 11 – Tolerance curve for human head (acceleration in gravity units, time in milliseconds) (Gurdjian et al., 1966)

In a review of published literature at the time, Stürtz (1980) found that children between 3-6 years of age had a maximum skull tolerance of 44-74 g in the anterior-posterior direction of the skull and 37-58 g in the medial-lateral direction of the skull. However, these were estimations and did not account for changes with development from 3 to 6 years of age.

Cory et al. (2001) discussed using peak linear head acceleration values as a means for assessment of head injury potential, where maximum recorded linear acceleration values during an impact event are related to a higher probability of injury. One limitation of this method is that it does not consider impact duration (Cory et al., 2001). Also, there are varying peak values that are considered the tolerance limits for children – one conservative estimate was reported to be 150-200g average acceleration for 3 ms in head-

first pediatric falls (Cory et al., 2001). Cory also reported the following: “Reichelderfer et al., referring to studies performed by the Franklin Institute Research Laboratories in Philadelphia at the behest of the Consumer Product Safety Commission (CPSC), suggested that ‘the maximal acceptable impact level was 50g; beyond this, serious injury begins to occur when a child’s [age not specified] head is dropped in a free-fall”” (Cory et al., 2001; Reichelderfer, Overbach, & Greensher, 1979). Overall, the literature generally accepts that peak linear acceleration values from 50 to 150g results in a small risk of head injury, peak linear acceleration values from 150 to 200g result in a definite risk of head injury, and above 200 g there is a “grave” risk for head injury (Cory 2001).

Much of the literature reviewed typically utilized the Head Injury Criterion, or HIC, scores as an assessment of injury potential resulting from the defined injury mechanisms (G. E. Bertocci et al., 2003; Gina E. Bertocci et al., 2004; Cory et al., 2001; Dufek et al., 2018; Forero Rueda & Gilchrist, 2009; Hajiaghamemar et al., 2015; Hughes et al., 2016). HIC is defined using equation 3.

$$HIC = \max \left[ (t_2 - t_1) \left[ \left( \frac{1}{t_2 - t_1} \right) \int_{t_1}^{t_2} a(t) dt \right]^{2.5} \right] \quad (3)$$

where  $(t_2 - t_1)$  is the sliding window in ms and  $a(t)$  is the resultant rotational head acceleration (g). The sliding window may be 36 ms ( $HIC_{36}$ ) or 15 ms ( $HIC_{15}$ ).

Dufek et al. (2018) found that pediatric falls with head-to-floor impacts have the greatest potential for injury. This study reviewed anthropomorphic and biomechanical components of patient falls from 26 children’s hospitals throughout the US and calculated the  $HIC_{15}$ . The study found a sample of 49 falls from heights of 72.5 to 1793.0 cm by

children ages 11 months through 17 years. Linear velocity from beginning to end was 2.81 to 6.16 m/s, and the mean linear acceleration was 19.5 to 95.3g. HIC<sub>15</sub> levels of impact ranged from 26.4 to 1,330.0, and seven children's HIC<sub>15</sub> levels exceeded age-specific thresholds. Their noted limitation was that exact determination of the mechanisms of brain injury may be difficult to establish due to the paucity of directly measured outcomes from the event. They concluded that the greatest HIC<sub>15</sub> values were from the greatest fall time durations and amount of force generated due to the gravitational acceleration over the longer time duration (Dufek et al., 2018). The researchers also presented the following HIC<sub>15</sub> thresholds for children: <1 year of age is 225; 1 to 2 years of age is 390; >2 to 5 years is 570 (Dufek et al., 2018). While the use of HIC is appropriate in contact-type injuries, the application of HIC is limited in that it is not an accurate representation of head injury potential following a rotational acceleration event (Gina E. Bertocci et al., 2004).

## 2. Thresholds based on rotational acceleration and rotational velocity

Rotational forces (and angular acceleration) cause shearing strain on the brain, and this is responsible for both superficial cortical injury and deep lesions in the brain (which can lead to concussions, coma). Furthermore, shearing forces are exaggerated along the interface of different brain density areas (junctions of gray and white matter, junction of corpus callosum, centrum semiovale) (Bagnato & Feldman, 1989). Ommaya et al. (2002) described rotational motion as being produced by the moment of a force about the center of gravity, or that by a "couple", two equal, parallel, oppositely-directed forces whose 'line of action are distinct' (Ommaya, Goldsmith, & Thibault, 2002). They discussed that rotation produces differential displacements of adjacent spherical brain layers due to

outwardly increasing translational velocity with respect to the axis of rotation (occipital condyles or base of the neck). This results in “shearing of the tissue, the cause of diffuse axonal injury (DAI) and various forms of vascular disruption” (Ommaya et al., 2002). The researchers referred to a previous study where animal models (live rhesus monkeys) were subjected to head impact and whiplash injuries to obtain injury tolerance thresholds for cerebral concussion (A. K. Ommaya & Hirsch, 1971). This study resulted in injury thresholds for the monkeys, and these thresholds were limited in that they were then scaled to human adult, young child, and neonate injury thresholds (FIGURE 12). They found that injury threshold value for a concussion in an infant approaches  $10,000 \text{ rad/s}^2$ , and for severe DAI it was just below  $40,000 \text{ rad/s}^2$ ; the reported time intervals were 10 ms (Ommaya et al., 2002). Margulies and Thibault also investigated the injury thresholds for DAI, and used primate experiments and scaling of brain mass to develop an injury tolerance curve based on peak change in rotational velocity and peak rotational acceleration (FIGURE 13) (Margulies & Thibault, 1992).

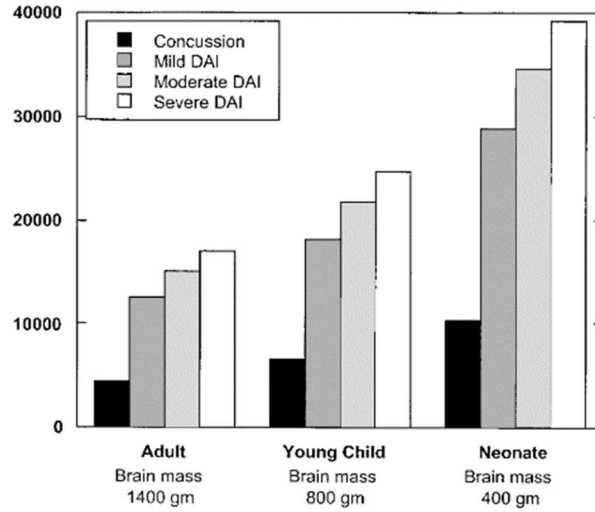


FIGURE 12 – Brain injury tolerance scaling in the adult, young child, and neonate (Ommaya et al., 2002)

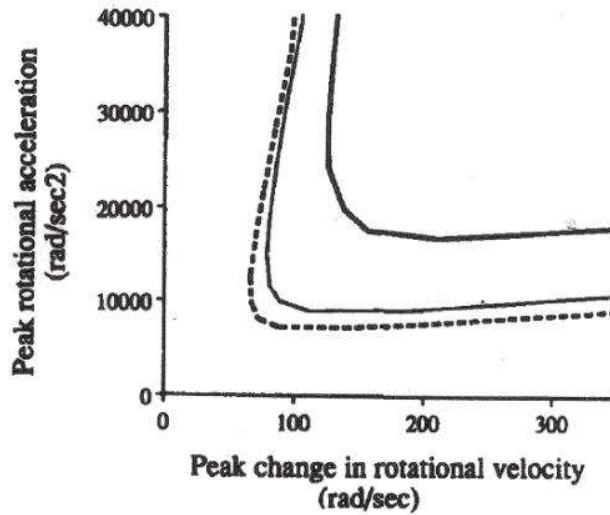


FIGURE 13 – DAI threshold developed from scaled brain mass; regions to the upper right of each curve represent injury Margulies (Margulies & Thibault, 1992). Thresholds shown are for an infant brain mass of 500 g (heavy solid line), adult brain mass of 1067 g (solid line), and primate brain mass of 1400 g (dashed line)



## G. Wearable accelerometers and the assessment of head impact biomechanics

### 1. Importance of reviewing video footage when subjects are equipped with biometric sensors

Cortes et al. investigated the utilization of video analysis to verify head impact events recorded by wearable sensors. This was a prospective cohort study with thirty male participants ( $16.6 \pm 1.2$  years) and 35 female participants ( $16.2 \pm 1.3$  years), who were high school lacrosse players. Female helmets were equipped with X-Patch triaxial accelerometer sensors, and male helmets were equipped with GForce Tracker sensors (triaxial accelerometers). The study recorded 3235 game-day head impacts that met or exceeded a 20g threshold. 690 game head impact events were verified via video analysis. The study concluded that 65% of all head impacts during the boys' games and 32% of all head impacts during the girls' games were verified to be true game play-related head impacts with by the video analysis. They suggested a high rate of false-positive impacts and an overestimation of verified head impact events by the wearable sensors, when they are not verified with video analysis (Cortes et al., 2017).

### 2. Wearable accelerometers and fall studies

Experiments with actual fall data are limited, and tend to focus on older populations and falls in a simulated environment, specifically for the development of a fall-detection algorithm to be used in elderly living homes that could immediately alert a nurse to a fall event (Kangas, Konttila, Lindgren, Winblad, & Jämsä, 2008). One of the only studies that was found that involved children equipped with a biometric sensor was one by Kakara et al. (2013). Researchers first developed a simulated daily living environment with the intention of children subjects replicating "natural human behaviors" to obtain

actual fall data. This environment was an ordinary apartment with couches, windows, desks, etc. and there were 12 cameras equipped in the room to capture unintentional falls from children subjects. They also used wearable acceleration-gyro sensors embedded in a vest that was worn on the subject's torso. Trials consisted of approximately 60-minute observation periods with a maximum of 2 participants per session. This study resulted in acceleration measurements collected from 19 children between 11 and 50 months. Data on 105 fall incidents were collected and videography was used in conjunction with the accelerometer data to eliminate false positives. They used this data to develop a fall motion database accessible online with information about each fall event, including child attributes (age, height, weight), fall characteristics (impact site, fall initiation, etc.), and fall dynamic data. They then used this information and the acceleration data collected from the wearable sensors to develop a MultiBody model (Kakara et al., 2013). Fall simulations using this model were used to calculate HIC, and HIC was used to assess severity of injury from impact. Biomechanical simulation was then used with finite element modeling to calculate the Mises stress from a reproduced impact of a head on an edge of a table. Kakara then used falls from their database with forward dynamics and modeled them in their MultiBody model. They simulated a head moving forward and assumed that the children failed to "defend themselves" during a fall. The model output a predicted HIC<sub>15</sub> (Head Injury Criteria) curve for the falls, and the authors concluded that life-threatening injuries were not likely to occur from simple forward-falling impacts. The paper did not go into detail regarding fall characteristics or acceleration values that were collected. Furthermore, the study was limited in that the environment for the children was simulated. However, they did conclude that computer models cannot fully

assess the risk of injury without actual fall data, and the addition of real biomechanical data will improve the accuracy of computational models (Kakara et al., 2013).

### 3. Wearable accelerometers in other applications

It is becoming increasingly popular for sports scientists to utilize the various resources available for measuring forces experienced in a game to analyze and mitigate the potential for head injuries players are exposed to. Andrew et al. (2017) studied impacts experienced by men (n=1063) and women (n=180; women's lacrosse is non-contact) lacrosse players who donned an accelerometer during gameplay for two seasons. Video footage was cross analyzed with the reported accelerometer impacts. 65% of the men's records and 32% of the women's were confirmed by the video footage (Andrew et al., 2017). It was determined that, while sensors offer valuable biomechanical information to the researchers, they can overestimate the number of significant impacts, so it is important to cross-analyze with a secondary impact detector, such as the videos, to decrease the amount of false-positives recorded. Other studies include the evaluation of hockey players via helmet-based instrumentation (Allison, Kang, Maltese, Bolte, & Arbogast, 2015; Wilcox et al., 2014); the evaluation of head impacts during collegiate football games with a standard football helmet equipped with the Head Impact Telemetry accelerometer system (Crisco et al., 2011); and the evaluation of head impacts during a youth soccer game with subject equipped with an X-Patch, a triaxial device that measured head accelerations (Chrisman et al., 2016).

## H. Pediatric short distance fall assessment in childcare setting and/or on a playground

Previous fall studies involving young children have been mostly performed via retrospective and clinical analysis, ATD testing, and computer modeling (N. G. Ibrahim & Margulies, 2010). There is a gap in the literature regarding human subject studies related to short distance falls in children. Chadwick et al. (2008) previously suggested using childcare sites for epidemiological, observational, and biomechanical studies because short distance falls on a variety of surfaces are quite common.

### 1. Previous study involving video-recorded falls in a childcare setting

Hilt performed a pilot study to characterize biomechanical measures and to examine differences in biomechanical measures based on child and fall characteristics in reliable witnessed video-recorded falls involving children equipped with a biomechanical measuring device. Video surveillance in the childcare center was used to capture fall dynamics and to provide reliable witnessed falls. A SIM G biomechanical sensor was used to measure and record linear and rotational head acceleration, linear and rotational head velocity, impact duration, and HIC (15). Whole-body impact biomechanics for each fall event were estimated including whole-body impact velocity, change impact momentum, and potential energy. The study resulted in 102 video-recorded falls with SIM G head biomechanical data; 19 subjects were involved (mean age 20.42 months). The mean biomechanical measures were obtained (TABLE 1).

TABLE 1

MEAN BIOMECHANICAL MEASURES OBTAINED IN HILT, 2018

<b>Biomechanical measure</b>	<b>Mean ± SD</b>
<b>Mean Peak Linear Head Acceleration (g)</b>	17.0 ± 5.5
<b>Mean Peak Rotational Head Acceleration (rad/s<sup>2</sup>)</b>	1820 ± 1019
<b>Mean Peak Linear Head Velocity (m/s)</b>	2.1 ± 0.7
<b>Mean Peak Rotational Head Velocity (rad/s)</b>	9.8 ± 4.5
<b>Mean HIC (15)</b>	8.3 ± 5.1
<b>Mean Impact Duration (ms)</b>	21.0 ± 6.3
<b>Mean Whole-body Impact Velocity (m/s)</b>	2.4 ± 0.5
<b>Mean Whole-body change in impact momentum (kgm/s)</b>	43.1 ± 10.8
<b>Mean whole-body potential energy (Nm)</b>	36.1 ± 16.2

There was no significant difference between child age and the calculated biomechanical measures, the child mass and all calculated measures, and no significant difference when the age and mass were considered together for any of the calculated measures. Fall characteristics and whether their effects had a significant impact on biomechanical measures were also analyzed (TABLE 2). COR referred to the coefficient of restitution of the impact surface (the closer the value to 1 the closer the impact was to a perfectly elastic collision). Hilt concluded that video-recorded pediatric short-distance falls did not lead to head injuries in children [in a childcare setting] and that fall biomechanical measures were associated with a low likelihood of head injury risk. He also concluded that differences in biomechanical measures based on fall characteristics

suggests that fall characteristics must be considered in the evaluation of injury risk for a given fall (Hilt, 2018).

TABLE 2  
FALL CHARACTERISTICS AND THEIR EFFECT ON BIOMECHANICAL  
MEASURES FROM HILT, 2018

Biomechanical measure analyzed	Ground based vs. height effect	Head impact vs non-head impact effect	Low vs high COR effect
Mean peak resultant linear head acceleration (g)	No	Yes	Yes
Mean peak resultant linear head velocity (m/s)	No	Yes	No
Mean peak resultant rotational head acceleration (rad/s <sup>2</sup> )	No	Yes	No
Mean peak resultant rotational head velocity (rad/s)	No	No	No
Mean HIC <sub>15</sub>	No	No	Yes
Mean impact duration (ms)	No	Yes	No
Mean whole-body impact velocity (m/s)	Yes	No	Yes
Change in impact momentum (kgm/s)	Yes	No	Yes
Mean potential energy (Nm)	Yes	No	No

## 2. Injuries resulting from falls involving playground equipment

When studying childcare centers, an important location for assessing pediatric injuries is the playground, as there is a high potential for accidental injuries on the playground. Ono et al. (2019) investigated playground equipment-related head injuries in children younger than 15 years of age. This study resulted in hospital records for 42 children (median age of 5 years) who were treated for head injuries that involved a slide (47.6%), a swing (26.2%), a jungle gym (11.9%), monkey bars, iron bars, trampoline, and unspecified equipment in the other cases (14.3%) (Ono, Sase, Takasuna, & Tanaka, 2019). The injuries that were presented and treated included: contusions, skull fractures, concussions, acute epidural hematomas, acute subdural hematomas, and traumatic subarachnoid hemorrhages. Also, the playground presents the opportunity to investigate falls from height. Ono et al. found that fall heights ranged from 1.2 to 2.5 m (Ono, 2019). Additionally, playgrounds typically have a harder surface, such as concrete or rubber material (as opposed to indoor surfaces, which may be linoleum or carpet).

Briss et al. (1995) performed a telephone survey of 1740 preschools to determine how frequent falls in playgrounds occur. They used the weighted total of 89.2 medically-attained playground fall injuries to estimate about 2700 injuries per year in US Childcare centers (Briss, Sacks, Addiss, Kresnow, & O'Neil, 1995). While this study did not include injury types, it supports the idea that preschools are a good location for studying fall frequencies in normal daily activities of children. Additionally, it validates the study of playground injuries in addition to classroom activities. Lillis et al. (1997) also performed a retrospective study on playground injuries at childcare facilities in Canada between March 1990-July 1991 (these were reported from the ED at the Hospital for Sick

Children and the Children's Hospital Injury Research and Prevention Project). They found 289 reported injuries (mean age 5.9 years with 39% <5 years old): 28% were fractures, 24% were lacerations, and 14% were hematomas (unspecified). Children younger than 5 years old had a higher incidence of head and neck injuries (58%) than those older than 5 (32%). Additionally, for children younger than 5 years old, 29% of injuries occurred on a climbing apparatus, while 40% occurred on slides. There were no fatalities, and the overall hospitalization rate was 18%. 77% of those hospitalized had fractures. They concluded that while young children overall sustained more head injuries on playground equipment than older children, an overwhelming majority were minor (Lillis & Jaffe, 1997). Kotch et al. (1993) performed a retrospective study on children under 5 years old in New Zealand between 1979 and 1988 who were admitted to a hospital with injuries associated with playground equipment either at home (n=528) or childcare facility (n=145). The most common injuries were fractures, and the head was the most common body part. Only one death was reported, where a 2-year-old male fell from a swing and suffered a subdural hemorrhage. 65% of cases stayed in the hospital less than 3 days, and 98% of cases were considered "routine" without severe injury (Kotch, Chalmers, Langley, & Marshall, 1993). While playgrounds are a good location to obtain actual fall data involving children, it is not expected that severe injuries will result from playground falls.

Forero et al. (2009) evaluated the biomechanics of injuries associated with playground equipment using a MADYMO 6-year-old child rigid body model based on 50<sup>th</sup> percentile anthropometrics (this was a model previously designed and validated by van Hoof et al. (2003)). The model was applicable to complex impact scenarios because



it was designed to be multi-dimensional. Adult head contact characteristics from experimental values were scaled to a 6-year-old child (Forero Rueda & Gilchrist, 2009). They simulated playground fall impacts from a free fall height of 2.7 m onto turf, concrete, tarmac, and rubber surfaces and they simulated seven body impact orientations (relative to the ground, these included: lateral 45-degree impact (feet-first); lateral side impact; prone impact; supine impact; anterior 45-degree impact (feet-first); posterior 45-degree impact (feet-first); 90 degree feet-first [standing] impact). The results showed that HIC decreased substantially from concrete to rubber (35% decrease) or turf (82% decrease). The results also showed that impact orientation also had an effect on HIC, with the highest HIC values resulting from a prone impact and the lowest values resulting from a posterior 45 degree (relative to the ground where feet impact first) impact (Forero Rueda & Gilchrist, 2009). This model was limited in that it could not guarantee biofidelity due to the head characteristics being based on scaled values; furthermore, the muscles and limbs of the model were “relaxed and loose” during the simulated impact, while humans tend to tense and activate muscles prior to impact (Forero Rueda & Gilchrist, 2009). The researchers noted that, “Computer reconstructions of actual falls that are intended to quantify the severity of physical injuries rely on accurate knowledge of initial conditions prior to falling, intermediate kinematics of the fall and the orientation of the body when it impacts against the ground” (Forero Rueda & Gilchrist, 2009). Having actual fall data from children may help improve the robustness of computer models.

## I. Current takeaways and gaps in the literature

1. Most researchers agree that short distance falls in the home and on playgrounds are not severe enough to cause significant injury, especially the kinds of injuries typically observed in abusive head cases.
2. Many studies have used HIC and linear motion measurements in injury assessment, but there is a lack of rotational motion injury assessment, specifically in injury assessment involving children.
3. Rotational accelerations play a very important role in injury mechanisms, but there is a paucity in measured rotational acceleration data from actual falls involving human children.
4. Having biomechanical measures from actual falls involving human children will help computational models become more accurate.
5. While wearable accelerometers are useful in identifying impacts, video recorded fall events are important in conjunction with these to eliminate false positives.
6. Only two studies involving children wearing accelerometers in their normal, everyday activities were found (Hilt, 2018). One of these studies involved a simulated environment (Kakara et al., 2013), and there is a paucity in “actual” fall data.

### III. SPECIFIC AIMS

The most common false history provided for a child presenting with injuries where the caregiver is concealing abuse is a fall. Falls accounted for an estimated 14.8 million nonfatal Emergency Department (ED) visits between 2001-2018 for children ages 0 to 3 years old (CDC, 2020). Benign, short-distance falls are very common in young children, but it is generally accepted that these rarely cause injuries; when injuries do occur, they are usually benign. However, there is a significant lack of reliably witnessed falls with known injury outcomes.

This prospective observational study characterized witnessed short-distance fall events and known outcomes. A childcare center was equipped with multiple video cameras and children between 1-3 years of age were monitored for falls during their normal activities. Additionally, children were equipped with wearable biomechanical sensors and head acceleration data (linear and angular head acceleration and head velocity) was collected. This project was accomplished through the following aims:

**Specific aim 1: Characterize video-recorded short distance falls involving young children in a childcare setting.** Various factors of the falls (dynamics, fall type, etc.) were analyzed, furthering the understanding of how children fall and what types of injuries occur.

**Specific aim 2: Identify body regions most commonly contacted or impacted during falls involving young children in a childcare setting.** Contacted/impacted body regions were analyzed and projected onto a representative child body map as a visual aid to identify the most commonly contacted/impacted body regions during these short-distance falls.

**Specific aim 3: Characterize the biomechanics of falls involving young children in a childcare setting by fall characteristics.** Falls with biomechanical data from the wearable devices were characterized for falls with and without head impact. A lumped mass, a single-link, and an inverted pendulum mathematical physics-based model were developed. These models were applied to replicated feet-first fall experiments with an anthropomorphic test device (ATD) as well as select childcare center falls with primary head impact and biomechanical data. Measured outcomes from the biometric sensor were compared to the outcomes from the physics-based models to determine their accuracy, as physics-based models are commonly used in forensics investigations.

*H1: Head accelerations and velocities will be greater in falls with head impact than falls without head impact.*

*H2: Lumped mass, single rod, and inverted pendulum physics-based models can accurately predict head biomechanical measures in common short-distance falls involving children.*

The study provided evidence-based data for reliably witnessed short-distance falls involving young children in a childcare setting. The evidence-based data from this project may assist in forensic investigations where child abuse is suspected but the mechanism of injury was reported to be a fall. This study may help investigators assess the biomechanical compatibility of a provided fall history, and it may further the differentiation between accidental and abusive injuries.

## IV. STUDY DESIGN AND METHODS

### A. Overview of study design and methodology

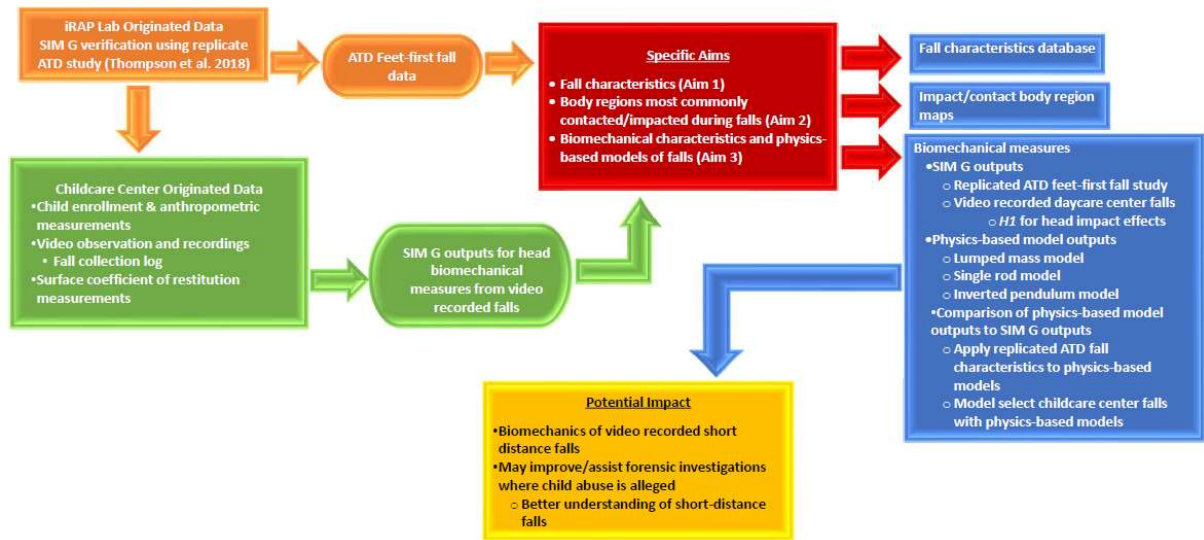


FIGURE 14 – Study design and methodology schematic

### B. Study design

The purpose of this study was to characterize video-recorded falls involving young children in a childcare setting. This study evaluated a subset of falls that were collected for a larger study. Four childcare classrooms and one playground were equipped with at least two digital video cameras each. The independent variables that were evaluated included fall characteristics such as whether the fall was from a height and what type of surface the subject impacted. Additionally, this study investigated the biomechanics associated with these short-distance falls, and the influence of fall characteristics on biomechanical measures (the dependent variables) were examined. To accomplish this,

children were equipped with biometric sensors embedded in a headband. The subjects were observed to record any falls and the observation period were video recorded. The video was reviewed to assess fall characteristics and to record falls that were missed during the observation period. Head biomechanical measures were obtained from the biometric sensors and the video recordings provided detailed fall dynamics. The study was approved by the University of Louisville IRB #16.1030.

1. Inclusion/exclusion criteria

This study included both male and female subjects between the ages of 12 months to 35 months (less than 3 years of age). Subjects participated in their normal activities in video-monitored classrooms and on the outdoor playground located in Bluegrass Academy Childcare Center (BACC) in Louisville, Kentucky. Caregiver written informed consent was obtained for participation. Once a subject exceeded 35 months, this child was no longer eligible for data collection. There were 4 classrooms that were equipped with video cameras. Two classrooms had children approximately 12 to 23 months of age and the other 2 had children 24-35 months of age. Subjects with musculoskeletal disorders or a disease that impeded their mobility, as well as those with a known metabolic bone disease or a bleeding disorder, were excluded from the study.

2. Fall monitoring duration and sample size

Data was collected at BACC over 2-hour periods conducted approximately 3 times per week. The observational periods included video monitored playground times for all classrooms. Fall events that were captured on video were extracted from the recordings and used for analysis. Data was collected from July 2018 through July 2019 and the first 100 video-recorded falls were obtained and analyzed for this study.

## C. Data collection

### 1. Anthropometrics

Once written informed consent was received from each subject's caregiver, anthropometric measurements of each subject were recorded. Measurements included: child's mass, head circumference, child's height, shoulder breadth, hip breadth, chin to sole length, hip to sole length, knee to sole length, and chest depth. For the child's mass, a Baby and Toddler Scale (Health o meter, McCook, Illinois) was used and the mass was recorded in kilograms. Length/height measurements were determined with a Hopkins Road Rod Portable Stadiometer (Hopkins Medical Products, Caledonia, Michigan) and were recorded in centimeters. Height measurements were recorded to the nearest 0.1 cm; chin to sole, hip to sole, and knee to sole lengths were recorded to the nearest 0.5 cm. For head circumference, a Gulick tape measure (Patterson Companies, Saint Paul, Minnesota) was used. The tape measure was wrapped around the widest circumference of the subject's head, just above the supraorbital ridge and above the superior aspect of the ears to the most prominent aspect of the posterior (occipital) head. These measurements were recorded to the nearest 0.1 cm. Shoulder breadth, hip breadth, and chest depth were measured with breadth calipers (Baseline, White Plains, New York) and were recorded to the nearest 0.1 cm.

### 2. Video monitoring

Digital video cameras were installed in each monitored location and in the outdoor playground area. Three classrooms were equipped with three cameras, and one classroom was equipped with four cameras due to its larger size. The playground was equipped with two cameras. There was a total of 15 cameras throughout the BGCC. In every

classroom/playground, cameras were placed at multiple locations and angles to ensure that the entirety of the space was visualized and so that all falls were recorded. The wall-mounted cameras (Lorex Technology, Markham, Canada) recorded at 1080p and 30 frames per second. All cameras transmitted to a network video recording (NVR) system (Lorex Technology, Markham, Canada) located in an isolated closet in BGCC.

### 3. Impact surfaces and coefficients of restitution

Impact surface was an important factor in the study. To analyze how an impact surface may affect the biomechanical outcomes of a fall, the coefficient of restitution (COR) of each impact surface was determined. The higher the COR, the closer the impact was to a perfectly elastic collision (usually varying between 0 and 1).

#### a. Impact surface and coefficients of restitution methods

To obtain the COR for each impact surface, a resiliency tester was used (IDM Instruments, Victoria, Australia) (FIGURE 15).

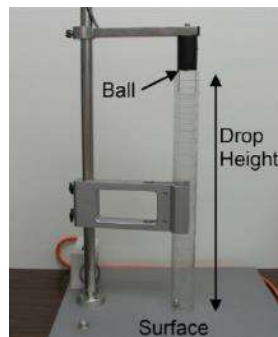


FIGURE 15 – COR Resiliency tester

To determine the COR, a small stainless-steel ball was dropped from a known height onto the evaluated impact surface. COR was calculated using equation 4.



$$COR = \sqrt{\frac{h_f}{h_i}} \quad (4)$$

where  $h_f$  was the final height of the ball after the first bounce from the impact surface (cm) and  $h_i$  was the initial height of the steel ball in the tube before it was released (cm). To obtain initial height and final height, each trial was video recorded using a HERO4 Silver camera (GoPro, San Mateo, California) recording at 240 frames per second. The camera was positioned parallel to the ball drop tube. Three ball drop trials were performed per surface type. The COR values were obtained from each surface type in every classroom as well as the surfaces on the playground (e.g., linoleum, carpet over concrete, playground mulch, etc.). This also included furniture surfaces and play equipment surfaces (e.g., carpeted stairs, plastic slide, butterfly bridge, etc.).

b. Impact surface and coefficient of restitution data analysis

The average COR value of the three trials was determined. Means and standard deviations were reported.

4. SIM G/SKYi System and biomechanical measure recordings

a. SIM G/SKYi System Methods

Each subject was assigned a triaxial accelerometer-gyroscope Smart Impact Monitoring (SIM G) device (Triax Technologies, Norwalk, Connecticut). These devices were inserted into a soft headband worn snugly around each subject's head. An appropriate headband size was chosen for each subject based off their individual head

circumference measurement. The headband sizes and circumferences were small (43 cm), medium (47 cm), and large (51 cm). The SIM G weighed 0.34 oz and measured 2.54 cm x 3.38 cm x 0.74 cm with an 8.4 cm antenna. The SIM G was inserted into a sleeve on the inside of the headband (FIGURE 16 (A), FIGURE 16 (B), FIGURE 16 (C)). The headbands were positioned so that the SIM G rested on the posterior head at the base of the skull in the occipital region (FIGURE 16 (D)). The blue logo of the Triax™ logo always faced upward while the green logo pointed toward the ground. The elastic part of the headband was placed on the child's forehead near the hairline.

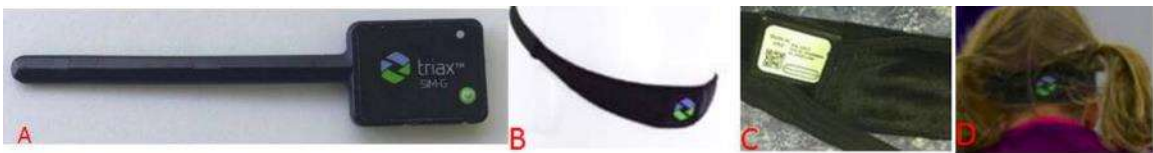


FIGURE 16 – (A) SIM G sensor; (B) Soft elastic headband; (C) SIM G inserted into posterior pouch on headband; (D) Child wearing headband with SIM G centered on occipital region of head

The SIM G collected data at 1,000 Hz and was activated when the resultant linear head acceleration was greater than or equal to 12 g during an impact. In other words, data from impacts with resultant linear head accelerations less than 12g was not recorded. Impacts were recorded for a total of 62 ms at the activation threshold; 10 ms was pre-trigger data and 52 ms was post-trigger data. When an impact met or exceeded the 12g threshold, the SIM G recorded triaxial (x, y, and z) data as well as the resultants for the following measurements: linear head acceleration (g), rotational head acceleration

( $\text{krad/s}^2$ ), and rotational head velocity ( $\text{rad/s}$ ). The SIM G also generated a 3D head model image that displayed head impact location (FIGURE 17).

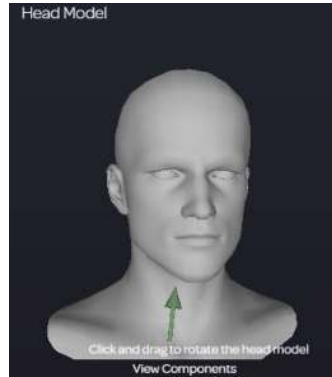


FIGURE 17 – Example of 3D head model showing a head impact at the right base of the chin

The SIM G data was transferred from the wearable device via a 900 MHz radio frequency to a SKYi aggregator receiver (FIGURE 18). The SKYi was placed in a central location within the childcare center during observation periods, and signals were transmitted to the SKYi up to 137 m. The SKYi was turned-on and programmed for each day's subset of subjects. Data was recorded in real time; onboard software processed and stored impacts that met or exceeded the threshold. These measurements were extracted to a Microsoft Excel file for post-observation processing.



FIGURE 18 – (A) SKYi aggregator receiver with power cord; (B) SIM G; (C) Headband

b. Verification of SIM G/SKYi system

The SKYi/SIM G system was tested and validated by comparing to head acceleration, velocity, and impact duration data from a previous anthropomorphic test device (ATD) fall study (A. Thompson, Bertocci, & Smalley, 2018). Feet-first falls were replicated from this study.

i. Previous fall experiment set-up

In Thompson et al.'s study, researchers examined femur loading and head acceleration in an infant during feet first falls using a 12-month-old Child Restraint Air Bag Interaction (CRABI) ATD (First Technology Safety Systems, Plymouth, Michigan). The ATD had onboard tri-axial head accelerometers (sampling rate of 10,000 Hz) and angular rate sensors, which were located at the center of mass of the ATD head. The previous study involved the ATD suspended from a rope attached to a release mechanism (bike brake), and the fall height in the previous study was 0.69 m. Fall height was measured

from the impact surface to the center of mass of the ATD. This fall height represented a child standing on a short (approx. 23 cm) stool (A. Thompson et al., 2018). Both surfaces were placed on a 1.83 m x 1.83 m wooden platform [1.9cm plywood covering 5.1 cm x 10.2 cm joists spaced 40.6 cm apart]. The padded carpet was 1.3 cm thick open loop over 0.32 cm thick padding; the linoleum tile was 1 mm thick self-adhesive no wax vinyl.

ii. Previous fall experiment data analysis and outcomes

Head acceleration data from the previous falls at 0.69 m onto padded carpet (n=13) and linoleum over wood (n=13) was obtained. In the previous study, the ATD was dropped feet-first onto two different impact surfaces (linoleum and carpet). X, y, and z linear head acceleration, anterior-posterior (AP) rotational head velocity, and medial-lateral (ML) rotational head velocity were measured in previous fall experiments. Rotational head acceleration was determined using equation 5.

$$\alpha = \left( \frac{\omega_f - \omega_i}{t_f - t_i} \right) \left( \frac{1}{1000} \right) \quad (5)$$

where  $\alpha$  is rotational head acceleration (krad/s<sup>2</sup>),  $\omega_f$  is the final rotational velocity (rad/s),  $\omega_i$  is the initial rotational velocity (rad/s),  $t_f$  is the final time (s), and  $t_i$  is the initial time (s) [dividing by 1000 converted the rotational acceleration to krad/s<sup>2</sup>]. The final and initial times were qualitatively obtained from the resultant linear head acceleration time history (an example showing how these times were determined is shown in FIGURE 19). The initial impact time was determined by qualitatively

identifying the time point on the graph where the peak acceleration began, and the final impact time was determined by qualitatively identifying the time point on the graph where the linear acceleration was no longer decreasing. The impact duration was calculated using equation 6.

$$\text{Impact Duration (ms)} = t_f - t_i \quad (6)$$

where  $t_f$  is the final impact duration time and  $t_i$  is the initial impact duration time.

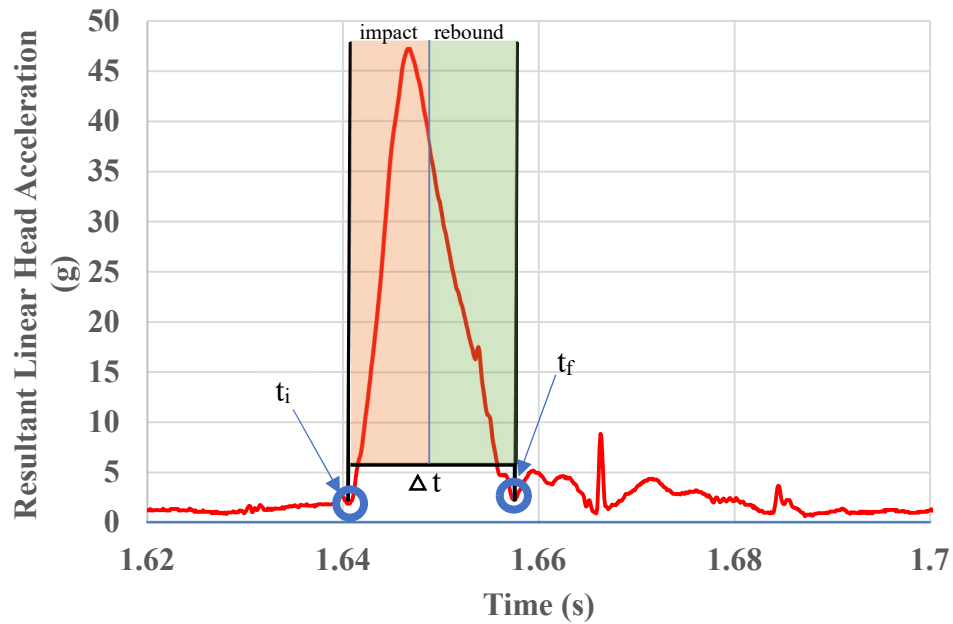


FIGURE 19 – Representative linear acceleration time history from ATD feet-first falls for determination of initial and final times associated with impact (where delta t is the full impact phase); orange shaded region is the impact of the head and green shaded region is the rebound of the head

Resultant linear head acceleration was determined using equation 7.

$$A_r = \sqrt{A_x^2 + A_y^2 + A_z^2} \quad (7)$$

where  $A_r$  is the resultant linear head acceleration (g),  $A_x$  is the linear head acceleration in the x direction (g),  $A_y$  is the linear head acceleration in the y direction, (g), and  $A_z$  is the linear head acceleration in the z direction (g). Resultant rotational head velocity was determined using equation 8.

$$\omega_r = \sqrt{\omega_{AP}^2 + \omega_{ML}^2} \quad (8)$$

where  $\omega_r$  is resultant rotational head velocity (rad/s),  $\omega_{AP}$  is anterior-posterior rotational head velocity (rad/s), and  $\omega_{ML}$  is medial-lateral rotational head velocity (rad/s).

Longitudinal rotation was not measured in the Thompson et al. study as it was expected to have a minimal effect on the resultant velocity. The linear head velocity along the x, y, and z axes (m/s) was calculated by numerical integration of the linear head acceleration using equation 9.

$$\text{Linear Head Velocity} = \int_{t_1}^{t_2} a(t)dt \quad (9)$$

where  $a(t)$  is linear head acceleration ( $m/s^2$ ), and  $t_1$  and  $t_2$  is based on the qualitatively determined impact duration. Finally, resultant rotational head acceleration was determined using equation 10.

$$\alpha_r = \sqrt{\alpha_{AP}^2 + \alpha_{ML}^2} \quad (10)$$

where  $\alpha_r$  is resultant rotational head acceleration ( $krad/s^2$ ),  $\alpha_{AP}$  is anterior-posterior rotational head acceleration ( $krad/s^2$ ), and  $\alpha_{ML}$  is medial-lateral rotational head acceleration ( $krad/s^2$ ).

### iii. Replicated fall experiment set-up and methods

The same CRABI ATD from the Thompson et al. study was equipped with a SIM G during falls. Feet-first falls were performed with the same set-up and impact surfaces used in the previous experiment (FIGURE 20).





FIGURE 20 – Experimental test set-up for 0.69 m fall to verify SIM G

A SIM G was placed into a headband, and the headband was positioned snugly on the head of the same 12-month-old CRABI ATD that was used in the Thompson et al. study. To protect the sensor during the ATD feet-first falls, the headband was positioned so that the SIM G was located on the anterior aspect (frontal skull) of the ATD head (FIGURE 21). This was a different orientation than was used on the human subjects, where the headband was positioned so that the SIM G was located on the posterior aspect of the head (occipital region).



FIGURE 21 –SIM G placement on 12-month-old CRABI ATD

A total of seven fall trials were performed on each surface. All replicated falls were video recorded with 2 HERO4 Silver GoPro cameras (GoPro, San Mateo, California). One camera was positioned to provide an anterior lateral view of the right side of the ATD (FIGURE 22A); the second camera was positioned on the ground to capture the left lateral view of the ATD (FIGURE 22B). The falls were recorded at 240 frames per second and allowed visual analysis of ATD fall dynamics. The cameras also allowed comparison with the previous ATD fall dynamics, which were recorded in the same manner.



FIGURE 22 – (A) Top-down right anterolateral view of ATD; (B) Left lateral view of ATD from the ground

iv. Replicated fall experiment outcomes

SIM G values that were recorded included triaxial linear head acceleration, triaxial rotational head acceleration, and triaxial rotational head velocity. The SIM G also reported each resultant for the linear head acceleration, rotational head acceleration, and rotational head velocity. This was calculated using equation 11.

$$Resultant = \sqrt{(x^2 + y^2 + z^2)} \quad (11)$$

where x, y, and z are the accelerations or velocities in the x, y, and z directions, respectively. The peak resultant linear head acceleration, peak resultant linear head velocity, peak resultant rotational head acceleration, and peak resultant rotational head velocity were determined. Additionally, impact duration was qualitatively determined (equation 6). Means and standard deviations were calculated.

v. Replicated fall experiment data comparison and statistical analysis

Replicated fall videos were reviewed for fall dynamics, and only fall trials with the same fall dynamics as those in the Thompson et al. study were compared. Replicated outcomes and previous outcomes were compared. Statistical analysis was performed in Minitab 19 (Minitab, LLC, State College, Pennsylvania) to determine if acceleration, velocity, and impact duration values from the SIM G were significantly different than outcomes from the Thompson et al. study using ATD onboard accelerometers. Data was checked for normality; if the data was normally distributed, then a two-sample t-test was conducted with a statistical significance set at  $p < 0.05$ . Means and 95% confidence intervals were reported. If the data was not normally distributed, a Mann-Whitney U-Test (non-parametric equivalent) was conducted with a statistical significance set at  $p < 0.05$ .

D. Childcare center procedures

1. Observation periods

Observation periods and data collection sessions were scheduled to monitor children while they were in their respective rooms. If weather permitted, observation periods also included a 30-minute playground session.

## 2. SIM G and SKYi system data collection

Based on the number of subjects present during the observation period, SIM G's (n=17) were assigned to those specific subjects. SIM G's were turned on and inserted into the assigned headband. The SIM G's were linked to the SKYi device. The SKYi time was synced with the NVR system at the beginning of each observation period to ensure that the times from the SIM G's were the same as the times in the video recordings. Time-synching also helped with associating a SIM G activation with a video recorded fall during post-observation review of the videos. Working with the teachers in the classrooms, the headbands were placed on each subject's head (FIGURE 23).

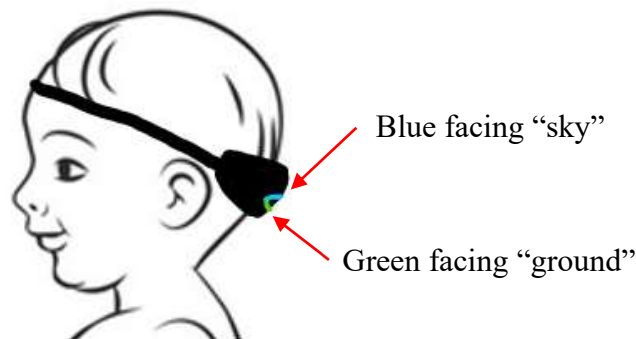


FIGURE 23 – SIM G placement on child subject's head

## 3. Video recording

A mirror drive storage device was connected to the NVR system located in the childcare. It generated a backup of all video monitoring during the observation period, so that video recordings could be reviewed during post-processing.

#### 4. Data collection log

Two observers were present during one session, one in each of two rooms monitored that day. Researchers monitored the children to ensure the headbands remained in place throughout the entire recording session. Researchers also recorded some fall characteristics and dynamics on a collection log (TABLE 3). Fall logs included the date of the observation period, room location (a new log sheet was made for observation periods on the playground), how many subjects were present during the observation period, the start time (operationalized as when the observer entered the classroom/playground), and the end time (operationalized as when the observer left the classroom/playground). This log supplemented post-observation processing by helping the researcher locate the fall in the video footage. The logs also provided more details to the events surrounding the fall and helpful identifiers (i.e., subject is wearing a blue shirt).

TABLE 3

CHILDCARE CENTER OBSERVATION LOG

Log field name	Operationalization
Impact time	Time of the witnessed fall
Subject ID	Unique identifier assigned at the time of the subject’s enrollment into the study
SIM G worn (y/n)	Circle yes or no if the subject was wearing their SIM G at the time of the fall
Fall type (circle)	Circle ground or height depending on whether the fall began with the child on the ground or from an elevated surface
Pre-fall condition (circle)	Circle running, standing, walking, pushed, other
Notes	Include explanation for “other” in pre-fall condition; include identifiers to aid in post-observation processing (such as the subject was wearing a yellow shirt; subject tripped over a ball)
Potential incident report (y/n)	Circle yes or no if an incident report was (or will be) filed by the childcare teacher as a result of the witnessed fall

5. Video review and data post-processing

A second NVR system was located at the Injury Risk Assessment and Prevention (iRAP) Laboratory at the University of Louisville. The video recordings were re-observed and reviewed after each observation period. All falls that occurred during the observation period, regardless of whether the team member in their respective classroom directly observed it, were located in the video footage, clipped, and stored for analysis.

The clipped videos were reviewed for fall time, and the videos were clipped to 10 seconds (which included 5 seconds pre-fall and 5 seconds post-fall). Additionally, falls that were missed on log sheets but found on video footage were added to the sample. Based on the fall time identified in the video footage, SIM G data was searched to identify corresponding SIM G activation(s). All clips were saved in a password-protected database.

E. Specific aim 1: Characterize video-recorded short distance falls involving young children in a childcare setting

1. Fall database and operationalization of data fields

The first 100 video-recorded falls collected from the larger childcare study were analyzed, regardless of whether a SIM G activation occurred during the fall. Each fall was characterized into its individual phases, and each database field referred to specific phases of the fall (TABLE 4). For classification purposes, and to characterize subjects by age and gender, the fall number, fall location (classroom or outdoor playground), subject ID number, and subject gender were recorded. An example of a characterization of a fall is provided in Appendix I.



TABLE 4

## OPERATIONALIZATION OF DATA FIELDS

Data field	Definition	Field options
<b>Fall ID</b>	Identification number assigned to the sequential fall event.	Numerical
<b>Classroom location</b>	The camera-equipped location in the childcare where the fall occurred.	Classroom 1; classroom 2; playground
<b>Subject ID</b>	Unique identification number assigned to each enrolled child.	Numerical
<b>Subject gender</b>	Gender of the enrolled child experiencing the fall event.	Male; female
<b>Fall description</b>	Full, detailed narration of all phases of the event, supplemented by fall log sheet and video recording.	Text field
<b>Initial condition</b>	Action/activity subject was performing prior to the fall being triggered.	Walking; running; standing; jumping; squatting; sitting; stepping; other [text field]

<b>Fall initiation</b>	The cause of the fall and the phase where the fall event began.	Loss of balance; tripped; slipped; pushed; other [text field]
<b>Fall type</b>	Judged visually; whether the fall began with the child on an elevated surface that was an appreciable distance from the impact surface height.	Ground; height; other [text field]
<b>Fall dynamics</b>	The direction(s) the subject moved during the fall.	Forward; rearward; left lateral; right lateral; feet first; headfirst
<b>Equipment/object involvement</b>	Whether an inanimate object(s) was involved during any phase of the fall.	Yes; no
<b>Type of equipment/object involved</b>	If yes for object(s) involvement, identify the object(s) involved.	Playground equipment; toy; classroom furniture; butterfly slide; pillow; container; carpeted steps; other [text field]
<b>Phase(s) of fall with equipment/object involvement</b>	If yes for object involvement, identify the phase(s) of the fall where	Initial condition; fall initiation; primary impact; secondary impact

	equipment/object was involved.	
<b>Another person(s) involvement</b>	Whether another person, not including the fall subject, was involved during any phase of the fall.	Yes; no
<b>Person(s) involved in the fall</b>	If yes for another person(s) involvement, identify the person(s) involved.	One other child; one adult; two other children; one other child and one adult; two other children and one adult; other [text field]
<b>Phase(s) of fall with another person(s) involvement</b>	If yes for another person(s) involvement, identify the phase(s) of the fall where another person(s) was involved.	Initial condition; fall initiation; primary impact; entire fall
<b>Head impact</b>	Whether the subject's head contacted any surface, item, person, etc. during any phase of the fall.	Yes; no; undetermined
<b>Primary impact surface</b>	The surface(s) on which the primary impact of the fall occurred.	Playground mulch; carpet; rug on carpet; linoleum; other [text field]

<p><b>First contact body region(s)</b></p>	<p>The phase of the fall where a body region(s) touched an impact surface after fall initiation; could be coincident with primary impact. Identify the body region(s) involved during this phase.</p>	<p>[Text field]</p>
<p><b>Primary impact body region(s)</b></p>	<p>The phase of the fall that was qualitatively judged to dissipate the most energy from the subject striking/forcibly coming into contact with a surface/object/person/etc. Identify the body region(s) involved during this phase.</p>	<p>[Text field]</p>
<p><b>Secondary impact body region(s)</b></p>	<p>The subsequent impact phase to primary impact. Fall events did not always include a secondary impact. Identify the body region(s) involved during this phase.</p>	<p>[Text field]</p>

<b>Body plane(s) impacted during primary impact</b>	The plane(s) of the body that struck a surface/object/person/etc. during the primary impact.	Anterior; posterior; left lateral; right lateral; left medial; right medial; Superior/inferior
<b>Final position</b>	The resting position/orientation of the subject at the end of the fall.	Sitting; lateral recumbent (right/left); on hands and knees; prone; on hands and feet; supine; other [text field]
<b>Equipped with SIM G</b>	Whether a subject was properly wearing a sensor during the fall event.	Yes; no
<b>Activation of SIM G</b>	Whether the SIM G was activated during the fall event.	Yes; no
<b>Injury outcomes</b>	Whether injury(s) was associated with the fall.	Yes; no
<b>Injury description</b>	Description of the injury(s) resulting from the fall. All incident reports of injury(s) related to the falls were collected from the childcare staff.	[Text field]

2. Equipment/object involvement operationalization

To evaluate how equipment or objects were involved in short distance falls, phases of the fall that involved at least one inanimate object were operationalized (TABLE 5).

Phases were limited to initial condition, fall initiation, primary impact, and secondary impact, as these phases were believed to be the most likely to have equipment or object involvement during a short distance fall.

TABLE 5  
TERMS OPERATIONALIZED FOR EQUIPMENT/OBJECT INVOLVEMENT IN  
THE FALLS

Phase	Criteria for object involvement in phase	Example
Initial condition	This phase of the fall was selected when the subject was interacting with any inanimate object prior to the fall being initiated, regardless of whether the object was involved in any other phase of the fall.	Subject was walking ( <b>initial condition</b> ) on the carpet while holding a ball in his right hand.
Fall initiation	This phase of the fall was selected when the fall was triggered by any inanimate object(s). This may or may not include the object from the initial condition, or it may be a completely different object.	The subject was walking on the carpet while carrying a ball ( <b>initial condition</b> ) and stubbed the toes of his left foot against the side of a toy bin; the subject tripped ( <b>fall initiation</b> ).
Primary impact	This phase of the fall was selected when an inanimate object was involved during the phase of the fall that was qualitatively judged to disperse the most energy from the subject striking the object. If a subject was holding onto an object during the initial condition and continued to hold onto it throughout the rest of the fall event, but the object had no effect during the primary impact, this phase was NOT selected.	The subject was walking on the carpet while carrying a ball ( <b>initial condition</b> ) and stubbed the toes of his left foot against the side of a toy bin, causing him to trip ( <b>fall initiation</b> ). The subject fell forward and impacted his left knee and shin on the toy bin ( <b>primary impact</b> ).
Secondary impact	This phase of the fall was selected when an inanimate object was involved in the subsequent phase to primary impact, when applicable. If a subject was holding onto an object during the initial condition and continued to hold onto it throughout the rest of the fall event, but the object did not have an effect during the secondary impact, this phase was NOT included.	The subject was walking on the carpet while carrying a ball ( <b>initial condition</b> ) and stubbed the toes of his left foot against the side of a toy bin, causing him to trip ( <b>fall initiation</b> ). The subject fell forward and impacted his left knee and shin on the toy bin ( <b>primary impact</b> ). The subject then fell forward and impacted his left hand and left posterior forearm against the edge of the toy bin ( <b>secondary impact</b> ).

3. Another person(s) (not including the fall subject) involvement operationalization

To evaluate how another person(s), not including the fall subject, was involved in short distance falls, phases of the fall that involved another person(s) were operationalized (TABLE 6). Phases were limited to initial condition, fall initiation, primary impact, and the entire fall, as these phases were believed to be the most likely to have another person(s) involved during a short distance fall.

TABLE 6

TERMS OPERATIONALIZED FOR ANOTHER PERSON(S)' INVOLVEMENT IN THE FALLS

Phase	Criteria for person(s)' involvement in phase	Example
Initial condition	This phase of the fall was selected when the subject was interacting with any person (teacher, other child, etc.) during the activity prior to fall trigger, regardless of whether the person was involved in any other phase of the fall.	Subject was walking on the linoleum and hugged another child ( <b>initial condition</b> ).
Fall initiation	This phase of the fall was selected when the fall was triggered by any person. This may or may not have included the person from the initial condition, or may have been a completely different person.	Subject was walking on the linoleum and hugged another child ( <b>initial condition</b> ). As the subject and child were hugging, they lost their balance ( <b>fall initiation</b> ) and fell laterally right.
Primary impact	This phase of the fall was selected when another person was involved when the subject struck an object, person, or surface with the greatest energy dissipation, judges qualitatively.	Subject was walking on the linoleum and hugged another child ( <b>initial condition</b> ). As the subject and child hugged, they lost their balance ( <b>fall initiation</b> ) and fell laterally right. The subject and other child impacted the linoleum, and the subject impacted her right lateral arm and right lateral leg ( <b>primary impact</b> ).
Entire fall	The entire fall was selected when another person was involved during all phases of the fall, from fall initiation to final position.	Subject was holding a teacher's hand and fell; he never released the teacher's hand during any phase of the fall ( <b>entire fall</b> ).

4. Specific aim 1 data analysis

From the database, each data field was analyzed to determine frequency. Descriptive statistics were performed on all outcome measures; means, standard deviations, and

frequencies were reported where appropriate. Not every field resulted in a mean or standard deviation calculation. Each fall was analyzed to determine how often an inanimate object was involved in each phase. Each fall was analyzed to determine how often another person(s) was involved in each phase

F. Specific aim 2: Identify body regions most commonly contacted/impacted during falls involving young children in a childcare setting.

1. Contact/impact operationalization

The following data fields were analyzed for frequencies: First contact body region(s); Primary impact body region(s); Secondary impact body region(s). Other impacts may have occurred, but they were not expected to have an influence on injury outcomes. The contact/impact terms were operationalized from the qualitative analysis of the recorded fall events (TABLE 7).



TABLE 7

OPERATIONALIZED DEFINITIONS FOR BODY REGION  
CONTACTED/IMPACTED

Term	Operationalized definition
<b>First contact body region(s)</b>	This was the first body region(s) to touch an impact surface after the fall initiation; it may have been coincident with primary impact. All body regions involved during first contact were counted.
<b>Primary impact body region(s)</b>	This was the body region(s) where the subject struck an object/person/surface/etc. after fall initiation with the greatest energy dissipation, judged qualitatively. All body regions involved were counted.
<b>Secondary impact body region(s)</b>	This was the body region(s) that was impacted subsequent to primary impact (judged qualitatively). Not every fall involved a secondary impact. All body regions involved were counted.

2. Determining body regions contacted/impacted

To determine body region(s) impacted, the body was divided into 11 major regions (TABLE 8). Upon reviewing each video-recorded fall, the body regions contacted/impacted during each phase of the fall were qualitatively determined.

TABLE 8

ALL BODY REGIONS INVOLVED IN THE FIRST CONTACT, PRIMARY IMPACT,  
AND SECONDARY IMPACT

Body region	Body subregions
<b>Head</b>	Face; anterior chin; lateral chin (left/right); base of chin; temple (left/right); superior parietal (left/right); occiput
<b>Anterior torso</b>	Anterior shoulder (left/right); full anterior torso; upper anterior torso; mid anterior torso; lower anterior torso; lateral anterior torso (left/right); pelvis; hip (left/right)
<b>Posterior torso</b>	Posterior shoulder (left/right); full posterior torso; upper posterior torso; mid posterior torso; lower posterior torso; lateral posterior torso (left/right); buttocks
<b>Right arm</b>	Full anterior arm; full posterior arm; upper anterior arm; upper posterior arm; anterior forearm; posterior forearm; full lateral arm; upper lateral arm; lateral forearm; full medial arm; upper medial arm; medial forearm
<b>Left arm</b>	Full anterior arm; full posterior arm; upper anterior arm; upper posterior arm; anterior forearm; posterior forearm; full lateral arm; upper lateral arm; lateral forearm; full medial arm; upper medial arm; medial forearm
<b>Right hand</b>	Right palm; right top of hand
<b>Left hand</b>	Left palm; left top of hand

<b>Right leg</b>	Full anterior leg; full posterior leg; anterior thigh; posterior thigh; anterior shin; posterior calf; full lateral leg; lateral thigh; lateral shin; full medial leg; medial thigh; medial shin; anterior knee; posterior knee
<b>Left leg</b>	Full anterior leg; full posterior leg; anterior thigh; posterior thigh; anterior shin; posterior calf; full lateral leg; lateral thigh; lateral shin; full medial leg; medial thigh; medial shin; anterior knee; posterior knee
<b>Right foot</b>	Top of foot; sole; lateral aspect of foot; medial aspect of foot
<b>Left foot</b>	Top of foot; sole; lateral aspect of foot; medial aspect of foot

### 3. Specific aim 2 data analysis

The frequencies of the different body regions involved were determined. Body region contact/impact maps were developed from these frequencies.

### 4. Body region contact/impact map

To best visualize body regions contacted/impacted, a body region map using a “heat map” concept was developed. Body regions on a human body map were edited to a color that corresponded to the frequency of contact/impact. To create the body contact/impact map, four views of an ungendered child were obtained and formatted in Microsoft PowerPoint software (PowerPoint for Office 365 MSO 64bit, Version 2002, Redmond, WA) (FIGURE 24). Body region masks were developed and overlaid onto the body with a color corresponding to the frequency of contact/impact on each view. Body region maps were generated for first contact, primary impact, and secondary impact.



FIGURE 24— Four views of child human body used in designing body region contact/impact maps

G. Specific aim 3: Characterize the biomechanics of falls involving young children in a childcare setting.

All biomechanical data from short distance falls with SIM G activations was collected. This biomechanical data was further analyzed for falls with and without head impact. Then, to investigate how accurate physics-based biomechanical models are to biomechanical data obtained from wearable SIM G devices, lumped mass, single rod, and inverted pendulum physics-based models were developed. The physics-based models were used to simulate the replicated ATD feet-first falls from the Thompson et al. (2018) study. Velocity and acceleration values from the physics-based models were compared to the SIM G measures from the replicated ATD study. Then, the physics-based models were used to simulate select childcare center falls with primary head impact (in other words, falls with impact to the head during the primary impact phase of the fall). Velocity and acceleration values were obtained from these models and compared to the select

childcare center falls that had both recorded SIM G measures and primary impact to the head. To select representative falls that had these criteria, the full fall dataset for the larger study was searched (unlike specific aim 1 and 2, the select falls were not limited to the first 100 falls from the dataset). These comparisons evaluated how useful physics-based models are in the evaluation of fall histories in forensic investigations.

#### 1. Falls with SIM G activation

Biomechanical data from falls where the SIM G device was triggered was extracted and reviewed with the video recordings. This verified the fall occurrence and removed any false positives from the dataset; previous studies have shown that head biosensors may overestimate the number of triggered events (Chrisman, 2015; Cortes, 2017).

SIM G data included linear head acceleration along the x, y, and z axes (g); rotational head acceleration along the x, y, and z axes (rad/s<sup>2</sup>); and rotational head velocity along the x, y, and z axes (rad/s). All SIM G data was timestamped. All data from the SIM G devices was exported to a Microsoft Excel file, and raw data was processed to calculate biomechanical outcome measures. The impact duration for the SIM G-triggered event was determined using the same methods that were used in the replicated ATD feet-first falls (equation 6). The linear head velocity along the x, y, and z axes (m/s) was calculated by numerical integration of the linear head acceleration using equation 12.

$$\text{Linear Head Velocity} = \int_{t_1}^{t_2} a(t)dt \quad (12)$$

where  $a(t)$  is linear head acceleration ( $m/s^2$ ), and  $t_1$  and  $t_2$  is based on the qualitatively determined impact duration (s). The resultant head accelerations and velocities were calculated using equation 13.

$$Resultant = \sqrt{(x^2 + y^2 + z^2)} \quad (13)$$

where  $x$ ,  $y$ , and  $z$  are the accelerations or velocities along the  $x$ ,  $y$ , and  $z$  axes, respectively. The peak value was determined for the resultant linear head acceleration, resultant rotational head acceleration, resultant linear head velocity, and resultant rotational head velocity. The Head Injury Criterion, or  $HIC_{15}$ , value was calculated using equation 14.

$$HIC_{15} = (t_2 - t_1) * \left[ \left( \frac{1}{t_2 - t_1} \right) * \int_{t_1}^{t_2} a(t) dt \right]^{2.5} \quad (14)$$

where  $(t_2 - t_1)$  is the sliding time window of 15 ms (0.015s) and  $a(t)$  is the resultant linear head acceleration (g).

## 2. Falls with SIM G activation data analysis

Biomechanical measures for each fall with verified SIM G data were reported. Mean head biomechanical measures and their standard deviations and ranges across all falls were also reported.

### 3. SIM G data analysis for head impacts

*H1: Head accelerations and velocities will be greater in falls with direct head impact than in falls without head impact.*

To test this hypothesis, videos were reviewed to determine whether head impact occurred during any phase of the fall. Head impact was operationalized as the subject's head impacting any surface, person, piece of furniture/equipment, etc. Furthermore, head impact was included for a fall when it occurred during any phase of the fall; it was not limited to the primary impact phase. Head impact was not considered if the head contacted the torso or tops of shoulders. For example, in fall 15, subject 4 fell forward and impacted his anterior bilateral shins and knees as well as the palms of both hands on the playground surface. His head rotated forward about the neck and his inferior chin may have contacted the anterior torso chest. The head only contacted the chest and was not visually judged to be a part of the impact sequence. This fall was counted in the "no head impact" category. The SIM G data for falls where head impact was determined to occur was reviewed to determine when the head impact occurred so that the proper corresponding peak on the head acceleration curve was selected for calculation of biomechanical outcomes. The data was checked for normality. If the data was normal, a two-sample t-test was used to test for significant difference in mean peak head accelerations and velocities between falls with and without head impact. A significance level of  $p < 0.05$  was used. Means, standard deviations, and 95% confidence intervals were reported. If the data was not normally distributed, a Mann-Whitney U-Test (non-parametric equivalent) was conducted with statistical significance set at  $p < 0.05$ .

4. Development of physics-based models for ATD feet-first falls and human subject childcare center falls with SIM G activation and primary head impact

*H2: Lumped mass, single rod, and inverted pendulum physics-based models can accurately predict head biomechanical measures in common short-distance falls involving children.*

To evaluate the accuracy and usefulness of physics-based models, three model types were selected to simulate both replicated ATD feet-first falls and select childcare center falls. These models included a lumped sum physics-based model, a single rod physics-based model, and an inverted pendulum physics-based model. The single rod and inverted pendulum models differed in their mass distribution and their moment of inertia. SIM G data from ATD feet-first falls (n=7 for linoleum impact surface and n=7 for carpet impact surface) was first compared by modeling these falls with the physics-based models. Then, a select subset of eight childcare center falls from the larger childcare center dataset with both SIM G data and primary head impact were modeled using physics-based models. Unlike the previously discussed hypothesis for falls with head impact versus those without head impact, the inclusion criteria for these select falls included head impact specifically during the primary impact phase of the fall. These model outcomes were then compared to the SIM G data. To test *H2*, the biomechanical outcomes from the physics-based models for both the replicated ATD feet-first falls and the simulated childcare center falls were compared to the respective SIM G outcomes (mean peak biomechanical measures from the replicated ATD falls and SIM G outputs from the childcare center falls); percent errors were calculated and categorized. Models with a percent error of 25% or less (in other words,  $0\% \leq \text{Percent error} \leq 25\%$ ) were



considered accurate, and it was assumed that more accurate models could accurately predict head biomechanical measures in common short distance falls.

a. ATD feet-first fall model known variables and assumptions

To model the replicated ATD feet-first falls, published impact surface characteristics were used. The replicated falls involved a carpet (n=7) and a linoleum (n=7) impact surface. The COR of each surface was obtained from the previous study using the same surfaces (Thompson et al 2009). Impact duration (ms) was based on the surface type as well, and published impact duration values were obtained (Thompson et al 2013). Anthropometric measurements of the 12-month-old CRABI ATD were obtained from a technical report published by the National Highway Traffic Safety Administration (NHTSA), including standing height (m), head height (m), neck length (m), etc. (Hagedorn & Pritz, 1999). Head center of mass (COM) was estimated to be half the head height (m). Analysis of the ATD falls began with the contact of the ATD soles on the impact surface, and any downward energy from the feet-first drop was assumed to not be converted into the rotational motion of the fall.

Additionally, it was unknown how the ATD biomechanical outcomes would differ by dynamic types. Following the methodology from the Thompson (2018) study, the video recordings of the replicated ATD feet-first falls onto carpet and linoleum were reviewed and categorized to each fall's respective dynamic type (TABLE 50, reproduced here). Mean peak ATD biomechanical outcomes from the physics-based models for each respective dynamic type were then compared to SIM G outcomes.

TABLE 50

DESCRIPTIONS OF ATD FALL DYNAMICS AND PREVIOUS FALL  
 FREQUENCIES (THOMPSON, 2018)

Nomenclature	Description
A	ATD fell to crouching position with hips and knees flexed; knees then extended while feet rotated forward from beneath torso as ATD pelvis continued to move downward. ATD landed in a seated position with knees fully extended before rotating rearward into a supine position or to one side (laterally).
B	ATD fell to crouching position with hips and knees flexed, left knee then extended while foot rotated forward from beneath torso, but right toes remained planted on the floor surface as ATD pelvis continued to move downward. ATD landed in a seated position (left knee extended, right knee flexed), torso then rotated rearward into a supine position.
C	ATD fell to crouching position with hips and knees flexed, heels then lifted off floor, while toes remained planted resulting in plantar flexion of ankles and rolling onto the dorsal surface of the foot as the ATD pelvis continued to move downward. Hips and knees extended after pelvis impact, launching ATD rearward to land in supine position.

b. Childcare center fall selection for physics-based models

To select the falls from the childcare center to be modeled with physics-based calculations, the dataset of short distance fall videos for the larger study was searched for falls that involved both SIM G activation and a head impact during the primary impact phase of the fall. These fall recordings were then reviewed, and falls were selected based on their complexity as well as the dynamics and planes impacted. Each fall recording was reviewed to determine where the fall analysis should begin. For example, fall 516 was reviewed. During the fall, the subject tripped, fell rearward, and contacted his buttocks on the impact surface. He then fell rearward and impacted his occiput on the carpeted flooring. Fall analysis was determined to begin at the point of contact of his buttocks on

the floor, and the fall height was the buttocks to head COM length (m). Anthropometric measurements and equipment/furniture measurements obtained during the study were used to estimate fall height in the video recordings.

c. Overview of methods for analyzing the childcare center and ATD physics-based models

To evaluate the three physics-based model types, four methods were chosen to calculate the expected physics-based outcomes. These four methods were chosen because it was not clear how the coefficient of restitution/rebound velocity of the head would affect biomechanical outcomes. It was expected that including COR/rebound velocity in the evaluation would lead to more accurate outcomes. To test this, four methods were used. Each method differed in the approach and what variables were included in the evaluation (TABLE 9). The different approaches were tested to determine if there was a more accurate starting point to obtaining the biomechanical outcomes (as compared to the SIM G outcomes). “Starting point” referred to the approach of the physics-based model. Methods A and B used the conservation of energy approach to calculate average head impact linear acceleration. Methods C and D set the force impulse equal to the momentum of the impact to determine average head impact linear acceleration. In methods B and C, surface properties, including coefficient of restitution and rebound velocity, were used in the analysis and assumed to influence the fall outcomes. The change in velocity was set as the difference between the impact velocity and the rebound velocity. Methods A and D were limited to only the crush phase of the impact (one-half the impact time duration), while methods B and C were analyzed over the entire pre-impact, impact, and post-impact phases of the fall (full impact time duration). See Figure

19 for a representative time history with defined impact time (including crush and rebound phases).

TABLE 9

METHODS USED TO EVALUATE THE PHYSICS-BASED MODELS

Method	Coefficient of restitution	Rebound Velocity	Starting Point	Phase <sup>1</sup>	Time duration
Method A	No	No	Conservation of energy	Crush phase only	½ Delta t
Method B	Yes	Yes	Conservation of energy	Crush and rebound phases	Delta t
Method C	Yes	Yes	Impulse set equal to momentum	Crush and rebound Phases	Delta t
Method D	No	No	Impulse set equal to momentum	Crush phase only	½ Delta t

<sup>1</sup>Phase of the fall referred to the primary head impact of the fall being evaluated; if only the crush phase was included, then rebound velocity was not included during evaluation; methods that evaluated crush and rebound phase included COR/rebound velocity.

d. Lumped mass physics-based model free body diagrams

i. Pre-fall initial conditions for lumped mass physics-based model

The lumped mass represented the mass of the whole body of the child/ATD (FIGURE 25). The lumped mass was assumed to free-fall under the force of gravity,  $g$ , where  $g$  is equal to  $9.81\text{m/s}^2$ . It was assumed that air resistance was negligible. The lumped mass modeled head accelerations and velocities at the head center of gravity. Head center of gravity height (m) was approximated to be half the head height of the respective subject/ATD head.

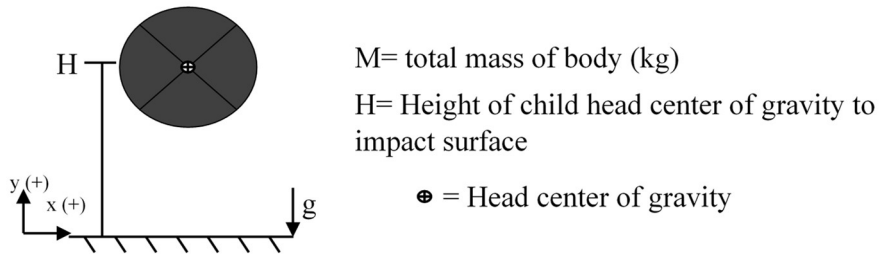


FIGURE 25 – Initial conditions for lumped mass physics-based model

ii. Free-fall of lumped mass physics-based model prior to impact

It was assumed that the lumped mass free-falls under the force of gravity (FIGURE 26).  $V_{\text{freefall\_CG}}$  (m/s) is the velocity of the lumped mass just prior to the impact.

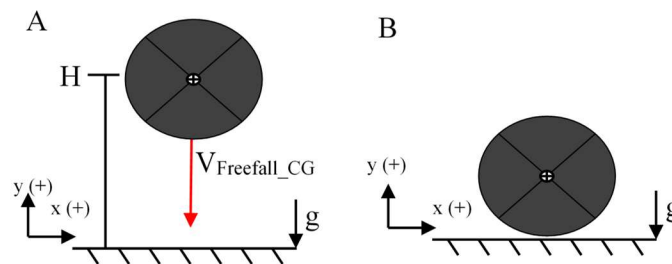


FIGURE 26 – Lumped mass just prior to impact

iii. Impact conditions for lumped mass physics-based model

The next figure demonstrates the impact phase and final resting phase of the lumped mass (FIGURE 27).

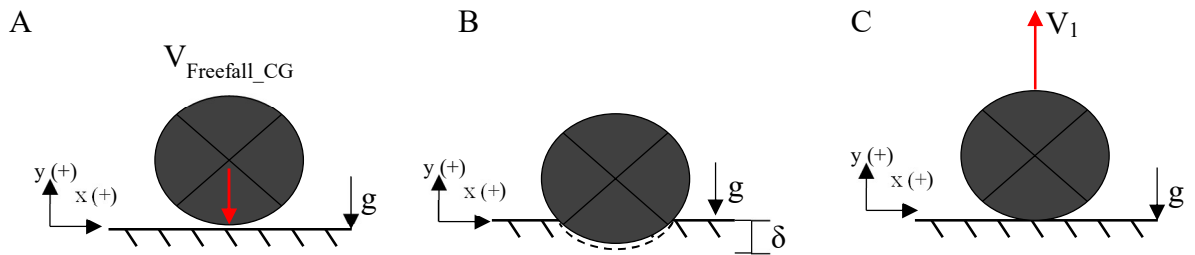


FIGURE 27 – (A) Lumped mass just prior to impact. (B) Lumped mass impacting the surface, where  $\delta$  is the surface deformation. (C) Lumped mass rebounding after the impact, where  $V_1$  is the rebound velocity of the mass before coming to rest.

e. Methods for analysis of lumped mass model

To evaluate the lumped mass models, four methods were used for each ATD/childcare center fall (TABLE 9).

i. Method A:

To calculate the free-fall velocity of the lumped mass just prior to impact, equation 15a was used.

$$(V_{freefall_{CG}})^2 = (V_o)^2 + 2 * a * H \quad (15a)$$

where  $V_{freefall_{CG}}$  (m/s) is the velocity of the lumped mass pass just prior to the impact,  $V_o$  is the initial downward velocity of the lumped mass (assumed to be 0 m/s; this was

assumed for all modeled falls), and  $a$  is gravitational acceleration ( $g$ ) equal to  $9.81 \text{ m/s}^2$ .

Rearranging equation 15a gives equation 15b.

$$V_{freefall_{CG}} = \sqrt{2 * g * H} \quad (15b)$$

To calculate the average linear acceleration of the impact head during impact, equation 16a was used.

$$a_{average} = \frac{\Delta v}{\Delta t} = \frac{v_{impact} - v_{rebound}}{\Delta t} \quad (16a)$$

where  $v_{impact}$  was equal to  $V_{freefall_{CG}}$  from equation 14, and the rebound velocity was found with equation 16b.

$$-v_{rebound} = COR * v_{impa} \quad (16b)$$

Equations 16a and 16b were combined and rearranged to produce equation 16c.

However, in this (method A) approach, it was assumed there was no rebound, so the rebound velocity was set to zero. The average linear impact acceleration was then calculated using equation 16c.

$$a_{average} = \frac{V_{freefall_{CG}}}{\Delta t} \quad (16c)$$

However, the SIM G device output the peak values for linear and rotational accelerations and velocities. To estimate the peak linear head acceleration, it was assumed that the linear acceleration curve was sinusoidal (Kuphaldt, 2001). This periodic wave was defined with equation 17.

$$a_{average} = a_{peak} * \sin(\theta t) \quad (17)$$

To calculate the average acceleration, the area under the curve was found with equation 18a where the average value is determined over one half a cycle (0 to  $\pi$ ).

$$a_{average} = \int_0^{\pi} a_{peak} * \sin(\theta * t) dt = \left(\frac{1}{\pi}\right) * (a_{peak}) * (-\cos(\pi) - (-\cos(0))) = \left(\frac{a_{peak}}{\pi}\right) * (2) \quad (18a)$$

where  $a_{average}$  is from equation 16. Simplifying and rearranging equation 18a produced equation 18b, which was used to determine peak linear head acceleration (g) during the impact.

$$a_{peak} = 1.57 * a_{average} \quad (18b)$$

To estimate the rotational velocity of the head COM during impact, it was assumed that the radius of rotation was equal to the neck length (from the head center of gravity to the base of the neck (m)) and equation 19 was used. For the purposes of these models, the radius of rotation was limited to neck length. However, to explore how radius length affected rotational outcomes, a parameter sensitivity analysis (PSA) was performed on all



outcomes after the initial model outcomes were obtained. The radius of rotation was varied, and the PSA started with the neck length and incrementally increased length, with the longest radius of rotation set as the length of the head center of gravity to sole length (m) (TABLE 10). Radius lengths for the replicated ATD falls were obtained from the CRABI ATD; radius lengths for the childcare center falls were obtained from subject anthropometric measurements. This PSA was performed for all physics-based model outcomes, for both the replicated ATD falls and the childcare center falls.

TABLE 10

RADIUS OF ROTATION LENGTHS FOR PARAMETER SENSITIVITY ANALYSIS

<b>Radius</b>	<b>Operationalization</b>
<b>About the neck</b>	From the head center of gravity to base of the neck (in line with the shoulders) length (m)
<b>About the hips</b>	From the head center of gravity to hip length (m)
<b>About the knees</b>	From the head center of center of gravity to the knees length (m)
<b>About the soles</b>	From the head center of gravity to the soles of the feet length (m)

For ATD replicated falls, neck length was obtained from the CRABI ATD. For childcare center falls, neck length was estimated to be approximately 12.7% of the full height of a child (Mahajan and Bharucha) [neck length could not be approximated from the anthropometric measurements].

$$\omega_{rotational} = \frac{V_{freefallCG}}{r_{neck}} \quad (19)$$

where  $\omega_{rotational}$  is the impact rotational velocity of the head about the neck (rad/s) and  $r_{neck}$  is the neck length (m). The neck length and  $a_{peak}$  from equation 18b were used to estimate the peak rotational acceleration using equation 20.

$$\alpha_{rotational} = \frac{a_{peak}}{r_{neck}} \quad (20)$$

where  $\alpha_{rotational}$  (rad/s<sup>2</sup>) is the impact rotational acceleration of the head about the neck and  $a_{peak}$  is the peak linear head acceleration (g) from equation 18b.

ii. Method B:

In method B, equations 15 and 16 were used again. However, for this approach, it was assumed that coefficient of restitution and rebound velocity did have an effect on the lumped mass during impact. Rather than setting COR equal to 0, equation 21a was used.

$$a_{impact} = \frac{\Delta v}{\Delta t} = \frac{v_{impact} - v_{rebound}}{\Delta t} = \frac{(V_{freefallCG} - (COR) * (-V_{FreefallCG}))}{\Delta t} \quad (21a)$$

where  $a_{impact}$  is the average linear head acceleration during impact. Equation 21a was further simplified to equation 21b.

$$a_{impact} = \frac{(V_{Freefall_{CG}}) * (COR + 1)}{\Delta t} \quad (21b)$$

Then, equation 18b was used to convert the result into peak linear head acceleration. Finally, to estimate the rotational velocity and rotational acceleration of the head COM during impact, it was assumed that the radius of rotation was equal to the neck length and equations 19 and 20 were used.

iii. Method C:

In method C, the approach to the analysis differed in that the starting point followed the impulse-momentum principle, which analyzed the force of the impact. Additionally, similar to method B, this method assumed that rebound velocity/COR had an effect during the impact. First, the impact velocity of the lumped mass was calculated by equating the impulse of the impact to the change in momentum using equation 22a.

$$F * \Delta t = m * \Delta v \quad (22a)$$

where F is the impact force (N),  $\Delta t$  is the impact time on the surface [from published values (s) for the replicated ATD falls and from SIM G impact duration from the childcare center falls], m is the mass of the lumped mass (kg), and  $\Delta v$  is the change in velocity using equation 16b, where  $V_{impact}$  is equal to  $V_{freefall\_CG}$  from equation 15 and  $V_{rebound}$  is the rebound from equation 16b. Rearranging equation 22a gave equation 22b.

$$F = \frac{m * (V_{Freefall_{CG}}) * (COR + 1)}{\Delta t} \quad (22b)$$

To determine the average linear impact acceleration, equation 23 was used.

$$a_{impact} = \frac{F_{impact}}{m} \quad (23)$$

where  $F_{impact}$  is the impact force (N),  $m$  (kg) is the mass of the lumped mass, and  $a_{impact}$  is the average linear impact acceleration ( $m/s^2$ ). Assuming that the force from the impulse is equal to the impact force, equation 22b was combined with equation 23 to obtain equation 24.

$$a_{impact} = \frac{(V_{freefall_{CG}}) * (COR + 1)}{\Delta t} \quad (24)$$

Then, equation 18b was used to convert the result into peak linear head acceleration.

Finally, to estimate the rotational velocity and rotational acceleration of the head COM during impact, it was assumed that the radius of rotation was equal to the neck length and equations 19 and 20 were used.

iv. Method D:

Method D followed the same procedures as method C; however, it was assumed that rebound velocity/COR had no effect on the head impact outcomes (as was assumed in

method A). Equation 24 was altered to reflect those assumptions; the coefficient of restitution was set to equal 0 and this produced equation 25.

$$a_{impact} = \frac{(V_{freefall_{CG}}) * (0 + 1)}{\Delta t} = \frac{V_{Freefall_{CG}}}{\Delta t} \quad (25)$$

Then, equation 18b was used to convert the result into peak linear head acceleration.

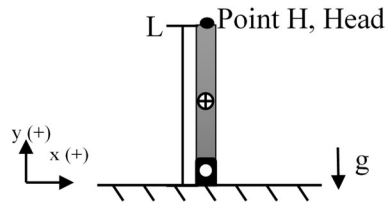
Finally, to estimate the rotational velocity and rotational acceleration of the head COM during impact, it was assumed that the radius of rotation was equal to the neck length and equations 19 and 20 were used.

f. Slender rod physics-based model free body diagrams

i. Pre-fall initial conditions for slender rod physics-based model

The model was assumed to be a light, single link rod with evenly distributed mass (kg); it was assumed that the rod rotates about a pivot point at one end of the rod on the horizontal, which represents an impact surface (FIGURE 28). Any distance between the end of rod and pivot point was considered negligible. In other words, there was no distance between the end of the rod, the pivot point, and the impact surface. It was assumed that the fall began with the feet soles contacting the impact surface, and any energy from a fall from height was not translated into rotational energy. The length of the rod was set as the sole to head center of mass (COM) (m) of the ATD/child. The pivot point was assumed to be frictionless and it was assumed there was no slipping. Point H of the model represented the location of the child/ATD's head center of mass on the single link rod. All anthropometric measurement values for the 12-month-old CRABI ATD

were obtained from a National Highway Traffic Safety Administration technical report publication (Hagedorn and Pritz, 1999).



•H= Location of center of mass (COM) of head on rod

L= Length of rod, from the soles of feet to the center of mass (COM) of head (m)

$$\text{COM head} = (1/2) * (\text{head height}),$$

(m)

FIGURE 28 – Initial conditions of single rod

ii. Falling conditions for single link rod physics-based model prior to impact

It was assumed that the rod rotated about the pivot point at angle  $\theta$  (degrees) to the surface and fell toward the horizontal impact surface (FIGURE 29).

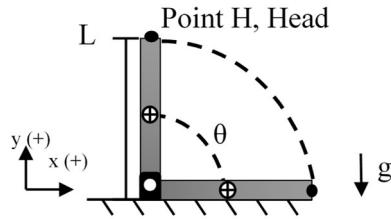


FIGURE 29 – Falling conditions of single rod

Depending on the initial orientation of the child from the pre-fall conditions, the angle,  $\theta$ , was set accordingly. For example, if the child's buttocks impacted the floor and the child's torso was approximately  $45^\circ$  to the horizontal, the angle was set accordingly. If the child's hip to head length was approximately  $90^\circ$  to the horizontal, then  $\sin(\theta)$  equaled 1.

iii. Impact conditions for single link rod physics-based model

During the impact, the rod impacted the surface (FIGURE 30a), and the impact surface deformed at distance,  $\delta$  (m) (FIGURE 30b). The rod rebounded with velocity  $V_{\text{Rebound}}$  (m/s), before coming to rest (FIGURE 30c).

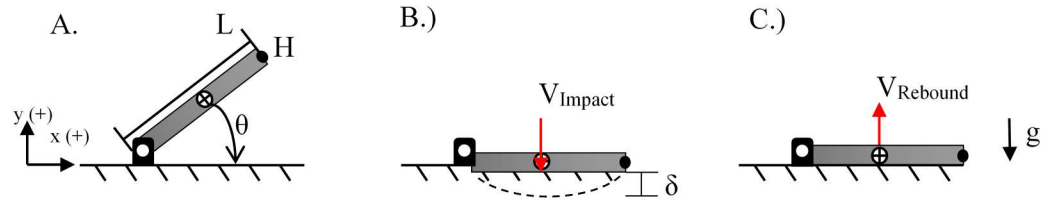


FIGURE 30 – (A) Single rod just prior to impact. (B) Single rod impacting the surface, where  $\delta$  is the surface deformation. (C) Single rod rebounding after the impact, where  $V_{\text{Rebound}}$  is the rebound velocity of the rod before coming to rest ( $V_{\text{final}}$  is 0 m/s).

g. Methods for analysis of slender rod physics-based model

To evaluate the slender rod models, four methods were used for each ATD/childcare center fall (TABLE 9).

i. Method A:

Conservation of energy was used to evaluate the falling conditions for the single link rod. The potential energy was set equal to the kinetic energy of the falling rod.

Potential energy was evaluated using equation 26a.

$$\text{Potential Energy} = m * g * h = m * g * (h) * \sin\theta \quad (26a)$$

where  $m$  is the mass of the child/ATD (kg),  $g$  is the gravitational constant ( $\text{m/s}^2$ ), and  $h$  is the length of the rod (m). The length of the rod varied based on the orientation of the child during the fall, which was judged visually. For example, if the child was on their buttocks and fell rearward, impacting the occiput of their head on the carpeted



flooring, then the height was judged as the buttocks to head COM height (m). Kinetic energy of the rod was evaluated using equation 26b.

$$Kinetic\ Energy = \left(\frac{1}{2}\right) * (I_{end}) * \omega^2 \quad (26b)$$

where  $I_{end}$  is the moment of inertia of the rod at its end and  $\omega$  is the rotational velocity of the rod (rad/s). The moment of inertia of the end of the rod was evaluated using equation 26c.

$$I_{end} = \left(\frac{1}{3}\right) * m * (h)^2 \quad (26c)$$

where  $m$  is the mass of the child/ATD (kg), and  $h$  is the origin point of the fall to head COM of the child/ATD (m). Combing and rearranging equations 26a, 26b, and 26c and setting the angle,  $\theta$ , yielded equation 26d, which was used to evaluate the rotational speed of the falling rod.

$$\omega = \sqrt{\frac{6 * g * \sin\theta}{h}} \quad (26d)$$

Depending on the initial orientation of the child from the pre-fall conditions, the angle,  $\theta$ , was set accordingly. For example, if the child's buttocks impacted the floor and the child's torso was approximately  $45^\circ$  to the horizontal, the angle was set accordingly. If

the child's hip to head length was approximately 90° to the horizontal, then  $\sin(\theta)$  equaled 1. To evaluate the impact of the rod, first the linear velocity of the end of the rod (which represented the child/ATD head COM) at impact was calculated from the rotational speed of the rod during the fall; equation 27 was used to find the impact speed,  $V_{impact}$ .

$$V_{impact} = \omega * L \quad (27)$$

where  $\omega$  is the rotational speed from equation 26d (rad/s) and L was the fall height (m). Then, to calculate the average linear acceleration of the impact head during impact, and because the assumptions were the same for this method, equation 16c was used (reproduced here), then equation 18b was used to convert the average to the peak linear head acceleration.

$$a_{average} = \frac{V_{impact}}{\Delta t} \quad (16c)$$

Finally, equations 19 and 20 were used to estimate the rotational velocity of the head COM during impact and the rotational acceleration of the head COM during impact, respectively.

ii. Method B:

First,  $V_{impact}$  from equation 27 was used to evaluate the linear head impact velocity (m/s).

However, this method assumed COR and rebound velocity had an effect on the biomechanical outcomes, and equation 28a was used.

$$a_{impact} = \frac{\Delta v}{\Delta t} = \frac{v_{impact} - v_{rebound}}{\Delta t} = \frac{(v_{impact} - (COR) * (-v_{impact}))}{\Delta t} \quad (28a)$$

Further simplifying equation 28a yielded equation 28b.

$$a_{impact} = \frac{((v_{impact}) * (COR + 1))}{\Delta t} \quad (28b)$$

Equation 18b was used to convert the average to the peak linear head acceleration.

Finally, equations 19 and 20 were used to estimate the rotational velocity of the head COM during impact and the rotational acceleration of the head COM during impact, respectively.

### iii. Method C:

Again, the approach to the analysis differed in that the starting point followed the impulse-momentum principle, which analyzed the force of the impact, and this method assumed that rebound velocity/COR had an effect during the impact. The impact velocity and acceleration of the lumped mass were calculated by equating the impulse of the impact to the change in momentum using equation 22a (reproduced here).

$$F * \Delta t = m * \Delta v \quad (22a)$$

where  $F$  is the impact force (N),  $\Delta t$  is the impact time on the surface from published values (s),  $m$  is the mass of the lumped mass (kg), and  $\Delta v$  is the change in velocity using equation 16b, where  $v_{\text{impact}}$  is from equation 27 and  $V_{\text{rebound}}$  is the rebound from equation 16b. Rearranging equation 22a, assuming that the impact force was equal to the impulse force, and setting it equal to equation 23 yielded equation 29.

$$a_{\text{impact}} = \frac{(v_{\text{impact}}) * (COR + 1)}{\Delta t} \quad (29)$$

Then, equation 17b was used to convert the result into peak linear head acceleration. Finally, to estimate the rotational velocity and rotational acceleration of the head COM during impact, it was assumed that the radius of rotation was equal to the neck length and equations 18 and 19 were used.

iv. Method D:

Method D followed the same procedures as method C; however, it was assumed that rebound velocity/COR had no effect on the head impact outcomes (as was assumed in method A). Equation 29 was altered to reflect those assumptions; the coefficient of restitution was set to equal 0 and this produced equation 30.

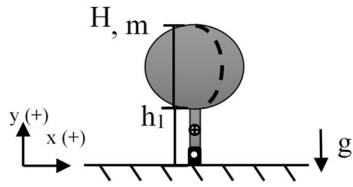
$$a_{\text{impact}} = \frac{(v_{\text{impact}}) * (0 + 1)}{\Delta t} = \frac{v_{\text{impact}}}{\Delta t} \quad (30)$$

Then, equation 18b was used to convert the result into peak linear head acceleration. Finally, to estimate the rotational velocity and rotational acceleration of the head COM during impact, it was assumed that the radius of rotation was equal to the neck length and equations 19 and 20 were used.

h. Inverted pendulum physics-based model free body diagrams

i. Pre-fall initial conditions for inverted pendulum physics-based model

The inverted pendulum model was represented with a single, massless rod with a point mass at the top. It was assumed that the inverted pendulum rotated about a pivot point at one end of the rod on the horizontal, which represented an impact surface (FIGURE 31). Like the single-link rod, any distance between the end of rod and pivot point was considered negligible. The length of the massless rod portion was set as the sole to top of neck length of the ATD/child (m). The point mass was set to the mass of the child/ATD (kg) and the height of the lumped mass was set as the sole to center of mass of the head of the child/ATD (assumed to be half of the height of the head of the child/ATD (m)). The pivot point was assumed to be frictionless and it was assumed there was no slipping. All anthropometric measurement values for the 12-month-old CRABI ATD were obtained from a National Highway Traffic Safety Administration technical report publication (Hagedorn and Pritz, 1999).



$H$  = Height from soles to head center  
of mass (m)

$$\text{COM}_{\text{Head}} = (1/2) * (\text{head height})$$

$h_1$  = Height of soles to top of neck (m)

$m$  = mass of the spherical lumped sum  
(kg)

$g$  = gravitational constant ( $\text{m/s}^2$ )

$\bullet$  = COM of the link (m) =  $(1/2) * (h_1)$

FIGURE 31 – Initial conditions of the inverted pendulum

ii. Falling conditions for inverted pendulum physics-based model prior to impact

It was assumed that the inverted pendulum rotated about the pivot point at angle  $\theta$  (degrees) to the surface, and it fell toward the horizontal impact surface (FIGURE 32).

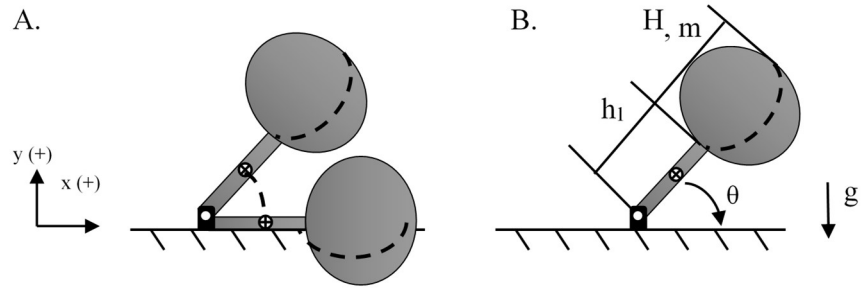


FIGURE 32 – Falling conditions of the inverted pendulum. (A) motion of the inverted pendulum and (B) angle of the inverted pendulum as it falls.

iii. Impact conditions for inverted pendulum physics-based model

During the impact, the inverted pendulum impacted the surface (FIGURE 33a), and the impact surface deformed at distance,  $\delta$  (m) (FIGURE 33b). The inverted pendulum rebounded with velocity  $V_{\text{Rebound}}$  (m/s), before coming to rest (FIGURE 33c).

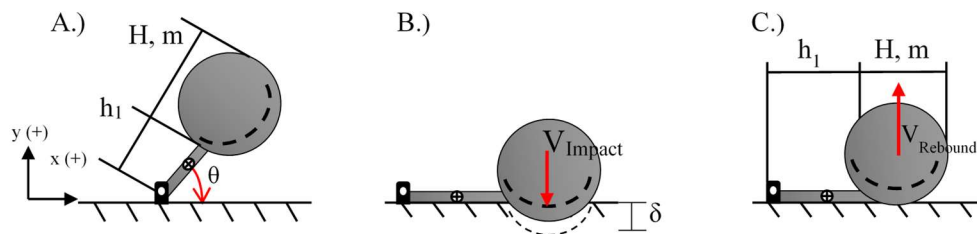


FIGURE 33 – (A) Inverted pendulum just prior to impact. (B) Inverted pendulum impacting the surface, where  $\delta$  is the surface deformation. (C) Inverted pendulum rebounding after the impact, where  $V_{\text{Rebound}}$  is the rebound velocity of the mass before coming to rest ( $V_{\text{final}}$  is 0 m/s).

i. Methods for analysis of inverted pendulum model

To evaluate the inverted pendulum models, four methods were used for each ATD/childcare center fall (TABLE 9).

i. Method A:

Conservation of energy was used to evaluate the falling conditions for the inverted pendulum. The potential energy was set equal to the kinetic energy of the inverted pendulum. Potential energy was evaluated using equation 31a.

$$Potential\ Energy = m * g * h = m * g * (H) * \sin\theta \quad (31a)$$

where m is the mass of the child/ATD (kg), and g is the gravitational constant (m/s<sup>2</sup>). H is the length of the rod to head COM (m) of the child/ATD. This length varied based on the fall, and the origin point (or end of the rod) was judged visually. For instance, if the child was on their buttocks and fell rearward, impacting their occiput on the floor, then the length of the rod to head COM was set as the buttocks to head COM height for that subject. Kinetic energy of the inverted pendulum was evaluated using equation 31b.

$$Kinetic\ Energy = \left(\frac{1}{2}\right) * (I_{point\ mass}) * (\omega)^2 \quad (31b)$$



where  $I_{point\ mass}$  is the moment of inertia for the point mass at the top of the rod and  $\omega$  is the rotational speed of the falling inverted pendulum (rad/s). The moment of inertia for the end of the massless rod was negated as the rod was assumed to be massless. The moment of inertia of the point mass was found with equation 31c, where the radius was the length of the rod.

$$I_{point\ mass} = (m) * (H)^2 \quad (31c)$$

Setting the potential energy equal to the kinetic energy, setting the angle  $\theta$  (based on fall characteristics), and combining and rearranging equations 31a, 31b, and 31c yielded equation 31d.

$$\omega = \sqrt{\frac{2g\sin\theta}{H}} \quad (31d)$$

To evaluate the impact of the inverted pendulum, first the speed of the end of the inverted pendulum at impact was calculated from the rotational speed of the rod during the fall; equation 25 was used to find the impact speed,  $v_{impact}$  (reproduced here).

$$v_{impact} = \omega * (H) \quad (25)$$

where  $\omega$  was the rotational speed from equation 31d (rad/s). For method A, it was assumed that COR/rebound velocity had no effect on the biomechanical outcomes, and the analysis began with the average linear head acceleration. This was calculated with equation 16c (reproduced here), where COR was set to 0.

$$a_{average} = \frac{v_{impact}}{\Delta t} \quad (16c)$$

where  $a_{average}$  is the average linear acceleration. Equation 18b was used to convert the result into peak linear head acceleration. Finally, to estimate the rotational velocity and rotational acceleration of the head COM during impact, it was assumed that the radius of rotation was equal to the neck length and equations 19 and 20 were used.

ii. Method B:

First,  $v_{impact}$  from equation 25 was used to evaluate the linear head impact velocity (m/s). However, this method assumed COR and rebound velocity had an effect on the biomechanical outcomes, and equation 28a was used (reproduced here).

$$a_{impact} = \frac{\Delta v}{\Delta t} = \frac{v_{impact} - v_{rebound}}{\Delta t} = \frac{(v_{impact} - (COR) * (-v_{impact}))}{\Delta t} \quad (28a)$$

Further simplifying equation 28a yielded equation 28b.

$$a_{impact} = \frac{\left( (v_{impact}) * (COR + 1) \right)}{\Delta t} \quad (28b)$$

Equation 18b was used to convert the average to the peak linear head acceleration.

Finally, equations 19 and 20 were used to estimate the rotational velocity of the head COM during impact and the rotational acceleration of the head COM during impact, respectively.

iii. Method C:

Again, the approach to the analysis differed in that the starting point followed the impulse-momentum principle (which analyzed the force of the impact), and this method assumed that rebound velocity/COR had an effect during the impact. The impact velocity and acceleration of the lumped mass were calculated by equating the impulse of the impact to the change in momentum using equation 22a (reproduced here).

$$F * \Delta t = m * \Delta v \quad (22a)$$

where F is the impact force (N),  $\Delta t$  is the impact time on the surface from published values (s), m is the mass of the lumped mass (kg), and  $\Delta v$  is the change in velocity using equation 16b, where  $v_{impact}$  is from equation 25 and  $V_{rebound}$  is the rebound from equation 16b. Rearranging equation 22a, assuming that the impact force was equal to the impulse force, and setting it equal to equation 23, yielded equation 32.

$$a_{impact} = \frac{(v_{impact}) * (COR + 1)}{\Delta t} \quad (32)$$

Then, equation 18b was used to convert the result into peak linear head acceleration.

Finally, to estimate the rotational velocity and rotational acceleration of the head COM during impact, it was assumed that the radius of rotation was equal to the neck length and equations 19 and 20 were used.

iv. Method D:

Method D followed the same procedures as method C; however, it was assumed that rebound velocity/COR had no effect on the head impact outcomes (as was assumed in method A). Equation 32 was altered to reflect those assumptions; the coefficient of restitution was set to equal 0 and this produced equation 33.

$$a_{impact} = \frac{(v_{impact}) * (0 + 1)}{\Delta t} = \frac{v_{impact}}{\Delta t} \quad (33)$$

Then, equation 18b was used to convert the result into peak linear head acceleration.

Finally, to estimate the rotational velocity and rotational acceleration of the head COM during impact, it was assumed that the radius of rotation was equal to the neck length and equations 19 and 20 were used.

5. Compare biomechanical outcomes from physics-based models to replicated ATD feet-first fall experiments using SIM G to measure head velocity and acceleration

The physics-based models were applied to the replicated feet-first ATD falls to estimate head biomechanical measures. All values obtained from the four methods used to evaluate the three physics-based models were compared to the mean peak value from each SIM G activation that was obtained in the replicated ATD study (n=7 for carpet surface and n=7 for linoleum surface). These values included peak linear head acceleration, peak linear head velocity, peak rotational head acceleration, and peak rotational head velocity. The percent error between each obtained physics-based model outcome and each mean peak value from the SIM G device was calculated. To visualize the results as compared to the SIM G outcomes, a number line for each biomechanical measure was produced and the SIM G range of each measure was displayed on the number line. Percent errors were reported and categorized (TABLE 11); the lower the percent error, the more accurate the model was to the SIM G outcome. To test *H2*, it was assumed that if a model had a 25% error or less, the model could accurately predict physics-based outcomes.

TABLE 11

PERCENT ERROR CATEGORIES FOR PHYSICS-BASED MODEL OUTCOMES

0-25.0% Error
25.01-50.0% Error
50.01-100.0% Error
>100.01% Error

6. Compare biomechanical outcomes from physics-based models to SIM G biomechanical data from select childcare center falls

Falls with SIM G data and primary head impact (n=8) from the childcare center that were selected to be modeled with physics-based models were used to estimate head biomechanical measures. The percent error for the results of each of the four methods for each of the three physics-based models was calculated based on the values obtained from the SIM G devices. Measures included peak linear head acceleration, peak linear head velocity, peak rotational head acceleration, and peak rotational head velocity. Percent errors were calculated, categorized (TABLE 11), and reported. As with the ATD replicated falls, to test *H2*, it was assumed that if a model had a 25% error or less, the model could accurately predict physics-based outcomes.

## V. RESULTS

### A. Video monitoring/video recorded falls

Falls 1 through 101 were collected from the video recording devices. These represented the first 100 falls (n=100) that were observed at the childcare. Fall 13 was excluded, as no fall event was visible in any of the camera views. Data was collected at the childcare center for 1.5 – 2 hours per day for a total of 7 collection days for this subset (over approximately 2 weeks). Data was collected only in the two younger classrooms and from the outdoor playground. No data was collected from any of the older classrooms. This dataset is a subset of a larger project (n=3354 falls; July 2018 through June 2019).

### B. Subject demographics

The first 100 video-recorded falls involving 8 children aged 17-25 months (mean  $\pm$  SD:  $20 \pm 2$  months) were characterized. This represented a subset (n=8) of the total number of subjects enrolled in the larger study (n=35). More subjects were female (62%) than male (38%). However, males fell more than females (FIGURE 34).

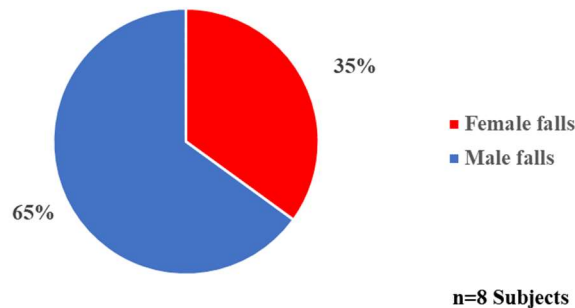


FIGURE 34 – Percent of falls (n=100) experienced by each gender

C. Anthropometric measurements of the subjects

Anthropometrics from the subjects (n=8) were obtained (TABLE 12). Subjects 6 and 11 were uncooperative and further measurements were not obtained.

TABLE 12

ANTHROPOMETRICS OF ENROLLED SUBJECTS

Subject ID	Age (months)	Gender	Mass (kg)	Height (cm)	Head circumference (cm)	Shoulder breadth (cm)	Hip breadth (cm)	Chin to sole length (cm)	Hip to sole length (cm)	Knee to sole length (cm)	Chest depth (cm)
1	25	M	12.0	84.4	49.0	20.5	19.0	67.0	36.5	18.5	12.5
2	25	M	16.6	90.3	51.0	24.5	19.5	71.5	37.0	20.5	13.0
3	20	F	12.3	82.3	49.0	21.0	19.5	62.5	36.0	18.0	13.0
4	21	M	11.4	80.9	48.5	21.0	17.5	62.5	31.0	18.5	13.3
5	19	F	12.5	78.1	47.5	20.5	19.0	59.3	31.0	19.0	12.5
6	21	F	10.8	76.0	45.5						
7	17	F	11.1	78.0	46.5	20.0	18.0	61.2	31.0	17.7	12.0
11	19	F	12.9	76.5	48.5						



#### D. Impact surfaces/object COR

Coefficient of restitution values were obtained in each interior room (linoleum, carpet, rug over carpet, etc.) and playground surfaces (playground synthetic mulch, playground equipment, etc.). The higher the COR, the closer the impact of the steel ball during measurement was to a perfectly elastic collision. Mean CORs and standard deviations for each impact surface/object involved in the 100 falls were determined (TABLE 13).

TABLE 13

## COEFFICIENT OF RESTITUTION MEANSUREMENT FOR IMPACT SURFACE/OBJECTS

Location	Surface type	COR $\pm$ SD
Classroom 1	Linoleum	0.45 $\pm$ 0.01
Classroom 1	Carpet	0.41 $\pm$ 0.018
Classroom 1	Area rug over carpet	0.56 $\pm$ 0.019
Classroom 1	Butterfly Pad	0.47 $\pm$ 0.039
Classroom 1	Butterfly Ramp	0.42 $\pm$ 0.01
Classroom 2	Linoleum	0.44 $\pm$ 0.012
Classroom 2	Carpet	0.41 $\pm$ 0.013
Classroom 2	Area Rug (over carpet)	0.55 $\pm$ 0.017
Classroom 2	Carpeted stairs	0.45 $\pm$ 0.015
Indoor Rooms	Drywall	0.26 $\pm$ 0.01
Indoor Rooms	Wood furniture	0.40 $\pm$ 0.006
Playground	Playground mulch	0.57 $\pm$ 0.028
Playground	Playground slide	0.22 $\pm$ 0.011
Playground	Playground slide edge	0.47 $\pm$ 0.02
Playground	Playground slide steps	0.17 $\pm$ 0.0087
Playground	Playground “mushrooms”	0.54 $\pm$ 0.008
Playground	Playground slide platform	0.34 $\pm$ 0.012
Playground	Slide structural support pole	0.24 $\pm$ 0.041

#### E. SIM G/SKYi Verification

Replicate fall experiments of Thompson's ATD feet first falls study (Thompson, 2018) were conducted to verify the SIM G sensor. Details and results of the SIM G/SKYi experimentation and testing can be found in APPENDIX II. SIM G values were found to be statistically consistent with the values obtained from the previous study. There were no significant differences in mean peak resultant linear head acceleration ( $p=0.571$ ), mean peak resultant linear head velocity ( $p=0.308$ ), mean peak resultant rotational head acceleration ( $p=0.248$ ), mean peak resultant rotational head velocity ( $p=0.863$ ), or mean impact duration ( $p=0.734$ ). The results verified the accuracy of the SIM G in relation to the onboard ATD accelerometers. The SIM G was determined to be acceptable instrumentation to obtain head biomechanics data for short-distance falls involving children.

#### F. Specific Aim 1: Characterize the video-recorded short distance falls involving young children in a childcare setting.

##### 1. Fall distribution by age

The fall distribution by age was developed with the age of the subjects at the median date of the collection period (between July 15, 2018 and July 28, 2018) (FIGURE 35). The ages were categorized into the following three groups: age group 1 represented 17-19 months; age group 2 represented 20-21 months; age group 3 represented 22-25 months. Of note, subject 4 (age group 2; male) represented 36% of total falls. Age group 1 was all female ( $n=3$ ); age group 2 was a mix of male and female ( $n=3$ ); age group 3 was all male ( $n=2$ ).

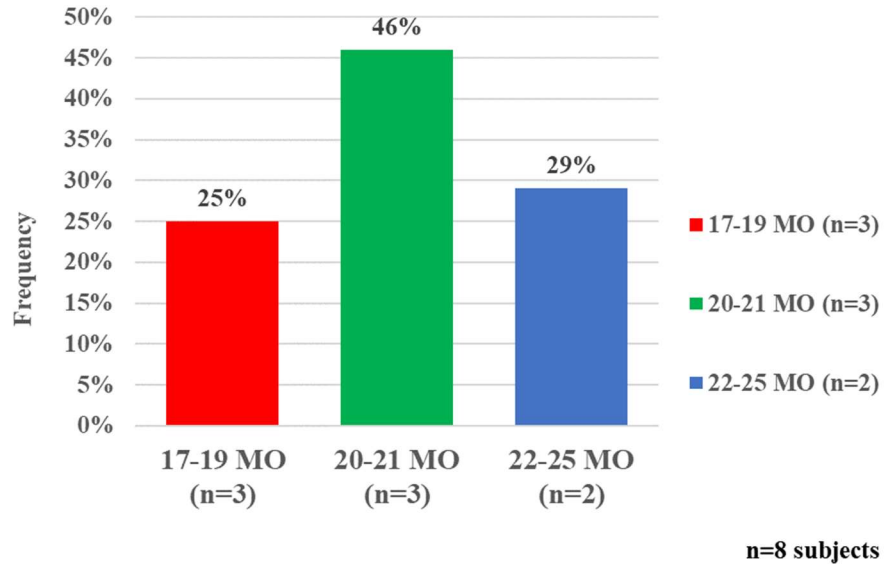


FIGURE 35 –Fall frequency by age distribution

2. Fall characterization by fall location

Three locations in the childcare were observed – the two younger classrooms and the playground (FIGURE 36). More of the observed falls occurred indoors (n=64) than outdoor (n=36).

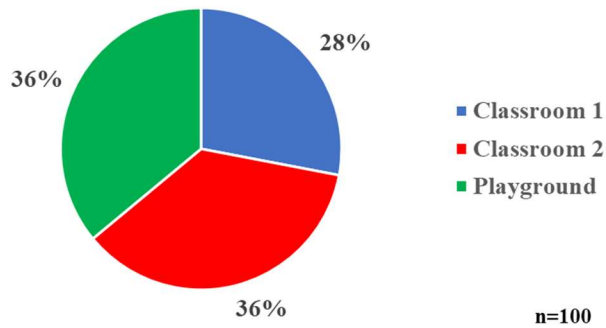


FIGURE 36 – Location where falls occurred

### 3. Fall characterization by fall type

The fall type was analyzed (FIGURE 37). The “other” category referred to 1 fall where the subject fell forward horizontally to the same surface she was standing on and impacted the palms of both hands on the surface (in this case, the playground slide), and her feet did not leave the supportive surface. Most falls were ground-type falls (82%). Ten falls from height occurred on the playground. To estimate the height of the falls from height, first the center of mass (COM) of each subject’s head was estimated from the obtained anthropomorphic measures. This was estimated to be half of the subject’s head height. Two female subjects did not have anthropomorphic measurements for chin to sole length. So, to estimate the COM of their heads, first the average ratio of head height to full height of all other female subjects was obtained, then this ratio was applied to the full height of the two subjects. The COM was then estimated to be half of this height. Once the COM was obtained for each subject, the height of the fall was estimated to be the difference of the COM of the head located at a point in space at the beginning of the fall versus at the end of the fall, judged visually. For example, in fall 57, subject 4 began the fall standing upright on the tall mushroom on the playground (FIGURE 38). The total starting height was the sum of the height of the tall mushroom, the chin to sole height, and the height of the COM of the head – this was 117.4 cm. The subject ended the fall prone on the playground surface, with his head on the ground. The difference from the ground to the COM of the head was assumed to be approximately the COM height, so this was chosen as the final height for this fall. The difference was calculated to be 108.2

cm. This was also the fall from the greatest height. The average fall height across all falls from height was  $64 \pm 21.1$  cm and the range was 17.8 cm to 108.2 cm.

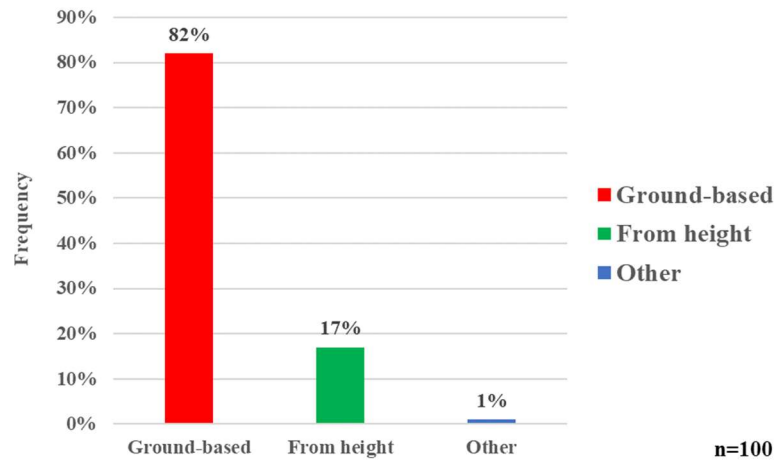


FIGURE 37 – Fall type



FIGURE 38 – Tall Mushroom (left; 45.7 cm) on playground next to short mushroom (right; 33.0 cm)

#### 4. Fall characterization by initial condition

The fall video recordings were analyzed to determine the initial conditions of the subjects just prior to the fall initiation (FIGURE 39). The most frequent initial condition of the subject was walking. Other common initial conditions included running, standing, jumping, squatting, and stepping (from a stationary position). “Other” included leaning, climbing, spinning, etc.

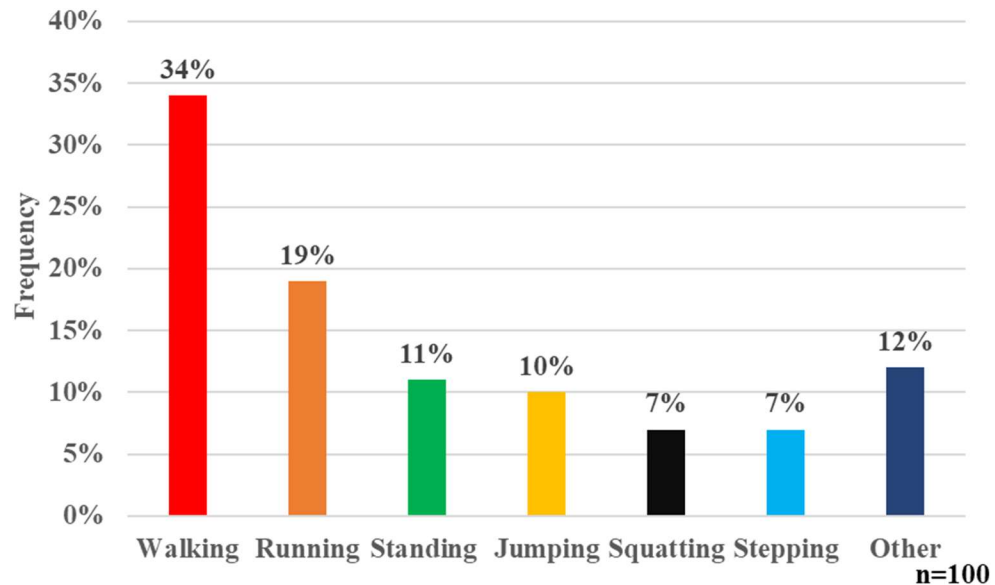


FIGURE 39 –Initial condition

#### 5. Fall characterization by fall initiation

Fall recordings were analyzed for fall initiations (FIGURE 40). The most common fall initiations included a loss of balance (or control) and tripping. Slipping and being

pushed, either by another person or object, were also seen in the falls. “Other” included a collision (either with another person or object), jumping, etc.

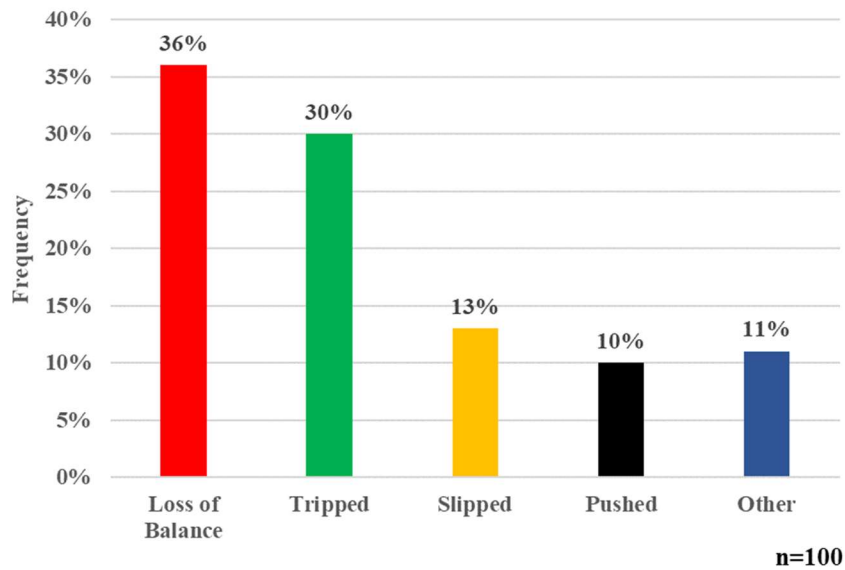


FIGURE 40 – Fall initiation

#### 6. Fall characterization by fall dynamic(s)

The videos were analyzed to determine the most frequent fall dynamics experienced during the fall events (FIGURE 41). Most falls involved forward dynamics, where the subject fell toward the anterior plane, or front, of their body. Some falls were rearward, where the subject fell toward the posterior plane, or back, of their body. Another portion of the falls were lateral falls, where the subject fell either right or left laterally (i.e., toward the right lateral arm). A few of the falls were feet-first falls where the subject fell from a height, typically by jumping and having the soles of their feet first contact the



supportive surface just prior to impact. Two falls involved head-first dynamics. 27% of falls involved more than one fall dynamic. Falls involved on average 1.3 unique fall dynamics.

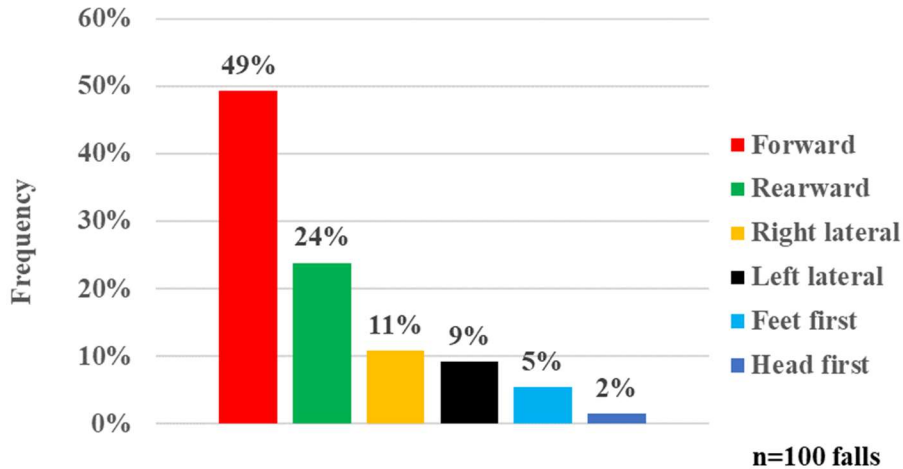


FIGURE 41 –Frequency of falls with each type of fall dynamics

a. Head-first falls

Two of the falls involved head-first fall dynamics. In fall 49, subject 4 was on his buttocks in the circular cutout of the playground panel play structure. He fell rearward and head-first, and the primary impact involved his head occiput and upper back on the playground surface (FIGURE 42). There was another subject who was near subject 4 when his fall occurred, but it was not clear in the video if this subject pushed the subject (or initiated the fall in any manner). The SIM G was not triggered for this event (in other words, this fall did not meet or exceed the 12 g linear head acceleration threshold).



FIGURE 42 – Subject 4 fell rearward and head-first out of the playground panel structure, impacting his occiput and upper back on the playground surface (indicated by white arrow)

In fall 54, subject 4 was initially standing on the tall mushroom on the playground, and he proceeded to fall forward off the mushroom head-first to the playground surface, impacting his face and superior head. In this fall, subject 4 (male) fell from the tall mushroom (45.7 cm) on the playground (FIGURE 43). Subject 4 was attempting to stand upward on the mushroom, and the fall was initiated by a slip. He fell forward and head-first from an initial squatting position, and he impacted the frontal skull and his face on both the playground surface and another child's leg (who was walking past the subject). The subject's teacher attempted to stop the fall by grabbing his left ankle, but the subject continued to fall forward. The primary impact included his anterior upper chest (torso body region), his face, his frontal lobe of his head, his medial right leg, and the bilateral palms of his hands. The secondary impact included his medial pelvis against the surface of the tall mushroom, and the anterior left leg impacted the playground surface. He was in a prone final position at the end of the fall. The SIM G was triggered, and the peak resultant linear head acceleration was 19g (FIGURE 44), and the HIC<sub>15</sub> was 12.9.



FIGURE 43 – Subject 4 falling from a height and impacting his head on the playground surface

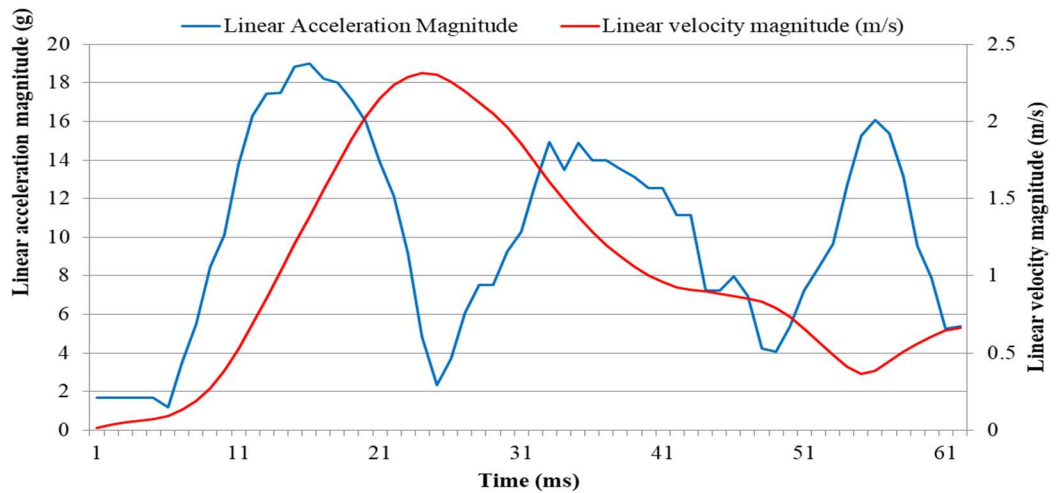


FIGURE 44 – Linear head acceleration magnitude (g) and linear head velocity magnitude (m/s) from SIM G output for fall 54

### 7. Fall characterization by equipment/object involvement

The video-recorded falls were analyzed to determine if an object was involved during any point of the fall (FIGURE 45). Of the 100 original falls, 59% (n=59) involved at least one inanimate object. Objects included, but were not limited to, a toy, a piece of

classroom furniture (i.e., a chair, table), a piece of playground equipment (i.e., the “mushrooms”, the slide), etc.

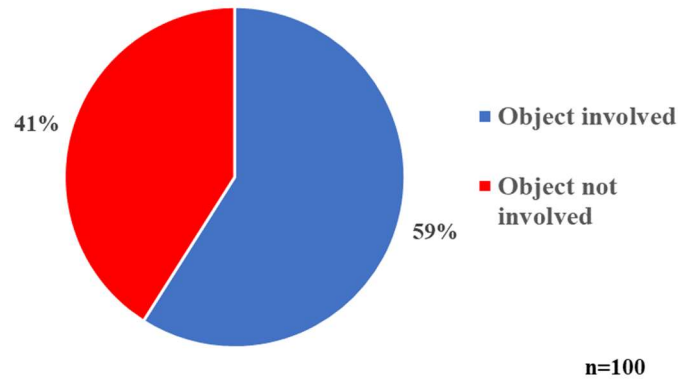


FIGURE 45 – Frequency of falls involving an object(s)

The subset of 59 falls that involved an object was analyzed for the type of objects that were involved during the fall (FIGURE 46). A total of (n=69) inanimate objects were involved (some falls involved more than one object). The most common objects involved during the fall event included playground equipment, a toy, and classroom furniture. Falls also occasionally involved the “butterfly slide,” which was a piece of furniture located in classroom 2 (FIGURE 47). Other objects that were involved less-frequently in the fall events included pillows, large clear plastic containers (used to store smaller objects), and the carpeted stairs play equipment in classroom 2 (FIGURE 48).

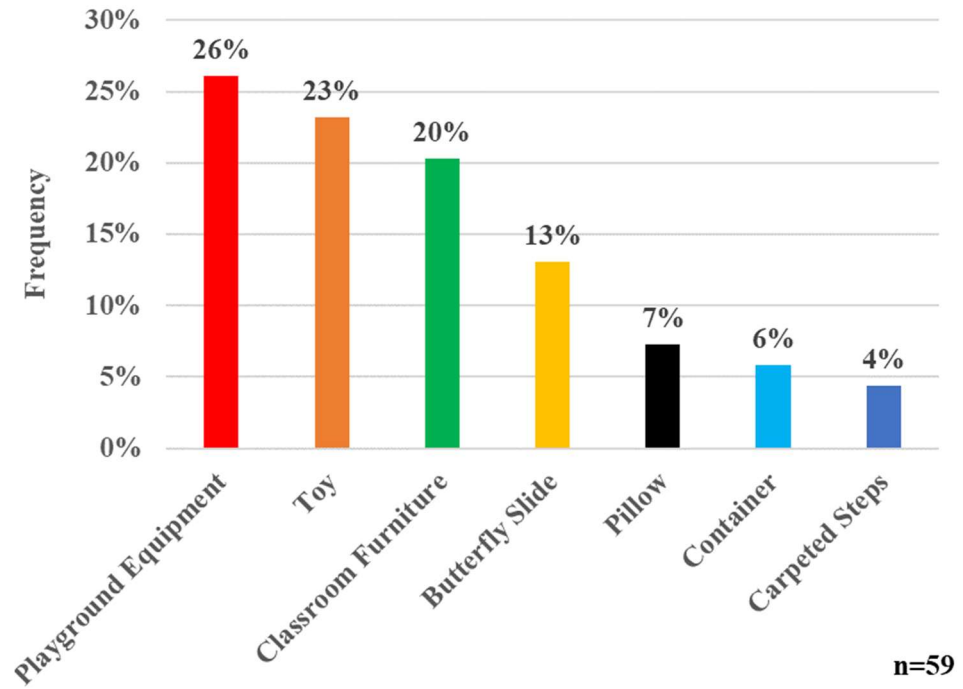


FIGURE 46 – Objects involved during the fall



FIGURE 47 – Butterfly slide in classroom 2



FIGURE 48 – Carpeted stair play equipment in classroom 2

The locations of the falls that included an inanimate object were also analyzed (FIGURE 49). More falls that involved an inanimate object occurred in a classroom (71%) rather than on the playground (29%).

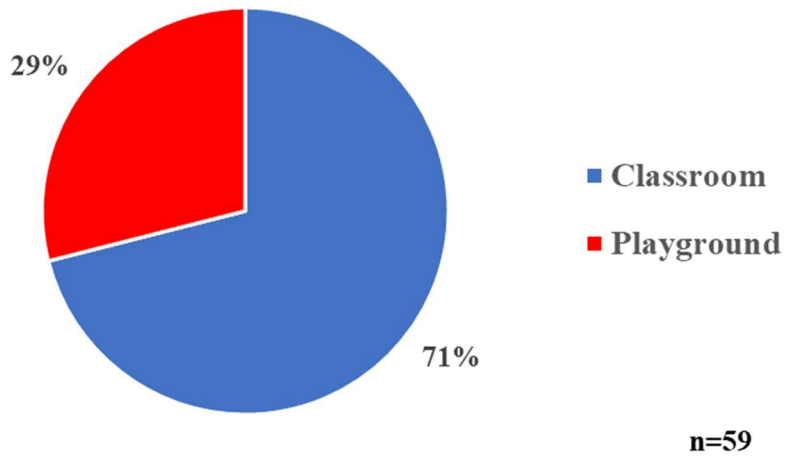


FIGURE 49 – Locations of falls that involved an object(s)

The phases of the fall that involved at least one inanimate object were analyzed. First, the total number of phases that were affected by at least one inanimate object was analyzed for its frequency (FIGURE 50). Most often, only one phase 1 or only two phases involved at least one (1) inanimate object. Only 7% of all falls involved an inanimate object during all 4 main phases of the fall.

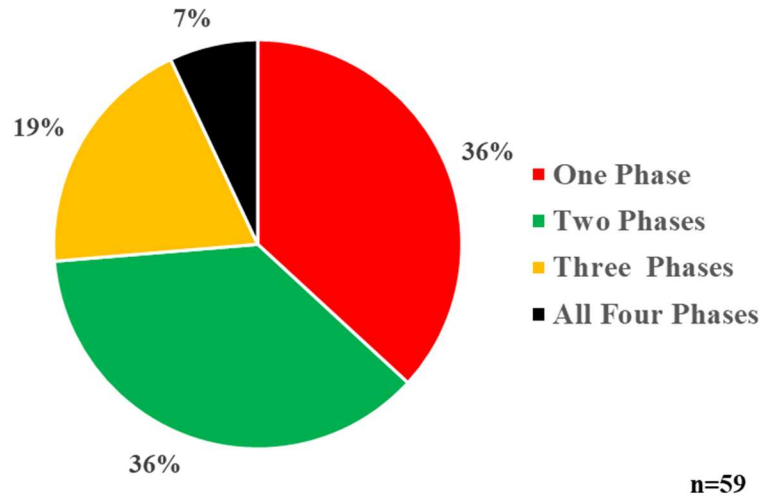


FIGURE 50 – Frequency of falls involving an object(s) by number of phases

The falls were then analyzed to determine how often an inanimate object(s) was involved in each phase (FIGURE 51). Of the total falls that involved at least one inanimate object, 64% had an object involved during the initial condition phase. 56% had an object involved during the fall initiation phase. Some falls involved an object during the primary and/or secondary phases.



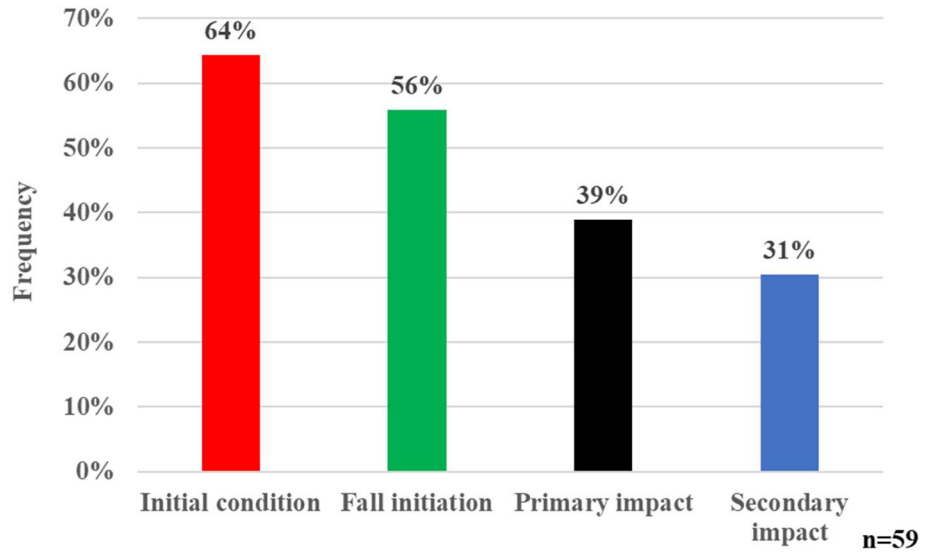


FIGURE 51 – Frequency of falls involving an object(s) in each phase

8. Fall characterization by another person(s) involvement

The video-recorded falls were analyzed to determine if at least one (1) other person was involved during any point of the fall (FIGURE 52). Of the 100 original falls, 26% (n=26) involved at least one other person.

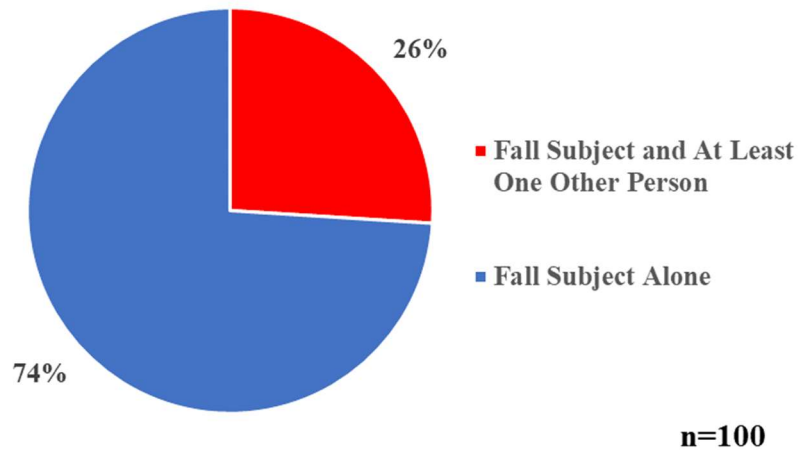


FIGURE 52 – Frequency of falls that involved another person(s), not including the fall subject

Then, the subset of 26 falls that involved at least one other person(s) was analyzed for the person(s) that was involved during the fall (FIGURE 53). For the 26 falls that involved at least one other person, most falls involved exactly one other child, not including the fall subject.

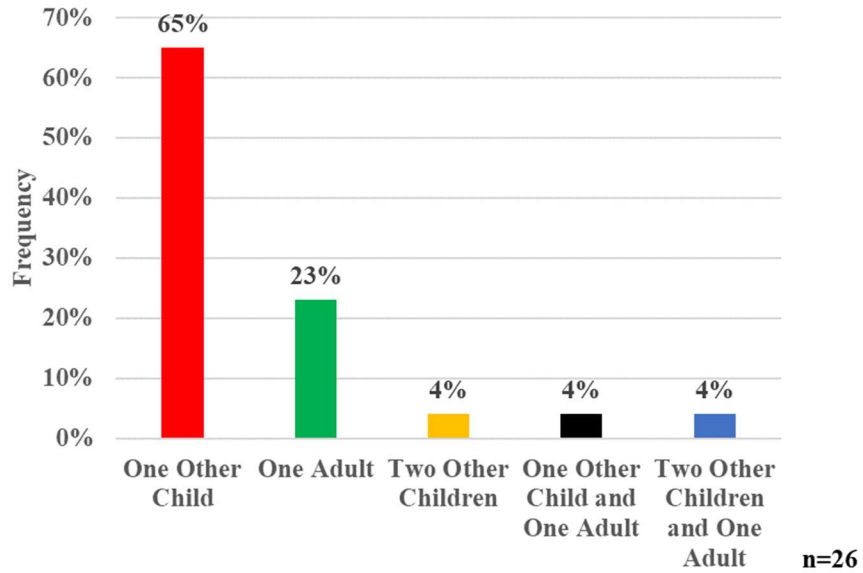


FIGURE 53 – Frequency of another person(s) involved in the falls

The locations of the falls that included at least one other person were also analyzed (FIGURE 54). Most falls that involved at least one other person occurred inside in a classroom (54%).

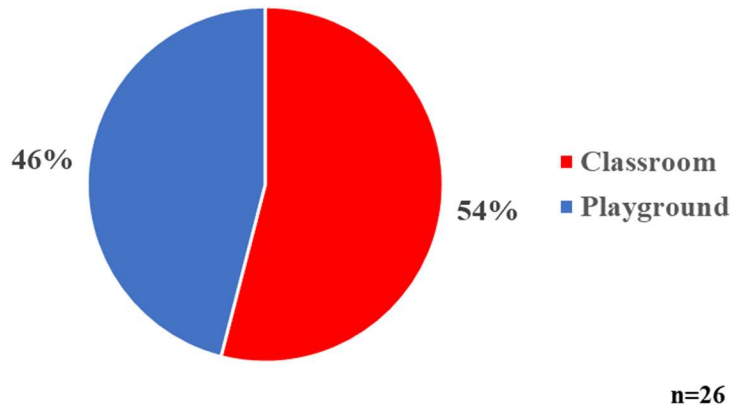
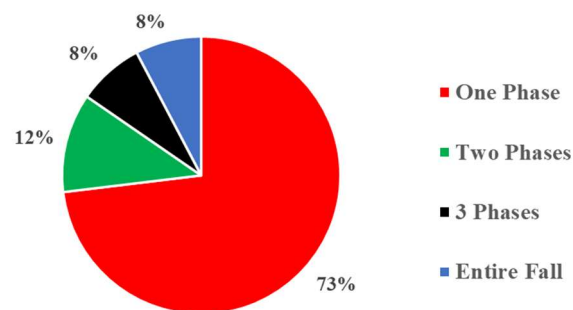


FIGURE 54 – Location of falls that involved another person(s)

The phases of the fall that involved another person were analyzed. Three fall phases were determined that involved another person, not including the subject – the initial condition phase; the fall initiation phase; and the primary impact phase. Additionally, some falls involved another person during the entire fall sequence. First, the total number of phases that were affected by at least one other person was analyzed for frequency (FIGURE 55). Most often (73%), only one phase involved another person, not including the fall subject. 20% of all falls involved another person during 2 or more phases of the fall. Two falls (8%) involved another person during the entire fall sequence. An example was a fall where subject 4 was standing on a mushroom (playground), proceeded to jump off, landed on the playground surface, and then fell forward and impacted his right hand on the playground surface. His left hand was held by a teacher during the entire fall sequence.



n=26

FIGURE 55 – Frequency of falls that involved another person(s) by number of phases

The falls were then analyzed to determine how often another person was involved in each phase (FIGURE 56). Of the total falls that involved at least one (1) other person, 75% had a person(s) involved during the fall initiation phase. 33% had a person(s) involved during the initial condition phase. 21% of falls involved a person during the primary impact phase.

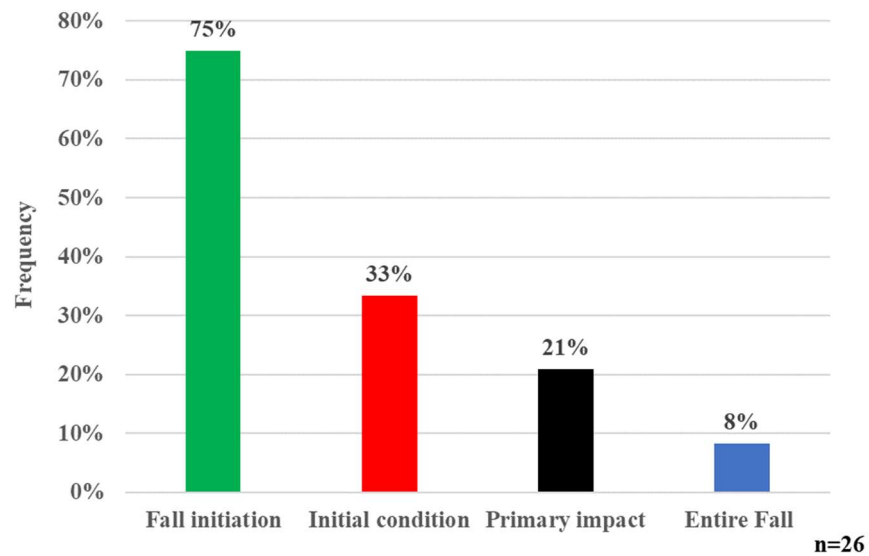


FIGURE 56 – Frequency of falls involving another person(s) by fall phases

#### 9. Fall characterization by head impact

Fall video recordings were then analyzed to determine if head impact occurred at any point across all fall events (FIGURE 57). 71% of falls did not have head impact occur at any point during the fall event. 19% of falls did have head impact occur at some point during the fall event, which could have occurred during fall initiation, primary impact,

etc. 10% of the falls were considered “undetermined” due to the camera angle being obscured.

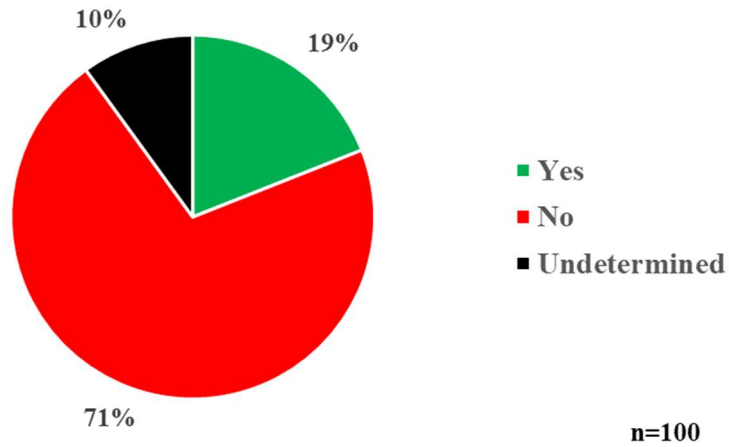


FIGURE 57 – Frequency of head impact

The subset of falls involving object(s) or another person(s) were analyzed to determine if head impact occurred during any point of the fall (FIGURE 58). Of the 59 falls that involved at least one other object, only 23% resulted in head impact at some point during the fall. Some falls were marked as “Undetermined” due to camera view obstruction. Of the 26 falls that involved at least one other person, 27% resulted in head impact at some point during the fall.

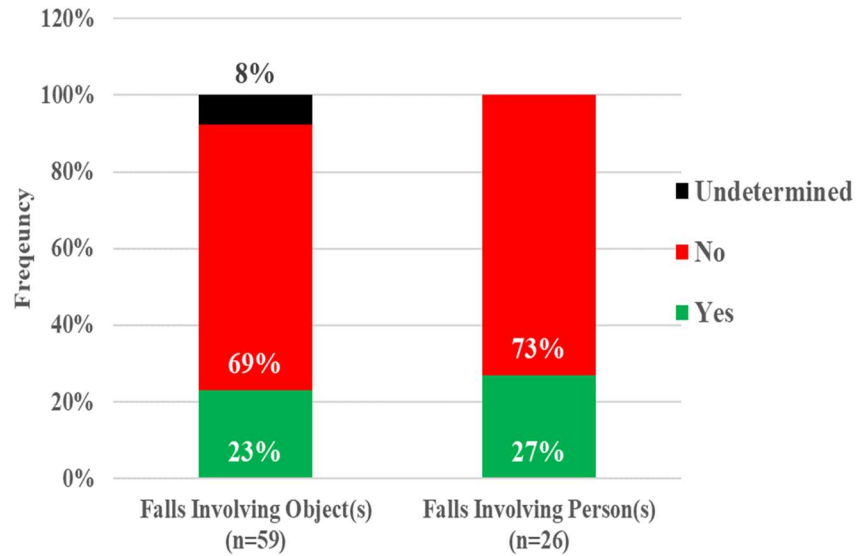


FIGURE 58 – Percentage of falls involving an object(s) or person(s) that resulted in head impact

#### 10. Fall characterization by impact surface

Fall video recordings were analyzed to determine the most frequent impact surfaces during the primary impact (FIGURE 59). Impact surface was only recorded for the primary impact, as that was determined to be the impact that was qualitatively judged to disperse the most energy. Most primary impacts occurred on playground mulch, carpet, and an area rug overlying carpet. Some falls occurred on linoleum in the classrooms. The other category included objects such as pillows, the butterfly slide, playground equipment, etc.

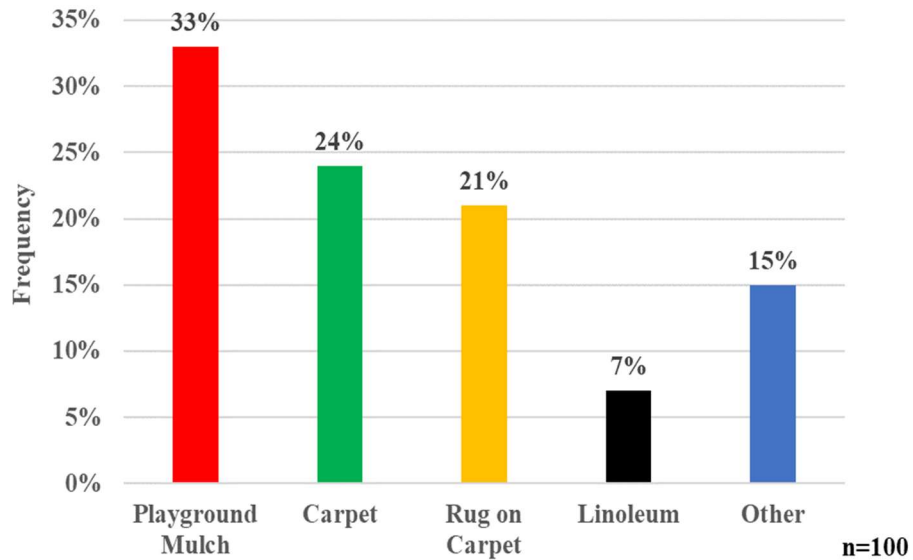


FIGURE 59 – Impact surfaces involved in the primary impact

11. Fall characterization by plane(s) impacted during primary impact

Fall video recordings were analyzed to determine the body plane(s) impacted during the primary impact (FIGURE 60). The most common plane impacted during the primary impact of a fall was the anterior (frontal) plane (FIGURE 61A). 26% of falls involved more than one plane during the primary impact. The average number of planes impacted per fall was 1.3.



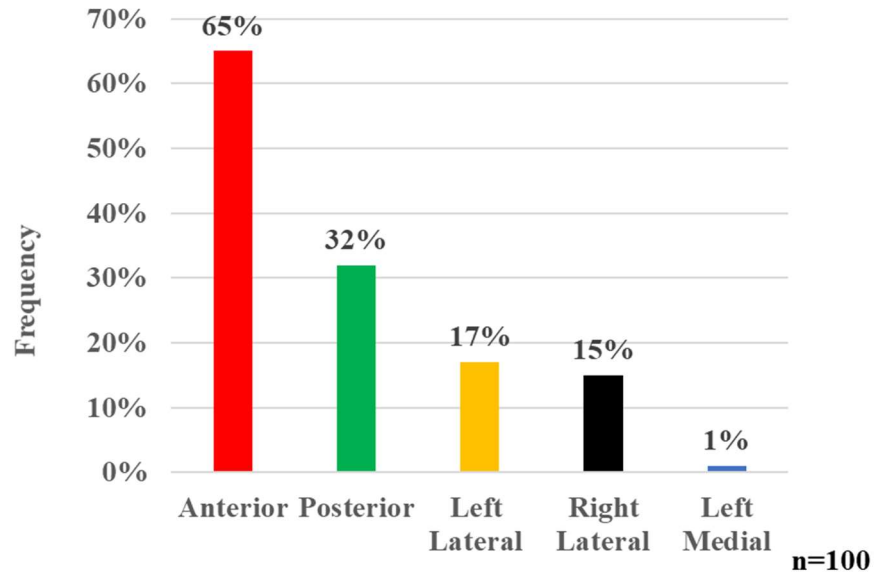


FIGURE 60 – Plane(s) impacted during the primary impact of a fall

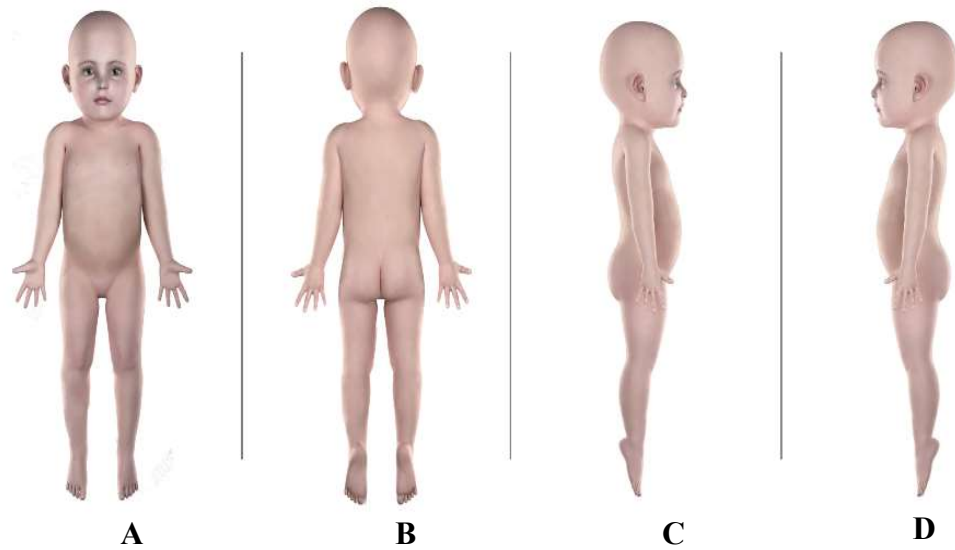


FIGURE 61 – (A) Anterior plane; (B) Posterior plane; (C) Right lateral plane; (D) Left lateral plane

## 12. Fall characterization by final position

The final phase of the fall was analyzed (FIGURE 62). Most falls ended in a sitting position on the final fall surface. The “sitting” position included a cross-legged position, as well as a “long sitting” position where the buttocks was on the floor and the posterior bilateral legs were extended out in front of the child. The subjects also demonstrated lateral recumbent positions, where they were laying on their right or left side. Many falls ended in a hands-and-knees position on the final surface; some subjects were prone. Similarly, some subjects were bent at the waist with their palms and feet on the final surface but their buttocks upright. A few falls ended in a supine position. The “other” category included squatting positions, kneeling positions, etc.

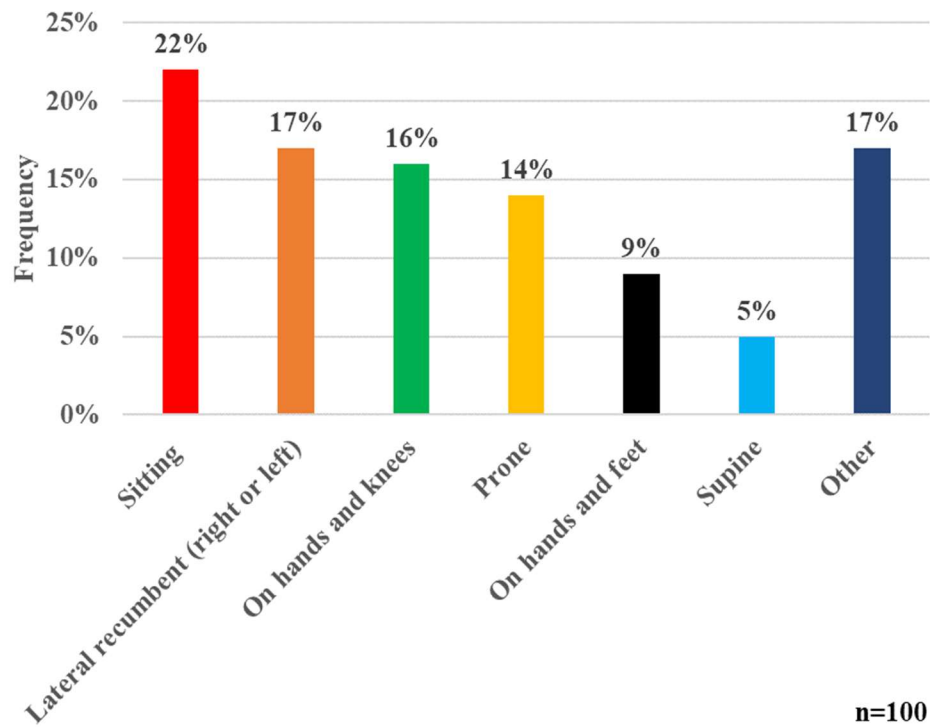


FIGURE 62 – Final position of the subject

13. Fall characterization by injury outcomes

**No injuries occurred in any fall.**

G. Specific Aim 2: Identify body regions most commonly impacted during falls involving young children in a childcare setting.

Body regions involved in the first contact, primary impact, and secondary impact were analyzed for frequency. Once frequencies of body regions impacted/contacted were determined, a 10% threshold was selected for displaying body regions involved in falls on the body maps. Many body regions were impacted only one or two times each, and they were considered outliers. Body regions were then colored according to a scale (FIGURE 63).



FIGURE 63 – Scale for percent of falls involving contact/impact to body region (n=100 falls)

1. First contact body map

The first contact body map displayed the most common body regions involved in the first contact of the fall (FIGURE 64). The soles of both feet were the most common body regions involved. No other body regions met the defined threshold of 10%.

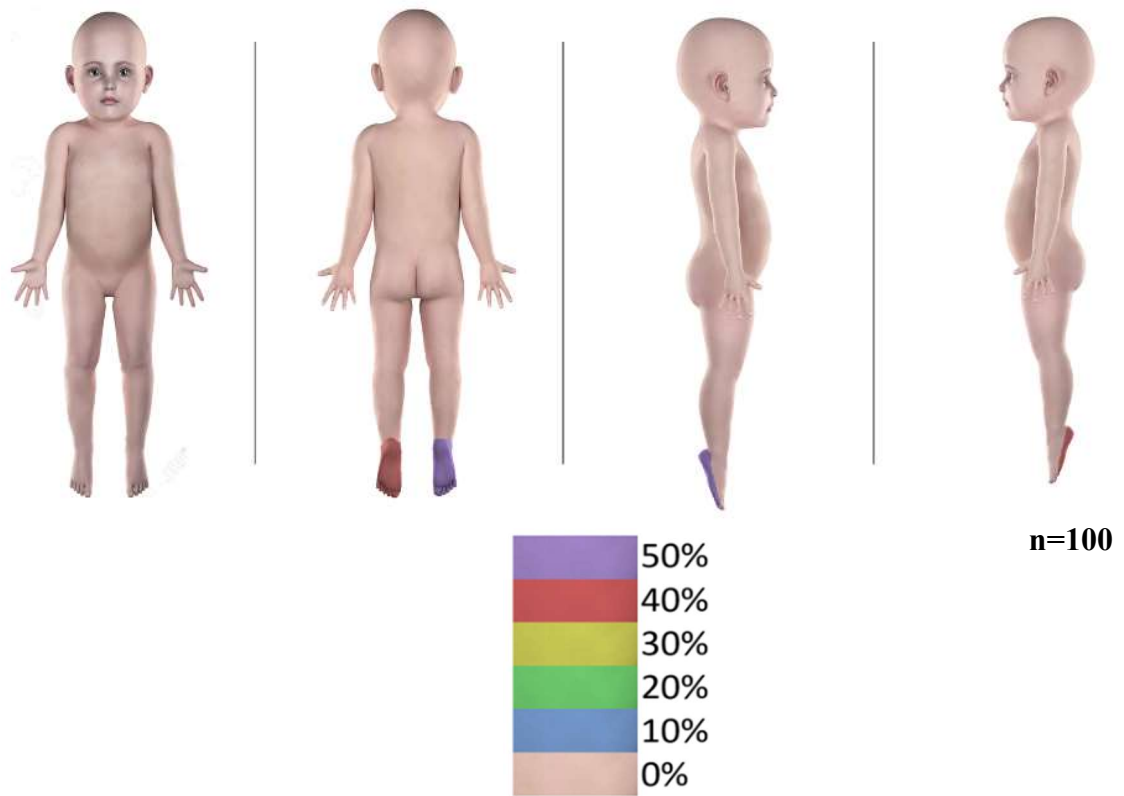


FIGURE 64 – First contact body contact map; legend represents percentage of falls involving contact to body region

## 2. Primary impact body map

The primary impact body map displayed the most common body regions involved in that phase of the fall (FIGURE 65). The palms of both hands were the most common body regions involved. The buttocks, anterior bilateral knees, and anterior bilateral shins were also often involved. The posterior forearms and lateral bilateral legs were sometimes but not always involved. No other body regions met the 10% threshold.

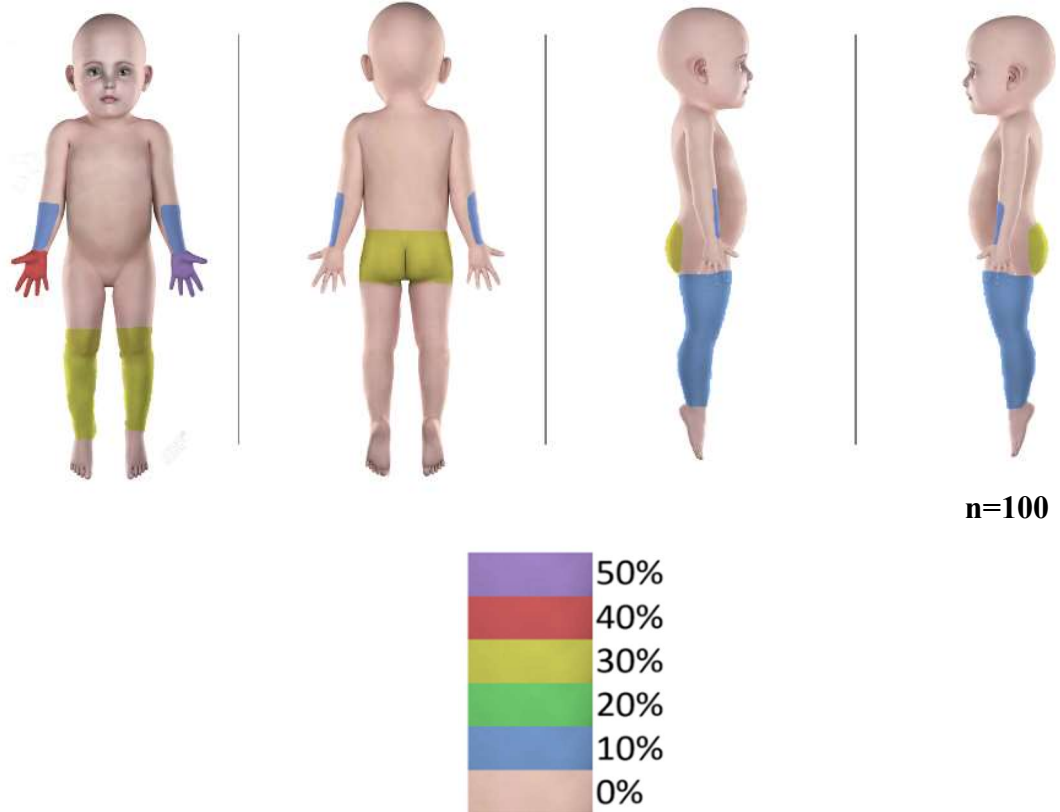


FIGURE 65 – Primary impact body impact map; Legend represents percentage of falls involving impact to body region

### 3. Secondary impact body map

The secondary impact body map displayed the most common body regions involved in that phase of the fall (FIGURE 66). The palms of both hands were the most common body regions involved. Not every fall involved a secondary impact; 42% of the falls involved a secondary impact. No other body regions met the 10% threshold.

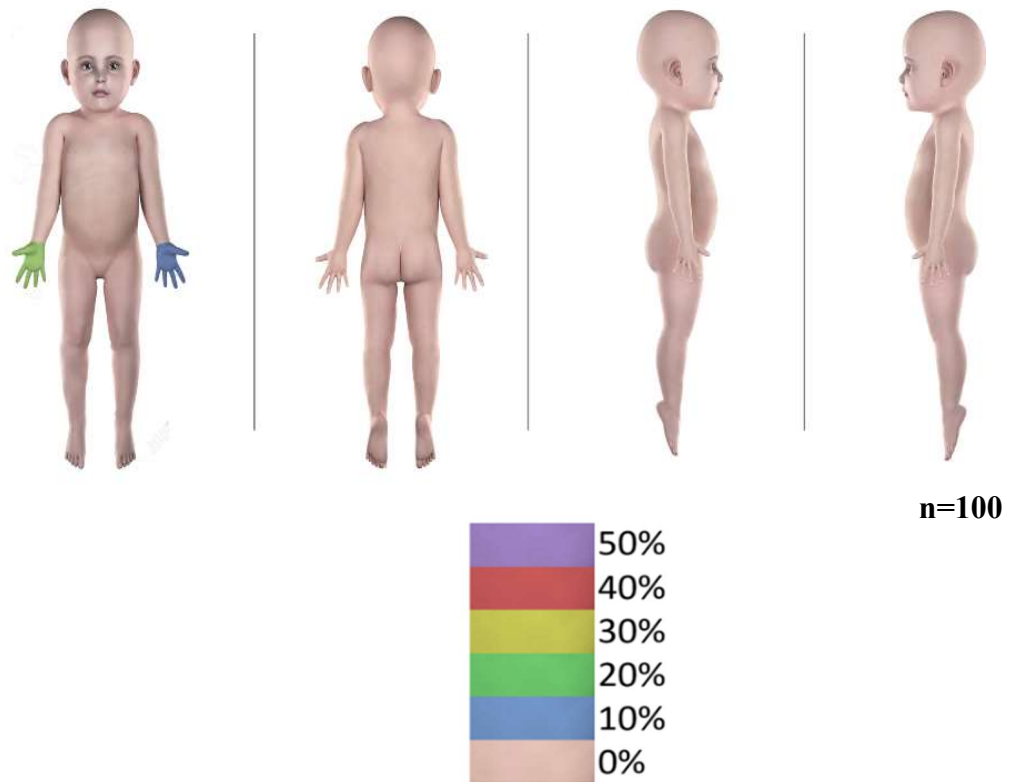


FIGURE 66 – Secondary impact body impact map; legend represent percentage of falls involving impact to body region

H. Specific aim 3: Characterize the biomechanics of falls involving young children in a childcare setting by fall characteristics.

1. Falls with SIM G activation

From the 100 collected video-recorded falls, 15% (n=15) resulted in activation of the SIM G device. However, one fall was disregarded because, while it resulted in two activations of the SIM G, it was out of view of the cameras and could not be verified. Out of the 14 verified falls, 2 falls (fall 57 and fall 97) resulted in more than one SIM G activation. These falls were reviewed to determine which activation corresponded to the respectful phase in the fall. It was determined that for fall 57, both the first and second SIM G activations corresponded to the impact phase of the fall. So, the greater SIM G activation was used for analysis and the lesser SIM G activation was disregarded. For fall 97, the first SIM G activation was determined to be from the fall initiation phase, when the subject collided with another child. This first activation was disregarded, and the second activation was determined to have occurred during the primary impact phase, so it was included in the analysis. Overall, 14 SIM G activations were used in this analysis. Most of the falls with SIM G activation involved male children (FIGURE 67). Specifically, every fall that involved a male child and SIM G activation involved the same subject (subject 4; no other male subjects experienced a fall that resulted in a SIM G activation). The average age of a child with a fall that resulted in a SIM G activation was  $19 \pm 2$  months.

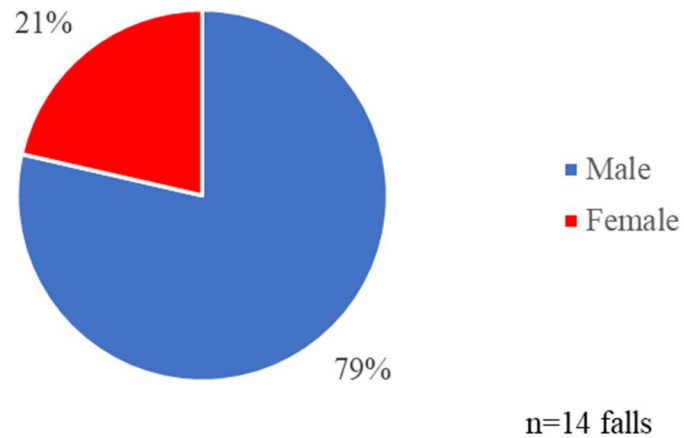


FIGURE 67 – Male vs. female subjects for falls with verified SIM G activation (n=14 falls)

FIGURE 68 displays peak resultant linear head acceleration (g) vs. peak resultant linear head velocity (m/s) across all falls with SIM G activation. FIGURE 69 displays peak resultant linear head acceleration (g) vs. peak resultant rotational head acceleration ( $\text{rad/s}^2$ ) across all falls with SIM G activation. FIGURE 70 displays peak resultant rotational head acceleration ( $\text{rad/s}^2$ ) vs. peak resultant rotational head velocity (rad/s) across all falls with SIM G activation. FIGURE 71 displays  $\text{HIC}_{15}$  vs. impact duration (ms) across all falls with SIM G activation. TABLE 14 displays the mean, standard deviations, and ranges for all head biomechanical measures across all verified SIM G activations.



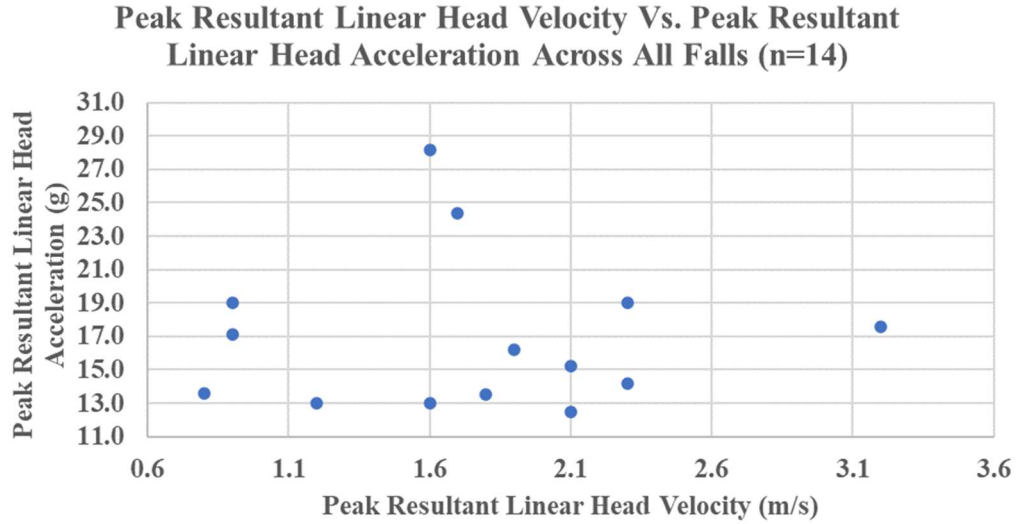


FIGURE 68 – Peak resultant linear head acceleration (g) vs. peak resultant linear head velocity (m/s) across all falls with SIM G activation.

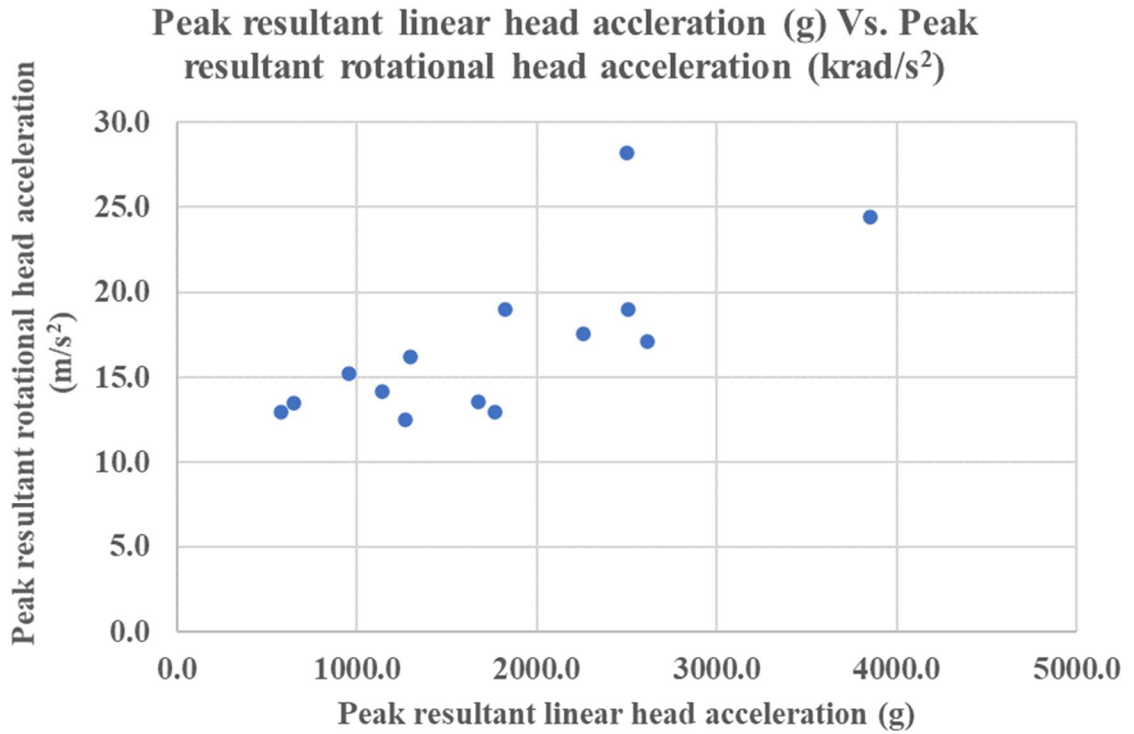


FIGURE 69 – Peak resultant linear head acceleration (g) vs. peak resultant rotational head acceleration ( $\text{rad/s}^2$ ) across all falls with SIM G activation.

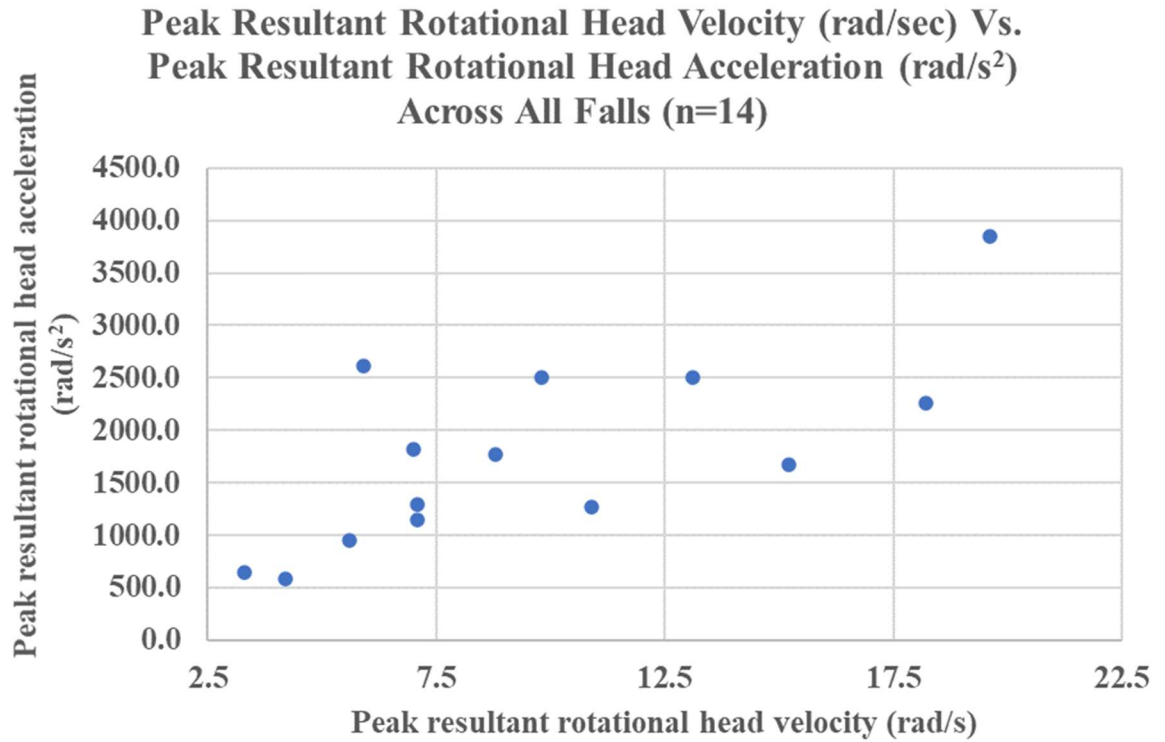


FIGURE 70 – Peak resultant rotational head acceleration ( $\text{rad/s}^2$ ) vs. peak resultant rotational head velocity (rad/s) across all falls with SIM G activation.

**Head Injury Criterion Vs. Impact Duration  
(ms) Across All Falls (n=14)**

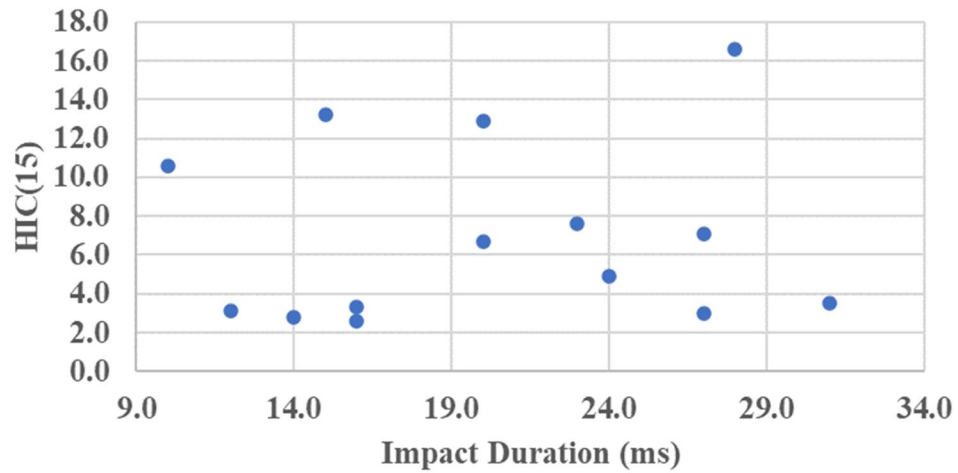


FIGURE 71 – HIC<sub>15</sub> vs. impact duration (ms) across all falls with SIM G activation.

TABLE 14

MEAN HEAD BIOMECHANICAL MEASURES ACROSS ALL VERIFIED SIM G  
ACTIVATIONS (N=14 ACTIVATIONS)

Biomechanical Measure	Mean ± SD	Range
Mean peak resultant linear head acceleration (g)	16.9 ± 4.6	12.5-28.2
Mean peak resultant linear head velocity (m/s)	1.7 ± 0.7	0.8-3.2
Mean peak resultant rotational head acceleration (rad/s <sup>2</sup> )	1778.0 ± 902.2	582.0-3853.0
Mean peak resultant rotational head velocity (rad/s)	9.7 ± 5.1	3.3-19.6
Mean HIC (15)	7.0 ± 4.6	2.6-16.6
Mean impact duration (ms)	20.2 ± 6.6	10.0-31.0

a. The fall with the largest peak resultant linear head acceleration (g)

The fall with the largest peak resultant linear head acceleration (g) from this sample was fall 72 (FIGURE 72), with a SIM G outcome of 28.2 g. This ground-type fall involved subject 4, a male child, who was initially jumping on a rug in his classroom. He lost control as he was jumping and fell rearward. He contacted his buttocks and right-hand palm on the rug surface, then continued to fall rearward. The primary impact involved his head occiput and his entire back. His left-hand palm also contacted the floor, and his head bumped a ball during the primary impact, which caused the ball to roll away. He was in a final supine position.



FIGURE 72 – Fall 72, the fall with the largest peak resultant linear head acceleration (28.2 g) from this sample

## 2. SIM G and Head Impacts

*H1: Head accelerations and velocities will be greater in falls with direct head impact than in falls without head impact.*

### a. Falls with SIM G activation and head impact

From the 14 verified SIM G activations, 50% (n=7) of the falls resulted in head impact (FIGURE 73). The average age of the child with a fall that resulted in a SIM G activation and head impact was  $20 \pm 1.6$  months.

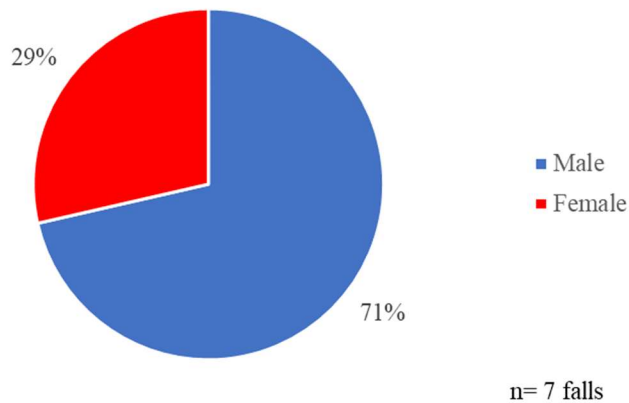


FIGURE 73 – Male vs. female subjects for falls with verified SIM G activations and head impact.

### b. Falls with SIM G activation and no head impact

From the 14 verified SIM G activations, 50% (n=7) of the falls resulted in no head impact (FIGURE 74). The average age of the child with a fall that resulted in a SIM G activation but no head impact was  $21 \pm 0.8$  months.

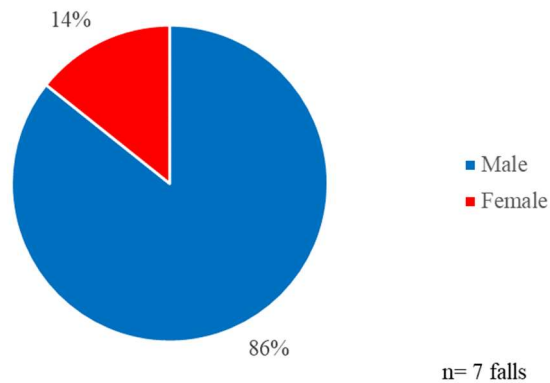


FIGURE 74 – Male vs. female subjects for falls with verified SIM G activations and no head impact.

c. Testing *HI* and comparing falls with SIM G activation and head vs. no head impact

TABLE 15 displays the collected data from all SIM G activations for falls that had head impact versus those that did not have head impact. Collected values include peak resultant linear head acceleration (g), peak resultant linear head velocity (m/s), peak resultant rotational head acceleration ( $\text{rad/s}^2$ ), peak resultant rotational head velocity (rad/s),  $\text{HIC}_{15}$ , and impact duration (ms). All data was tested for statistical difference ( $p < 0.05$ ). The only value that was found to have a significant difference was peak resultant rotational head acceleration ( $\text{rad/s}^2$ ), where the average value was larger for falls with head impact than for falls without head impact. Therefore, *HI* was rejected. It was determined that head accelerations and velocities were not significantly different in these falls with direct head impact compared to falls without head impact.

TABLE 15

MEAN HEAD BIOMECHANICAL MEASURES ACROSS ALL VERIFIED SIM G

ACTIVATION (N=14 FALLS)

Biomechanical Measure	Head impact (n=7)		No head impact (n=7)		p-value
	Mean $\pm$ SD	Range	Mean $\pm$ SD	Range	
PEAK RESULTANT LINEAR HEAD ACCELERATION (G)	18.8 $\pm$ 5.63	13.0-28.2	15.0 $\pm$ 2.45	12.5-19.0	0.141
PEAK RESULTANT LINEAR HEAD VELOCITY (M/S)	1.5 $\pm$ 0.53	0.8-2.3	1.9 $\pm$ 0.76	0.9-3.2	0.278
PEAK RESULTANT ROTATIONAL HEAD ACCELERATION (RAD/S <sup>2</sup> )	2316 $\pm$ 844	1299-3853	1240 $\pm$ 612	582-2258	0.021
PEAK RESULTANT ROTATIONAL HEAD VELOCITY (RAD/S)	11.4 $\pm$ 4.9	5.9-19.6	8.0 $\pm$ 5.1	3.3-18.2	0.240
HIC <sub>15</sub>	7.4 $\pm$ 4.7	2.6-13.2	6.5 $\pm$ 4.8	2.8-16.6	0.731
IMPACT DURATION (MS)	17.1 $\pm$ 5.7	10.0-27.0	23.3 $\pm$ 6.3	14.0-31.0	0.082

d. Comparing peak resultant linear head acceleration (g) for head impact vs. no head impact

The peak resultant linear head acceleration values for falls with head impact and falls without head impact were tested for normality. The data was normally distributed, so a two-sample T-test was performed. It was determined that there was no significant difference between the peak resultant linear head accelerations for falls with and without head impact ( $p=0.141$ ) (FIGURE 75).

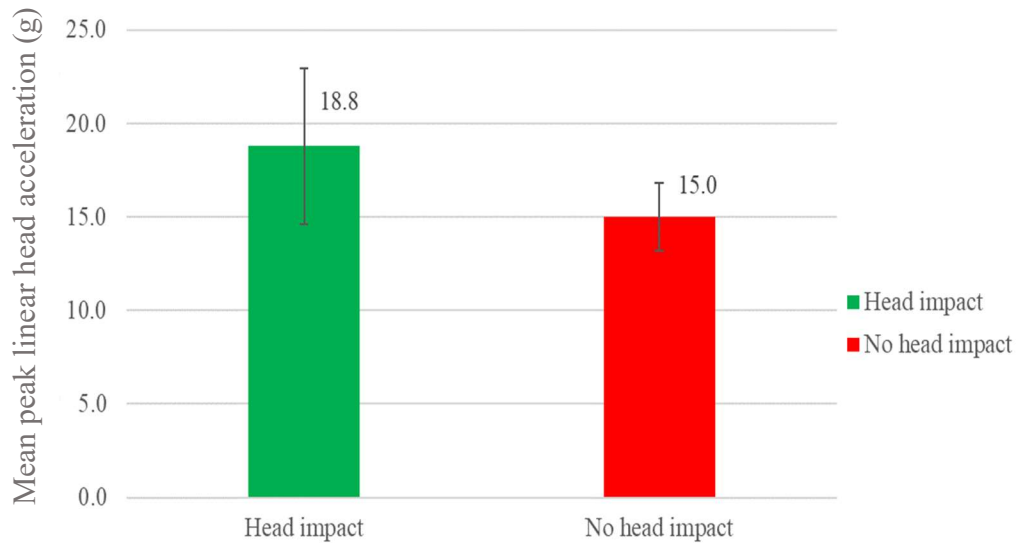


FIGURE 75 – Mean peak linear head acceleration (g) for falls with SIM G activation and head impact (n=7) vs. no head impact (n=7). Error bars represent 95% confidence interval.



e. Comparing peak resultant linear head velocity (m/s) for head impact vs. no head impact

The peak resultant linear head velocity values for falls with head impact and falls without head impact were tested for normality. The data was normally distributed, so a two-sample T-test was performed. It was determined that there was no significant difference between the peak resultant linear head velocities for falls with and without head impact ( $p=0.278$ ) (FIGURE 76).

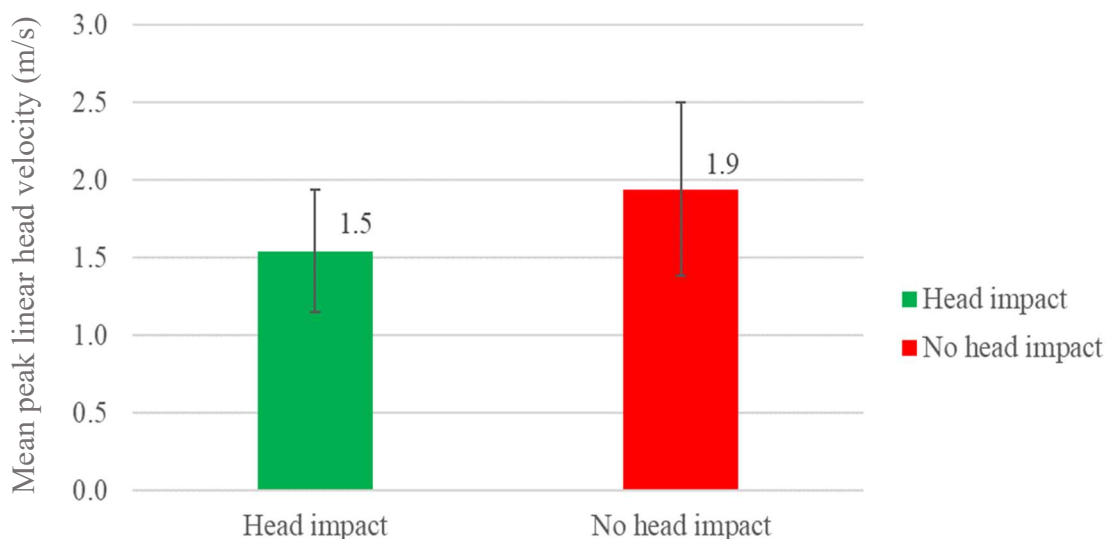


FIGURE 76 – Mean peak linear head velocity (m/s) for falls with SIM G activation and head impact ( $n=7$ ) vs. no head impact ( $n=7$ ). Error bars represent 95% confidence interval.

f. Comparing peak resultant rotational head acceleration ( $\text{rad/s}^2$ ) for head impact vs. no head impact

The peak resultant rotational head acceleration values for falls with head impact and falls without head impact were tested for normality. The data was normally

distributed, so a two-sample T-test was performed. It was determined that there was a significant difference between the peak resultant rotational head accelerations for falls with and without head impact ( $p=0.021$ ). The average value for falls with head impact was larger than the average value for falls without head impact (FIGURE 77).

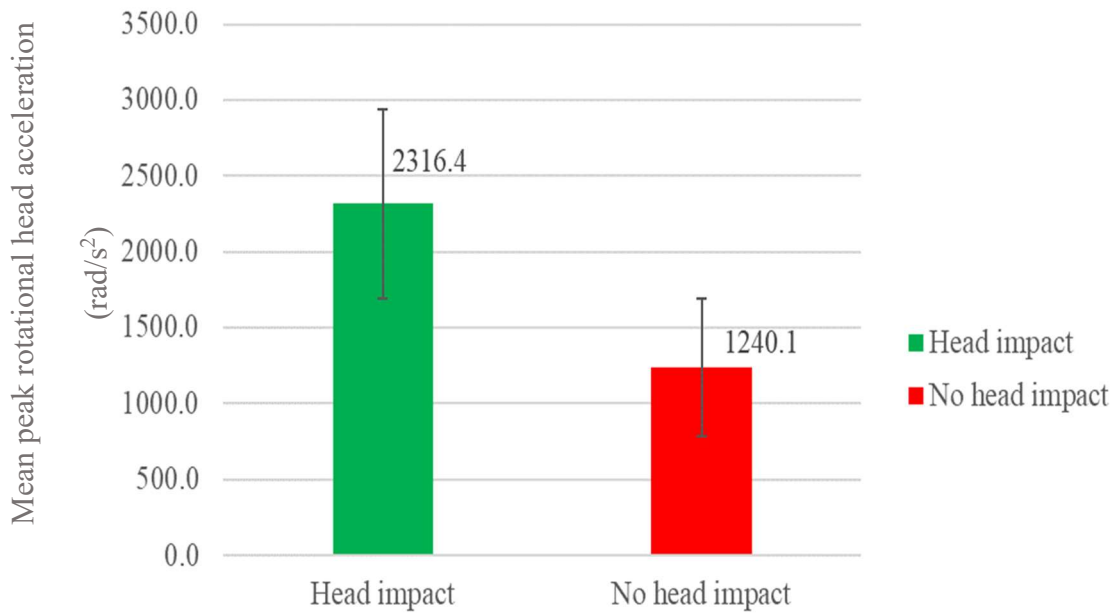


FIGURE 77 – Mean peak rotational head acceleration (rad/s<sup>2</sup>) for falls with SIM G activation and head impact (n=7) vs. no head impact (n=7). Error bars represent 95% confidence interval.

g. Comparing peak resultant rotational head velocity (rad/s) for head impact vs. no head impact

The peak resultant rotational head velocity values for falls with head impact and falls without head impact were tested for normality. The data was normally distributed, so a two-sample T-test was performed. It was determined that there was no significant

difference between the peak resultant rotational head velocities for falls with and without head impact ( $p=0.240$ ) (FIGURE 78).

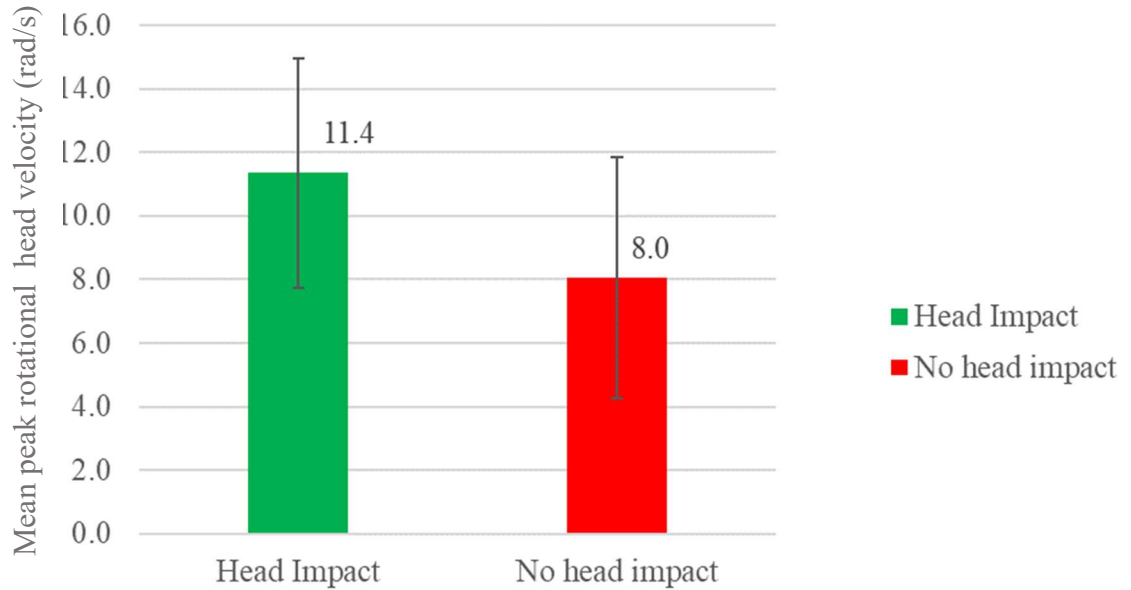


FIGURE 78 – Mean peak rotational head velocity (rad/s) for falls with SIM G activation and head impact ( $n=7$ ) vs. no head impact ( $n=7$ ). Error bars represent 95% confidence interval.

#### h. Comparing HIC<sub>15</sub> for head impact vs. no head impact

The HIC<sub>15</sub> values for falls with head impact and falls without head impact were tested for normality. The data was normally distributed, so a two-sample T-test was performed. It was determined that there was not a significant difference between the HIC<sub>15</sub> values for falls with and without head impact ( $p=0.731$ ) (FIGURE 79).

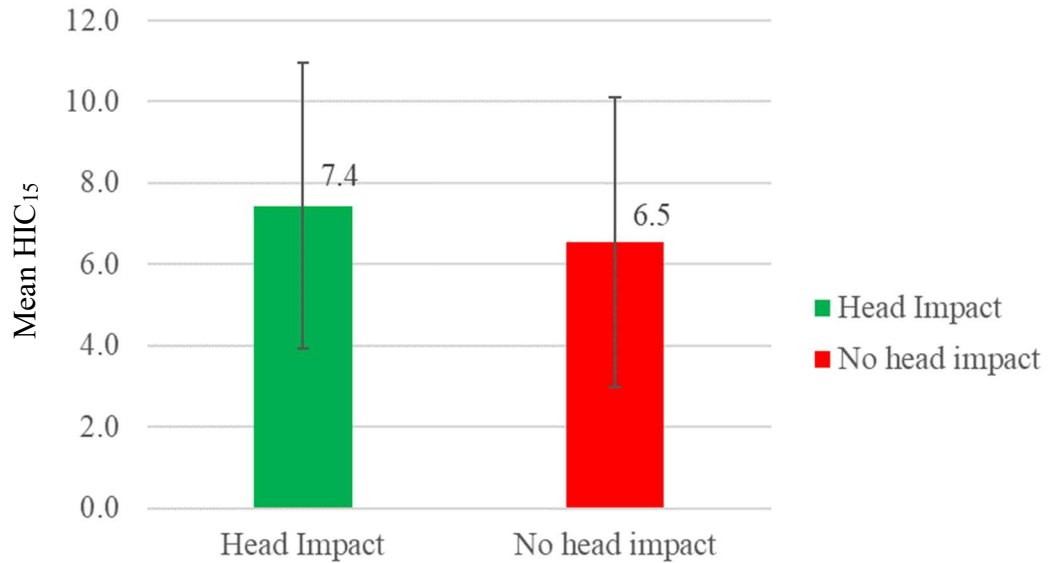


FIGURE 79 – Mean HIC<sub>15</sub> for falls with SIM G activation and head impact (n=7) vs. no head impact (n=7). Error bars represent 95% confidence interval.

i. Comparing impact time (ms) for head impact vs. no head impact

The impact duration values for falls with head impact and falls without head impact were tested for normality. The data was normally distributed, so a two-sample T-Test was performed. It was determined that there was no significant difference between the impact duration values for falls with and without head impact ( $p=0.082$ ) (FIGURE 80).

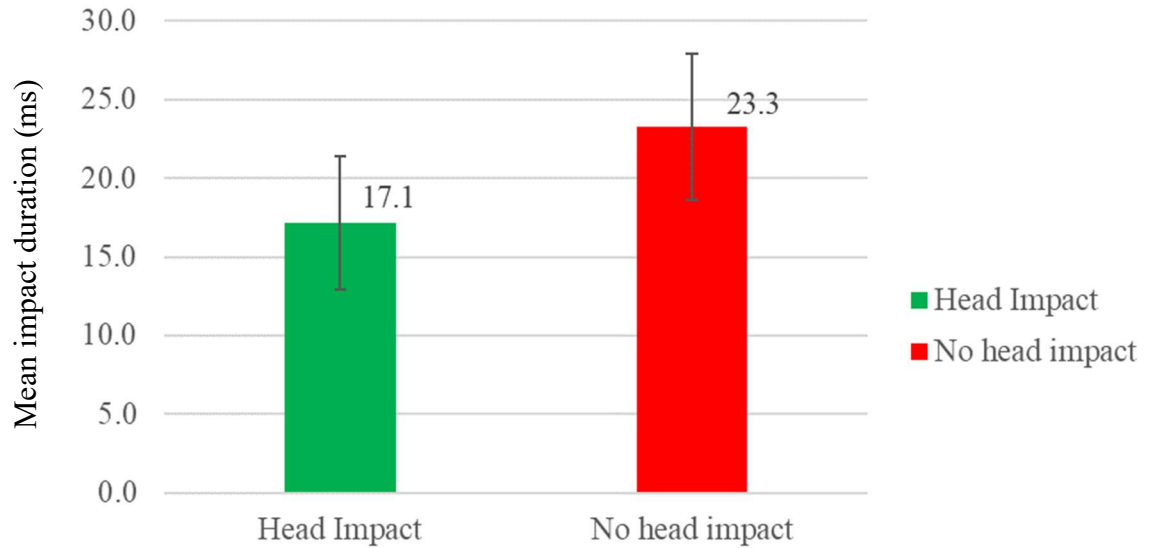


FIGURE 80 – Mean impact duration (ms) for falls with SIM G activation and head impact (n=7) vs. no head impact (n=7). Error bars represent 95% confidence interval.

3. Development of physics-based models for ATD feet-first falls and human subject childcare center falls with SIM G activation and primary head impact

a. Results for physics-based model predictions for replicated ATD feet-first falls

From the replicated ATD feet-first fall study that was used to validate the SIM G devices, the mean peak biomechanical measure values from two tested surfaces were used to compare to physics-based model outcomes (carpet (n=7) and linoleum (n=7)). For full results, see Appendix III. Each of the physics-based models (lumped mass, single rod, and inverted pendulum) were tested with each of the four methods (Table 9, reproduced here).

TABLE 9

METHODS USED TO EVALUATE THE PHYSICS-BASED MODELS

Method	Coefficient of restitution	Rebound Velocity	Starting Point	Phase <sup>1</sup>	Time duration
Method A	No	No	Conservation of energy	Crush phase only	½ Delta t
Method B	Yes	Yes	Conservation of energy	Crush and rebound phases	Delta t
Method C	Yes	Yes	Impulse set equal to momentum	Crush and rebound Phases	Delta t
Method D	No	No	Impulse set equal to momentum	Crush phase only	½ Delta t

<sup>1</sup>Phase of the fall referred to the primary head impact of the fall being evaluated; if only the crush phase was included, then rebound velocity was not included during evaluation; methods that evaluated crush and rebound phase included COR/rebound velocity.

Overall, it was determined that method A resulted in the most accurate values for head impact acceleration and velocity measures. Method D was more accurate for some PBMs but very inaccurate for others. Methods B and C resulted in similar yet inaccurate values for head impact acceleration and velocity measures. Therefore, only methods A and B will be presented in this section. See Appendix III for full results.

i. Replicated ATD feet-first falls onto carpet physics-based model outcomes

Percent error outcomes were obtained and reported for methods A and B used to analyze the lumped mass, single rod, and inverted pendulum physics-based models (TABLE 16).

TABLE 16

REPLICATED ATD FEET-FIRST FALLS ONTO CARPET METHODS A AND B  
 PERCENT ERROR OUTCOMES FOR PHYSICS-BASED MODELS AS COMPARED  
 TO MEAN PEAK SIM G OUTCOMES (N=7)

Model type	Biomechanical measures	Mean peak SIM G $\pm$ SD	METHOD A	METHOD B
LUMPED MASS	Linear Acceleration (g)	34 $\pm$ 1.9	14%	70%
	Change in Linear Velocity (m/s)	5.9 $\pm$ 0.6	39%	39%
	Angular Acceleration (rad/s <sup>2</sup> )	2085 $\pm$ 402	116%	223%
	Angular Velocity (rad/s)	7.14 $\pm$ 1.6	504%	505%
SINGLE ROD	Linear Acceleration (g)	34 $\pm$ 1.9	22%	194%
	Change in Linear Velocity (m/s)	5.9 $\pm$ 0.6	58%	7%
	Angular Acceleration (rad/s <sup>2</sup> )	2085 $\pm$ 402	48%	459%
	Angular Velocity (rad/s)	7.14 $\pm$ 1.6	312%	947%
INVERTED PENDULUM	Linear Acceleration (g)	34 $\pm$ 1.9	14%	70%
	Change in Linear Velocity (m/s)	5.9 $\pm$ 0.6	39%	39%
	Angular Acceleration (rad/s <sup>2</sup> )	2085 $\pm$ 402	116%	223%
	Angular Velocity (rad/s)	7.14 $\pm$ 1.6	504%	505%

From the percent error outcomes, it was determined that the most accurate physics-based models were the lumped mass and inverted pendulum; it was also determined that method A was the best method of analysis for these falls.

ii. Replicated ATD feet-first falls onto linoleum physics-based model outcomes

Percent error outcomes were obtained and reported for methods A and B used to analyze the lumped mass, single rod, and inverted pendulum physics-based models (TABLE 17). From the percent error outcomes, it was determined that the most accurate physics-based models were the lumped mass and inverted pendulum; it was also determined that method A was the best method of analysis for these falls.

TABLE 17

REPLICATED ATD FEET-FIRST FALLS ONTO LINOLEUM METHODS A AND B  
 PERCENT ERROR OUTCOMES FOR PHYSICS-BASED MODELS AS COMPARED  
 TO MEAN PEAK SIM G OUTCOMES (N=7)

Model type	Biomechanical measures	Mean peak SIM G $\pm$ SD	METHOD A	METHOD B
LUMPED MASS	Linear Acceleration (g)	38 $\pm$ 14.2	39%	87%
	Change in Linear Velocity (m/s)	6.51 $\pm$ 2	45%	45%
	Angular Acceleration (rad/s <sup>2</sup> )	2086 $\pm$ 402	195%	299%
	Angular Velocity (rad/s)	7.1 $\pm$ 1.6	504%	505%
SINGLE ROD	Linear Acceleration (g)	38 $\pm$ 14.2	5%	225%
	Change in Linear Velocity (m/s)	6.51 $\pm$ 2	62%	3%
	Angular Acceleration (rad/s <sup>2</sup> )	2086 $\pm$ 402	101%	591%
	Angular Velocity (rad/s)	7.1 $\pm$ 1.6	312%	947%
INVERTED PENDULUM	Linear Acceleration (g)	38 $\pm$ 14.2	39%	87%
	Change in Linear Velocity (m/s)	6.51 $\pm$ 2	45%	45%
	Angular Acceleration (rad/s <sup>2</sup> )	2086 $\pm$ 402	195%	299%
	Angular Velocity (rad/s)	7.1 $\pm$ 1.6	504%	505%



iii. Comparing replicated ATD feet-first fall dynamics and biomechanical outcomes

The replicated ATD feet-first fall video recordings were reviewed and the falls were categorized into their respective dynamic characterizations (TABLE 51, reproduced here).

TABLE 51

REPLICATE FALL DYNAMICS AND FREQUENCIES

Dynamics	Carpet surface frequency	Linoleum surface frequency
<b>A</b>	0	5
<b>B</b>	0	0
<b>C</b>	7	2

Because all carpet replicate feet-first falls resulted in the same dynamic type, they were not evaluated for difference in dynamics. However, for the falls onto the linoleum surface, five falls exhibited dynamic type A, and two falls exhibited dynamic type C. The fall outcomes were compared; all results may be found in Appendix III. Only overall results for methods A and B will be presented here. The first table includes the methods A and B outcomes for feet-first falls onto linoleum with dynamic type A (TABLE 18). The second table includes the methods A and B outcomes for feet-first falls onto linoleum with dynamic type C (TABLE 19).

TABLE 18

ATD FALLS ONTO LINOLEUM WITH DYNAMIC A METHODS A AND B  
 PERCENT ERROR OUTCOMES FOR PHYSICS-BASED MODELS AS COMPARED  
 TO MEAN PEAK SIM G OUTCOMES (N=5)

Model type	Biomechanical measures	Mean peak SIM G $\pm$ SD	METHOD A	METHOD B
LUMPED MASS	Linear Acceleration (g)	31 $\pm$ 1	70%	130%
	Change in Linear Velocity (m/s)	5.5 $\pm$ 0.6	35%	35%
	Angular Acceleration (rad/s <sup>2</sup> )	1900 $\pm$ 283	224%	338%
	Angular Velocity (rad/s)	7.3 $\pm$ 1.9	491%	491%
SINGLE ROD	Linear Acceleration (g)	31 $\pm$ 1	16%	298%
	Change in Linear Velocity (m/s)	5.5 $\pm$ 0.6	55%	15%
	Angular Acceleration (rad/s <sup>2</sup> )	1900 $\pm$ 283	121%	658%
	Angular Velocity (rad/s)	7.3 $\pm$ 1.9	303%	924%
INVERTED PENDULUM	Linear Acceleration (g)	31 $\pm$ 1	70%	130%
	Change in Linear Velocity (m/s)	5.5 $\pm$ 0.6	35%	35%
	Angular Acceleration (rad/s <sup>2</sup> )	1900 $\pm$ 283	224%	338%
	Angular Velocity (rad/s)	7.3 $\pm$ 1.9	491%	491%

TABLE 19

ATD FALLS ONTO LINOLEUM WITH DYNAMIC C METHODS A AND B  
 PERCENT ERROR OUTCOMES FOR PHYSICS-BASED MODELS AS COMPARED  
 TO MEAN PEAK SIM G OUTCOMES (N=2)

Model type	Biomechanical measures	Mean peak SIM G $\pm$ SD	METHOD A	METHOD B
LUMPED MASS	Linear Acceleration (g)	56 $\pm$ 17	6%	27%
	Change in Linear Velocity (m/s)	9.1 $\pm$ 2.3	60%	60%
	Angular Acceleration (rad/s <sup>2</sup> )	2550 $\pm$ 212	141%	226%
	Angular Velocity (rad/s)	6.7 $\pm$ 0.4	544%	544%
SINGLE ROD	Linear Acceleration (g)	56 $\pm$ 17	36%	120%
	Change in Linear Velocity (m/s)	9.1 $\pm$ 2.3	73%	31%
	Angular Acceleration (rad/s <sup>2</sup> )	2550 $\pm$ 212	65%	465%
	Angular Velocity (rad/s)	6.7 $\pm$ 0.4	339%	1016%
INVERTED PENDULUM	Linear Acceleration (g)	56 $\pm$ 17	6%	27%
	Change in Linear Velocity (m/s)	9.1 $\pm$ 2.3	60%	60%
	Angular Acceleration (rad/s <sup>2</sup> )	2550 $\pm$ 212	141%	226%
	Angular Velocity (rad/s)	6.7 $\pm$ 0.4	544%	544%

b. Results for parameter sensitivity analysis of rotational motion for replicated ATD feet-first falls

To explore how the selected radius of rotation effects the rotational motion outcomes during a fall, a parameter sensitivity analysis was performed on the replicated ATD feet-first falls. Because analysis Method A resulted in the most accurate outcomes, only A was used in this PSA. The lengths of rotation were varied (TABLE 10, reproduced here).

TABLE 10

RADIUS OF ROTATION LENGTHS FOR PARAMETER SENSITIVITY ANALYSIS

Radius	Operationalization
About the neck	From the head center of gravity to base of the neck (in line with the shoulders) length (m)
About the hips	From the head center of gravity to hip length (m)
About the knees	From the head center of center of gravity to the knees length (m)
About the soles	From the head center of gravity to the soles of the feet length (m)

- i. Replicated ATD feet-first falls onto carpet parameter sensitivity analysis outcomes

The measurements used for the ATD were reported (TABLE 20) and the mean peak SIM G values were reported (TABLE 21). All outcomes for the lumped mass, single rod, and inverted pendulum were reported (TABLE 22).

TABLE 20

ATD MEASUREMENTS USED FOR PARAMETER SENSITIVITY ANALYSIS

Length with respect to ATD	Measurement (m)
About the neck (m)	0.084
About the hips (sitting height, m)	0.475
About the knees (Head COM to knees, m)	0.503
Sole to head COM (m)	0.67

TABLE 21

MEAN PEAK SIM G VALUES FROM REPLICATED ATD FEET-FIRST FALLS  
ONTO CARPET (N=7)

BIOMECHANICAL MEASURE	MEAN PEAK SIM G ± SD
Linear Acceleration (g)	34 ± 1.9
Change in Linear Velocity (m/s)	5.9 ± 0.6
Angular Acceleration (rad/s <sup>2</sup> )	2085.71 ± 402
Angular Velocity (rad/s)	7.14 ± 1.6

TABLE 22

PARAMETER SENSITIVITY ANALYSIS RESULTS (METHOD A) REPLICATED  
 ATD FEET-FIRST FALLS ONTO CARPET, AS COMPARED TO SIM G (N=7)

PHYSICS-BASED MODEL	PHYSICS-BASED MODEL PARAMETER SENSITIVITY ANALYSIS OUTCOMES				Percent error				
	ROTATIONAL MOTION	About the neck	About the hips	About the knees	About the soles	About the neck	About the hips	About the knees	About the soles
LUMPED MASS	Angular Acceleration (rad/s <sup>2</sup> )	4519	799	755	567	117%	62%	64%	73%
	Angular Velocity (rad/s)	42.9	7.6	7.2	5.4	504%	7%	1%	24%
SINGLE ROD	Angular Acceleration (rad/s <sup>2</sup> )	3082	545	515	386	48%	74%	75%	81%
	Angular Velocity (rad/s)	29.8	5.3	5.0	3.7	314%	26%	30%	47%
INVERTED PENDULUM	Angular Acceleration (rad/s <sup>2</sup> )	4519	799	755	567	117%	62%	64%	73%
	Angular Velocity (rad/s)	42.9	7.6	7.2	5.4	504%	7%	1%	24%

ii. Replicated ATD feet-first falls onto linoleum parameter sensitivity analysis outcomes

The measurements used for the ATD were reported (TABLE 20, as this involved the same ATD) and the mean peak SIM G values were reported (TABLE 23). All outcomes for the lumped mass, single rod, and inverted pendulum were reported (TABLE 24).

TABLE 23

MEAN PEAK SIM G VALUES FROM REPLICATED ATD FEET-FIRST FALLS ONTO LINOLEUM (N=7)

BIOMECHANICAL MEASURE	MEAN PEAK SIM G ± SD
Linear Acceleration (g)	38 ± 14.2
Change in Linear Velocity (m/s)	6.51 ± 2
Angular Acceleration (rad/s <sup>2</sup> )	2086 ± 402
Angular Velocity (rad/s)	7.1 ± 1.6

TABLE 24

PARAMETER SENSITIVITY ANALYSIS RESULTS (METHOD A) REPLICATED ATD FEET-FIRST FALLS ONTO LINOLEUM, AS COMPARED TO SIM G (N=7)

PHYSICS-BASED MODEL	PHYSICS-BASED MODEL PARAMETER SENSITIVITY ANALYSIS OUTCOMES				Percent error				
	ROTATIONAL MOTION	About the neck	About the hips	About the knees	About the soles	About the neck	About the hips	About the knees	About the soles
Lumped mass	Angular Acceleration (rad/s <sup>2</sup> )	6162	1090	1029	773	195%	48%	51%	63%
	Angular Velocity (rad/s)	42.9	7.6	7.2	5.4	504%	7%	1%	24%
Single rod	Angular Acceleration (rad/s <sup>2</sup> )	4204	743	702	527	102%	64%	66%	75%
	Angular Velocity (rad/s)	29.8	5.3	5.0	3.7	314%	26%	30%	47%
Inverted pendulum	Angular Acceleration (rad/s <sup>2</sup> )	6190	1095	1034	776	197%	48%	50%	63%
	Angular Velocity (rad/s)	42.9	7.6	7.2	5.4	504%	7%	1%	24%

iii. Replicated ATD feet-first falls onto linoleum with dynamic A parameter sensitivity analysis outcomes

The measurements used for the ATD were reported (TABLE 20, as this involved the same ATD) and the mean peak SIM G values for falls onto linoleum with dynamic A (n=5) were reported (TABLE 25). All outcomes for the lumped mass, single rod, and inverted pendulum were reported (TABLE 26).

TABLE 25

MEAN PEAK SIM G VALUES FROM REPLICATED ATD FEET-FIRST FALLS ONTO LINOLEUM WITH DYNAMIC A (N=5)

Biomechanical measure	Mean peak SIM G $\pm$ SD
Linear Acceleration (g)	31 $\pm$ 1
Change in Linear Velocity (m/s)	5.5 $\pm$ 0.6
Angular Acceleration (rad/s <sup>2</sup> )	1900 $\pm$ 283
Angular Velocity (rad/s)	7.3 $\pm$ 1.9

TABLE 26

PARAMETER SENSITIVITY ANALYSIS RESULTS (METHOD A) REPLICATED ATD FEET-FIRST FALLS ONTO LINOLEUM WITH DYNAMIC A (N=5), AS COMPARED TO SIM G

PHYSICS-BASED MODEL	PHYSICS-BASED MODEL PARAMETER SENSITIVITY ANALYSIS OUTCOMES				Percent error				
	ROTATIONAL MOTION	About the neck	About the hips	About the knees	About the soles	About the neck	About the hips	About the knees	About the soles
Lumped mass	Angular Acceleration (rad/s <sup>2</sup> )	6162	1090	1029	773	224%	43%	46%	59%
	Angular Velocity (rad/s)	43.0	7.6	7.2	5.4	489%	4%	2%	26%
Single rod	Angular Acceleration (rad/s <sup>2</sup> )	4204	743	702	527	121%	61%	63%	72%
	Angular Velocity (rad/s)	29.4	5.2	4.9	3.7	303%	29%	33%	49%
Inverted pendulum	Angular Acceleration (rad/s <sup>2</sup> )	6190	1095	1034	776	226%	42%	46%	59%
	Angular Velocity (rad/s)	43.1	7.6	7.2	5.4	490%	4%	2%	26%

iv. Replicated ATD feet-first falls onto linoleum with dynamic C parameter sensitivity analysis outcomes

The measurements used for the ATD were reported (TABLE 20, as this involved the same ATD) and the mean peak SIM G values for falls onto linoleum with dynamic C (n=2) were reported (TABLE 27). All outcomes for the lumped mass, single rod, and inverted pendulum were reported (TABLE 28).



TABLE 27

MEAN PEAK SIM G VALUES FROM REPLICATED ATD FEET-FIRST FALLS ONTO LINOLEUM WITH DYNAMIC C (N=2)

Biomechanical measure	Mean peak SIM G ± SD
Linear Acceleration (g)	56 ± 17
Change in Linear Velocity (m/s)	9.1 ± 2.3
Angular Acceleration (rad/s <sup>2</sup> )	2550 ± 212
Angular Velocity (rad/s)	6.7 ± 0.4

TABLE 28

PARAMETER SENSITIVITY ANALYSIS RESULTS FOR REPLICATED ATD FEET-FIRST FALLS ONTO LINOLEUM WITH DYNAMIC C (N=2), AS COMPARED TO SIM G

PHYSICS-BASED MODEL	PHYSICS-BASED MODEL PARAMETER SENSITIVITY ANALYSIS OUTCOMES				Percent error				
	ROTATIONAL MOTION	About the neck	About the hips	About the knees	About the soles	About the neck	About the hips	About the knees	About the soles
Lumped mass	Angular Acceleration (rad/s <sup>2</sup> )	6162	1090	1029	773	142%	57%	60%	70%
	Angular Velocity (rad/s)	42.9	7.6	7.2	5.4	543%	14%	7%	19%
Single rod	Angular Acceleration (rad/s <sup>2</sup> )	4204	743	702	527	65%	71%	72%	79%
	Angular Velocity (rad/s)	29.8	5.3	5.0	3.7	339%	22%	27%	45%
Inverted pendulum	Angular Acceleration (rad/s <sup>2</sup> )	6190	1095	1034	776	143%	57%	59%	70%
	Angular Velocity (rad/s)	42.9	7.6	7.2	5.4	543%	14%	7%	19%

c. Results for physics-based model predictions for subset of childcare center falls with primary head impact (n=8)

The complete dataset for the childcare center study was searched for falls with both a verified SIM G activation and primary head impact. Videos of falls that matched these criteria were reviewed. Falls that were selected for simulation with physics-based models were those that were not impeded by another person(s) (all of the falls selected only involved the subject). Furthermore, qualitative assessment was used to choose falls that had simple dynamics. In other words, falls were selected when they had distinct impacts

that were easy to visualize from the video recordings. Falls were not selected if a majority of the recording was blocked by furniture, a teacher/student, etc. Falls were also not selected when there were multiple impacts (e.g., if a child fell down more than one step on a staircase). After reviewing the full dataset with the selection criteria, seven falls were selected for simulation with the physics-based models. However, one fall (fall 676) resulted in two distinct head impacts with two SIM G activations. Because there was an appreciable difference between the first head impact and the second head impact, it was determined that the two SIM G activations could be compared separately with two different physics-based model analyses. So, this resulted in eight (n=8) childcare center falls for simulation with physics-based models. See Appendix III for screenshots and a brief narration of all falls chosen for simulation.

The biomechanical measure values from the simulated childcare center falls with primary head impact and SIM G outcomes (n=8 falls) were used to compare to physics-based model outcomes. For full results, see Appendix III. Each of the physics-based models (lumped mass, single rod, and inverted pendulum) were tested with each of the four methods (Table 9, reproduced here).

TABLE 9

## METHODS USED TO EVALUATE THE PHYSICS-BASED MODELS

Method	Coefficient of restitution	Rebound Velocity	Starting Point	Phase <sup>1</sup>	Time duration
Method A	No	No	Conservation of energy	Crush phase only	½ Delta t
Method B	Yes	Yes	Conservation of energy	Crush and rebound phases	Delta t
Method C	Yes	Yes	Impulse set equal to momentum	Crush and rebound Phases	Delta t
Method D	No	No	Impulse set equal to momentum	Crush phase only	½ Delta t

<sup>1</sup>Phase of the fall referred to the primary head impact of the fall being evaluated; if only the crush phase was included, then rebound velocity was not included during evaluation; methods that evaluated crush and rebound phase included COR/rebound velocity.

Overall, it was determined that method A resulted in the most accurate values for head impact acceleration and velocity measures. Method D was more accurate for some PBMs but very inaccurate for others. Methods B and C resulted in similar yet inaccurate values for head impact acceleration and velocity measures. Therefore, only methods A and B will be presented in this section (TABLE 29 and TABLE 30, respectively). See Appendix III for full results.

TABLE 29

OVERALL PERCENT ERROR OUTCOMES FOR METHOD A ANALYSIS OF SIMULATED CHILDCARE CENTER FALLS FOR LUMPED MASS, SINGLE ROD, AND INVERTED PENDULUM PHYSICS-BASED MODELS AS COMPARED TO MEAN PEAK SIM G OUTCOMES (N=8)

SIM G OUTPUTS			MODEL METHOD A RESULTS		
Fall #	Biomechanical measures	SIM G	Lumped mass	Single rod	Inverted pendulum
146	Linear Acceleration (g)	15	24%	15%	24%
	Change in Linear Velocity (m/s)	1.5	47%	0%	47%
	Angular Acceleration (rad/s <sup>2</sup> )	1145	12%	40%	12%
	Angular Velocity (rad/s)	11.3	8%	27%	8%
238	Linear Acceleration (g)	18	0%	31%	0%
	Change in Linear Velocity (m/s)	3.1	19%	19%	19%
	Angular Acceleration (rad/s <sup>2</sup> )	1281	23%	47%	23%
	Angular Velocity (rad/s)	17.5	15%	21%	15%
241	Linear Acceleration (g)	14	36%	8%	36%
	Change in Linear Velocity (m/s)	1.7	18%	18%	18%
	Angular Acceleration (rad/s <sup>2</sup> )	1151	16%	43%	16%
	Angular Velocity (rad/s)	9.5	10%	25%	10%
321	Linear Acceleration (g)	12	47%	0%	47%
	Change in Linear Velocity (m/s)	1.7	41%	0%	41%
	Angular Acceleration (rad/s <sup>2</sup> )	599	48%	1%	48%
	Angular Velocity (rad/s)	11.9	4%	29%	4%
516	Linear Acceleration (g)	31	5%	35%	5%
	Change in Linear Velocity (m/s)	1.3	112%	45%	115%
	Angular Acceleration (rad/s <sup>2</sup> )	2336	18%	44%	18%
	Angular Velocity (rad/s)	8.5	117%	48%	117%
545	Linear Acceleration (g)	50	6%	36%	6%
	Change in Linear Velocity (m/s)	1.8	78%	22%	78%
	Angular Acceleration (rad/s <sup>2</sup> )	5388	55%	69%	55%
	Angular Velocity (rad/s)	13.3	28%	13%	28%
676 (1)	Linear Acceleration (g)	18	0%	32%	0%
	Change in Linear Velocity (m/s)	2.5	12%	40%	12%
	Angular Acceleration (rad/s <sup>2</sup> )	1159	20%	45%	20%
	Angular Velocity (rad/s)	14.8	20%	45%	20%
676 (2)	Linear Acceleration (g)	13	89%	29%	89%
	Change in Linear Velocity (m/s)	1.6	75%	19%	75%
	Angular Acceleration (rad/s <sup>2</sup> )	1684	25%	49%	25%
	Angular Velocity (rad/s)	12.3	18%	19%	18%
Percent error categories:		0.0% to 25.0%	25.01% to 50.0%	50.01% to 100.0%	≥ 100.01%

TABLE 30

OVERALL PERCENT ERROR OUTCOMES FOR METHOD B ANALYSIS OF SIMULATED CHILDCARE CENTER FALLS FOR LUMPED MASS, SINGLE ROD, AND INVERTED PENDULUM PHYSICS-BASED MODELS AS COMPARED TO MEAN PEAK SIM G OUTCOMES (N=8)

SIM G OUTPUTS			MODEL METHOD B RESULTS		
Fall #	Biomechanical measures	SIM G	Lumped mass	Single rod	Inverted pendulum
146	Linear Acceleration (g)	15	57%	171%	57%
	Change in Linear Velocity (m/s)	1.5	47%	153%	47%
	Angular Acceleration (rad/s <sup>2</sup> )	1145	11%	92%	11%
	Angular Velocity (rad/s)	11.3	8%	86%	8%
238	Linear Acceleration (g)	18	56%	172%	57%
	Change in Linear Velocity (m/s)	3.1	19%	106%	19%
	Angular Acceleration (rad/s <sup>2</sup> )	1281	20%	109%	21%
	Angular Velocity (rad/s)	17.5	15%	100%	16%
241	Linear Acceleration (g)	14	92%	232%	92%
	Change in Linear Velocity (m/s)	1.7	18%	106%	18%
	Angular Acceleration (rad/s <sup>2</sup> )	1151	19%	105%	18%
	Angular Velocity (rad/s)	9.5	10%	90%	10%
321	Linear Acceleration (g)	12	85%	221%	85%
	Change in Linear Velocity (m/s)	1.7	41%	147%	41%
	Angular Acceleration (rad/s <sup>2</sup> )	599	87%	223%	87%
	Angular Velocity (rad/s)	11.9	5%	81%	5%
516	Linear Acceleration (g)	31	34%	131%	34%
	Change in Linear Velocity (m/s)	1.3	115%	269%	115%
	Angular Acceleration (rad/s <sup>2</sup> )	2336	16%	101%	16%
	Angular Velocity (rad/s)	8.5	116%	275%	116%
545	Linear Acceleration (g)	50	32%	128%	32%
	Change in Linear Velocity (m/s)	1.8	78%	211%	78%
	Angular Acceleration (rad/s <sup>2</sup> )	5388	37%	9%	37%
	Angular Velocity (rad/s)	13.3	28%	122%	28%
676 (1)	Linear Acceleration (g)	18	54%	167%	54%
	Change in Linear Velocity (m/s)	2.5	12%	56%	8%
	Angular Acceleration (rad/s <sup>2</sup> )	1159	24%	114%	24%
	Angular Velocity (rad/s)	14.8	20%	39%	20%
676 (2)	Linear Acceleration (g)	13	197%	414%	197%
	Change in Linear Velocity (m/s)	1.6	75%	200%	75%
	Angular Acceleration (rad/s <sup>2</sup> )	1684	18%	105%	18%
	Angular Velocity (rad/s)	12.3	18%	105%	18%
Percent error categories:		0.0% to 25.0%	25.01% to 50.0%	50.01% to 100.0%	≥ 100.01%

d. Results for parameter sensitivity analysis of rotational motion childcare center falls with SIM G activation and primary head impact

To explore how the selected radius of rotation effects the rotational motion outcomes during a fall, a parameter sensitivity analysis was performed on the simulated childcare center falls. Because analysis Method A resulted in the most accurate outcomes, only A was used in this PSA. The lengths of rotation were varied (TABLE 10, reproduced here).

TABLE 10

RADIUS OF ROTATION LENGTHS FOR PARAMETER SENSITIVITY ANALYSIS

<b>Radius</b>	<b>Operationalization</b>
<b>About the neck</b>	From the head center of gravity to base of the neck (in line with the shoulders) length (m)
<b>About the hips</b>	From the head center of gravity to hip length (m)
<b>About the knees</b>	From the head center of center of gravity to the knees length (m)
<b>About the soles</b>	From the head center of gravity to the soles of the feet length (m)

i. Parameter sensitivity analysis outcomes for fall 146

The parameter sensitivity analysis was performed on childcare center fall 146, with the radius of rotation set to the respective subject’s measurements, and the rotational

motion outcomes were compared to the original SIM G outcomes (TABLE 31). At the time of the anthropometric measurements for this subject, the subject was not cooperative and only full height and chin to sole height measurements were obtained. Therefore, lengths for the parameter sensitivity analysis were estimated from published children anthropometrics (Snyder et al., 1975). The height for this subject fit the height for the fifth percentile measurements for female children of her age, so these 5<sup>th</sup> percentile measurements were used. The overall outcomes were reported (TABLE 32).

TABLE 31

SUBJECT 11 PARAMETER SENSITIVITY ANALYSIS MEASUREMENTS AND FALL 146 SIM G OUTCOMES

Subject 11		FALL 146 BIOMECHANICAL OUTCOMES	
Length wrt Body region:	Value:	OUTCOME	SIM G OUTCOME
About the neck (m)	0.182	Linear Acceleration (g)	15
About the hips (Hip to head COM, m)	0.397	Change in Linear Velocity (m/s)	1.5
About the knees (Knees to head COM, m)	0.585	Angular Acceleration (rad/s <sup>2</sup> )	1145
About the soles (Soles to head COM, m)	0.681	Angular Velocity (rad/s)	11.3

TABLE 32

OVERALL PARAMETER SENSITIVITY ANALYSIS OUTCOMES FOR  
SIMULATED CHILDCARE CENTER FALL 146

PHYSICS-BASED MODEL	FALL 146								
	PHYSICS-BASED MODEL PARAMETER SENSITIVITY ANALYSIS OUTCOMES				PERCENT ERROR				
	ROTATIONAL MOTION	About the neck	About the hips	About the knees	About the soles	About the neck	About the hips	About the knees	About the soles
LUMPED MASS	Angular Acceleration (rad/s <sup>2</sup> )	1006	462	313	269	12%	60%	73%	77%
	Angular Velocity (rad/s)	12.1	5.5	3.8	3.2	7%	51%	67%	71%
SINGLE ROD	Angular Acceleration (rad/s <sup>2</sup> )	686	315	213	183	40%	73%	81%	84%
	Angular Velocity (rad/s)	8.2	3.8	2.6	2.2	27%	67%	77%	80%
INVERTED PENDULUM	Angular Acceleration (rad/s <sup>2</sup> )	1024	470	319	274	11%	59%	72%	76%
	Angular Velocity (rad/s)	12.1	5.5	3.8	3.2	7%	51%	67%	71%

ii. Parameter sensitivity analysis outcomes for fall 238

The parameter sensitivity analysis was performed on childcare center fall 238, with the radius of rotation set to the respective subject’s measurements, and the rotational motion outcomes were compared to the original SIM G outcomes (TABLE 33). At the time of the anthropometric measurements for this subject, the subject was not cooperative and only full height and chin to sole height measurements were obtained. Therefore, lengths for the parameter sensitivity analysis were estimated from published children anthropometrics (Snyder et al., 1975). The height for this subject fit the height for the fifth percentile measurements for female children of her age, so these 5<sup>th</sup> percentile measurements were used. The overall outcomes were reported (TABLE 34).



TABLE 33

SUBJECT 11 PARAMETER SENSITIVITY ANALYSIS MEASUREMENTS AND FALL 238 SIM G OUTCOMES

Subject 11		FALL 238 BIOMECHANICAL OUTCOMES	
Length wrt Body region:	Value:	OUTCOME	SIM G OUTCOME
About the neck (m)	0.182	Linear Acceleration (g)	18
About the hips (Hip to head COM, m)	0.397	Change in Linear Velocity (m/s)	3.1
About the knees (Knees to head COM, m)	0.585	Angular Acceleration (rad/s <sup>2</sup> )	1281
About the soles (Soles to head COM, m)	0.681	Angular Velocity (rad/s)	17.5

TABLE 34

OVERALL PARAMETER SENSITIVITY ANALYSIS OUTCOMES FOR SIMULATED CHILDCARE CENTER FALL 238

PHYSICS-BASED MODEL	FALL 238								
	PHYSICS-BASED MODEL PARAMETER SENSITIVITY ANALYSIS OUTCOMES				PERCENT ERROR				
	ROTATIONAL MOTION	About the neck	About the hips	About the knees	About the soles	About the neck	About the hips	About the knees	About the soles
LUMPED MASS	Angular Acceleration (rad/s <sup>2</sup> )	989	454	308	265	23%	65%	76%	79%
	Angular Velocity (rad/s)	20.3	9.3	6.3	5.4	16%	47%	64%	69%
SINGLE ROD	Angular Acceleration (rad/s <sup>2</sup> )	680	312	212	182	47%	76%	83%	86%
	Angular Velocity (rad/s)	13.7	6.3	4.3	3.7	22%	64%	76%	79%
INVERTED PENDULUM	Angular Acceleration (rad/s <sup>2</sup> )	970	445	302	259	24%	65%	76%	80%
	Angular Velocity (rad/s)	20.3	9.3	6.3	5.4	16%	47%	64%	69%

iii. Parameter sensitivity analysis outcomes for fall 241

The parameter sensitivity analysis was performed on childcare center fall 241, with the radius of rotation set to the respective subject's measurements, and the rotational

motion outcomes were compared to the original SIM G outcomes (TABLE 35). The overall outcomes were reported (TABLE 36).

TABLE 35

SUBJECT 5 PARAMETER SENSITIVITY ANALYSIS MEASUREMENTS AND FALL 241 SIM G OUTCOMES

Subject 5		FALL 241 BIOMECHANICAL OUTCOMES	
Length wrt Body region:	Value:	OUTCOME	SIM G OUTCOME
About the neck (m)	0.193	Linear Acceleration (g)	14
About the hips (Hip to head COM, m)	0.377	Change in Linear Velocity (m/s)	1.7
About the knees (Knees to head COM, m)	0.497	Angular Acceleration (rad/s <sup>2</sup> )	1151
About the soles (Soles to head COM, m)	0.687	Angular Velocity (rad/s)	9.5

TABLE 36

OVERALL PARAMETER SENSITIVITY ANALYSIS OUTCOMES FOR SIMULATED CHILDCARE CENTER FALL 241

PHYSICS-BASED MODEL	FALL 241								
	PHYSICS-BASED MODEL PARAMETER SENSITIVITY ANALYSIS OUTCOMES				PERCENT ERROR				
	ROTATIONAL MOTION	About the neck	About the hips	About the knees	About the soles	About the neck	About the hips	About the knees	About the soles
LUMPED MASS	Angular Acceleration (rad/s <sup>2</sup> )	965	494	375	271	16%	57%	67%	76%
	Angular Velocity (rad/s)	10.4	5.3	4.0	2.9	9%	44%	58%	69%
SINGLE ROD	Angular Acceleration (rad/s <sup>2</sup> )	658	337	255	185	43%	71%	78%	84%
	Angular Velocity (rad/s)	7.3	3.7	2.8	2.0	24%	61%	70%	79%
INVERTED PENDULUM	Angular Acceleration (rad/s <sup>2</sup> )	966	494	375	271	16%	57%	67%	76%
	Angular Velocity (rad/s)	10.4	5.3	4.0	2.9	9%	44%	58%	69%

iv. Parameter sensitivity analysis outcomes for fall 321

The parameter sensitivity analysis was performed on childcare center fall 321, with the radius of rotation set to the respective subject's measurements, and the rotational motion outcomes were compared to the original SIM G outcomes (TABLE 37). The overall outcomes were reported (TABLE 38).

TABLE 37

SUBJECT 4 PARAMETER SENSITIVITY ANALYSIS MEASUREMENTS AND FALL 321 SIM G OUTCOMES

Subject 4		FALL 321 BIOMECHANICAL OUTCOMES	
Length wrt Body region:	Value:	OUTCOME	SIM G OUTCOME
About the neck (m)	0.195	Linear Acceleration (g)	12
About the hips (Hip to head COM, m)	0.407	Change in Linear Velocity (m/s)	1.7
About the knees (Knees to head COM, m)	0.532	Angular Acceleration (rad/s <sup>2</sup> )	599
About the soles (Soles to head COM, m)	0.717	Angular Velocity (rad/s)	11.9

TABLE 38

OVERALL PARAMETER SENSITIVITY ANALYSIS OUTCOMES FOR  
SIMULATED CHILDCARE CENTER FALL 321

PHYSICS-BASED MODEL	FALL 321								
	PHYSICS-BASED MODEL PARAMETER SENSITIVITY ANALYSIS OUTCOMES				PERCENT ERROR				
	ROTATIONAL MOTION	About the neck	About the hips	About the knees	About the soles	About the neck	About the hips	About the knees	About the soles
LUMPED MASS	Angular Acceleration (rad/s <sup>2</sup> )	888	425	325	242	48%	29%	46%	60%
	Angular Velocity (rad/s)	12.3	5.9	4.5	3.3	3%	50%	62%	72%
SINGLE ROD	Angular Acceleration (rad/s <sup>2</sup> )	605	290	222	165	1%	52%	63%	73%
	Angular Velocity (rad/s)	8.7	4.2	3.2	2.4	27%	65%	73%	80%
INVERTED PENDULUM	Angular Acceleration (rad/s <sup>2</sup> )	906	434	332	246	51%	28%	45%	59%
	Angular Velocity (rad/s)	12.3	5.9	4.5	3.3	3%	50%	62%	72%

v. Parameter sensitivity analysis outcomes for fall 516

The parameter sensitivity analysis was performed on childcare center fall 516, with the radius of rotation set to the respective subject’s measurements, and the rotational motion outcomes were compared to the original SIM G outcomes (TABLE 39). At the time of the anthropometric measurements for this subject, the subject was not cooperative and only full height and chin to sole height measurements were obtained. Therefore, lengths for the parameter sensitivity analysis were estimated from published children anthropometrics (Snyder et al., 1975). The height for this subject fit the height for the fifth percentile measurements for male children of his age, so these 5<sup>th</sup> percentile measurements were used. The overall outcomes were reported (TABLE 40).

TABLE 39

SUBJECT 15 PARAMETER SENSITIVITY ANALYSIS MEASUREMENTS AND FALL 516 SIM G OUTCOMES

Subject 15		FALL 516 BIOMECHANICAL OUTCOMES	
Length wrt Body region:	Value:	OUTCOME	SIM G OUTCOME
About the neck (m)	0.150	Linear Acceleration (g)	31
About the hips (Hip to head COM, m)	0.388	Change in Linear Velocity (m/s)	1.3
About the knees (Knees to head COM, m)	0.553	Angular Acceleration (rad/s <sup>2</sup> )	2336
About the soles (Soles to head COM, m)	0.650	Angular Velocity (rad/s)	8.5

TABLE 40

OVERALL PARAMETER SENSITIVITY ANALYSIS OUTCOMES FOR SIMULATED CHILDCARE CENTER FALL 516

PHYSICS-BASED MODEL	FALL 516								
	PHYSICS-BASED MODEL PARAMETER SENSITIVITY ANALYSIS OUTCOMES	ROTATIONAL MOTION				PERCENT ERROR			
		About the neck	About the hips	About the knees	About the soles	About the neck	About the hips	About the knees	About the soles
LUMPED MASS	Angular Acceleration (rad/s <sup>2</sup> )	1897	733	514	438	19%	69%	78%	81%
	Angular Velocity (rad/s)	18.7	7.2	5.1	4.3	120%	15%	40%	49%
SINGLE ROD	Angular Acceleration (rad/s <sup>2</sup> )	1308	506	355	302	44%	78%	85%	87%
	Angular Velocity (rad/s)	12.7	4.9	3.4	2.9	49%	42%	60%	66%
INVERTED PENDULUM	Angular Acceleration (rad/s <sup>2</sup> )	1897	733	514	438	19%	69%	78%	81%
	Angular Velocity (rad/s)	18.7	7.2	5.1	4.3	120%	15%	40%	49%

vi. Parameter sensitivity analysis outcomes for fall 545

The parameter sensitivity analysis was performed on childcare center fall 545, with the radius of rotation set to the respective subject's measurements, and the rotational motion outcomes were compared to the original SIM G outcomes (TABLE 41). The overall outcomes were reported (TABLE 42).

TABLE 41

SUBJECT 21 PARAMETER SENSITIVITY ANALYSIS MEASUREMENTS AND FALL 545 SIM G OUTCOMES

Subject 21		FALL 545 BIOMECHANICAL OUTCOMES	
Length wrt Body region:	Value:	OUTCOME	SIM G OUTCOME
About the neck (m)	0.190	Linear Acceleration (g)	50
About the hips (Hip to head COM, m)	0.386	Change in Linear Velocity (m/s)	1.8
About the knees (Knees to head COM, m)	0.521	Angular Acceleration (rad/s <sup>2</sup> )	5388
About the soles (Soles to head COM, m)	0.686	Angular Velocity (rad/s)	13.3

TABLE 42

OVERALL PARAMETER SENSITIVITY ANALYSIS OUTCOMES FOR  
SIMULATED CHILDCARE CENTER FALL 545

PHYSICS-BASED MODEL	FALL 545								
	PHYSICS-BASED MODEL PARAMETER SENSITIVITY ANALYSIS OUTCOMES					PERCENT ERROR			
	ROTATIONAL MOTION	About the neck	About the hips	About the knees	About the soles	About the neck	About the hips	About the knees	About the soles
LUMPED MASS	Angular Acceleration (rad/s <sup>2</sup> )	2427	1194	885	672	55%	78%	84%	88%
	Angular Velocity (rad/s)	16.8	8.3	6.1	4.7	27%	38%	54%	65%
SINGLE ROD	Angular Acceleration (rad/s <sup>2</sup> )	1652	813	603	458	69%	85%	89%	92%
	Angular Velocity (rad/s)	11.6	5.7	4.2	3.2	13%	57%	68%	76%
INVERTED PENDULUM	Angular Acceleration (rad/s <sup>2</sup> )	2427	1194	885	672	55%	78%	84%	88%
	Angular Velocity (rad/s)	16.8	8.3	6.1	4.7	27%	38%	54%	65%

vii. Parameter sensitivity analysis outcomes for fall 676 (1)

The parameter sensitivity analysis was performed on childcare center fall 676 (1), with the radius of rotation set to the respective subject’s measurements, and the rotational motion outcomes were compared to the original SIM G outcomes (TABLE 43). The overall outcomes were reported (TABLE 44).

TABLE 43

SUBJECT 21 PARAMETER SENSITIVITY ANALYSIS MEASUREMENTS AND FALL 676 (1) SIM G OUTCOMES

Subject 21		FALL 676 (1) BIOMECHANICAL OUTCOMES	
Length wrt Body region:	Value:	OUTCOME	SIM G OUTCOME
About the neck (m)	0.190	Linear Acceleration (g)	18
About the hips (Hip to head COM, m)	0.386	Change in Linear Velocity (m/s)	2.5
About the knees (Knees to head COM, m)	0.521	Angular Acceleration (rad/s <sup>2</sup> )	1159
About the soles (Soles to head COM, m)	0.686	Angular Velocity (rad/s)	14.8

TABLE 44

OVERALL PARAMETER SENSITIVITY ANALYSIS OUTCOMES FOR SIMULATED CHILDCARE CENTER FALL 676 (1)

PHYSICS-BASED MODEL	FALL 676 (1)								
	PHYSICS-BASED MODEL PARAMETER SENSITIVITY ANALYSIS OUTCOMES				PERCENT ERROR				
	ROTATIONAL MOTION	About the neck	About the hips	About the knees	About the soles	About the neck	About the hips	About the knees	About the soles
LUMPED MASS	Angular Acceleration (rad/s <sup>2</sup> )	930	458	339	258	20%	61%	71%	78%
	Angular Velocity (rad/s)	11.6	5.7	4.2	3.2	22%	61%	71%	79%
SINGLE ROD	Angular Acceleration (rad/s <sup>2</sup> )	634	312	231	176	45%	73%	80%	85%
	Angular Velocity (rad/s)	7.9	3.9	2.9	2.2	47%	74%	81%	85%
INVERTED PENDULUM	Angular Acceleration (rad/s <sup>2</sup> )	929	457	339	257	20%	61%	71%	78%
	Angular Velocity (rad/s)	11.6	5.7	4.2	3.2	22%	61%	71%	78%



viii. Parameter sensitivity analysis outcomes for fall 676 (2)

The parameter sensitivity analysis was performed on childcare center fall 676 (2), with the radius of rotation set to the respective subject's measurements, and the rotational motion outcomes were compared to the original SIM G outcomes (TABLE 45). The overall outcomes were reported (TABLE 46).

TABLE 45

SUBJECT 21 PARAMETER SENSITIVITY ANALYSIS MEASUREMENTS AND FALL 676 (2) SIM G OUTCOMES

Subject 21		FALL 676 (2) BIOMECHANICAL OUTCOMES	
Length wrt Body region:	Value:	OUTCOME	SIM G OUTCOME
About the neck (m)	0.190	Linear Acceleration (g)	13
About the hips (Hip to head COM, m)	0.386	Change in Linear Velocity (m/s)	1.6
About the knees (Knees to head COM, m)	0.521	Angular Acceleration (rad/s <sup>2</sup> )	1684
About the soles (Soles to head COM, m)	0.686	Angular Velocity (rad/s)	12.3

TABLE 46

OVERALL PARAMETER SENSITIVITY ANALYSIS OUTCOMES FOR  
SIMULATED CHILDCARE CENTER FALL 676 (2)

PHYSICS-BASED MODEL	FALL 676 (2)								
	PHYSICS-BASED MODEL PARAMETER SENSITIVITY ANALYSIS OUTCOMES					PERCENT ERROR			
	ROTATIONAL MOTION	About the neck	About the hips	About the knees	About the soles	About the neck	About the hips	About the knees	About the soles
LUMPED MASS	Angular Acceleration (rad/s <sup>2</sup> )	1270	625	463	352	25%	63%	72%	79%
	Angular Velocity (rad/s)	14.7	7.3	5.4	4.1	18%	38%	52%	62%
SINGLE ROD	Angular Acceleration (rad/s <sup>2</sup> )	866	426	316	240	49%	75%	81%	86%
	Angular Velocity (rad/s)	10.0	4.9	3.6	2.8	19%	60%	70%	77%
INVERTED PENDULUM	Angular Acceleration (rad/s <sup>2</sup> )	1291	635	471	358	25%	63%	72%	79%
	Angular Velocity (rad/s)	14.7	7.3	5.4	4.1	20%	41%	56%	67%

e. Evaluation of H2

*H2: Lumped mass, single rod, and inverted pendulum physics-based models can accurately predict head biomechanical measures in common short-distance falls involving children.*

Overall, based on the physics-based model (PBM) outcomes for all head biomechanical measures for both the ATD and simulated childcare center falls, it was determined that when using method A the PBMs could reasonably predict a probable range of head biomechanical measures in common short-distance falls involving children. Results where the percent error was 25% or less were determined to be very accurate. However, it was also determined that models within 25% to 50% error were reasonable because when one model resulted in an error within this range, the other model(s) for the same fall tended to result in more accurate outcomes (for instance, one fall may result in a linear head acceleration percent error of 39% for the lumped mass and inverted pendulum PBMs, but a 10% error for the single rod). There was no clear explanation for why one model produced better outcomes for a given fall based on the dynamics of the

fall, and further study is needed to better understand which model(s) can best predict biomechanical outcomes based on the dynamics of a fall. However, when all models were taken into consideration, a range of reasonable outcomes for the ATD falls and the childcare center falls was obtained. Thus, *H2* was accepted.

i. Replicated ATD feet-first falls (n=7 onto carpet; n=7 onto linoleum)

For replicated ATD feet-first falls onto **carpet**, it was determined that the mathematical physics-based models could reasonably predict biomechanical outcomes. Both the lumped mass and inverted pendulum mathematical PBMs (using Method A) resulted in more accurate predictions of outcomes than the single rod PBM. Linear head accelerations were predicted less than 25% error for ATD falls onto carpet, and predictions of linear head velocities were less accurate yet still resulted in less than 50% error. For replicated ATD feet-first falls onto **linoleum**, it was determined that the mathematical PBMs using method A could accurately predict linear head acceleration when a single rod model was used, where the model resulted in a 5% error. The lumped mass and inverted pendulum models were slightly less accurate than the single rod PBM for linear head acceleration (with both models resulting in a 39% error). However, the single rod was less accurate for change in linear head velocity (with a 62% error) than the lumped mass and inverted pendulum models (with both models resulting in a 45% error). Therefore, it was determined that for these falls, the use of all three models provided a reasonable range of expected biomechanical outcomes.

All models overestimated rotational head acceleration and rotational head velocity when using the neck length as the radius of rotation. However, the rotational head outcomes decreased and became more accurate as the radius of rotation increased. It was

determined that PBMs of these replicated ATD falls were sensitive to radius length, and that rotation “about the hips” and sometimes “about the knees” improved accuracy. For falls onto carpet, the percent error decreased and the radius of rotation was similar and most accurate for about the hips and about knees for all 3 models. However, the rotational head acceleration was still greater than 50% error. The angular velocity was equal to or less than 26% error for all 3 models, so the angular velocity was accurate. For falls onto linoleum, rotation about the hips was the most accurate point of rotation, and rotational head acceleration outcomes were 48% for the lumped mass and inverted pendulum models. Rotational head velocities had a 7% error for the lumped mass and inverted pendulum models. For falls onto both the carpet and linoleum, the rotational outcomes were overestimated when the radius was set at the neck; however, with radius set at the hips and knees, the rotational acceleration values were underestimated yet more accurate. Therefore, calculating the rotational outcomes using all three model types and a range of radius length may improve the understanding of what the worst-case scenario of a fall may be. It is noted that it was not surprising that the PSM indicated that rotation about the hips and sometimes about the knees was more accurate than the neck, given that the dynamics of ATD falls onto carpet had a predominant rotation about the hips as well as sometimes about the knees (which occurred when the ATD fell into a crouching position before rotating rearward). The results of the PSA highlight the sensitivity of biomechanical outcomes to radius of rotation, as well as the importance of using an appropriate radius of rotation.

To determine the effect of fall dynamics, falls onto linoleum were evaluated which involved two different types of dynamics (all falls onto carpet demonstrated the same

dynamics). For falls onto linoleum, dynamic A (n=5) (where the ATD fell into a crouching position, then the knees extended causing the pelvis to impact in a seated position; then the torso rotated rearward) and dynamic C (n=2) (where the ATD fell to a crouching position, then feet rotated forward exhibiting plantar flexion; hips and knees extended after the pelvis impacted the surface, and launched the ATD into a rearward supine position) were observed. For falls with dynamic type A, the single rod PBM accurately predicted the linear head acceleration with a 16% error, but the lumped mass and inverted pendulum PBMs more accurately predicted the change in linear head velocity with both models resulting in a 35% error. When the radius of rotation was set to the neck length for falls with dynamic A, the rotational outcomes were overestimated in every model with a 100% or greater error. However, the parameter sensitivity analysis demonstrated that the lumped mass and inverted pendulum PBMs underestimated but resulted in more accurate rotational acceleration outcomes when the radius of rotation was set as “about the hips” or “about the knees” with 43% or less error and a 4% error for rotational velocity outcomes. For falls with dynamic type C, the lumped mass and inverted pendulum PBMs accurately predicted the linear head acceleration outcomes with both models resulting in 6% error, and these models were more accurate than the single rod model (which resulted in 36% error). The change in linear velocity for all three models resulted in 60% error or greater, but it was determined that these models still performed appropriately as experts tend to evaluate linear acceleration versus change in linear velocity. When the radius of rotation was set to the neck length (for falls with dynamic C), the rotational outcomes were overestimated by every model. However, the parameter sensitivity analysis for all models predicted more accurate rotational motion

outcomes when the radius of rotation was set as “about the hips” and “about the knees”. Overall, PBMs more accurately predicted biomechanical outcomes for falls with dynamic C than for falls with dynamic A. Despite the small sample size, the findings from the comparison of ATD fall dynamics in this cohort suggest PBMs can be used to reasonably predict biomechanical outcomes for ATD feet-first falls. Furthermore, PBM selection must parallel fall dynamics and radius of rotation must be about the hips or knees rather than the neck.

ii. Subset of childcare center falls with primary head impact (n=8)

Overall, the lumped mass, single rod, and inverted pendulum PBMs (using method A) predicted more accurate biomechanical outcomes for childcare center falls with primary head impact. In general, the lumped mass and inverted pendulum PBMs tended to be more accurate than the single rod PBM. The lumped mass and inverted pendulum PBMs accurately predicted linear head acceleration in five of these simulated falls (<25% error), slightly overestimated the linear head acceleration in two falls (<50% error), and overestimated the linear head acceleration in one fall (89% error). However, for the latter fall the single rod model only slightly overestimated the linear head acceleration outcome (29% error). The change in linear head velocity was less accurately predicted in some of the falls; however, when the lumped mass and inverted pendulum were inaccurate, the single rod model resulted in more accurate outcomes. For example, when fall 516 was modeled with a lumped mass and an inverted pendulum, both models resulted in a 112% error in change in linear velocity. However, when the fall was modeled with a single rod, the change in linear velocity resulted in a 45% error. For linear motion outcomes, all three PBMs were sensitive to estimated fall height, and it was

determined that no one model for these simulated falls was more accurate than the others. There was no clear explanation as to why no one model(s) was best at predicting biomechanical outcomes. Overall, it was determined that if a bioengineer expert used all three models when evaluating a history of a fall, they can obtain a range of linear outcomes that reasonably represent the biomechanical outcomes from these real-world falls.

For rotational motion outcomes across the simulated childcare center falls, it was determined that using the point of rotation about the neck generated accurate and reasonable predictions. As shown by the parametric sensitivity analysis, as radius of rotation lengths increased, rotational outcomes tended to be underestimated (i.e. rotational outcomes decreased). Similar to the linear outcomes, when the lumped mass and inverted pendulum PBMs resulted in less accurate rotational motion predictions, the single rod PBM resulted in more accurate outcomes. 88% of this subset of childcare center falls resulted in PSA rotational head acceleration outcomes that were <25% error for at least one of the PBMs.

In summary, it was determined that neck length was the most appropriate radius of rotation for simulated childcare center falls in this cohort. Furthermore, all three model types enabled a reasonable range of biomechanical outcomes for a given fall. Therefore, when using PBMs to predict biomechanical outcomes when presented with a history of a short-distant fall, the neck length should be used as the radius of rotation and all three PBMs should be used to predict the range of probable biomechanical outcomes. However, further study is needed to better understand which model(s) can best predict biomechanical outcomes based on the dynamics of a fall. Because the PBMs resulted in

reasonable linear and rotational outcomes (<25% error for 88% of predicted outcomes), *H2* was accepted for these simulated childcare center falls. However, further study is needed to understand which model(s) can best predict biomechanical outcomes based on fall dynamics.



## VI. DISCUSSION

### A. Injury outcomes and injury risk

100 video-recorded and witnessed short-distance falls occurring in a childcare setting were reviewed in this study. No head injuries occurred in any of the falls. Furthermore, no moderate or minor injuries to any body region that required medical attention were witnessed during observation and post-observation periods or documented in incident reports. It is possible that contusions and abrasions occurred to clothed areas, such as the buttocks, that may have arisen at a later time. However, even if a child sustained a contusion or abrasion from a short-distance fall, these are minor injuries that would not require medical attention. Based on these findings, the potential for moderate to severe injury resulting from these short distance falls in a childcare setting remains low.

#### 1. Mean peak resultant linear head acceleration across all falls

The mean peak resultant linear head acceleration (g) across all falls (n=14 falls with SIM G output) was  $16.6 \pm 4.4$  g, with a maximum value of 28.2 g. Because no injuries occurred in these falls, these results indicated that these peak linear head acceleration values at or below 28.2 g are below published linear skull fracture injury thresholds, which ranged from 37 g to 74 g (Gurdjian, Roberts, & Thomas, 1966; Stürtz, 1980; Cory et al, 2001; Reichelderfer, Overbach, & Greensher, 1979).

#### 2. Mean peak resultant rotational head acceleration and velocity across all falls

The mean peak resultant rotational head acceleration ( $\text{rad/s}^2$ ) across all falls was  $1838.0 \pm 1000$   $\text{rad/s}^2$ , with a maximum value of 3853.0  $\text{rad/s}^2$ . The mean peak resultant rotational head velocity ( $\text{rad/s}$ ) across all falls was  $10.0 \pm 5.7$   $\text{rad/s}$ , with a maximum value of 20.5  $\text{rad/s}$ . Ommaya et al. (2002) used scaled brain masses from animal [primate]

models to young child to develop rotational head acceleration threshold values. For a young child, the following was determined: approximately 6000-7000 rad/s<sup>2</sup> could result in a concussion; approaching 20 krad/s<sup>2</sup> could result in a mild DAI; approaching 23 krad/s<sup>2</sup> could result in a moderate DAI; and 25 krad/s<sup>2</sup> and above could result in a severe DAI. Rotational head accelerations in this study were well below these thresholds.

Margulies and Thibault (1992) also investigated the relation between peak rotational head acceleration and peak change in rotational head velocity for brain masses scaled from primate to infant. They established that DAI thresholds for infants (brain mass averages 1.0 to 1.1 kg for both male and females from 18 to 30 months of age; Dekaban and Sadowsky, 1978) begin with approximately 150 rad/s for peak change in rotational head velocity and 20 krad/s<sup>2</sup> for peak rotational head acceleration. Rotational head accelerations and velocities in this study were below these thresholds.

### 3. Mean HIC<sub>15</sub> value across all falls

The mean peak HIC<sub>15</sub> value across all falls was 7.1±4.4, with a maximum value of 16.6. This may be low because most of the falls did not result in primary head impact. Previous studies have indicated that, for young children, HIC values below 500 result in a very low likelihood of linear-type injuries, such as skull fractures (Cory, 2001). Despite having instances of head impact during these falls, these results suggested that these HIC values at or below 16.6 are below linear-type (i.e. fracture) injury thresholds.

### 4. Mean impact duration across all falls

The mean impact duration (ms) across all falls was 20.6±6.4 ms, The minimum value recorded was 10.0 ms. Shorter impact durations have been associated with higher peak linear head acceleration values, and studies have indicated that longer impact durations

are less likely to cause head injury (Cory, 2001). The fall that had the shortest impact duration resulted in a peak linear head acceleration of 28.2 g, which was also the largest peak linear head acceleration from these falls. During this fall, subject 4 fell rearward and his buttocks contacted the rug overlying carpet in a classroom; he then rotated about his buttocks and fell rearward, impacting his head occiput on the rug overlying carpet. The results from this study are consistent with previous findings.

### B. Specific aim 1 discussion

The first specific aim of this thesis was to characterize video-recorded short distance falls involving children aged 1-3 years in a childcare setting. This was accomplished through the successful development of a database that characterized various factors of 100 video-recorded falls from the childcare center. Overall, the collected falls ranged from simple falls in one direction onto one surface and impacting a single body region, to complex falls from height involving multiple people, multiple planes of impact, and multiple dynamics. Complex falls may dissipate more energy as they may involve more impact planes. Therefore, “complex” falls may actually result in a lower risk of injury, and “simple” head-first falls may be considered more severe than falls with more complex dynamics and impacts. No injury was witnessed or documented with an incident report from the childcare center. These factors provide an overall understanding of the common dynamics and body region impacts that are experienced in common short-distance falls.

#### 1. Fall type

Most falls were ground-based falls (82%). When falls from height did occur, 59% of them were located on the playground. Falls from height in the classroom may have been

less common due to the lack of equipment/furniture height in the classrooms; furthermore, furniture in childcare rooms is smaller than furniture for adults and designed specifically for young children. Also, the children were monitored and may be less likely to climb or have access to higher surfaces.

## 2. Initial condition and fall initiation

An interesting finding from this category was that children could fall even when they are standing still (11%). It demonstrated that young developing children commonly fall due to a loss of balance (36%). In other words, a child standing still does not need to be acted upon by an external force (e.g., another child running into them) for a fall to be initiated.

## 3. Fall dynamics

The average number of unique fall dynamics per fall event was 1.3, indicating that on average, more than one fall dynamic was involved during these short-distance falls. For example, fall 79 involved two fall dynamics. In this fall, subject 2 was standing upright on the butterfly slide (see FIGURE 47 in results for butterfly slide). The fall was initiated by a loss of stability, which caused his right foot to slip off the slide right laterally. He fell rearward and right laterally to the “wing” mat of the slide (overlying carpeted surface). His buttocks contacted the butterfly slide, and then the primary impact involved his right lateral leg and the lateral aspect of his right foot. The secondary impact of this fall involved his right palm and posterior distal right arm (i.e., forearm) on the edge of the “wing” mat. Overall, it was determined that these common short-distance falls can be more complex and still not result in any injury. In fact, complex fall dynamics with

impact to various body regions may dissipate more energy, which potentially decreases risk of injury.

a. Head-first falls compared to fall maximum SIM G linear acceleration output

As was mentioned in the Results, falls 49 and 54 were two falls that involved the rare head-first dynamics from this sample. Fall 49 involved more than one fall dynamics (rearward and head-first) and was a ground type (the change of height of the head center of mass [COM] was approximately 58 cm from the initial position in the structure to the playground surface). Fall 54 involved more than one fall dynamics (forward and head-first) and was from a height (the change of height of the head COM was approximately 99 cm from the top of the tall mushroom to the playground surface). An interesting outcome was that, despite both head-first fall dynamics, primary head impact, and fall types from height, neither of these falls resulted in the maximum SIM G output. In fact, fall 49 did not result in a peak resultant linear head acceleration that met or exceeded the 12 g threshold, so biomechanical measures were not obtained from this fall. Fall 54 resulted in a peak resultant linear head acceleration of 19 g. This fall, however, also involved the intervention of a teacher who witnessed the fall. The teacher grabbed the subject's ankle and this appeared to slow the fall, which may be why the overall outcomes were lower than expected.

The fall with the maximum SIM G output, fall 72, was a rearward ground-based fall (the fall height was the sole to head COM length of the fall subject, approximately 72 cm) onto a rug overlying carpet in a classroom. This fall resulted in a peak resultant linear head acceleration of 28 g. The biomechanical outcomes in fall 72 may have been

higher than those in fall 49 because the subject fell from a greater height. It is possible that the fall 72 outcomes were higher than outcomes in fall 54 because no person (i.e., teacher) intervened during this fall.

#### 4. Equipment/Object involvement

The most common object that was involved in these falls (n=59 falls with equipment/object involvement) was the playground equipment (26%). 36% of all falls (n=100 total falls) occurred on the playground, so based off these findings short distance falls may commonly be the result of falling from playground equipment to the playground surface. These findings also support the previously proposed idea that playgrounds are a good location to obtain actual fall data involving children where severe injuries are not expected to occur (Kotch, Chalmers, Langley, & Marshall, 1993). Objects were involved most frequently during one or two phases of the fall, most commonly either the initial condition of the fall or the fall initiation. Sometimes objects were involved during primary impact; however, due to the operationalization of object involvement, a child may have been carrying an object during the primary impact (and not impact the object). Based on this information, short distance falls may be initiated by objects such as toys and furniture (i.e., chairs, tables, small toy balls, etc.). The butterfly slide (see FIGURE 47 in Results) was involved in 13% of the falls that involved an object(s) during the fall (n=59 falls). This slide was made of a soft, deformable material (similar to foam used in furniture) and when a child attempted to stand upright on top of it, they sometimes lost their footing and the deformable material caused their foot to slip off of the edge, which resulted in a fall. However, this soft deformable material allowed

for fall impact absorption, which may be why falls from height on this object did not result in injury.

5. Another person(s) involvement, not including the subject

Only 26% of all falls (n=100 total falls) involved another person(s); most falls subjects were alone during the fall event. When the fall did involve another person, it was most commonly one other child (65%), or one adult (23%). More falls involving another person occurred indoors (54%). While it was more common for an equipment or object to be involved in one or more phases (72%, n=59 falls involving an object(s)), it was more common for another person(s) to be involved in only one phase of the fall (73%, n=26 falls involving another person(s)). Most falls were affected by another person during fall initiation (73%, n=26 falls involving another person(s)), often involving a push. Based on this information, short distance falls may be initiated by an external force from another person(s).

6. Head impact during any phase of the fall

An important finding from the study was that while these short-distance falls could result in a head impact, even the more complex of the falls did not usually result in a head impact. Only 19% of falls involved head impact during any phase of the fall (not limited to primary impact). This supports the theory that short-distance falls do not usually result in serious head injury.

7. Impact surface and planes impacted

The most common impact surfaces were playground mulch (33%), carpet (24%), and rug on carpet (21%). These surfaces were expected to be the most common, due to the design of both classrooms. As stated in the results, 36% of falls occurred on the

playground while 64% occurred inside a classroom. Both classrooms were designed so that half of the room was a linoleum floor, and the other half was carpet overlying concrete. Both rooms also had an area rug overlying a portion of the carpet.

Hilt (2018) previously measured and classified the coefficient of restitution (COR) for various impact surfaces at the same childcare center as the one in this study. The range of COR's for all surfaces (from Hilt (2018)) was  $0.23 \pm 0.01$  to  $0.57 \pm 0.03$ ; the median surface COR (0.43) was used to classify a surface as having a "high" COR versus "low" COR. Table 40 demonstrates the most common impact surfaces involved in this study and their associated COR classification based on Hilt's findings.

TABLE 40

MOST COMMON IMPACT SURFACES (FROM THIS STUDY) AND THEIR RESPECTIVE COEFFICIENT OF RESTITUTION MEASUREMENT AND CLASSIFICATION (FROM HILT (2018))

Most common impact surface (from this study)	Coefficient of restitution mean $\pm$ SD (from Hilt (2018))	Coefficient of restitution classification (from Hilt (2018))
Playground mulch	$0.57 \pm 0.03$	High
Carpet	$0.41 \pm 0.02$	Low
Area rug overlaying carpet	$0.55 \pm 0.02$	High
Linoleum	$0.45 \pm 0.01$	High

Hilt's study found that surface COR influenced the peak resultant linear head accelerations. Specifically, falls onto surfaces with lower COR were associated with significantly greater peak resultant linear head acceleration than falls onto higher COR.



Hilt also found that falls onto surfaces with lower COR were associated with significantly greater HIC<sub>15</sub> values than falls onto surfaces with higher COR. Based on Hilt's findings, because most of the common impact surfaces from this study involved surfaces with high COR (playground mulch, area rug overlaying carpet, linoleum), it was expected that the peak resultant linear head acceleration and HIC<sub>15</sub> values would be lower, and therefore lead to less potential for injury. For falls onto carpet alone, because carpet was classified as having a low COR in Hilt (2018), it was expected that the peak resultant linear head acceleration and HIC<sub>15</sub> values would be greater, which could lead to greater potential for head injury. However, no injuries were documented from any of these witnessed short-distance falls.

#### 8. Final landing position

Most subjects were in a sitting position (22%), a lateral recumbent position (right or left; 17%), on their hands and knees (16%), or prone (14%) at the end of the fall. Because most children were upright and walking/running/standing/jumping just prior to fall initiation, this suggests that the center of mass (COM) of the subjects moved from an appreciable point above ground to the ground/surface level. The COM height was estimated to be about half the height of the child, on average 40 cm in ground-based falls, and this distance was higher in falls from height.

#### C. Specific aim 2 discussion

Body regions involved in the first contact, primary impact, and secondary impact were analyzed. Overall, impacts occurred to multiple body regions, including the head and face. Head impact occurred in 19% of these falls at some phase during the entire fall sequence. However, less than 10% of primary impacts involved the head suggesting that

head impact was not a common primary impact in these short distance falls. Body region contact/impact maps also suggest that subjects responded with active muscle response during a fall. The soles of both feet were the most common first contact in falls. This was witnessed when the subject attempted to step to regain their balance – the step was a common reaction. The body region impact maps also suggest that a forward fall onto hands was the most common occurrence when a fall included a secondary impact. A small number of falls involved a tertiary impact. Due to the rarity of a tertiary impact, tertiary impacts were not included as the body impact maps would not reflect any valuable information as the threshold for inclusion was set at 10% or greater. It is worth noting that the tertiary impacts indicated a more complex fall. As discussed earlier, these “complex” falls with primary, secondary, and tertiary impacts may have a lesser potential for injury outcomes than simple falls with only a primary impact.

The results from these body region contact/impact maps may be used to better understand body regions that have the highest potential to have evidence of impact (such as a bruise). In other words, the body regions involved in the primary impact of a fall may be thought as the region(s) that have the greatest potential for injury. This is an important finding because these maps were based on reliably-witnessed falls with known outcomes. Outcomes indicated that the average number of body planes involved in the primary impact of a fall was 1.3. This is relevant information for clinicians when assessing a child’s injuries in the presence of a short distance fall history. Most falls resulted in impacts that involved a combination of a lateral body plane with either the anterior or posterior body planes. It was extremely rare, however, for falls to involve multiple planes of impact that were opposite each other. In other words, if the primary

impact body plane involved the anterior plane, the posterior plane was not involved in almost all cases. Extremely rare cases involved both the anterior and posterior plane when a subject lost their balance, fell one direction and impacted that region, then rebounded and impacted another region (e.g., in fall 95, the subject stumbled, fell rearward and impacted her posterior torso against a wall; she then rebounded and fell forward, impacting her anterior shins and knees on carpeted flooring).

The body region contact/impact maps may be used as tools by physicians (i.e., those in pediatric emergency departments and pediatric primary care practices) to have a better understanding of which body regions are expected to be involved in an impact(s) during these common short-distance falls, as well as how many planes of the body could be expected to have injuries. For example, it is expected that short distance falls will typically have evidence of impact or injury on 1 plane of the body or 2 contiguous planes of the body. Body region contact/impact maps may help clinicians to have a better understanding of which body regions are expected to have the highest potential for evidence of an impact (e.g., contusion) when evaluating a history where a short-distance fall was provided in young children. The body region contact/impact maps from this study were consistent with previous studies as discussed below (Dsouza and Bertocci (2015); Dsouza and Bertocci (2018); Pierce et al. (2018)).

1. Body region impact maps from ATD falls

Two previous studies developed body region impact maps for falls using a sensing skin applied to an ATD. The first study was Dsouza and Bertocci (2015), which used the same 12-month-old CRABI ATD that was used in the replicated ATD feet-first falls in this study. Researchers wanted to identify potential bruising locations (body regions)

associated with a rearward short-distance fall (operationalized as a young child falling rearward and impacting the occiput), which is a common fall experienced by children in the early stages of walking (mobility) development. The ATD was instrumented with a custom-developed force sensing skin, which was linked to display recorded force data onto a computerized body mapping image system. The force sensors were activated during the rearward impacts (threshold of 5% the ATD body weight, approx. 4.5 N). The ATD was dropped (a total of n=32 falls) with a manual release system onto two different impact surfaces (padded carpet over wood and linoleum tile over concrete) and two different initial positions were tested (mostly upright and at a 20° angle to the vertical, and inclined falls at a 30° angle to the vertical; both positions involved the feet in contact with the impact surface). This study resulted in potential bruising regions that included the occiput, posterior torso, and some upper posterior legs/lower posterior arms (FIGURE 81 and FIGURE 82). The outcomes from Dsouza and Bertocci (2015) indicated that fall dynamics played a role in which body regions were impacted. For instance, falls from an inclined position commonly involved the upper posterior legs as the ATD fell into a seated position with the legs fully extended. Although Dsouza and Bertocci (2015) was limited to rearward fall types, the outcomes indicated that falls with simple dynamics did not result in impacts to multiple planes of impact (in other words, none of these ATD falls resulted in impacts to the anterior or lateral body planes in addition to the posterior plane). This was consistent with the falls from this study, as the body impact planes also did not result in impacts to opposite body planes, as discussed earlier.

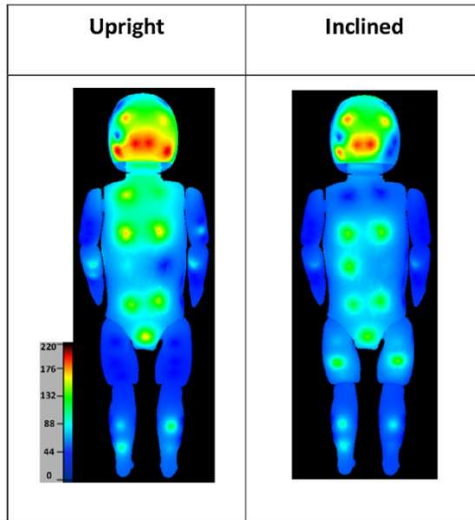


FIGURE 81 – The posterior ATD body maps from Dsouza and Bertocci (2015) for each initial position scenario for rearward fall impacts onto linoleum; colors and intensities varied depending on the level of impact force (N)

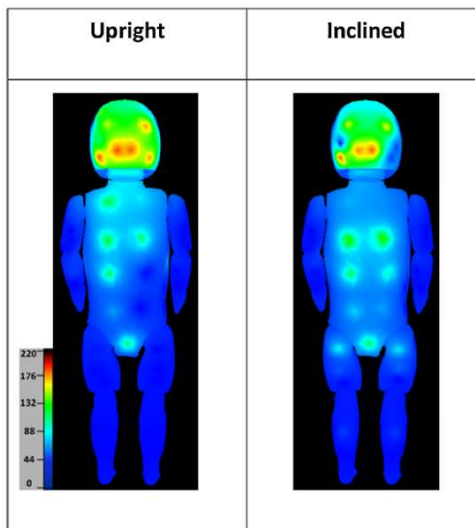


FIGURE 82 – The posterior ATD body maps from Dsouza and Bertocci (2015) for each initial position scenario for rearward fall impacts onto carpet; colors and intensities varied depending on the level of impact force (N)

Another similar study conducted by Dsouza and Bertocci (2018), where the same set up in the previous study (Dsouza and Bertocci [2015]) was used to develop body impact maps for simulated bed falls. In this study, pneumatic actuator was used to push the side-lying ATD from a horizontal surface that represented a couch or a bed. The ATD rolled off the bed and impacted a carpet over wood surface. Falls (n=20) with two initial positions (forward facing, where the face looked toward the edge of the horizontal surface, and rearward facing, where the face looked toward the middle of the horizontal surface) and two bed heights (61 cm and 91 cm) were conducted. It was found that body regions impacted did depend on the initial position of the ATD (for instance, forward-facing ATD falls commonly involved impacts to the left shoulder and left parietal head). Representative impact maps are included (FIGURE 83 and FIGURE 84). Although the overall fall dynamics differed between the two initial positions of the ATD, the overall results from Dsouza and Bertocci (2018) indicated that body impact regions involved at most 2 impact planes, which were adjoining and not opposite (i.e., anterior and lateral right, but not anterior and posterior). These findings were consistent in this study of childcare center falls. Furthermore, Dsouza and Bertocci found that most impact regions and the greatest forces were recorded in one plane, and fewer regions of impact (and decreased force) in a second plane, which was consistent with the outcomes in this study. Similar to the previous study outcomes (Dsouza and Bertocci 2015), they also found that the outcomes suggested no possibility of impact to opposite impact planes in a single given fall, which was consistent with this study.

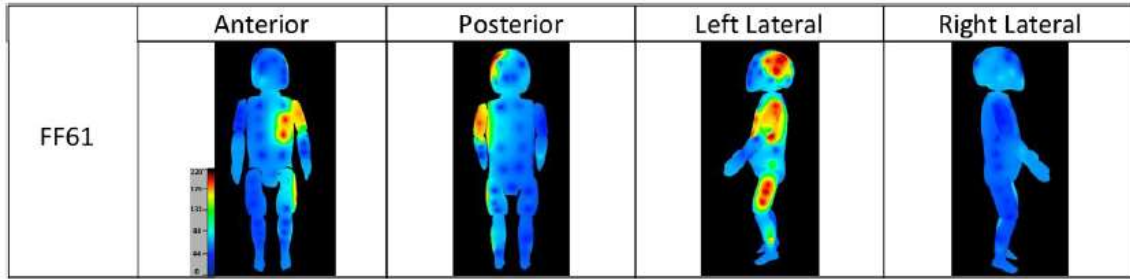


FIGURE 83 – Cumulative body impact maps for forward bed falls at 61 cm (n=5); impact body regions included anterior, some posterior, left lateral, and very few right lateral regions (note: these are cumulative contact region maps across all trials; in individual trials, it was observed that if more than one body plane was impacted, only 2 adjoining planes were involved, such as anterior and left lateral). (Dsouza and Bertocci, 2018). Colors and intensities varied depending on the level of impact force (N)

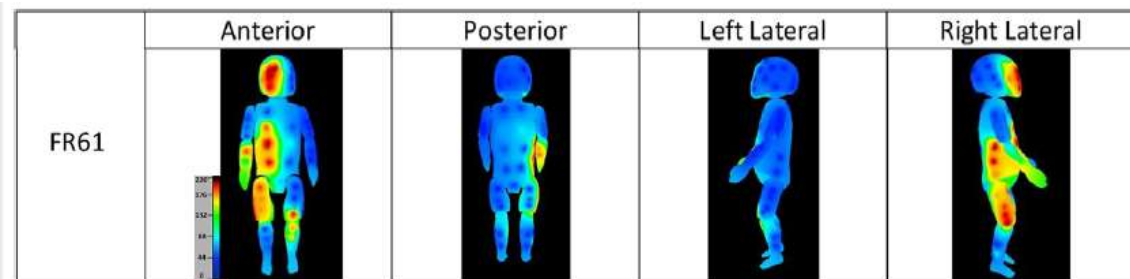


FIGURE 84 – Cumulative body impact maps for rearward bed falls at 61 cm (n=5); impact body regions included anterior, some posterior, right lateral, and very few left lateral regions (note: these are cumulative contact region maps across all trials; in individual trials, it was observed that if more than one body plane was impacted, only 2 adjoining planes were involved, such as anterior and right lateral) (Dsouza and Bertocci, 2018). Colors and intensities varied depending on the level of impact force (N)

2. Body region bruising maps from prospective cross-sectional clinical study

Pierce, et al. (2021) recently published a prospective cross-sectional study that involved young children (less than 4 years of age) who presented to urban children's hospitals (n=5 locations) with contusions. The goal of this study was to evaluate the ability of the Bruising Clinical Decision Rule (BCDR) to predict if bruising patterns could delineate between accidental and abusive trauma. The BCDR initially included injuries to the torso, ear, and neck body regions for children under 4 years of age (i.e., TEN-4 BCDR). Cases were reviewed and subjects were enrolled if they had at least one contusion. This study included otherwise healthy children. Researchers at the hospitals documented skin findings characteristics including injury types, the number of injuries, and injury location(s) on body maps. Deidentified cases were then reviewed by a panel of experts (including child abuse pediatric physicians, pediatric emergency medicine physicians and one biomedical engineer), and experts determined if the injuries were the outcome of an accident or abuse. Any cases deemed indeterminate by the panel were excluded. This study resulted in n=2123 cases (n=1713 were non-abuse and n=410 were abuse) of children with an average age of 2.1 years. The study concluded that the initial TEN-4 BCDR could not delineate between accident and abuse with a high level of sensitivity and specificity, and it was suggested that the rule be refined to include the frenulum (of the mouth), the angle of the jaw(s), the cheeks (soft portion), the eyelids, and the subconjunctiva of the eyes (i.e. TEN-4-FACESp BCDR). This study also resulted in composite body bruising location maps for cases that were determined to be the result of an accident and those that were determined to be the result of abuse (FIGURE 85 and FIGURE 86). When the non-abuse bruising locations (Pierce et al., 2021) are compared



to the body region primary impact maps from this study (for children aged 12 to 35 months of age), the locations of potential evidence of impact are consistent with actual outcomes (i.e. bruising locations) from this clinical study. Pierce et al. found that, in accidental cases, bruises in the anterior plane occurred on the bilateral shins and knees, which was consistent with this study. For the posterior plane, Pierce et al. also found that, in accidental cases, bruises were not only less common, but mostly involved the lower posterior arms and the lower torso. In both the left and right lateral planes, bruises were limited to the lateral extremities, which was consistent with this study, and the lateral torso was extremely rare. A finding in the Pierce et al. study that was not consistent with the outcomes in this study was that the body region bruising maps suggested that bruises often occurred to the face, occiput, and lateral (temporal/parietal) head. However, because these children were presented to hospitals with injuries, it was expected that injuries to the head and face would be a more common finding.

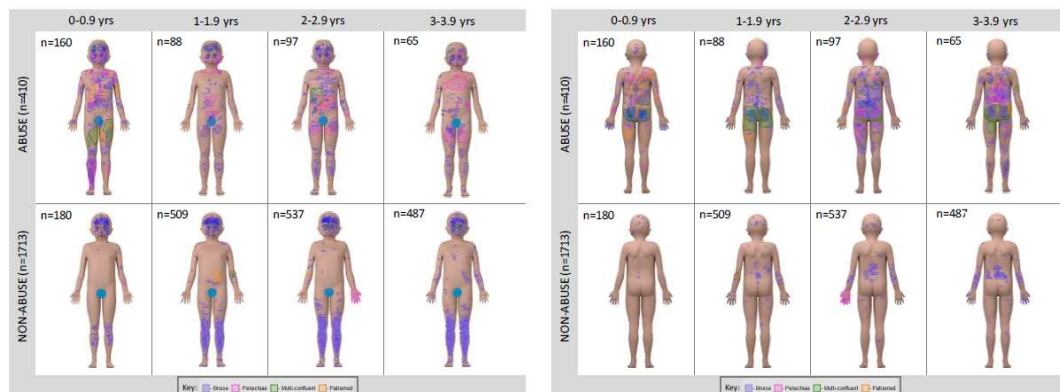


FIGURE 85 – Composite anterior and posterior bruising locations for abuse (top) and non-abuse (bottom) cases from Pierce et al. (2021)

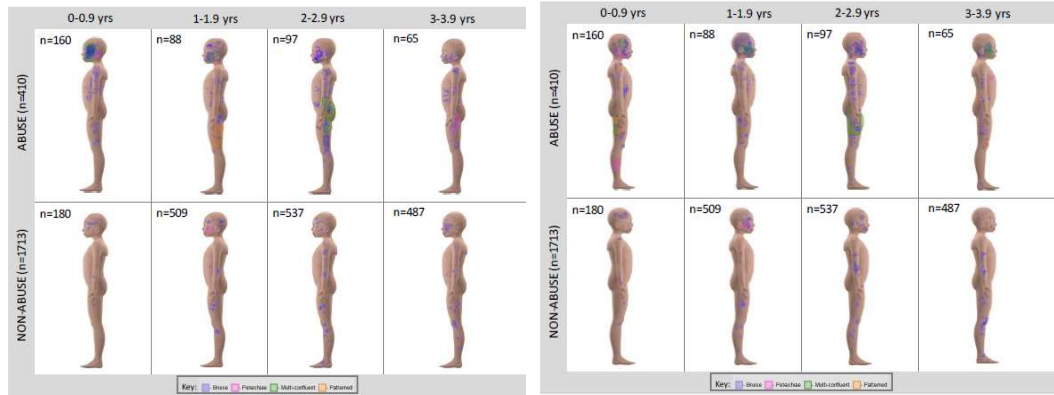


FIGURE 86 – Composite lateral left and lateral right bruising locations for abuse (top) and non-abuse (bottom) cases from Pierce et al. (2021)

#### D. Specific aim 3 discussion

##### 9. SIM G Falls with Head Impact vs No Head Impact

*H1: Head accelerations and velocities will be greater in falls with direct head impact than in falls without head impact.*

Outcome measures for this hypothesis included peak resultant linear head acceleration (g), peak resultant linear head velocity (m/s), peak resultant rotational head acceleration (rad/s<sup>2</sup>), peak resultant rotational head velocity (rad/s), HIC<sub>15</sub>, and impact duration (ms). All data were tested for statistical differences between falls with (n=7) and without (n=7) direct head impact (p<0.05), and the only measure that was found to have a significant difference was peak resultant rotational head acceleration (rad/s<sup>2</sup>). The average peak rotational head acceleration was larger for falls with head impact than for falls without head impact. As only 1 of the 4 head acceleration and velocity measures was significant, *H1* was rejected. It was surprising that there was no significant difference between most of the biomechanical measures. With respect to falls without head impact,

other body regions were involved in the primary impact, which likely dissipated more energy. Hilt (2018) found significant differences in peak linear acceleration and linear velocity, as well as peak rotational acceleration and impact duration between falls with and without primary head impact (TABLE 48). A difference between this study and Hilt (2018) was the sample size. Hilt evaluated a total of 102 falls with SIM G data including those with (75%) and without head impact (25%), which was much larger than this study (n=14). Because Hilt used a much larger sample size, the results from Hilt’s study present a better understanding of biomechanical outcomes from falls with and without head impact.

TABLE 48

PEAK HEAD BIOMECHANICAL MEASURES FOR HEAD IMPACT VS. NO HEAD IMPACT FROM HILT (2018) (N=102 FALLS)

Biomechanical measure	Hilt (2018) Head impact (Mean±SD)	Hilt (2018) No head impact (Mean±SD)	This Study Head Impact (Mean±SD)	This Study No Head Impact (Mean±SD)
Peak linear head acceleration (g)	20.57 ± 9.35	15.47 ± 2.26	18.8 ± 5.63	15.0 ± 2.45
Peak rotational head acceleration (rad/s <sup>2</sup> )	2265 ± 1423	1662 ± 776	2316 ± 844	1240 ± 612
Peak linear head velocity (m/s)	1.35 ± 0.67	2.16 ± 0.61	1.5 ± 0.53	1.9 ± 0.76
Peak rotational head velocity (rad/s)	10.76 ± 4.91	9.42 ± 4.28	11.4 ± 4.9	8.0 ± 5.1
HIC <sub>15</sub>	9.00 ± 7.93	8.06 ± 3.77	7.4 ± 4.7	6.5 ± 4.8
Impact duration (ms)	14.58 ± 5.67	23.24 ± 4.82	17.1 ± 5.7	23.3 ± 6.3

10. Development of physics-based models for replicated ATD feet-first falls and human subject childcare center falls with SIM G activation and primary head impact

*H2: Lumped mass, single rod, and inverted pendulum physics-based models can accurately predict head biomechanical measures in common short-distance falls involving children.*

The overall outcomes from all tested models indicated that lumped mass, single rod, and inverted mathematical pendulum physics-based models (PBMs) could reasonably predict head biomechanical measures. Therefore, *H2* was accepted. Method A was the most accurate methodology, and that is the method that will be addressed in the following sections. In general, the PBMs were found to overestimate biomechanical outcomes, but this was not surprising given the PBMs did not account for energy absorption that occurs within the body and on the impact surface. The PBMs also did not account for active muscle reactions during the fall, and these responses were observed in the childcare center falls. In other words, children were commonly observed to attempt to correct themselves before a fall, and it was also observed that children braced themselves during impacts. Additionally, models did not account for impact surface and head stiffness/compliance - all surfaces and the modeled head were assumed to be rigid. Not surprisingly this would lead to overestimations in cases where the impact surface was something other than the linoleum over concrete. However, the tendency of these PBMs to overestimate biomechanical measures provides a worst-case scenario in the prediction of these outcomes.

b. Replicated ATD feet-first falls versus select childcare center falls

It was surprising that the model predictions for ATD falls were less accurate than for the simulated select childcare center falls, as the ATD falls were performed in a controlled setting. When the calculations were performed, the analysis began after the buttocks impacted the floor surface, and any initial velocity prior to this impact was assumed to not transfer into rotational motion. This assumption may not be correct, and the physics-based models may require the inclusion of the initial velocity right after the feet-first drop to be more accurate. Furthermore, there were only two fall dynamics observed in the replicated ATD feet-first falls, while the selected childcare center falls involving real children resulted in a variety of fall dynamics and impact planes. Therefore, further evaluation is recommended to explore how fall dynamics affect overall outcomes of these models.

c. Physics-based models and linear biomechanical outcomes

An observation of the performance of these models was that the PBMs were sensitive to height, and linear acceleration outcomes increased when height increased. Therefore, it is critical that those using PBMs consider a range of fall heights, especially if the exact fall height is unknown. The outcomes from this study indicate that a range of fall heights may allow bioengineering experts who are evaluating a given fall scenario to provide a reasonable range of probable biomechanical outcomes (which may then be used to evaluate the biomechanical compatibility of the given scenario). It is worth noting that greater priority can be placed on accurately estimating linear acceleration since many head injury thresholds utilize this metric.

Method A was found to result in the most accurate outcomes for all falls. However, this approach did not evaluate the rebound of the head impact, it only considered the crush phase. In other words, method A (and method D as well) may be considered an inelastic collision. This may account for overestimation of the change in linear velocity in some of the falls, as the model may better represent the impact velocity and not the change in linear velocity. It was not surprising that this was the most accurate method to estimate peak linear acceleration as it typically occurs at the end of the crush phase, or at  $\frac{1}{2}$  of the impact duration.

Another observation of these models was that the lumped mass and inverted pendulum PBMs tended to, but did not always, more accurately predict biomechanical outcomes compared to the single rod model. This was not surprising, as these models used a lumped point mass versus the single rod, which used evenly distributed mass. The lumped mass and inverted pendulum models may better represent the mass distribution of a child (more concentrated in the head and upper body) than a single rod (which is evenly distributed). What was surprising, though, was that when a researcher reviewed the video recordings and attempted to predict which PBM would be the most accurate type for that fall scenario, the prediction did not always match the PBM outcomes. For instance, in fall 321, the subject fell forward and impacted his knees on the classroom floor. He then fell forward and impacted the frontal region of his head on a drywall wall. In reviewing the fall dynamics, it was predicted that perhaps the inverted pendulum may result in the best outcomes. However, the single rod very closely predicted almost all biomechanical outcomes with a linear head acceleration of 0% error; change in linear head velocity of 0% error; rotational head acceleration [with radius about the neck] of 1% error; rotational

head velocity [about the neck] as 29% error. The results of the lumped mass and inverted pendulums were less accurate with a linear head acceleration of 47% error for both models; change in linear head velocity of 41% error for both models; rotational head acceleration [with radius about the neck] of 48% error for both models; rotational head velocity [about the neck] as 4% error for both models. This overestimation of biomechanical outcomes is likely due to the head impacting the drywall wall which is relatively compliant; this overestimation would be more pronounced with models employing a concentrated mass. However, further evaluation is recommended to explore best model selection based on fall dynamics.

One of the simulated childcare center falls, fall 516, resulted in large overestimations of the change in linear velocity (with 112% error for a lumped mass modeled with method A and a 115% error for an inverted pendulum modeled with method A). In this fall, the subject slipped on a small ball and impacted his buttocks on the classroom floor; he then fell rearward and impacted his occiput on possibly a toy and then the carpeted floor. However, right before the occiput impacted the floor, it appeared (from the video recording) that his left posterior shoulder may have impacted a toy truck that was on the floor behind him, and this was further evidenced by the truck moving away from the child (as viewed in the video recording). It is possible that the change in linear velocity of the head impacting the surface was smaller than expected because some of the energy in the fall was transferred to the truck when the posterior left shoulder impacted it. This is further indicated by the SIM G linear acceleration and velocity curve that was produced by the SIM G (FIGURE 122, reproduced here). The shape of this curve was not typical of the other SIM G impacts, and the presence of two acceleration peaks may indicate that

the first, larger peak (approx. 30 g) may be from the impact of the shoulder right before the head impacted the carpeted floor, resulting in the second peak (approx. 27 g). This head acceleration time history curve indicates that the abstraction of details may be an important factor in the evaluation of fall scenarios.

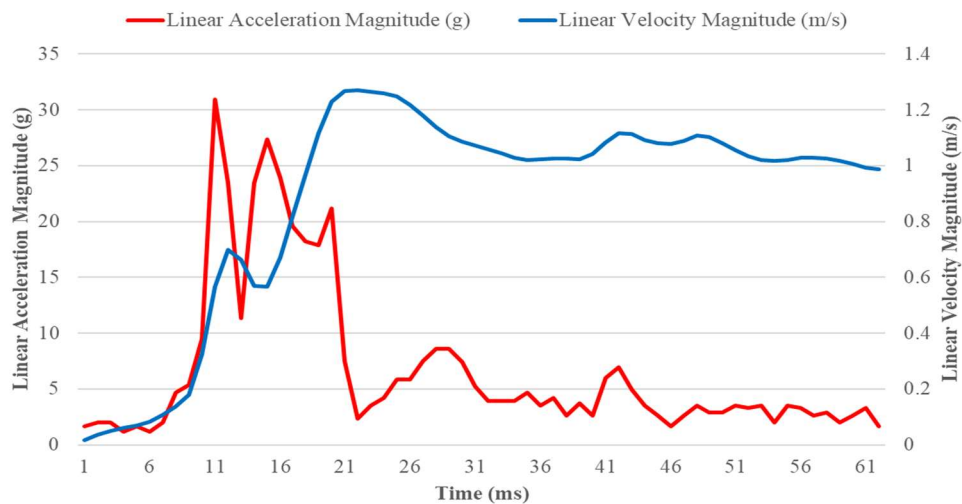


FIGURE 122 – Linear acceleration magnitude (g) and linear velocity magnitude (m/s) from SIM G output for fall 516

d. Physics-based models and rotational biomechanical outcomes

When the parameter sensitivity analysis (PSA) was performed on the replicated ATD falls, it was found that the rotational acceleration and rotational velocity were more accurate when the radius of rotation was set as “about the hips” (i.e., length from the head COM of the ATD to the buttocks) and approximately the same for “about the knees” (i.e., length from the head COM of the ATD to the knees). This made sense, as the ATD buttocks first impacted the flooring surface during the fall. Furthermore, because the



ATD rotated about the hips then impacted the occiput, the PSA outcomes were consistent with the qualitative assessment that rotation “about the hips” would be more accurate than just “about the neck”. In contrast, the PSA demonstrated that rotation about the neck for childcare center falls yielded more accurate PBM predictions. This may have been due to differences in fall dynamics when comparing ATD falls to childcare center falls, or it may be due to differences in compliance of the ATD neck vs that of a child. The ATD neck is much stiffer and less compliant than the relatively flexible neck of a child. In the ATD neck design, there is a cable that connects the head to the torso of the ATD, which introduces resistance to head rotation. This may partially explain why the PSA for the childcare center falls indicated that the neck was the most appropriate radius of rotation to evaluate rotational outcomes. For the childcare center falls, as the radius of rotation increased, the overall rotational outcomes decreased and became less accurate.

e. Surface properties, rebound, and COR

An unexpected outcome of this study was that, when surface coefficient of restitution was included in the analysis methodology for the physics-based models (i.e., methods B and C), the replicated ATD feet-first fall outcomes for peak linear head acceleration, rotational head acceleration, and rotational head velocity were overestimated. For change in linear head velocity in these ATD falls, the outcomes were consistently underestimated. For the simulated childcare center falls, Methods B and C for all three model types consistently overestimated all biomechanical measures.

When the analysis methodology was developed for PBMs, it was assumed that surface coefficient of restitution was an important factor in modeling these falls. Previous studies have shown that impact surface has a significant effect on head biomechanical

outcomes (Hu, 2017; Thompson 2013; Jones & Theobald, 2011; Pierce et al. 2002; Cory et al. 2001; Snyder & Civil Aeromedical research, 1963). Furthermore, Hilt (2018) found that the surface COR had an effect on mean peak resultant linear accelerations, mean HIC<sub>15</sub>, mean whole-body impact velocity, and change in impact momentum from common short-distance falls involving children in a childcare setting. This was why surface COR was collected and included in this study. However, using methods A and D in the PBMs, where COR and therefore rebound velocity were assumed to not influence biomechanical outcomes, resulted in the most accurate outcomes. The less accurate predictions associated with Methods B and C may be associated with calculating peak linear acceleration from the average linear acceleration since the full impact duration is utilized in these methods. Peak linear acceleration is therefore indirectly calculated from average linear acceleration. Additionally, there may be limitations in the methodology used to obtain COR. COR measurements of impact surfaces were obtained by dropping a small (0.625-inch diameter; 17.5 g), stainless steel ball from a known height and measuring its rebound height. This may not be an accurate method, as a child's head has a larger mass and is less homogenous (skull, scalp, etc.) than the steel ball (Jackson, Green, and Marghitu, 2009; Imre, Raepsamen, and Springman, 2007). It is expected that the lightweight steel ball will cause less surface deformation than a child or ATD head and will rebound from the surface differently. Additionally, the COR only characterizes the rebound or unloading phase of impact representative of a damper in mechanical analogue models. A more direct measure of surface stiffness, or a spring constant, is needed to describe the loading phase of an object impacting a surface. Perhaps a

combined spring-damper system may yield more accurate model predictions of the interaction between the head and the impact surface.

#### E. Clinical and judicial relevance

##### 1. Clinical relevance

This study resulted in a comprehensive fall dataset that will allow clinical and forensic investigators to learn more about short distance fall characteristics and expected outcomes in young children. Furthermore, the body region contact/impact maps that were developed could help investigators have a better understanding of the commonly impacted body regions and body planes that are involved in short-distance falls involving young children. Body region contact/impact maps may be used to better understand body regions that have the highest frequency of potential evidence of impact, such as a bruise. In other words, the body regions involved in the primary impact of a fall may be thought as the region(s) that have the greatest potential for injury. This is an important finding because these maps were based on reliably witnessed and video recorded falls with known outcomes. These body region contact/impact maps and the dataset may be used as tools by physicians and investigators to better understand expected outcomes of common short-distance falls, which may improve their ability to assess whether a fall history provided by a caregiver could adequately explain a child's presenting injuries. The outcomes from the physics-based models indicated that, when clinicians or forensic investigators are obtaining a history of a short-distance fall, details for the fall scenario and from the fall scene may be useful in modeling the falls with mathematical physics-based models.

## 2. Judicial relevance

As discussed in the introduction, a fall is the most common false history provided by caregivers in cases of abuse. When a forensic investigation is undertaken as part of a litigation to determine the plausibility of a short distance fall history causing a child's injury, bioengineers may be called in as expert witnesses. Bioengineers evaluate the biomechanical compatibility of a given fall scenario and a child's presenting injuries. In these cases, these experts are often provided certain details (e.g., impact surface, estimated fall height, child characteristics, how the child fell, etc.) regarding an alleged fall that was observed by a caregiver. They then use these details to evaluate the provided fall scenario, often using mathematical physics-based models to predict the biomechanical outcomes for the scenario. Published ATD studies are also used to estimate potential biomechanical outcomes for comparison, but fall scenarios may differ and biofidelity of ATDs may be limited. Furthermore, previously there were no studies that involved video recorded falls involving children in a real-world setting (e.g., childcare center) with biomechanical data from these falls. This study not only resulted in biomechanical data for witnessed video recorded short-distance falls, but it also determined that mathematical physics-based models provide reasonable predictions of biomechanical outcomes for both replicated ATD falls and in the simulation of childcare center falls with actual children. These findings are important because they indicate that the use of mathematical PBMs by expert witnesses to evaluate cases regarding short-distance falls involving young children may be an appropriate and useful tool in estimating biomechanical outcomes to aid in determining whether the provided fall scenario could result in the presenting injuries.

## F. Limitations

A limitation of this study is that subject ages ranged from 17 to 25 months and development status may differ across this range. Given the small sample size it was not possible to analyze the effects of differences in mobility/abilities of the children. Perhaps children who are closer to 3 years of age will have more stability and fall less than children closer to 1 year of age, who are just developing the ability to walk. Also, because this was a pilot study, a convenience sample of the first 100 falls was used and there was no effort to distribute falls across the age range. In this study, no injuries resulted from falls, but it is important to note that falls occurred in a supervised childcare setting where the environment was designed to be safe. If the same falls occurred in a non-supervised setting without regard to safety of the environment (i.e., limited playground equipment height, compliant playground surface) injury outcomes may have varied.

When the replicated ATD feet-first falls were evaluated to determine the effects of fall dynamics, only falls onto linoleum were evaluated because all falls onto carpet resulted in the same type of dynamics (i.e., no variation in fall dynamics). However, the sample sizes were small for the falls onto linoleum (n=7), with most representing dynamic A (n=5) and only two falls representing dynamic C. Dynamic C, however, is a dynamic that is not expected to occur in actual falls involving children and resulted due to ATD foot and ankle design (i.e., rubber foot and ankle). This limitation was discussed in a previous study by Thompson, et al. (2018). Researchers in the previous study indicated that the lower leg (foot and ankle) of the 12-month-old CRABI ATD were not modified to be more biofidelic. This influenced impact dynamics; the ATD fell into a

crouch position where the heels of the feet lifted off the floor, while the toes remained on the floor leading to plantar flexion of the ankles and rolling onto the dorsal surface of the feet as the ATD pelvis continued to move downward. Then, the hips and knees extended after the pelvis impacted, which caused the ATD to launch rearward, landing in a final supine position (Thompson, 2018). As the researchers mentioned, this dynamic may be an “artifact given the lower leg design” (Thompson, 2018). In the ATD design, the lower leg consisted of a rod representing the tibia which ended just proximal to the ankle, and did not connect to the ankle. Furthermore, the ankle joint and foot are a rubber and foam structure. This design led to some of the falls resulting in dynamics that were not realistic, as none of the observed childcare center falls in this study resulted in such dynamics. Despite some ATD falls including unrealistic impact dynamics, it is important to note that this did not adversely affect the validation of the SIM G device.

There were several limitations with respect to use of the SIM G devices. SIM G devices were activated only when linear acceleration met or exceeded the 12 g threshold; this occurred in a 14 of the first verified 100 falls. Head biomechanical data was not available for the remainder of falls. Also, although measures were taken to obtain a snug fit, if the SIM G headband was not snugly fit on a subject’s head, inaccurate biomechanical data may have been obtained. The headbands were available in three sizes (i.e., small, medium, and large) and were matched to child head circumference, but were not customized to each individual subject. Another limitation was that linear velocity was not directly measured by the SIM G and derived from integration of linear acceleration to obtain the change in velocity. Although 3 video cameras were installed in each monitored space, a small number of were not in view of the cameras; these were not included in the

study. Some falls were blocked by furniture and some occurred in an area of the childcare center that was not equipped with cameras (i.e., the hallways).

The physics-based models were limited in that they simplified a child's body down to a simple design with uniform or concentrated mass (i.e., lumped mass, single rod, and inverted pendulum). In reality, children differ in their mass distribution. Furthermore, these childcare center falls are more complex than, for example, a single rod rotating about a fixed point. Real-world falls often involve multiple or moving centers of rotation. Additionally, these models represent rigid bodies and do not account for energy absorption that occurs within the body and impact surface, thus overestimating biomechanical outcomes and representing worst-case scenarios. The models did not include active muscle response when children braced themselves during falls, thus, it is not surprising that the models often overestimated biomechanical measures. Additionally, the models did not account for falls having more than one impact to multiple body regions (select falls from the childcare center were limited to those with primary head impact). Another limitation of the physics-based model predictions was that fall heights were estimated from video recordings and child anthropometrics, and it was determined that these models were sensitive to these estimated fall heights.

#### G. Future work and recommendations

This pilot study evaluated biomechanical measures recorded in video monitored short distance falls involving children in a childcare setting. Data from this pilot study will be used by the researchers to perform a power analysis to determine an adequate sample size to test for significant differences between falls with head impact and without head impact. Future work will include a larger sample of SIM G biomechanical measures and

monitoring of injury outcomes, including collection of injury incident reports from the childcare center; researchers will use these outcomes to characterize injury outcomes and determine the rate of severe head injury in these video-recorded pediatric falls. Future work will also include developing a predictive model that will estimate head impact acceleration and velocity based upon fall, environment, and child characteristics. Finally, a searchable web-based knowledgebase will be created that will include information from these video-recorded pediatric falls, with the overall goal of facilitating the biomechanical assessment of fall injury and injury compatibility.

This study also resulted in a comparison of SIM G outcomes to outcomes predicted using mathematical physics-based models. It was determined that the tested models (i.e., lumped mass, single rod, and inverted pendulum) provided reasonable estimations for biomechanical measures. However, there was no one PBM that performed best as compared to the other models. Therefore, further study is needed to understand which PBM(s) can best predict biomechanical outcomes based on fall dynamics. Further investigation is recommended to determine which PBM best predicts outcomes for certain fall dynamics or scenarios. This may lead to the development of guidelines for bioengineer experts that recommend a suitable PBM for a given fall scenario. This study resulted in biomechanical data from real falls involving children, and these SIM G outcomes could be used to make physics-based models that involve more segments (i.e., multibody models) more accurate (Kakara, 2013).

It is suggested that further evaluation of how coefficient of restitution is obtained and how it effects biomechanical outcomes is needed. Head impact on a surface may be modeled more accurately with a 3-parameter viscoelastic model as suggested by Prange



(2004). In Prange et al. (2004), researchers compared both 6-month-old CRABI ATD head and infant cadaveric head specimens (1, 3, and 11 days old) free-falling and impacting a flat anvil surface from two different fall heights (15 cm and 30 cm). They then compared the ATD and infant cadaveric impact outcomes (including peak linear head acceleration, impact pulse (time) duration, and HIC values) to two developed mathematical models. Two different force-time models were developed – a simple mass-spring system and a second model that coupled a head mass model to a three-parameter viscoelastic model. This study determined that the simple spring-mass model could not fully represent impact data. However, the 3-parameter viscoelastic model was more accurate. By introducing a viscoelastic component, a damping unloading response after the impact was better represented. While mathematical models used by Prange accurately predicted biomechanical outcomes, their specific models were applied to controlled experiments and would not be suitable for use in predicting biomechanical outcomes from falls occurring in a real-world setting. However, if the physics-based models in this study were represented with a similar 3-parameter model to the Prange study that better represents the unloading response of the head, then the replicated ATD falls and the childcare center falls may be more accurate to the SIM G outcomes.

## VII. CONCLUSIONS

This pilot study resulted in a comprehensive dataset of 100 reliably witnessed video-recorded falls involving young children in a childcare center setting with known outcomes. This study also resulted in body region contact/impact maps that demonstrated the most frequently involved body regions in these common short-distance falls. These maps demonstrated that the head was not commonly impacted in these falls. This study also found that head biomechanical measures were not significantly different in falls with head impact versus without head impact, except for peak resultant rotational head acceleration. These findings were different than previous findings, which found that most biomechanical measures were greater in falls with head impact than those without head impact. This study also found that the methodology used in lumped mass, single rod, and inverted pendulum models was an important factor in predicting head biomechanical outcomes. The lumped mass and inverted pendulum physics-based models were the most accurate, when surface coefficient of restitution/rebound velocity was not included in the model. It was determined that the models in this study resulted in reasonable predictions of biomechanical outcomes. No falls in this study resulted in injury or the generation of an incident report by childcare center staff. This study addressed several current gaps in the literature. Child rotational head velocity and acceleration were measured in video-recorded and witnessed falls. Along with Hilt (2018), these studies are valuable because they are the only known studies that involve falls of young children equipped with head-mounted accelerometers occurring during normal daily activities in a childcare center setting. Findings from this study may further increase the understanding of falls involving

young children and can potentially aid in the differentiation of accidental versus abusive injuries in the presence of a fall history.

## VIII. REFERENCES CITED

- Aghakhani, K., Heidari, M., Ameri, M., Mehrpisheh, S., & Memarian, A. (2015). Characteristics of Traumatic Brain Injury among Accident and Falling Down Cases. *Acta medica Iranica*, 53(10), 652-655.
- Allison, M. A., Kang, Y. S., Maltese, M. R., Bolte, J. H. t., & Arbogast, K. B. (2015). Measurement of Hybrid III Head Impact Kinematics Using an Accelerometer and Gyroscope System in Ice Hockey Helmets. *Annals of biomedical engineering*, 43(8), 1896-1906. doi:10.1007/s10439-014-1197-z
- Andrew, E. L., Michael, H., Lisa, H., Nelson, C., Gregory, D. M., Margot, P., & Shane, V. C. (2017). Video Analysis Verification of Head Impact Events Measured by Wearable Sensors. *The American journal of sports medicine*.
- Arregui-Dalmases, C., Teijeira, R., Forman, J., & Geneva. (2010). Injury biomechanics as a necessary tool in the field of forensic science: A pedestrian run-over case study. *Forensic Science International*, 198(1-3), e5-e9. doi:10.1016/j.forsciint.2010.01.008
- Bagala, F., Becker, C., Cappello, A., Chiari, L., Aminian, K., Hausdorff, J. M., . . . Klenk, J. (2012). Evaluation of Accelerometer-Based Fall Detection Algorithms on Real-World Falls. *PLoS ONE*, 7(5).
- Bagnato, S. J., & Feldman, H. (1989). Closed head injury in infants and preschool children: Research and practice issues. *Infants & Young Children*, 2(1), 1-13.
- Bandak, F. A. (2005). Shaken baby syndrome: A biomechanics analysis of injury mechanisms. *Forensic Science International*, 151(1), 71-79. doi:10.1016/j.forsciint.2005.02.033
- Bertocci, G. E., Pierce, M. C., Deemer, E., Aguel, F., Janosky, J. E., & Vogeley, E. (2003). Using test dummy experiments to investigate pediatric injury risk in simulated short-distance falls. *Archives of pediatrics & adolescent medicine*, 157(5), 480-486.
- Bertocci, G. E., Pierce, M. C., Deemer, E., Aguel, F., Janosky, J. E., & Vogeley, E. (2004). Influence of fall height and impact surface on biomechanics of feet-first free falls in children. *Injury*, 35(4), 417-424. doi:[https://doi.org/10.1016/S0020-1383\(03\)00062-7](https://doi.org/10.1016/S0020-1383(03)00062-7)
- Briss, P. A., Sacks, J. J., Addiss, D. G., Kresnow, M., & O'Neil, J. (1995). Injuries from falls on playgrounds: Effects of day care center regulation and enforcement. *Archives of pediatrics & adolescent medicine*, 149(8), 906-911. doi:10.1001/archpedi.1995.02170210080014
- Burrows, P., Trefan, L., Houston, R., Hughes, J., Pearson, G., Edwards, R. J., . . . Kemp, A. M. (2015). Head injury from falls in children younger than 6 years of age. *Archives of Disease in Childhood*, 100(11), 1032-1037. doi:10.1136/archdischild-2014-307119
- Case, M. E. (2008). Accidental Traumatic Head Injury in Infants and Young Children. *Brain Pathology*, 18(4), 583-589. doi:doi:10.1111/j.1750-3639.2008.00203.x
- Case, M. E. (2008). Forensic pathology of child brain trauma. *Brain pathology (Zurich, Switzerland)*, 18(4), 562-564.
- Case, M. E. (2014). Distinguishing accidental from inflicted head trauma at autopsy. *Pediatric Radiology*, 44(4), 632-640.

- Chadwick, D. L., Bertocci, G., Castillo, E., Frasier, L., Guenther, E., Hansen, K., . . . Krous, H. F. (2008). Annual Risk of Death Resulting From Short Falls Among Young Children: Less Than 1 in 1 Million. *Pediatrics*, *121*(6), 1213-1224.
- Chadwick, D. L., Chin, S., Salerno, C., Landsverk, J., & Kitchen, L. (1991). Deaths from falls in children: how far is fatal? *The Journal of trauma*, *31*(10), 1353-1355.
- Children's Bureau: An Office of the Administration for Children & Families, U.S. Department of Health & Human Services. *Child Maltreatment 2018*. 2020. Web.
- Chrisman, S. P., Mac Donald, C. L., Friedman, S., Andre, J., Rowhani-Rahbar, A., Drescher, S., . . . Rivara, F. P. (2016). Head Impact Exposure During a Weekend Youth Soccer Tournament. *Journal of child neurology*, *31*(8), 971-978. doi:10.1177/0883073816634857
- Coats, B., & Margulies, S. S. (2008). Potential for head injuries in infants from low-height falls. *J Neurosurg Pediatr*, *2*(5), 321-330. doi:10.3171/ped.2008.2.11.321
- Cortes, N., Lincoln, A. E., Myer, G. D., Hepburn, L., Higgins, M., Putukian, M., & Caswell, S. V. (2017). Video Analysis Verification of Head Impact Events Measured by Wearable Sensors. *The American journal of sports medicine*, *45*(10), 2379-2387. doi:10.1177/0363546517706703
- Cory, C. Z., Jones, M. D., James, D. S., Leadbeater, S., & Nokes, L. D. M. (2001). The potential and limitations of utilising head impact injury models to assess the likelihood of significant head injury in infants after a fall. *Forensic Science International*, *123*(2), 89-106. doi:[https://doi.org/10.1016/S0379-0738\(01\)00523-0](https://doi.org/10.1016/S0379-0738(01)00523-0)
- Cory, Z. C., & M, D. J. (2003). Can Shaking Alone Cause Fatal Brain Injury? : A biomechanical assessment of the Duhaime shaken baby syndrome model. *Medicine, Science and the Law*, *43*(4), 317-333.
- Crisco, J. J., Wilcox, B. J., Beckwith, J. G., Chu, J. J., Duhaime, A.-C., Rowson, S., . . . Greenwald, R. M. (2011). Head impact exposure in collegiate football players. *Journal of Biomechanics*, *44*(15), 2673-2678. doi:10.1016/j.jbiomech.2011.08.003
- Dekaban, A. and Sadowsky, D. (1978). Changes in Brain Weights During the Span of Human Life: Relation of Brain Weights to Body Heights and Body Weights. *Annals of Neurology*, *4*(4), p. 345-356.
- Dsouza, R. and Bertocci, G. (2016). Impact sites representing potential bruising locations associated with rearward falls in children. *Forensic Science International*, *261*, 129-136.
- Dsouza, R. and Bertocci, G. (2018). Impact sites representing potential bruising locations associated with bed falls in children. *Forensic Science International*, *286*, 86-95.
- Dufek, J. S., Ryan-Wenger, N. A., Eggleston, J. D., & Mefferd, K. C. (2018). A Novel Approach to Assessing Head Injury Severity in Pediatric Patient Falls. *Journal of Pediatric Health Care*, *32*(2), e59-e66. doi:<https://doi.org/10.1016/j.pedhc.2017.09.012>
- Duhaime, A. C., Alario, A. J., Lewander, W. J., Schut, L., Sutton, L. N., Seidl, T. S., . . . Loporchio, S. (1992). Head Injury in Very Young Children: Mechanisms, Injury Types, and Ophthalmologic Findings in 100 Hospitalized Patients Younger Than 2 Years of Age. *Pediatrics*, *90*(2), 179-185. Retrieved from <http://pediatrics.aappublications.org/content/pediatrics/90/2/179.full.pdf>

- Duhaime, A. C., Gennarelli, T. A., Thibault, L. E., Bruce, D. A., Margulies, S. S., & Wisner, R. (1987). The shaken baby syndrome. A clinical, pathological, and biomechanical study. *Journal of neurosurgery*, 66(3), 409-415.
- Forero Rueda, M. A., & Gilchrist, M. D. (2009). Comparative multibody dynamics analysis of falls from playground climbing frames. *Forensic Science International*, 191(1), 52-57. doi:<https://doi.org/10.1016/j.forsciint.2009.06.007>
- Girard, N., Brunel, H., Dory-Lautrec, P., & Chabrol, B. (2016). Neuroimaging differential diagnoses to abusive head trauma. *Pediatric Radiology*, 46(5), 603-614. doi:10.1007/s00247-015-3509-3
- Gurdjian, E. S., Roberts, V. L., & Thomas, L. M. (1966). Tolerance curves of acceleration and intracranial pressure and protective index in experimental head injury. *The Journal of trauma*, 6(5), 600-604.
- Hagedorn, A. V. & Pritz, H. B. (1999). Evaluation of the CRABI 12-month-old infant and its comparison with the TNO P3/4. *NHTSA Docket # 99-5156*.
- Hajiaghameh, M., Seidi, M., Ferguson, J. R., & Caccese, V. (2015). Measurement of Head Impact Due to Standing Fall in Adults Using Anthropomorphic Test Dummies. *Annals of biomedical engineering*, 43(9), 2143-2152. doi:10.1007/s10439-015-1255-1
- Helfer, R. E., Slovis, T. L., & Black, M. (1977). Injuries resulting when small children fall out of bed. *Pediatrics*, 60(4), 533-535.
- Hu, J. (2017). Height of head centre of gravity predicts paediatric head injury severity in short-distance falls. *Evidence Based Medicine*, 22(1), 36-36. doi:10.1136/ebmed-2016-110558
- Hughes, J., Maguire, S., Jones, M., Theobald, P., & Kemp, A. (2016). Biomechanical characteristics of head injuries from falls in children younger than 48 months. *Archives of Disease in Childhood*, 101(4), 310-315. doi:10.1136/archdischild-2014-306803
- Hilt, Bret. 2018. Biomechanical characterization of video-recorded short-distance falls involving children equipped with a biometric device: A pilot study. Master's thesis. University of Louisville, Louisville.
- Ibrahim, N. G., & Margulies, S. S. (2010). Biomechanics of the toddler head during low-height falls: an anthropomorphic dummy analysis. *J Neurosurg Pediatr*, 6(1), 57-68. doi:10.3171/2010.3.peds09357
- Ibrahim, N. G., Wood, J., Margulies, S. S., & Christian, C. W. (2012). Influence of age and fall type on head injuries in infants and toddlers. *International Journal of Developmental Neuroscience*, 30(3), 201-206. doi:<https://doi.org/10.1016/j.ijdevneu.2011.10.007>
- Imre, B., Raepsamen, S., and Springman, S. M. (2007). A coefficient of restitution of rock materials. *Computers & Geosciences*, 34(2008), 339-350.
- Jackson, R., Green, I., and Marghitu, D. Predicting the coefficient of restitution of impacting elastic-perfectly plastic spheres. *Journal of Nonlinear Dynamics*, 60 (2010), 217-229.
- Jenny, C. A., Bertocci, G., Fukuda, T., Rangarajan, N., & Shams, T. (2017). Biomechanical Response of the Infant Head to Shaking: An Experimental Investigation. *Journal of Neurotrauma*, 34(8), 1579-1588.
- Jones, M. D., & Theobald, P. S. (2011). The potential effects of floor impact surfaces on

- infant head injury outcome during a short fall. *Medicine, science, and the law*, 51(4), 203-207. doi:10.1258/msl.2011.011006
- Kakara, H., Nishida, Y., Yoon, S. M., Miyazaki, Y., Koizumi, Y., Mizoguchi, H., & Yamanaka, T. (2013). Development of childhood fall motion database and browser based on behavior measurements. *Accident Analysis & Prevention*, 59(Supplement C), 432-442. doi:<https://doi.org/10.1016/j.aap.2013.06.015>
- Kangas, M., Konttila, A., Lindgren, P., Winblad, I., & Jämsä, T. (2008). Comparison of low-complexity fall detection algorithms for body attached accelerometers. *Gait & Posture*, 28(2), 285-291. doi:<https://doi.org/10.1016/j.gaitpost.2008.01.003>
- Kleiven, S. (2013). Why Most Traumatic Brain Injuries are Not Caused by Linear Acceleration but Skull Fractures are. *Frontiers in bioengineering and biotechnology*, 1, 15. doi:10.3389/fbioe.2013.00015
- Kotch, J. B., Chalmers, D. J., Langley, J. D., & Marshall, S. W. (1993). Child day care and home injuries involving playground equipment. *Journal of Paediatrics and Child Health*, 29(3), 222-227.
- Lillis, K. A., & Jaffe, D. M. (1997). Playground injuries in children. *Pediatric emergency care*, 13(2), 149-153.
- Loyd, A. M., Nightingale, R. W., Luck, J. F., Song, Y., Fronheiser, L., Cutcliffe, H., . . . Dale Bass, C. R. (2015). The compressive stiffness of human pediatric heads. *Journal of Biomechanics*, 48(14), 3766-3775.
- Lyons, T. J., & Oates, R. K. (1993). Falling out of bed: a relatively benign occurrence. *Pediatrics*, 92(1), 125-127.
- Mahajan, P V, and B A Bharucha. "Evaluation of short neck: new neck length percentiles and linear correlations with height and sitting height." *Indian pediatrics* vol. 31,10 (1994): 1193-203.
- Margulies, S. S., & Thibault, L. E. (1992). A proposed tolerance criterion for diffuse axonal injury in man. *Journal of Biomechanics*, 25(8), 917-923.
- Mohan, D., Bowman, B. M., Snyder, R. G., & Foust, D. R. (1979). A Biomechanical Analysis of Head Impact Injuries to Children. *J Biomech Eng*, 101(4), 250-260. doi:10.1115/1.3426254
- Morrison, L., Chalmers, D., Parry, M., & Wright, C. (2002). Infant-furniture-related injuries among preschool children in New Zealand, 1987–1996. *Journal of Paediatrics and Child Health*, 38(6), 587-592. doi:doi:10.1046/j.1440-1754.2002.00059.x
- Mulligan, C. S., Adams, S., Tzioumi, D., & Brown, J. (2017). Injury from falls in infants under one year. *Journal of Paediatrics and Child Health*, 53(8), 754-760. doi:doi:10.1111/jpc.13568
- National Center for Injury Prevention and Control – Division of Violence Prevention. *Child maltreatment*. 2014. Web.
- Nimityongskul, P., & Anderson, L. D. (1987). The likelihood of injuries when children fall out of bed. *Journal of pediatric orthopedics*, 7(2), 184-186.
- Ommaya, A. K., Goldsmith, W., & Thibault, L. (2002). Biomechanics and neuropathology of adult and paediatric head injury. *British Journal of Neurosurgery*, 16(3), 220-242. doi:10.1080/02688690220148824
- Ommaya, A. K., & Hirsch, A. E. (1971). Tolerances for cerebral concussion from head impact and whiplash in primates. *Journal of Biomechanics*, 4(1), 13-21.

- doi:[https://doi.org/10.1016/0021-9290\(71\)90011-X](https://doi.org/10.1016/0021-9290(71)90011-X)
- Ono, H., Sase, T., Takasuna, H., & Tanaka, Y. (2019). Playground equipment-related head injuries requiring hospitalization in children. *Pediatrics International*, 61(3), 293-297. doi:10.1111/ped.13765
- Overall Fall Nonfatal Emergency Department Visits and Rates per 100,00. Web-based Injury Statistics Query and Reporting System, Center for Disease Control. 2020. Web.
- Pierce, M. C., Bertocci, G. E., Berger, R., & Vogeley, E. (2002). Injury biomechanics for aiding in the diagnosis of abusive head trauma. *Neurosurgery Clinics of North America*, 13(2), 155-168. doi:[https://doi.org/10.1016/S1042-3680\(01\)00006-7](https://doi.org/10.1016/S1042-3680(01)00006-7)
- Powell, E. C., Jovtis, E., & Tanz, R. R. (2002). Incidence and Description of Highchair-Related Injuries to Children. *Ambulatory Pediatrics*, 2(4), 276-278. doi:[https://doi.org/10.1367/1539-4409\(2002\)002<0276:IADOHC>2.0.CO;2](https://doi.org/10.1367/1539-4409(2002)002<0276:IADOHC>2.0.CO;2)
- Reichelderfer, T. E., Overbach, A., & Greensher, J. (1979). Unsafe playgrounds. *Pediatrics*, 64(6), 962-963.
- Snyder, R. G., & Civil Aeromedical Research, I. (1963). *Human survivability of extreme impacts in free-fall*. Washington, D.C.: United States Government Printing Office.
- Snyder, R., Spencer, M., Owings, C., and Schneider, L. (1975). Physical characteristics of children as related to death and injury for consumer product design and use. *Highway Safety Research Institute at The University of Michigan*. 241 p. UM-HSRI-BI-75-75.
- Stürtz, G. (1980). Biomechanical Data of Children. *SAE Transactions*, 89, 4008-4030.
- Thompson, A., Bertocci, G., & Pierce, M. C. (2013). Assessment of injury potential in pediatric bed fall experiments using an anthropomorphic test device. *Accident Analysis & Prevention*, 50, 16-24. doi:<https://doi.org/10.1016/j.aap.2012.09.011>
- Thompson, A., Bertocci, G., & Smalley, C. (2018). Femur loading in feet-first fall experiments using an anthropomorphic test device. *Journal of Forensic and Legal Medicine*, 58, 25-33. doi: 10.1016/j.jflm.2018.03.017
- Thompson, A. K., Bertocci, G., Rice, W., & Pierce, M. C. (2011). Pediatric short-distance household falls: Biomechanics and associated injury severity. *Accident Analysis & Prevention*, 43(1), 143-150. doi:<https://doi.org/10.1016/j.aap.2010.07.020>
- Thompson, A. K., Bertocci, G., & Pierce, M. C. (2009). Assessment of head injury risk associated with feet-first free falls in 12-month-old children using an anthropomorphic test device. *The Journal of Trauma Injury, Infection, and Critical Care*, 66(4), 1019-1029.
- van den Kroonenberg, A. J., Hayes, W. C., & McMahon, T. A. (1995). Dynamic Models for Sideways Falls From Standing Height. *Journal of Biomechanical Engineering*, 117(3), 309-318. doi:10.1115/1.2794186
- van Hoof, J., de Lange, R., and Wismans, J. Improving pedestrian safety using numerical human models, *Stapp Car Crash Journal* 47 (2003) 401-436.
- Wilcox, B. J., Beckwith, J. G., Greenwald, R. M., Chu, J. J., McAllister, T. W., Flashman, L. A., . . . Crisco, J. J. (2014). Head impact exposure in male and female collegiate ice hockey players. *Journal of Biomechanics*, 47(1), 109-114. doi:10.1016/j.jbiomech.2013.10.004
- Williams, R. A. (1991). Injuries in infants and small children resulting from witnessed



and corroborated free falls. *The Journal of trauma*, 31(10), 1350-1352.

Yoganandan, N., Stemper, B. D., Pintar, F. A., & Maiman, D. J. (2011). Use of postmortem human subjects to describe injury responses and tolerances. *Clinical Anatomy*, 24(3), 282-293.

IX. APPENDIX I

A. Example from fall database

Fall 14 from the database is included here to demonstrate how a fall was analyzed (TABLE 49).

TABLE 49

EXAMPLE OF FALL ANALYSIS

<b>Data field</b>	<b>Definition</b>	<b>Field options</b>	<b>Example</b>
<b>Fall ID</b>	Identification number assigned to the sequential fall event.	Numerical	14
<b>Classroom location</b>	The camera-equipped location in the childcare where the fall occurred.	Classroom 1; classroom 2; playground	Playground
<b>Subject ID</b>	Unique identification number assigned to each enrolled child.	Numerical	4
<b>Subject gender</b>	Gender of the enrolled child experiencing the fall event.	Male; female	Male
<b>Fall description</b>	Full, detailed narration of all phases of the event,	Open response	See footnote <sup>1</sup>

	supplemented by fall log sheet and video recording.		
<b>Initial condition</b>	Action/activity subject is performing prior to the fall being triggered.	Walking; running; standing; jumping; squatting; sitting; stepping; other [open response]	Walking
<b>Fall initiation</b>	The cause of the fall and the phase where the fall event begins.	Loss of balance; tripped; slipped; pushed; other [open response]	Pushed; other (collision)
<b>Fall type</b>	Judged visually; whether the fall began with the child on an elevated surface that was an appreciable distance from the impact surface height.	Ground; height; other [open response]	Ground

<b>Fall dynamics</b>	The direction(s) the subject moves during the fall.  (forward, rearward, lateral, feet-first).	Forward; rearward; left lateral; right lateral; feet first	Right lateral
<b>Equipment/object involvement</b>	Whether an inanimate object is involved during any phase of the fall.	Yes; no	No
<b>Type of equipment/object involved</b>	If yes for an object(s) involvement, identify the object(s) involved.	Playground equipment; toy; classroom furniture; butterfly slide; pillow; container; carpeted steps; other [open response]	
<b>Phase(s) of fall with equipment/object involvement</b>	If yes for object involvement, identify the phase(s) of the fall where equipment/object is involved.	Initial condition; fall initiation; primary impact; secondary impact	

<b>Another person(s) involvement</b>	Whether another person, not including the fall subject, is involved during any phase of the fall.	Yes; no	Yes
<b>Person(s) involved in the fall</b>	If yes for another person(s) involvement, identify the person(s) involved.	One other child; one adult; two other children; one other child and one adult; two other children and one adult; other [open response]	One other child
<b>Phase(s) of fall with another person(s) involvement</b>	If yes for another person(s) involvement, identify the phase(s) of the fall where another person(s) is involved.	Initial condition; fall initiation; primary impact; entire fall	Fall initiation
<b>Head impact</b>	Whether the subject's head comes into contact with any surface, item, person, etc. during any phase of the fall.	Yes; no; undetermined	Yes

<p><b>Primary impact surface</b></p>	<p>The surface(s) on which the primary impact of the fall occurs.</p>	<p>Playground mulch; carpet; rug on carpet; linoleum; other [open response]</p>	<p>Playground mulch</p>
<p><b>First contact body region(s)</b></p>	<p>The phase of the fall after fall initiation where a body part touches any surface prior to impact. Not all falls will have first contact. Identify the body region(s) involved during this phase.</p>	<p>Open response [see Table 8 in section IV.F.2]</p>	<p>Left lateral torso; left lateral arm; head occiput</p>
<p><b>Primary impact body region(s)</b></p>	<p>The phase of the fall that is qualitatively judged to dissipate the most energy from the subject striking/forcibly coming into contact with a surface/object/person/etc. Identify the body region(s) involved during this phase.</p>	<p>Open response [see Table 8 in section IV.F.2]</p>	<p>Right lateral leg; right hip; right hand; right forearm</p>

<p><b>Secondary impact body region(s)</b></p>	<p>The subsequent impact phase to primary impact.</p> <p>Fall events did not always include a secondary impact.</p> <p>Identify the body region(s) involved during this phase.</p>	<p>Open response [see Table 8 in section IV.E.2]</p>	<p>Left hand palm</p>
<p><b>Body plane(s) impacted during primary impact</b></p>	<p>The plane(s) of the body that strike a surface/object/person/etc. during the primary impact.</p>	<p>Anterior; posterior; left lateral; right lateral; left medial; right medial</p>	<p>Right lateral</p>
<p><b>Final position</b></p>	<p>Resting position/orientation of the subject at the end of the fall.</p>	<p>Sitting; lateral recumbent (right/left); on hands and knees; prone; on hands and feet; supine; other [open response]</p>	<p>Lateral recumbent (right)</p>

<b>Equipped with SIM G</b>	Whether a subject was properly wearing a sensor during the fall event.	Yes; no	Yes
<b>Activation of SIM G</b>	Whether the SIM G was activated during the fall event.	Yes; no	Yes
<b>Injury outcomes</b>	Whether injury(s) was associated with the fall.	Yes; no	No
<b>Injury description</b>	Description of the injury(s) resulting from the fall. All incident reports of injury(s) related to the falls will be collected from the childcare staff.		

<sup>1</sup>Fall description: Subject 4 is slowly walking on the playground and a second child collides with the left lateral side of his torso and the occipital region of his head. Subject falls right laterally and impacts the right lateral side on the playground surface. His right arm is extended under him and his legs are extended behind him. He impacts his right knee and the lateral side of his right leg; he also impacts his right hand and the posterior side of the distal portion of his right arm. He then impacts his left hand. He is laying in a right lateral recumbent position on the playground surface.

#### B. Screen grabs from the clipped fall 14 video

To visualize the fall, the previously described fall (fall 14) was clipped from the video recording. Then, screenshots of the video to capture the fall dynamics were obtained. The first image shows the fall initiation (FIGURE 87A). The second and third images show the first contact (FIGURE 87B) then the fall dynamics (FIGURE 87C). The fourth image



shows the primary impact of the fall (FIGURE 87D). The final image shows the final position of the subject post-fall (FIGURE 87E).



FIGURE 87 – Captured screen shots of fall 14 dynamics from the video recording

## X. APPENDIX II

### A. SIM G/SKYi Verification

Replicate fall experiments from Thompson's ATD feet first falls study (Thompson, 2018) were performed to verify the SIM G sensor accuracy. Thompson's data, referred to as "previous data," were obtained. The data represented an ATD falling feet-first onto carpet and linoleum floor surface types from a short distance height, 0.69 m.

#### 1. Fall dynamics

In the previous study, fall dynamics were grouped into three categories (TABLE 50). For the replicate falls, each video recording for each fall was reviewed and the fall was categorized into one of three fall dynamics previously described (TABLE 51). Replicate falls onto carpet resulted in all seven falls demonstrating the C-type fall dynamic; however, none of the previous falls onto carpet resulted in a C-type dynamic. Replicate falls onto linoleum resulted in 5 out of 7 falls demonstrating the A-type dynamic, while 2 out of 7 represented the C-type. None represented the B-type. Because there was a lack of similar fall dynamics onto the carpet surface, only replicate falls onto linoleum were analyzed for verification purposes. Furthermore, only replicate falls with A-type dynamics were analyzed.

TABLE 50

DESCRIPTIONS OF ATD FALL DYNAMICS AND PREVIOUS FALL FREQUENCIES (THOMPSON, 2018)

Nomenclature	Description	0.69 m Carpet frequency	0.69 m Linoleum frequency
<b>A</b>	ATD fell to crouching position with hips and knees flexed; knees then extended while feet rotated forward from beneath torso as ATD pelvis continued to move downward. ATD landed in a seated position with knees fully extended before rotating rearward into a supine position or to one side (laterally).	9	11
<b>B</b>	ATD fell to crouching position with hips and knees flexed, left knee then extended while foot rotated forward from beneath torso, but right toes remained planted on the floor surface as ATD pelvis continued to move downward. ATD landed in a seated position (left knee extended, right knee flexed), torso then rotated rearward into a supine position.	3	2
<b>C</b>	ATD fell to crouching position with hips and knees flexed, heels then lifted off floor, while toes remained planted resulting in plantar flexion of ankles and rolling onto the dorsal surface of the foot as the ATD pelvis continued to move downward. Hips and knees extended after pelvis impact, launching ATD rearward to land in supine position.	0	0

TABLE 51

REPLICATE FALL DYNAMICS AND FREQUENCIES

Dynamics	Carpet surface frequency	Linoleum surface frequency
<b>A</b>	0	5
<b>B</b>	0	0
<b>C</b>	7	2

## 2. Comparison of results

To validate the SIM G data with the onboard accelerometer data, mean peak resultant values for all biomechanical measures were compared. These measures included peak resultant linear head acceleration, peak resultant rotational head acceleration, peak resultant rotational head velocity, and impact duration (TABLE 52). All data was tested for significant differences between the previous falls data and the replicate falls data (p value < 0.05).

TABLE 52

### ATD ONBOARD INSTRUMENTATION AND SIM G COMPARISON

Biomechanical measure	ATD Onboard instrumentation <sup>1</sup> (n=11)		SIM G Instrumentation <sup>2</sup> (n=5)		p-Value
	Mean ± SD	Range	Mean ± SD	Range	
Peak resultant linear head acceleration (g)	32.7 ± 9.2	25.1-47.8	31.0 ± 1.4	29.4-33.2	0.571
Peak resultant linear head velocity (m/s)	0.52 ± 0.13	0.41-0.75	0.52 ± 0.05	0.44-0.58	0.308
Peak resultant rotational head acceleration (rad/s <sup>2</sup> )	3.2 ± 1.2	1.6-5.5	2.8 ± 0.3	2.3-3.2	0.248
Peak resultant rotational head velocity (rad/s)	12.5 ± 3.5	7.6-18.3	12.9 ± 3.81	6.3-15.7	0.863
Impact duration (ms)	16.1 ± 1.6	13.0-17.0	16.8 ± 1.5	15.0-19.0	0.734

<sup>1</sup>ATD Onboard instrumentation was used in previous experiment (Thompson 2018).

<sup>2</sup>SIM G instrumentation was used in replicated falls.

a. Linear head acceleration

The mean peak resultant linear head acceleration value for the onboard accelerometers from Thompson’s experiments was 32.7 g. The mean peak resultant linear head acceleration value for the SIM G (replicated falls) was 31.0 g (FIGURE 88). Resultant linear head acceleration from both falls was tested for normal distribution and it was found that the data from the onboard accelerometers was not normally distributed, while the data for the SIM G was normally distributed. A nonparametric Mann-Whitney U-Test was performed, and it was found that the peak resultant linear head acceleration between the SIM G and onboard accelerometers was not significantly different (p=0.571).

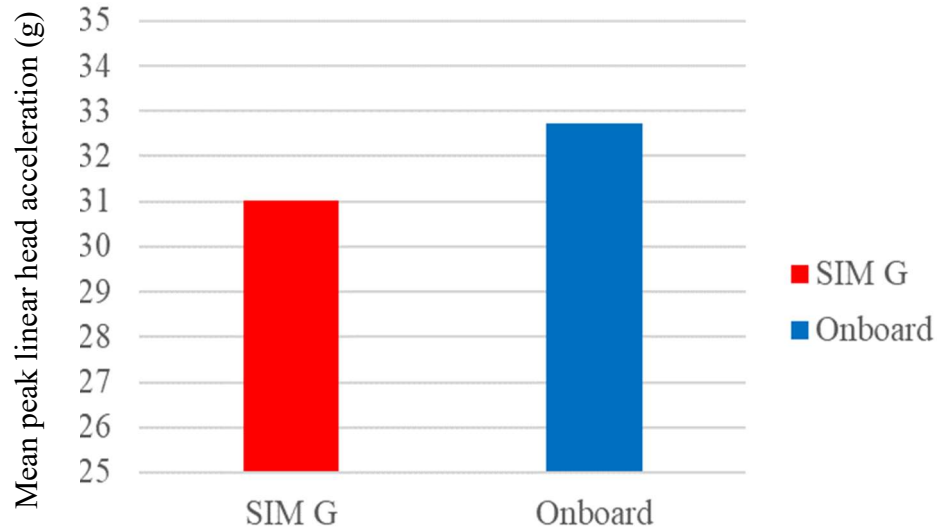


FIGURE 88 – SIM G verification with mean peak resultant linear head acceleration (g) from replicated ATD feet-first falls onto linoleum.

b. Linear head velocity

The mean peak resultant linear head velocity value for the onboard accelerometers from Thompson's experiments was 0.52 m/s. The mean peak resultant linear head acceleration value for the SIM G (replicated falls) was 0.52 m/s (FIGURE 89). Resultant linear head velocity from both falls was tested for normal distribution and it was found that the data from the onboard accelerometers was not normally distributed, while the data for the SIM G was normally distributed. A nonparametric Mann-Whitney U-Test was performed, and it was found that the peak resultant linear head velocity between the SIM G and onboard accelerometers was not significantly different ( $p=0.308$ ).

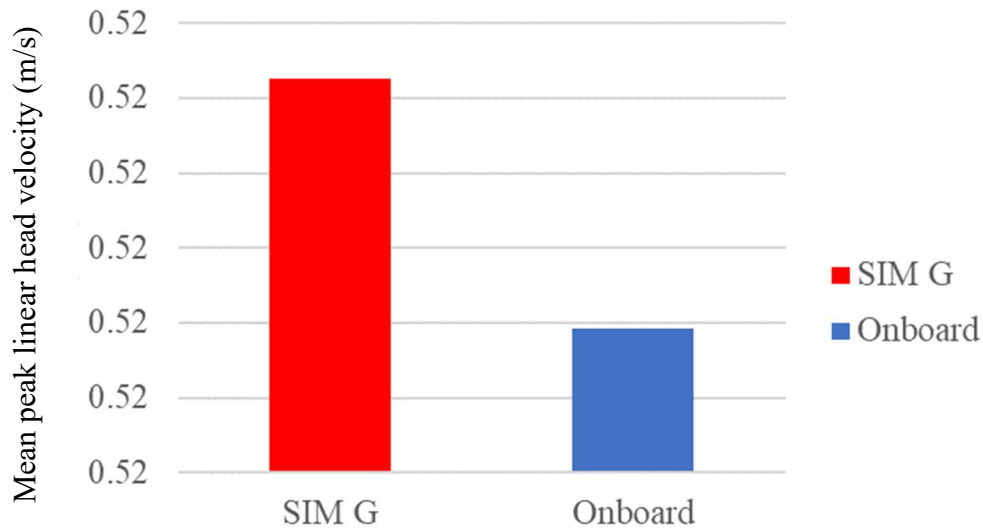


FIGURE 89 – SIM G verification with mean peak resultant linear head velocity (m/s) from replicated ATD feet-first falls onto linoleum.

c. Rotational head acceleration

The mean peak resultant rotational head acceleration value for the onboard accelerometers from Thompson's experiments was 3.2 krad/s<sup>2</sup> with a 95% CI of [2.54, 3.92]. The mean peak resultant linear head acceleration value for the SIM G (replicated falls) was 2.8 krad/s<sup>2</sup> with a 95% CI of [2.5, 3.1] (FIGURE 90). Resultant rotational head acceleration data from both fall tests was tested for normal distribution and it was found that the data from both instrumentations was normally distributed. A two-sample T-test was performed, and it was found that the peak resultant rotational head acceleration between the SIM G and onboard accelerometers was not significantly different (p=0.248).

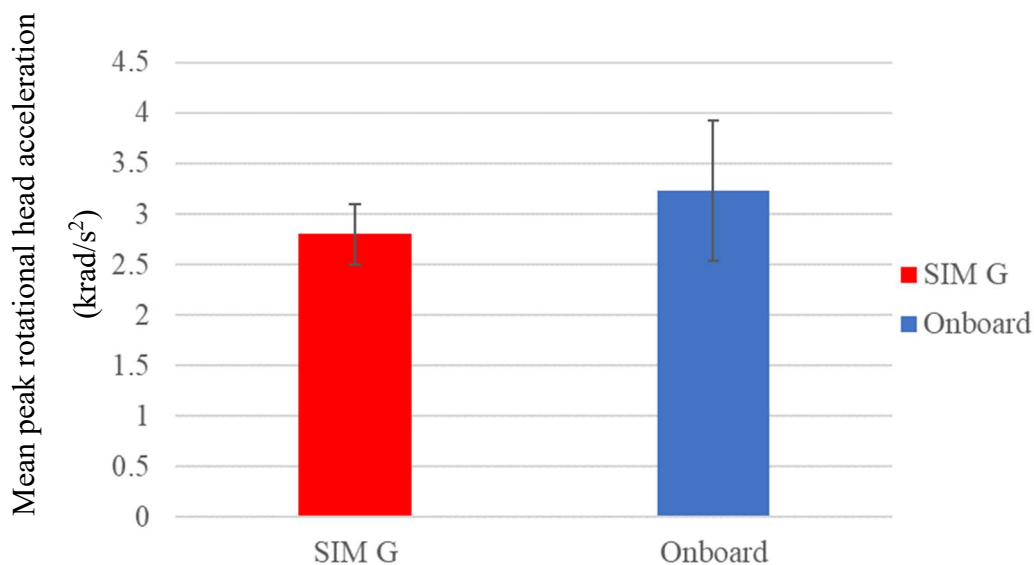


FIGURE 90 – SIM G verification with mean peak resultant rotational head acceleration (krad/s<sup>2</sup>) from replicated ATD feet-first falls onto linoleum. Error bars represent 95% CI

d. Rotational head velocity

The mean peak resultant rotational head velocity value for the onboard accelerometers from Thompson's experiments was 12.5 krad/s with a 95% CI of [10.4, 14.6]. The mean peak resultant linear head acceleration value for the SIM G (replicated falls) was 12.9 krad/s with a 95% CI of [9.5, 16.2] (FIGURE 91). Resultant rotational head velocity data from both fall tests was tested for normal distribution and it was found that the data from both instrumentations was normally distributed. A two-sample T-test was performed, and it was found that the peak resultant rotational head velocity between the SIM G and onboard accelerometers was not significantly different ( $p=0.863$ ).

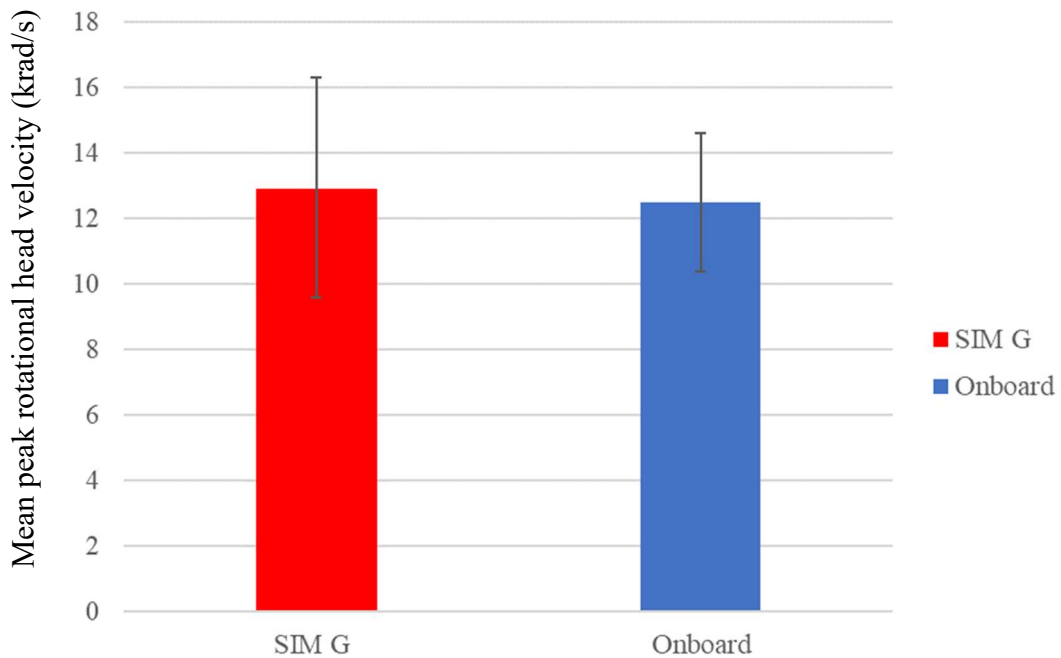


FIGURE 91 – SIM G verification with mean peak resultant rotational head velocity (krad/s) from replicated ATD feet-first falls onto linoleum. Error bars represent 95% CI



e. Impact duration

The mean impact time duration value for the onboard accelerometers from Thompson's experiments was 16.1 ms. The mean impact duration value for the SIM G (replicated falls) was 16.8 ms (FIGURE 92). Impact duration data from both fall tests was tested for normal distribution and it was found that the data from the onboard accelerometers was not normal, while the data from the SIM G was normal. A nonparametric Mann-Whitney U-Test was performed, and it was found that the mean impact duration between the SIM G and onboard accelerometers was not significantly different ( $p=0.734$ ).

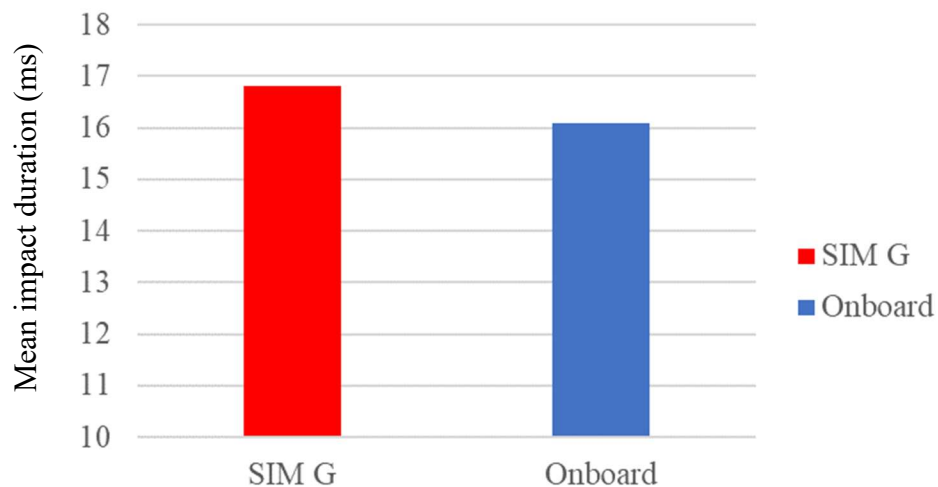


FIGURE 92 – SIM G verification with mean impact duration (ms) from replicated ATD feet-first falls onto linoleum.

XI. APPENDIX III

APPENDIX III details the results for all methods of analysis for each of the physics-based models for the feet-first ATD falls and the childcare center falls. The percent errors between the physics-based models and the SIM G outcomes were categorized (TABLE 11, reproduced here). Also, TABLE 9 is reproduced here to display the differences between the methods of analysis used for each of the three physics-based models (lumped mass, single rod, and inverted pendulum).

TABLE 9

METHODS USED TO EVALUATE THE PHYSICS-BASED MODELS

Method	Coefficient of restitution	Rebound Velocity	Starting Point	Phase <sup>1</sup>	Time duration
Method A	No	No	Conservation of momentum	Crush phase only	½ Delta t
Method B	Yes	Yes	Conservation of momentum	Crush and rebound phases	Delta t
Method C	Yes	Yes	Impulse	Crush and rebound Phases	Delta t
Method D	No	No	Impulse	Crush phase only	½ Delta t

<sup>1</sup>Phase of the fall referred to the primary head impact of the fall being evaluated; if only the crush phase was included, then rebound velocity was not included during evaluation; methods that evaluated crush and rebound phase included COR/rebound velocity.

TABLE 11

PERCENT ERROR CATEGORIES FOR PHYSICS-BASED MODEL OUTCOMES

0-25.0% Error
25.01-50.0% Error
50.01-100.0% Error
>100.01% Error

A. Physics-based model results for replicated ATD feet-first falls

The first section of this Appendix details all physics-based model results for each of the four methods (methods A through D) for each of the three physics-based models for the replicated ATD feet-first falls. The feet-first falls involved two different surfaces, which were carpet and linoleum.

1. Physics-based model results for ATD feet-first falls onto carpet

Testing the four methods with each of the three physics-based model types resulted in outcomes and comparisons for each of the physics-based models for ATD feet-first falls onto a carpet surface.

a. ATD feet-first falls onto carpet modeled with lumped mass physics-based model

The table (TABLE 53) displays the physics-based model outcomes for a lumped mass model type as compared to the SIM G outputs, and their respective percent error (as compared to the mean peak SIM G outcome).

TABLE 53

LUMPED MASS PHYSICS-BASED MODEL OUTCOMES VS. SIM G OUTCOMES (N=7) FOR FEET-FIRST ATD FALLS ONTO CARPET

BIOMECHANICAL MEASURE		LUMPED MASS MODEL OUTCOMES				PERCENT ERROR			
Outcome	Mean peak SIM G ± SD	METHOD A	METHOD B	METHOD C	METHOD D	METHOD A	METHOD B	METHOD C	METHOD D
Linear Acceleration (g)	34 ± 1.9	39	58	58	49	14%	70%	70%	45%
Change in Linear Velocity (m/s)	5.9 ± 0.6	3.6	3.6	5.4	3.6	39%	39%	8%	39%
Angular Acceleration (rad/s <sup>2</sup> )	2085.71 ± 402	4513	6731	6731	5755	116%	223%	223%	176%
Angular Velocity (rad/s)	7.14 ± 1.6	43.1	43.2	43.2	43.2	504%	505%	505%	505%
Impact Force (N)		935	1409	898	1205				

b. ATD feet-first falls onto carpet modeled with single rod physics-based model

The table (TABLE 54) displays the physics-based model outcomes for a single rod model type as compared to the SIM G outputs, and their respective percent error (as compared to the mean peak SIM G outcome).

TABLE 54

SINGLE ROD PHYSICS-BASED MODEL OUTCOMES VS. SIM G OUTCOMES (N=7) FOR FEET-FIRST ATD FALLS ONTO CARPET

BIOMECHANICAL MEASURE		SINGLE ROD MODEL OUTCOMES				PERCENT ERROR			
Outcome	Mean peak SIM G ± SD	METHOD A	METHOD B	METHOD C	METHOD D	METHOD A	METHOD B	METHOD C	METHOD D
Linear Acceleration (g)	34 ± 1.9	26	100	100	85	22%	194%	194%	151%
Change in Linear Velocity (m/s)	5.9 ± 0.6	2.5	6.3	9.4	6.3	58%	7%	59%	6%
Angular Acceleration (rad/s <sup>2</sup> )	2085.71 ± 402	3078	11660	11659	9968	48%	459%	459%	378%
Angular Velocity (rad/s)	7.14 ± 1.6	29.4	74.8	74.8	74.8	312%	947%	947%	947%
Impact Force (N)		638	2441	1555	2087				

c. ATD feet-first falls onto carpet modeled with inverted pendulum physics-based model

The table (TABLE 55) displays the physics-based model outcomes for an inverted pendulum model type as compared to the SIM G outputs, and their respective percent error (as compared to the mean peak SIM G outcome).

TABLE 55

INVERTED PENDULUM PHYSICS-BASED MODEL OUTCOMES VS. SIM G OUTCOMES (N=7) FOR FEET-FIRST ATD FALLS ONTO CARPET

BIOMECHANICAL MEASURE Outcome	Mean peak SIM G ± SD	INVERTED PENDULUM MODEL OUTCOMES				PERCENT ERROR			
		METHOD A	METHOD B	METHOD C	METHOD D	METHOD A	METHOD B	METHOD C	METHOD D
Linear Acceleration (g)	34 ± 1.9	39	58	58	49	14%	70%	70%	45%
Change in Linear Velocity (m/s)	5.9 ± 0.6	3.6	3.6	5.4	3.6	39%	39%	8%	39%
Angular Acceleration (rad/s <sup>2</sup> )	2085.71 ± 402	4513	6732	6731	5755	116%	223%	223%	176%
Angular Velocity (rad/s)	7.14 ± 1.6	43.1	43.2	43.2	43.2	504%	505%	505%	505%
Impact Force (N)		935	1409	898	1205				

d. Graphic representation of physics-based model outcomes as compared to SIM G outputs for ATD feet-first falls onto a carpet surface

The following number lines display the SIM G output range for each of the four biomechanical measures: linear head acceleration (FIGURE 93), linear head velocity (FIGURE 94), rotational head acceleration (FIGURE 95), and rotational head velocity (FIGURE 96). On each of the number lines, the physics-based model outcome is displayed. The color of the square and the letter displayed on the square correspond to the respective method and model type.

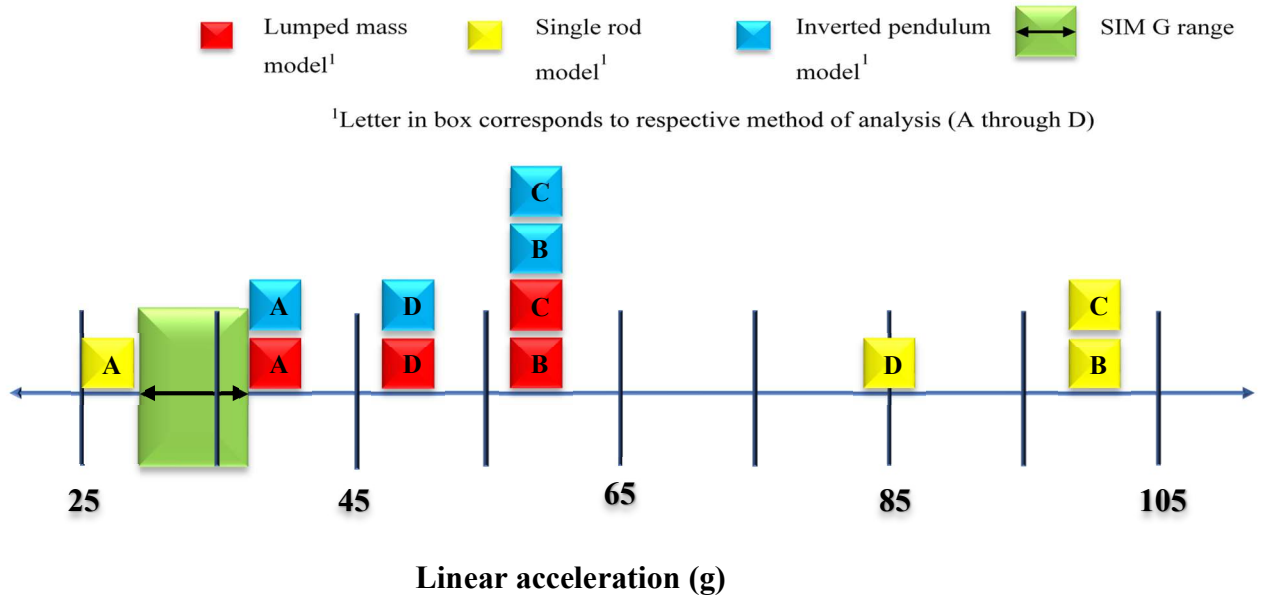


FIGURE 93 – Number line for comparison of linear acceleration (g) measured in ATD feet-first falls (SIM G range) onto carpet (n=7) to physics-based model predictions

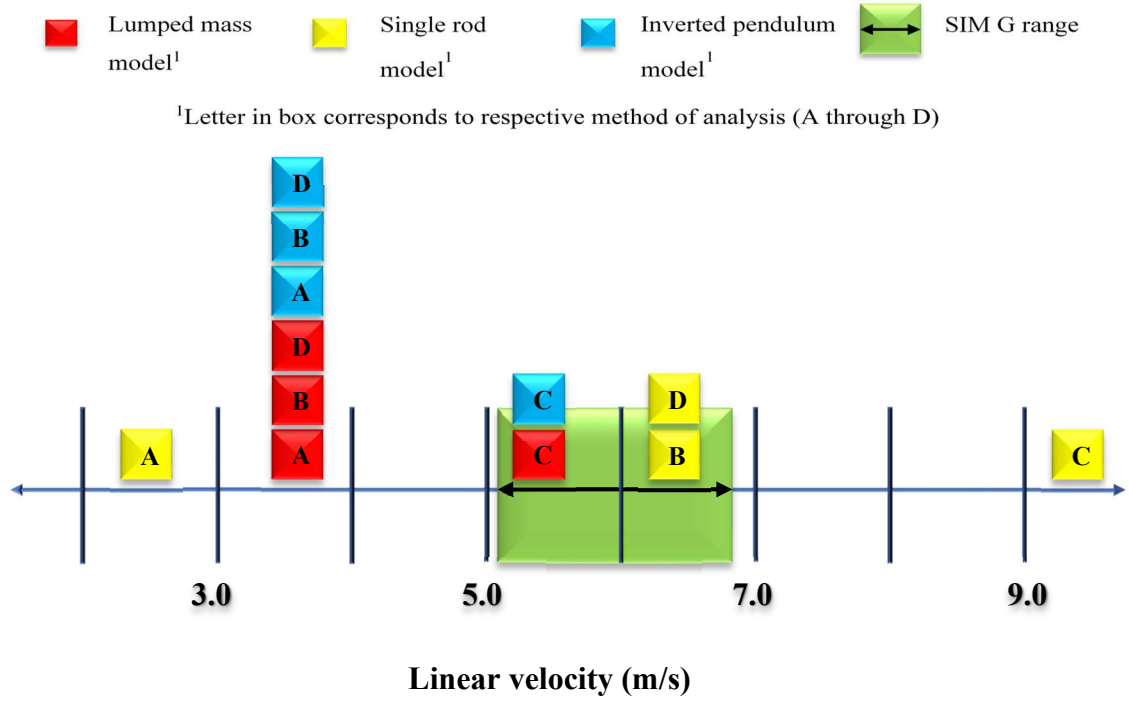


FIGURE 94 –Number line for comparison of linear velocity (m/s) measured in ATD feet-first falls (SIM G range) onto carpet (n=7) to physics-based model predictions

■ Lumped mass model<sup>1</sup>    
 ■ Single rod model<sup>1</sup>    
 ■ Inverted pendulum model<sup>1</sup>    
 ■ SIM G range

<sup>1</sup>Letter in box corresponds to respective method of analysis (A through D)

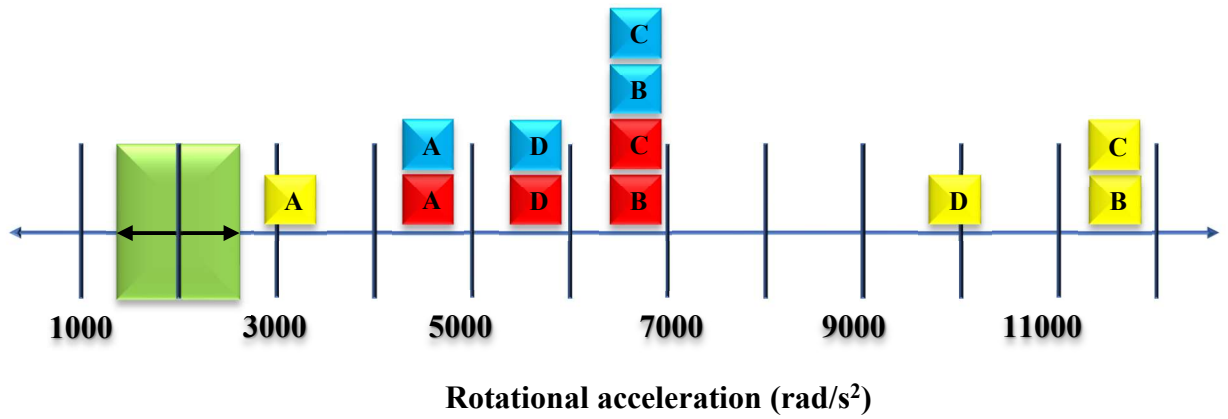


FIGURE 95 –Number line for comparison of rotational acceleration ( $\text{rad/s}^2$ ) measured in ATD feet-first falls (SIM G range) onto carpet ( $n=7$ ) to physics-based model predictions



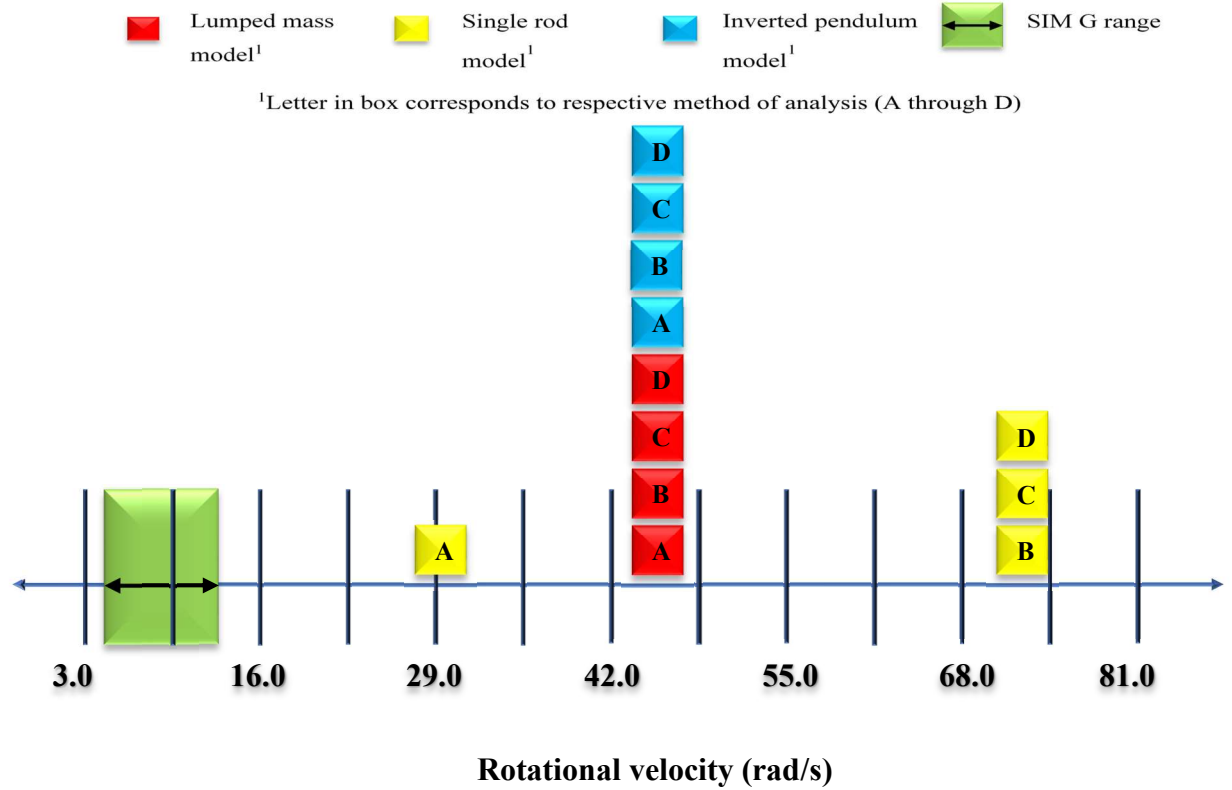


FIGURE 96 –Number line for comparison of rotational velocity (rad/s) measured in ATD feet-first falls (SIM G range) onto carpet (n=7) to physics-based model predictions

2. Physics-based model results for ATD feet-first falls onto linoleum

Testing the four methods with each of the three physics-based model types resulted in outcomes and comparisons for each of the physics-based models for ATD feet-first falls onto a linoleum surface.

a. ATD feet-first falls onto linoleum modeled with lumped mass physics-based model

The table (TABLE 55) displays the physics-based model outcomes for a lumped mass model type as compared to the SIM G outputs, and their respective percent error (as compared to the mean peak SIM G outcome).

TABLE 55

LUMPED MASS PHYSICS-BASED MODEL OUTCOMES VS. SIM G OUTCOMES (N=7) FOR FEET-FIRST ATD FALLS ONTO LINOLEUM

Outcome	BIOMECHANICAL MEASURES Mean peak SIM G ± SD	LUMPED MASS MODEL OUTCOMES				PERCENT ERROR			
		METHOD A	METHOD B	METHOD C	METHOD D	METHOD A	METHOD B	METHOD C	METHOD D
Linear Acceleration (g)	38 ± 14.2	53	71	71	67	39%	87%	87%	77%
Change in Linear Velocity (m/s)	6.51 ± 2	3.6	3.6	4.9	3.6	45%	45%	25%	44%
Angular Acceleration (rad/s <sup>2</sup> )	2086 ± 402	6154	8317	8317	7848	195%	299%	299%	276%
Angular Velocity (rad/s)	7.1 ± 1.6	43.1	43.2	43.2	43.2	504%	505%	505%	505%
Impact Force (N)		1276	1741	1109	1643				

b. ATD feet-first falls onto linoleum modeled with single rod physics-based model

The table (TABLE 56) displays the physics-based model outcomes for a single rod model type as compared to the SIM G outputs, and their respective percent error (as compared to the mean peak SIM G outcome).

TABLE 56

SINGLE ROD PHYSICS-BASED MODEL OUTCOMES VS. SIM G OUTCOMES (N=7) FOR FEET-FIRST ATD FALLS ONTO LINOLEUM

Outcome	BIOMECHANICAL MEASURES	SINGLE ROD MODEL OUTCOMES				PERCENT ERROR			
	Mean peak SIM G ± SD	METHOD A	METHOD B	METHOD C	METHOD D	METHOD A	METHOD B	METHOD C	METHOD D
Linear Acceleration (g)	38 ± 14.2	36	123	123	116	5%	225%	225%	206%
Change in Linear Velocity (m/s)	6.51 ± 2	2.5	6.3	8.5	6.3	62%	3%	30%	3%
Angular Acceleration (rad/s <sup>2</sup> )	2086 ± 402	4197	14406	14405	13593	101%	591%	591%	552%
Angular Velocity (rad/s)	7.1 ± 1.6	29.4	74.8	74.8	74.8	312%	947%	947%	947%
Impact Force (N)		870	3016	1921	2846				

c. ATD feet-first falls onto linoleum modeled with inverted pendulum physics-based model

The table (TABLE 57) displays the physics-based model outcomes for an inverted pendulum model type as compared to the SIM G outputs, and their respective percent error (as compared to the mean peak SIM G outcome).

TABLE 57

INVERTED PENDULUM PHYSICS-BASED MODEL OUTCOMES VS. SIM G OUTCOMES (N=7) FOR FEET-FIRST ATD FALLS ONTO LINOLEUM

Outcome	BIOMECHANICAL MEASURES	INVERTED PENDULUM MODEL OUTCOMES				PERCENT ERROR			
	Mean peak SIM G ± SD	METHOD A	METHOD B	METHOD C	METHOD D	METHOD A	METHOD B	METHOD C	METHOD D
Linear Acceleration (g)	38 ± 14.2	53	71	71	67	39%	87%	87%	77%
Change in Linear Velocity (m/s)	6.51 ± 2	3.6	3.6	4.9	3.6	45%	45%	25%	44%
Angular Acceleration (rad/s <sup>2</sup> )	2086 ± 402	6154	8317	8317	7848	195%	299%	299%	276%
Angular Velocity (rad/s)	7.1 ± 1.6	43.1	43.2	43.2	43.2	504%	505%	505%	505%
Impact Force (N)		1276	1741	1109	1643				

d. Graphic representation of physics-based model outcomes as compared to SIM G outputs for ATD feet-first falls onto a linoleum surface

The following number lines display the SIM G output range for each of the four biomechanical measures: linear head acceleration (FIGURE 97), linear head velocity (FIGURE 98), rotational head acceleration (FIGURE 99), and rotational head velocity (FIGURE 100). On each of the number lines, the physics-based model outcome is displayed. The color of the square and the letter displayed on the square correspond to the respective method and model type.



<sup>1</sup>Letter in box corresponds to respective method of analysis (A through D)

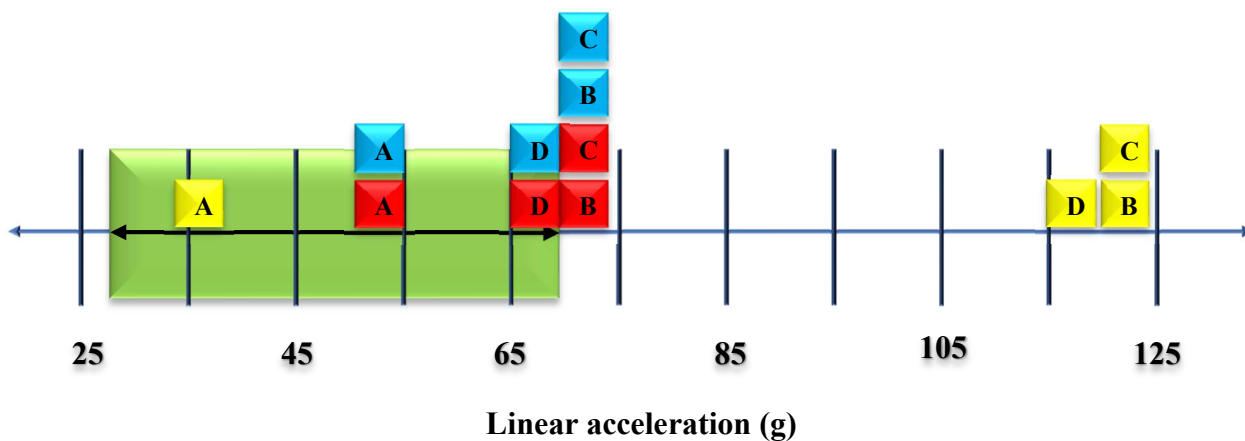


FIGURE 97 – Number line for comparison of linear acceleration (g) measured in ATD feet-first falls (SIM G range) onto linoleum (n=7) to physics-based model predictions

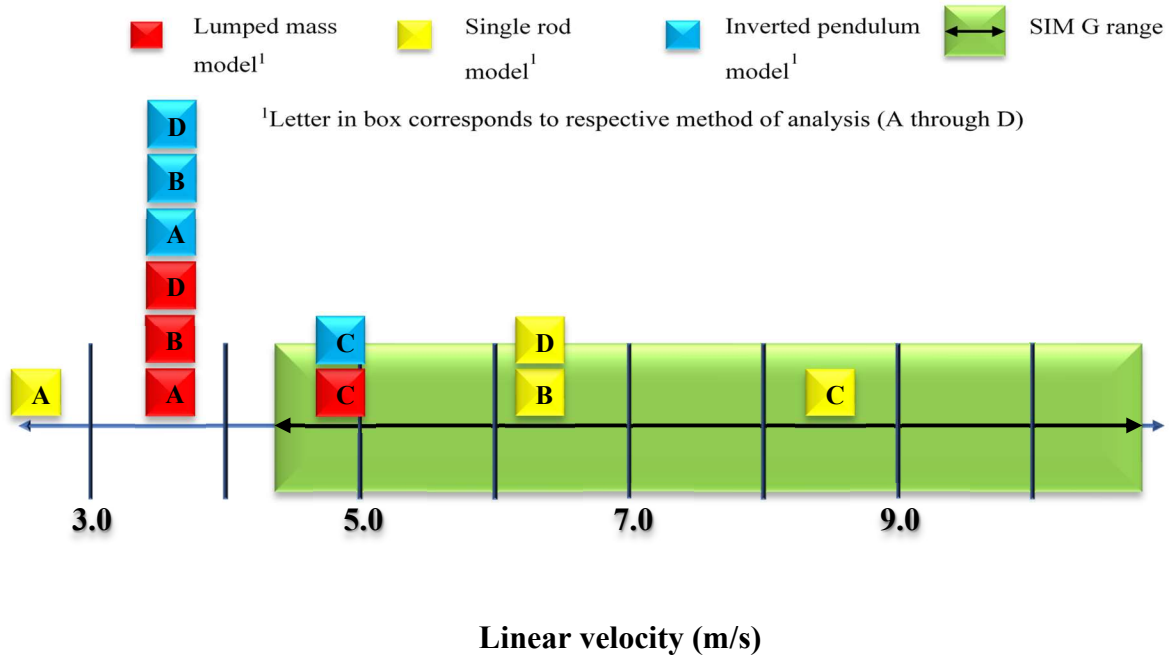


FIGURE 98 – Number line for comparison of linear velocity (m/s) measured in ATD feet-first falls (SIM G range) onto linoleum (n=7) to physics-based model predictions



¹Letter in box corresponds to respective method of analysis (A through D)

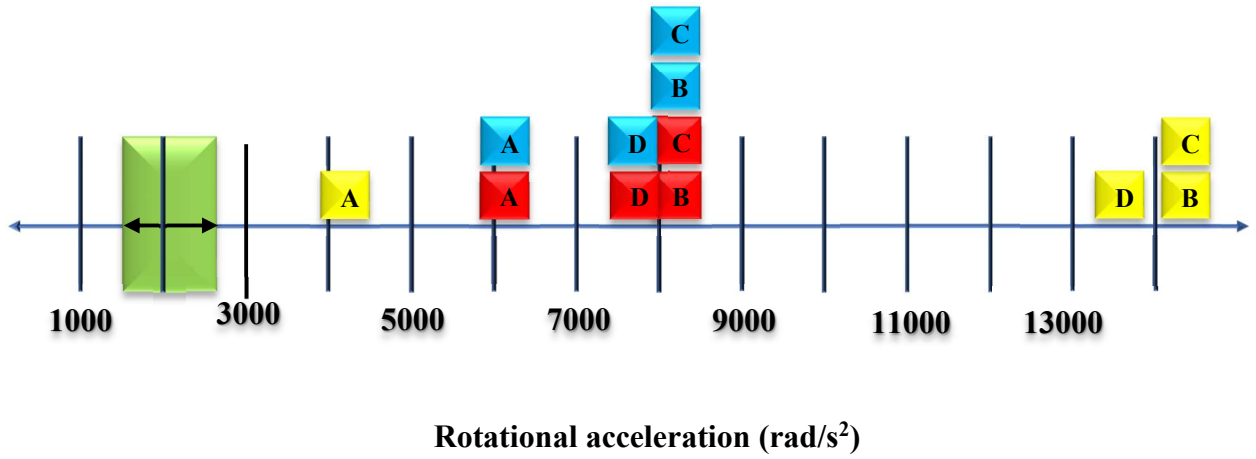


FIGURE 99 – Number line for comparison of rotational acceleration ( $\text{rad/s}^2$ ) measured in ATD feet-first falls (SIM G range) onto linoleum ( $n=7$ ) to physics-based model predictions

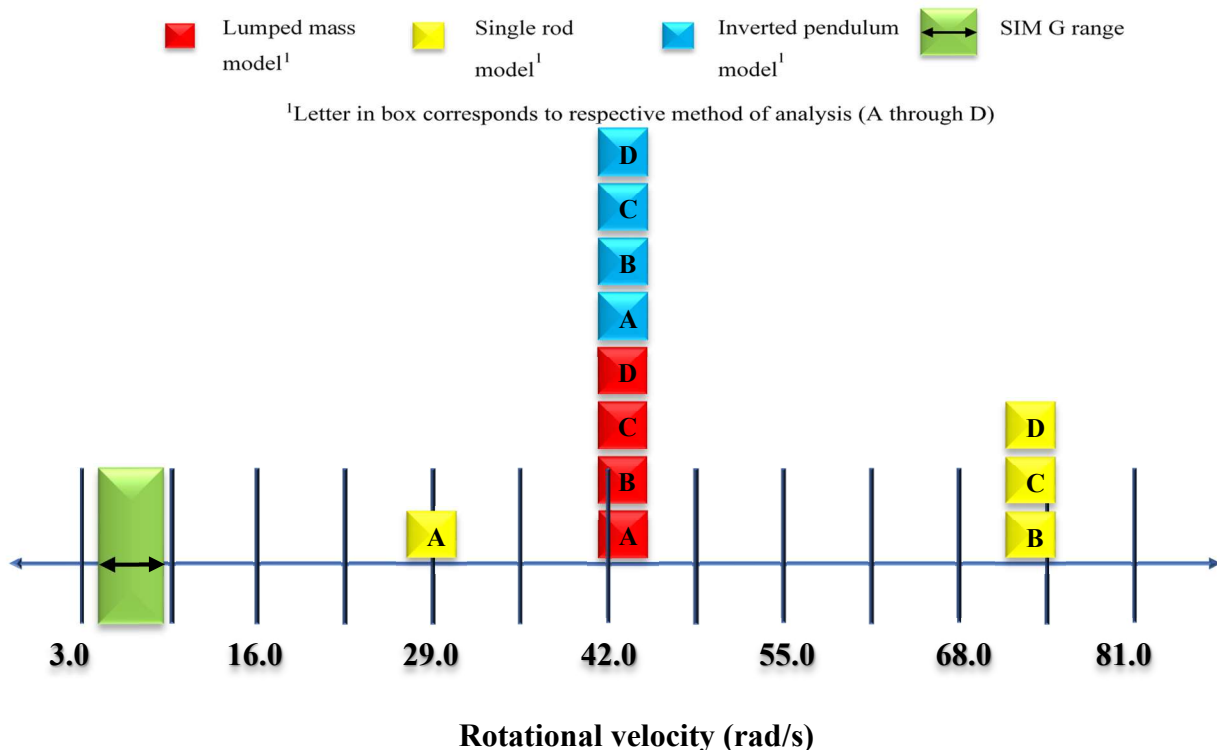


FIGURE 100 – Number line for comparison of rotational velocity (rad/s) measured in ATD feet-first falls (SIM G range) onto linoleum (n=7) to physics-based model predictions

### 3. Comparison of replicated ATD feet-first fall outcomes by fall dynamics

The replicated ATD feet-first fall video recordings were reviewed, and it was determined that the falls onto the carpeted surface (n=7) all exhibited the same fall dynamics.

Therefore, the falls onto carpet were not evaluated for how outcomes differed based on dynamics. For the linoleum surface (n=7), though, two unique dynamic types were observed, dynamics A (n=5) and C (n=2) (TABLE 50, reproduced here). The outcomes from the physics-based models for those falls will be compared to SIM G outcomes to evaluate if a dynamic type resulted in more or less accurate outcomes.



TABLE 50

DESCRIPTIONS OF ATD FALL DYNAMICS AND PREVIOUS FALL FREQUENCIES (THOMPSON, 2018)

Nomenclature	Description
<b>A</b>	ATD fell to crouching position with hips and knees flexed; knees then extended while feet rotated forward from beneath torso as ATD pelvis continued to move downward. ATD landed in a seated position with knees fully extended before rotating rearward into a supine position or to one side (laterally).
<b>B</b>	ATD fell to crouching position with hips and knees flexed, left knee then extended while foot rotated forward from beneath torso, but right toes remained planted on the floor surface as ATD pelvis continued to move downward. ATD landed in a seated position (left knee extended, right knee flexed), torso then rotated rearward into a supine position.
<b>C</b>	ATD fell to crouching position with hips and knees flexed, heels then lifted off floor, while toes remained planted resulting in plantar flexion of ankles and rolling onto the dorsal surface of the foot as the ATD pelvis continued to move downward. Hips and knees extended after pelvis impact, launching ATD rearward to land in supine position.

- a. Replicate ATD feet-first falls onto linoleum with dynamic A (n=5)

Falls with dynamic-type A were evaluated for mean peak biomechanical outcomes from the SIM G, and these were compared to physics-based model outcomes for these falls onto linoleum. The first table displays the physics-based model outcomes for a lumped mass model type as compared to the SIM G outputs, and their respective percent error (as compared to the mean peak SIM G outcome) (TABLE 58). The second table displays the physics-based model outcomes for a single rod model type as compared to the SIM G outputs, and their respective percent error (as compared to the mean peak

SIM G outcome) (TABLE 59). The third table displays the physics-based model outcomes for an inverted pendulum model type as compared to the SIM G outputs, and their respective percent error (as compared to the mean peak SIM G outcome) (TABLE 60).

TABLE 58

REPLICATED ATD FEET-FIRST FALLS ONTO LINOLEUM WITH DYNAMIC A LUMPED MASS OUTCOMES

BIOMECHANICAL MEASURES		LUMPED MASS MODEL OUTCOMES				PERCENT ERROR			
Outcome	Mean peak SIM G $\pm$ SD	METHOD A	METHOD B	METHOD C	METHOD D	METHOD A	METHOD B	METHOD C	METHOD D
Linear Acceleration (g)	31 $\pm$ 1	53	71	71	67	70%	130%	130%	117%
Change in Linear Velocity (m/s)	5.5 $\pm$ 0.6	3.6	3.6	4.9	3.6	35%	35%	11%	34%
Angular Acceleration (rad/s <sup>2</sup> )	1900 $\pm$ 283	6154	8317	8317	7848	224%	338%	338%	313%
Angular Velocity (rad/s)	7.3 $\pm$ 1.9	43.1	43.2	43.2	43.2	491%	491%	491%	491%
Impact Force (N)		1276	1741	1109	1643				

TABLE 59

REPLICATED ATD FEET-FIRST FALLS ONTO LINOLEUM WITH DYNAMIC A SINGLE ROD OUTCOMES

BIOMECHANICAL MEASURES		SINGLE ROD MODEL OUTCOMES				PERCENT ERROR			
Outcome	Mean peak SIM G $\pm$ SD	METHOD A	METHOD B	METHOD C	METHOD D	METHOD A	METHOD B	METHOD C	METHOD D
Linear Acceleration (g)	31 $\pm$ 1	36	123	123	116	16%	298%	298%	275%
Change in Linear Velocity (m/s)	5.5 $\pm$ 0.6	2.5	6.3	8.5	6.3	55%	15%	54%	14%
Angular Acceleration (rad/s <sup>2</sup> )	1900 $\pm$ 283	4197	14406	14405	13593	121%	658%	658%	615%
Angular Velocity (rad/s)	7.3 $\pm$ 1.9	29.4	74.8	74.8	74.8	303%	924%	924%	924%
Impact Force (N)		870	3016	1921	2846				

TABLE 60

REPLICATED ATD FEET-FIRST FALLS ONTO LINOLEUM WITH DYNAMIC A  
INVERTED PENDULUM OUTCOMES

BIOMECHANICAL MEASURES		INVERTED PENDULUM MODEL OUTCOMES				PERCENT ERROR			
Outcome	Mean peak SIM G ± SD	METHOD A	METHOD B	METHOD C	METHOD D	METHOD A	METHOD B	METHOD C	METHOD D
Linear Acceleration (g)	31 ± 1	53	71	71	67	70%	130%	130%	117%
Change in Linear Velocity (m/s)	5.5 ± 0.6	3.6	3.6	4.9	3.6	35%	35%	11%	34%
Angular Acceleration (rad/s <sup>2</sup> )	1900 ± 283	6154	8317	8317	7848	224%	338%	338%	313%
Angular Velocity (rad/s)	7.3 ± 1.9	43.1	43.2	43.2	43.2	491%	491%	491%	491%
Impact Force (N)		1276	1741	1109	1643				

- b. Graphic representation of physics-based model outcomes as compared to SIM G outputs for ATD feet-first falls onto a linoleum surface with dynamic A

The following number lines display the SIM G output range for each of the four biomechanical measures: linear head acceleration (FIGURE 101), linear head velocity (FIGURE 102), rotational head acceleration (FIGURE 103), and rotational head velocity (FIGURE 104). On each of the number lines, the physics-based model outcome is displayed. The color of the square and the letter displayed on the square correspond to the respective method and model type.

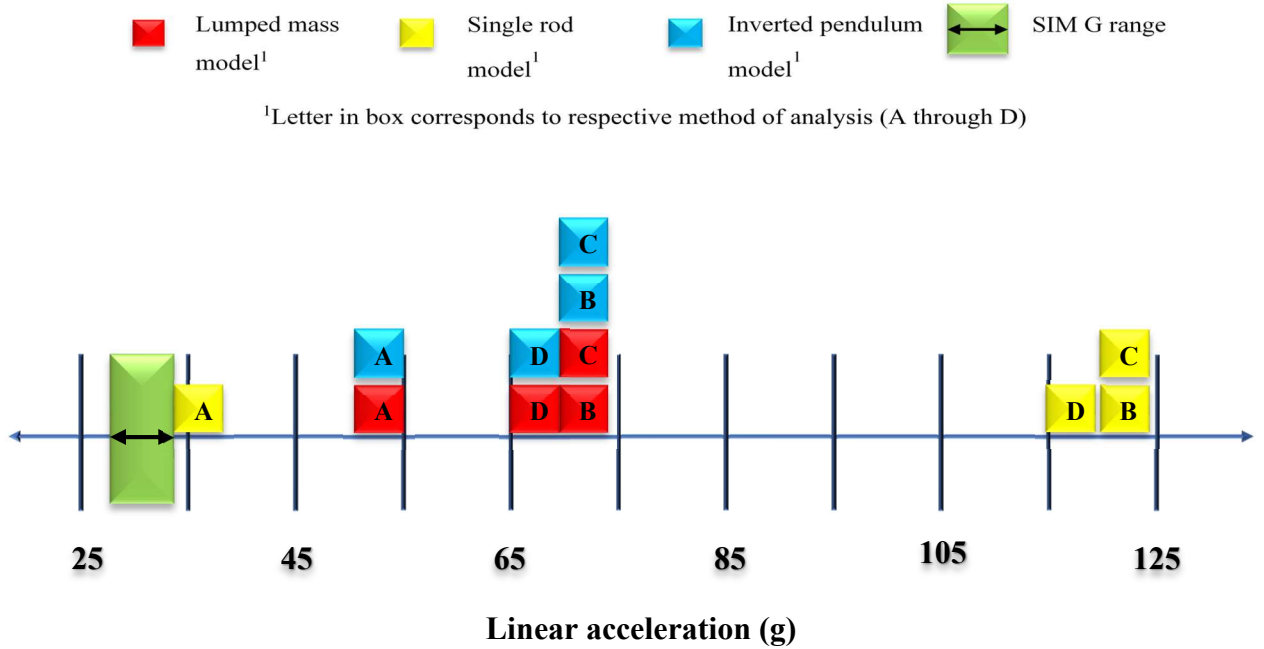


FIGURE 101 – Number line for comparison of linear acceleration (g) measured in ATD feet-first falls (SIM G range) onto linoleum with dynamic A (n=5) to physics-based model predictions

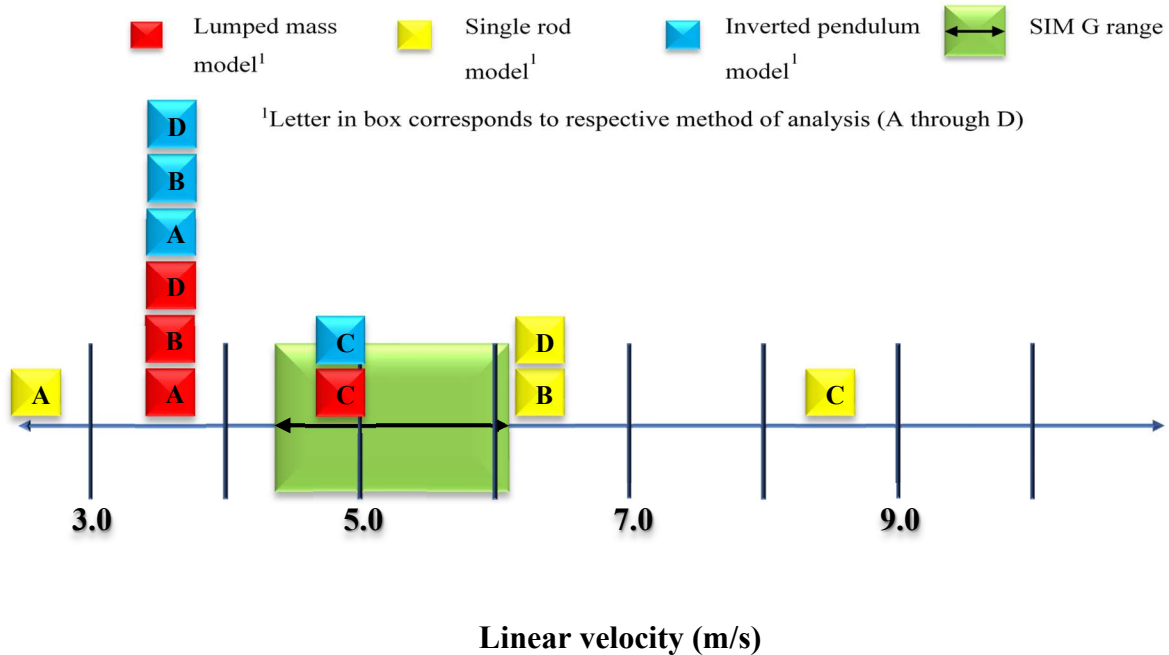


FIGURE 102 – Number line for comparison of linear velocity (m/s) measured in ATD feet-first falls (SIM G range) onto linoleum with dynamic A (n=5) to physics-based model predictions

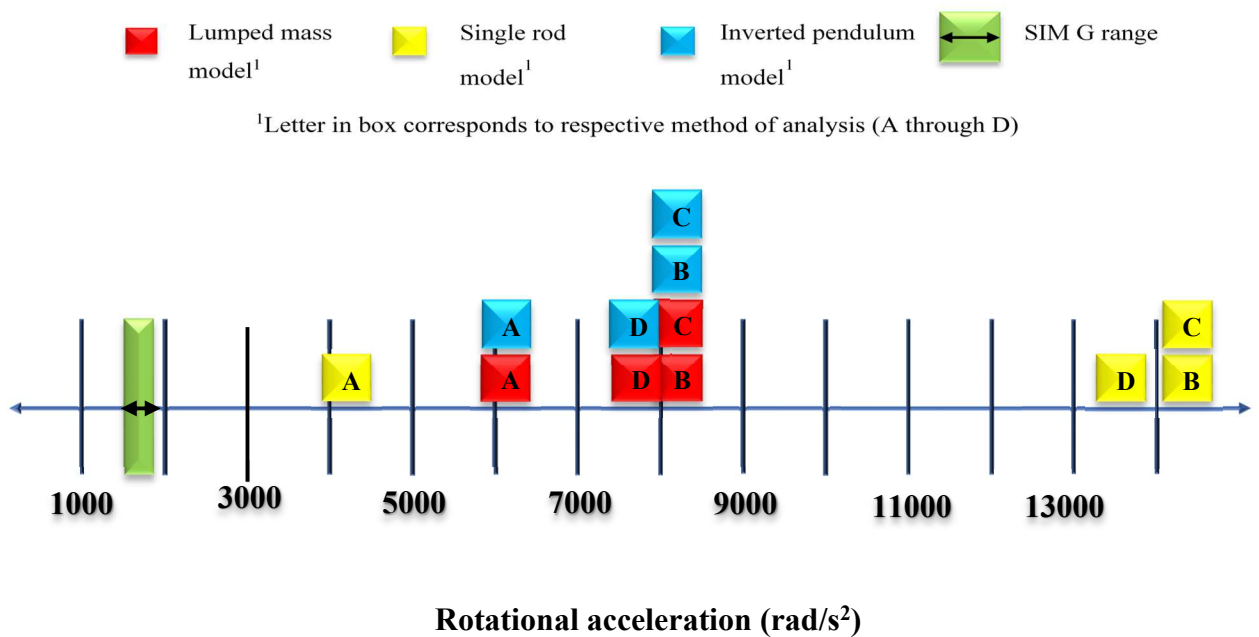


FIGURE 103 – Number line for comparison of rotational acceleration ( $\text{rad/s}^2$ ) measured in ATD feet-first falls (SIM G range) onto linoleum with dynamic A ( $n=5$ ) to physics-based model predictions

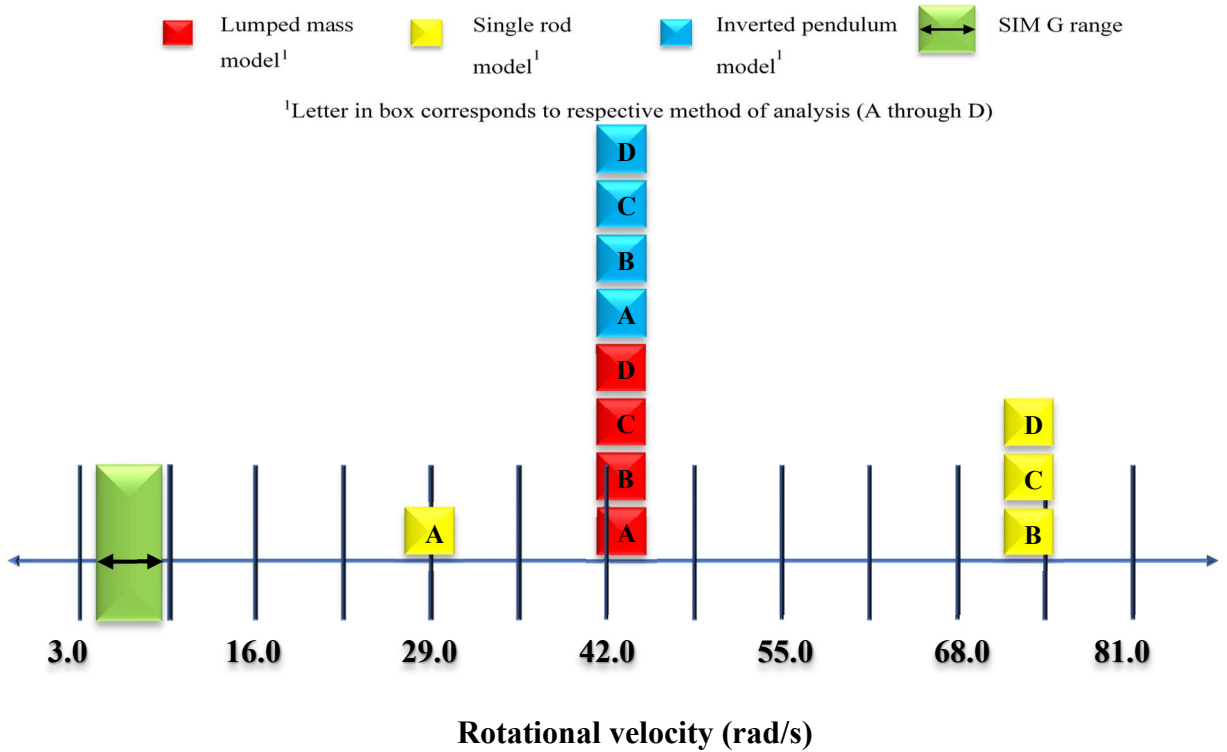


FIGURE 104 – Number line for comparison of rotational velocity ( $\text{rad/s}$ ) measured in ATD feet-first falls (SIM G range) onto linoleum with dynamic A ( $n=5$ ) to physics-based model predictions

c. Replicate ATD feet-first falls onto linoleum with dynamic C ( $n=2$ )

Falls with dynamic-type C were evaluated for mean peak biomechanical outcomes from the SIM G, and these were compared to physics-based model outcomes for these falls onto linoleum. The first table displays the physics-based model outcomes for a lumped mass model type as compared to the SIM G outputs, and their respective percent error (as compared to the mean peak SIM G outcome) (TABLE 61). The second

table displays the physics-based model outcomes for a single rod model type as compared to the SIM G outputs, and their respective percent error (as compared to the mean peak SIM G outcome) (TABLE 62). The third table displays the physics-based model outcomes for an inverted pendulum model type as compared to the SIM G outputs, and their respective percent error (as compared to the mean peak SIM G outcome) (TABLE 63).

TABLE 61

REPLICATED ATD FEET-FIRST FALLS ONTO LINOLEUM WITH DYNAMIC C LUMPED MASS OUTCOMES

BIOMECHANICAL MEASURES		LUMPED MASS MODEL OUTCOMES				PERCENT ERROR			
Outcome	Mean peak SIM G $\pm$ SD	METHOD A	METHOD B	METHOD C	METHOD D	METHOD A	METHOD B	METHOD C	METHOD D
Linear Acceleration (g)	56 $\pm$ 17	53	71	71	67	6%	27%	27%	20%
Change in Linear Velocity (m/s)	9.1 $\pm$ 2.3	3.6	3.6	4.9	3.6	60%	60%	46%	60%
Angular Acceleration (rad/s <sup>2</sup> )	2550 $\pm$ 212	6154	8317	8317	7848	141%	226%	226%	208%
Angular Velocity (rad/s)	6.7 $\pm$ 0.4	43.1	43.2	43.2	43.2	544%	544%	544%	544%
Impact Force (N)		1276	1741	1109	1643				

TABLE 62

REPLICATED ATD FEET-FIRST FALLS ONTO LINOLEUM WITH DYNAMIC C SINGLE ROD OUTCOMES

BIOMECHANICAL MEASURES		SINGLE ROD MODEL OUTCOMES				PERCENT ERROR			
Outcome	Mean peak SIM G $\pm$ SD	METHOD A	METHOD B	METHOD C	METHOD D	METHOD A	METHOD B	METHOD C	METHOD D
Linear Acceleration (g)	56 $\pm$ 17	36	123	123	116	36%	120%	120%	108%
Change in Linear Velocity (m/s)	9.1 $\pm$ 2.3	2.5	6.3	8.5	6.3	73%	31%	7%	31%
Angular Acceleration (rad/s <sup>2</sup> )	2550 $\pm$ 212	4197	14406	14405	13593	65%	465%	465%	433%
Angular Velocity (rad/s)	6.7 $\pm$ 0.4	29.4	74.8	74.8	74.8	339%	1016%	1016%	1016%
Impact Force (N)		870	3016	1921	2846				

TABLE 63

REPLICATED ATD FEET-FIRST FALLS ONTO LINOLEUM WITH DYNAMIC C  
INVERTED PENDULUM OUTCOMES

Outcome	BIOMECHANICAL MEASURES Mean peak SIM G ± SD	INVERTED PENDULUM MODEL OUTCOMES				PERCENT ERROR			
		METHOD A	METHOD B	METHOD C	METHOD D	METHOD A	METHOD B	METHOD C	METHOD D
Linear Acceleration (g)	56 ± 17	53	71	71	67	6%	27%	27%	20%
Change in Linear Velocity (m/s)	9.1 ± 2.3	3.6	3.6	4.9	3.6	60%	60%	46%	60%
Angular Acceleration (rad/s <sup>2</sup> )	2550 ± 212	6154	8317	8317	7848	141%	226%	226%	208%
Angular Velocity (rad/s)	6.7 ± 0.4	43.1	43.2	43.2	43.2	544%	544%	544%	544%
Impact Force (N)		1276	1741	1109	1643				

- d. Graphic representation of physics-based model outcomes as compared to SIM G outputs for ATD feet-first falls onto a linoleum surface with dynamic A

The following number lines display the SIM G output range for each of the four biomechanical measures: linear head acceleration (FIGURE 105), linear head velocity (FIGURE 106), rotational head acceleration (FIGURE 107), and rotational head velocity (FIGURE 108). On each of the number lines, the physics-based model outcome is displayed. The color of the square and the letter displayed on the square correspond to the respective method and model type.



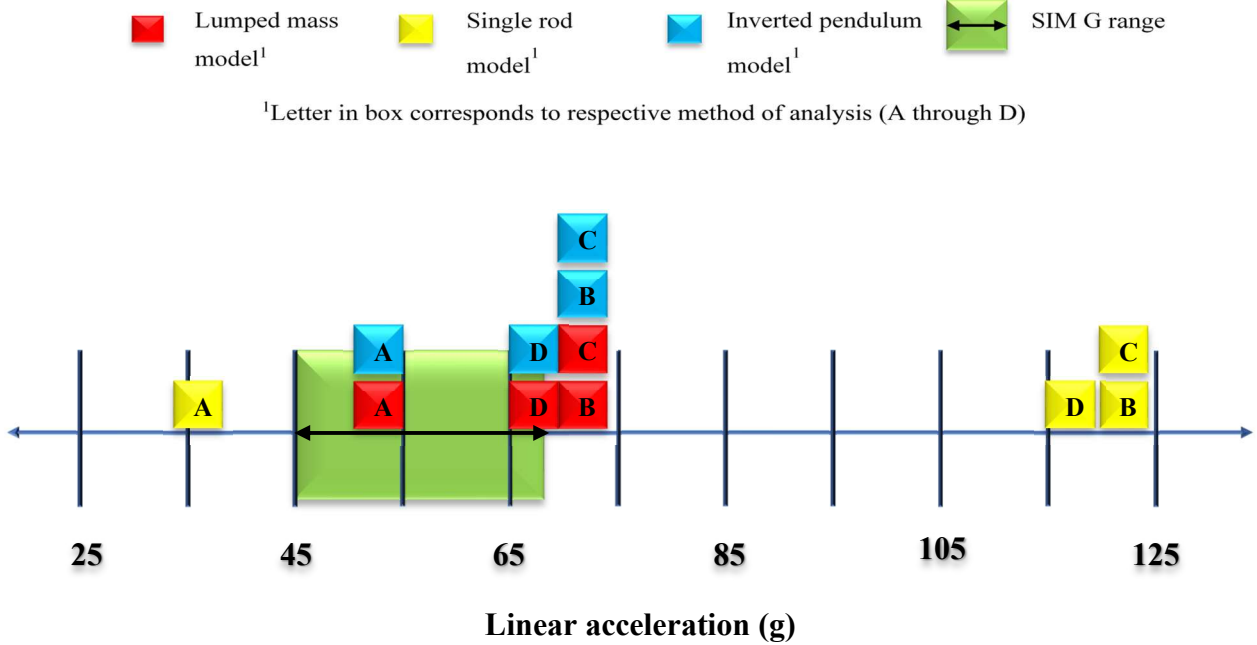


FIGURE 105 – Number line for comparison of linear acceleration (g) measured in ATD feet-first falls (SIM G range) onto linoleum with dynamic C (n=2) to physics-based model predictions

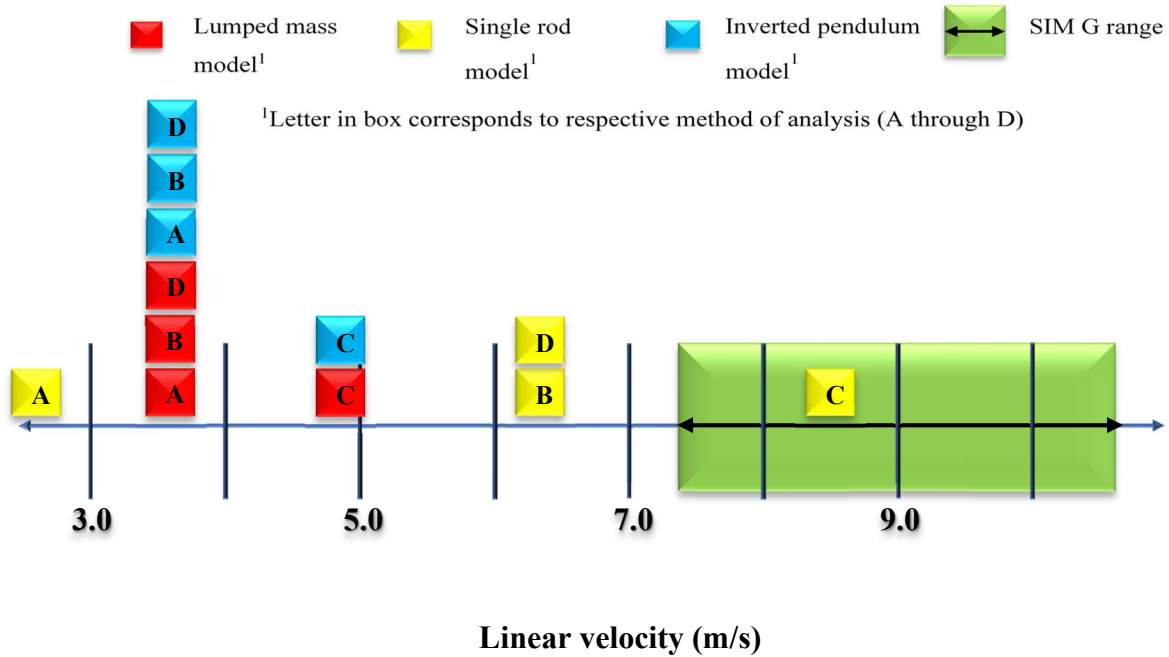


FIGURE 106 – Number line for comparison of linear velocity (m/s) measured in ATD feet-first falls (SIM G range) onto linoleum with dynamic C (n=2) to physics-based model predictions

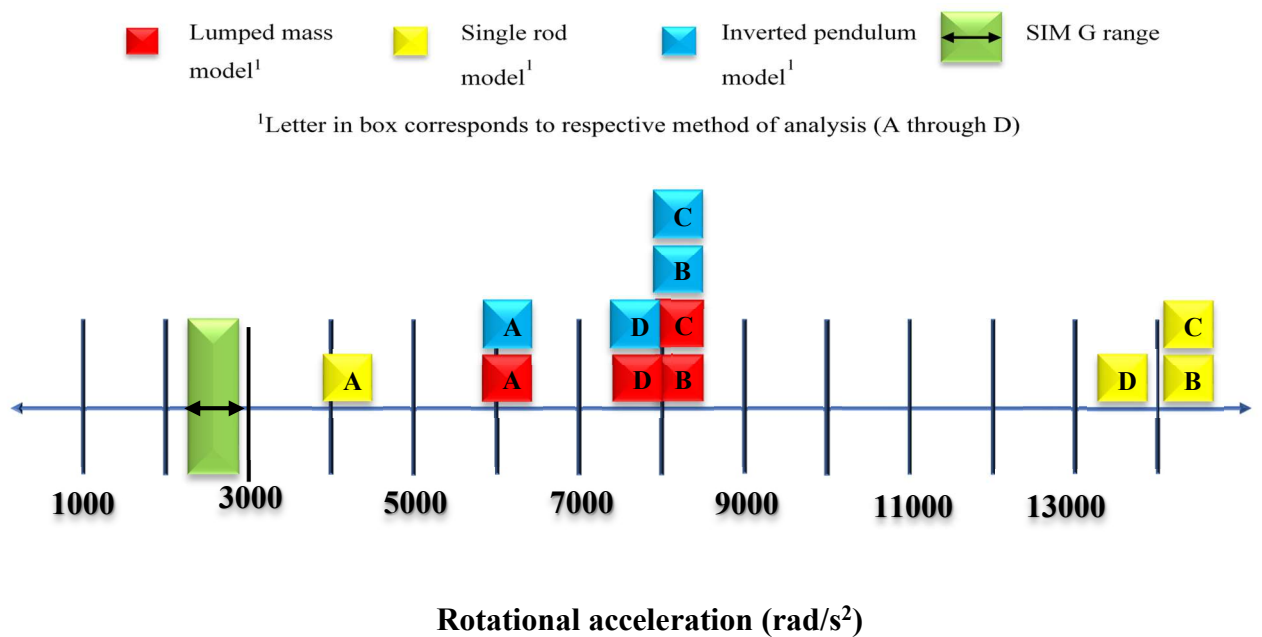


FIGURE 107 – Number line for comparison of rotational acceleration ( $\text{rad/s}^2$ ) measured in ATD feet-first falls (SIM G range) onto linoleum with dynamic C ( $n=2$ ) to physics-based model predictions

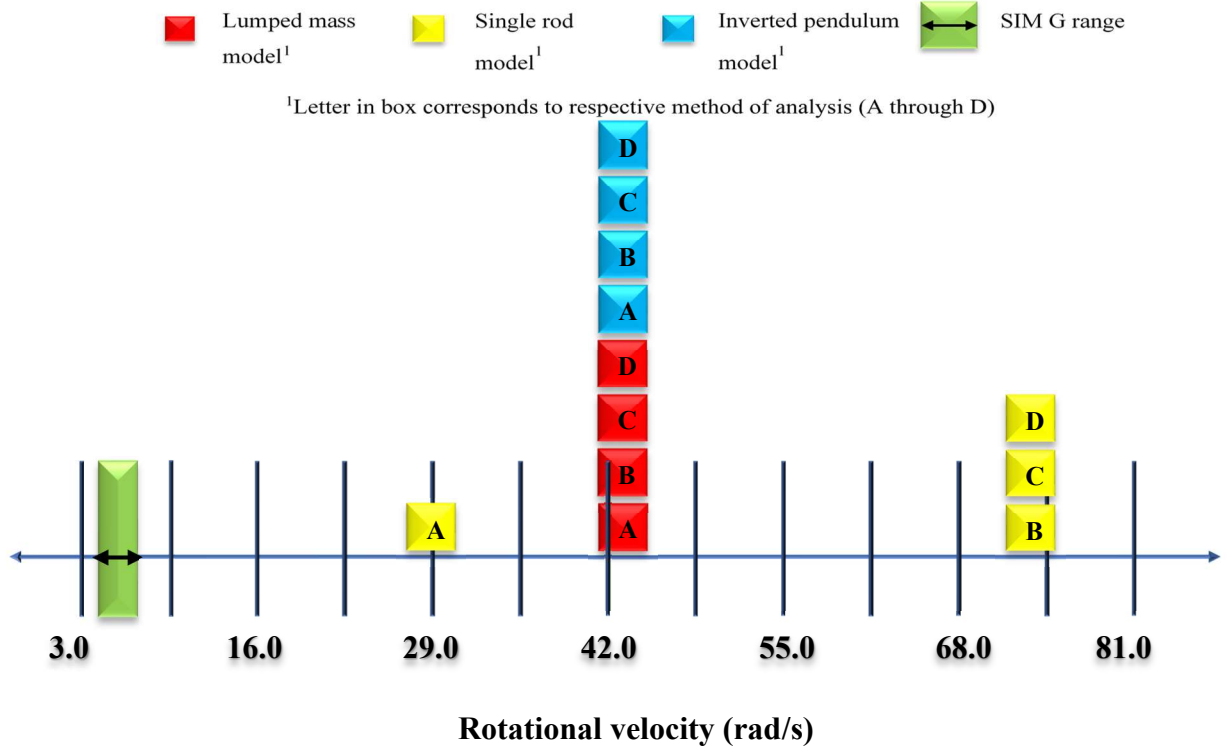


FIGURE 108 – Number line for comparison of rotational velocity ( $\text{rad/s}$ ) measured in ATD feet-first falls (SIM G range) onto linoleum with dynamic C ( $n=2$ ) to physics-based model predictions

B. Physics-based model results for childcare center falls with SIM G activation and primary head impact

The second section of this Appendix details all results for each of the four methods (methods A through D) for each of the three physics-based models for every fall with SIM G activation and primary head impact.

1. Childcare center fall 146

The results for all four methods for fall 146 are detailed below (TABLE 64, TABLE 65, TABLE 66). In fall 146, subject 11 (female) was sitting on her buttocks and proceeded to fall rearward at an angle. Her occiput impacted the dry wall behind her (FIGURE 109). The SIM G was triggered and a graph was produced (FIGURE 110). A head impact location image was generated (FIGURE 111).



FIGURE 109 – The yellow arrow indicates subject 11, who was initially sitting on her buttocks (A) when she lost balance and fell rearward (B). She impacted her head occiput on the bulletin board and impacted her upper posterior torso on the carpeted flooring (C/D). Her final position was supine on the carpeted flooring (D).

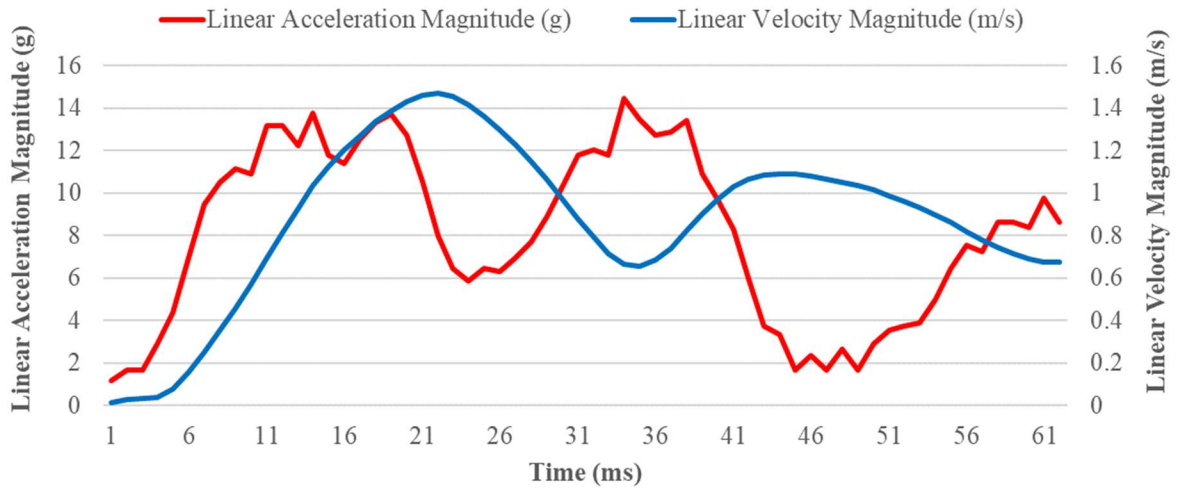


FIGURE 110 – Linear acceleration magnitude (g) and linear velocity magnitude (m/s) from SIM G output for fall 146

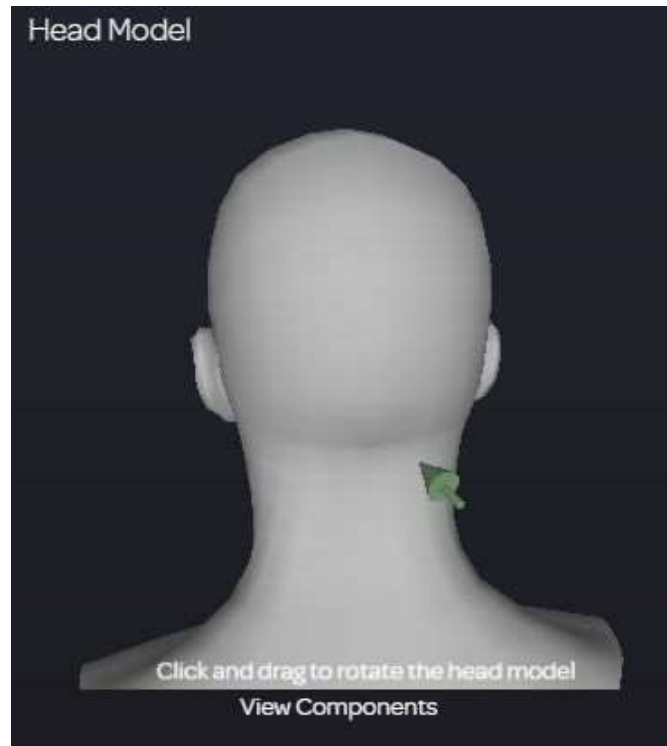


FIGURE 111 – Head impact location image generated from SIM G activation

TABLE 64

RESULTS FOR FALL 146 LUMPED MASS PHYSICS-BASED MODEL

BIOMECHANICAL MEASURE		PHYSICS-BASED MODEL OUTCOMES				PERCENT ERROR			
Outcome	SIM G	METHOD A	METHOD B	METHOD C	METHOD D	METHOD A	METHOD B	METHOD C	METHOD D
Linear Acceleration (g)	15	19	24	24	24	24%	57%	57%	58%
Change in Linear Velocity (m/s)	1.5	2.2	2.2	2.8	2.2	47%	47%	64%	30%
Angular Acceleration (rad/s <sup>2</sup> )	1145	1006	1267	1267	1281	12%	11%	11%	12%
Angular Velocity (rad/s)	11.3	12.2	12.2	12.2	12.2	8%	8%	8%	8%
Impact Force (N)		584	744	474	752				

TABLE 65

RESULTS FOR FALL 146 SINGLE ROD PHYSICS-BASED MODEL

BIOMECHANICAL MEASURE		PHYSICS-BASED MODEL OUTCOMES				PERCENT ERROR			
Outcome	SIM G	METHOD A	METHOD B	METHOD C	METHOD D	METHOD A	METHOD B	METHOD C	METHOD D
Linear Acceleration (g)	15	13	41	41	41	15%	171%	171%	174%
Change in Linear Velocity (m/s)	1.5	1.5	3.8	4.8	3.8	0%	153%	222%	156%
Angular Acceleration (rad/s <sup>2</sup> )	1145	686	2194	2194	2219	40%	92%	92%	94%
Angular Velocity (rad/s)	11.3	8.3	21.1	21.1	21.1	27%	86%	87%	87%
Impact Force (N)		398	1288	820	1302				

TABLE 66

RESULTS FOR FALL 146 INVERTED PENDULUM PHYSICS-BASED MODEL

BIOMECHANICAL MEASURE	SIM G	PHYSICS-BASED MODEL OUTCOMES				PERCENT ERROR			
		METHOD A	METHOD B	METHOD C	METHOD D	METHOD A	METHOD B	METHOD C	METHOD D
Linear Acceleration (g)	15	19	23	24	24	24%	57%	57%	58%
Change in Linear Velocity (m/s)	1.5	2.2	2.2	2.8	2.2	47%	47%	86%	48%
Angular Acceleration (rad/s <sup>2</sup> )	1145	1006	1267	1267	1281	12%	11%	11%	12%
Angular Velocity (rad/s)	11.3	12.2	12.2	12.2	12.2	8%	8%	8%	8%
Impact Force (N)		584	743	474	752				

2. Childcare center fall 238

The results for all four methods for fall 238 are detailed below (Table 67, TABLE 68, TABLE 69). In fall 238, subject 11 (female) fell from the base of the playground slide. Her face impacted the playground surface (FIGURE 112). The SIM G was triggered and a graph was produced (FIGURE 113). A head impact location image was generated (FIGURE 114).

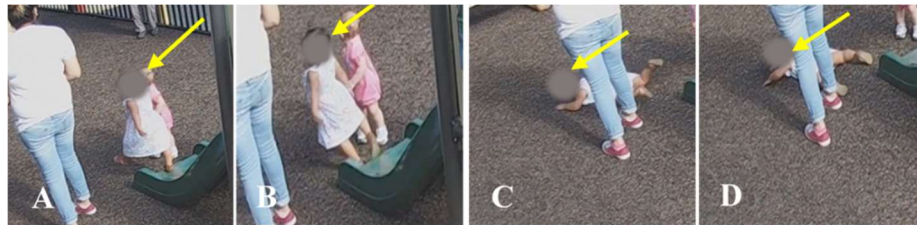


FIGURE 112 – The yellow arrow indicates subject 11, who was initially standing upright on the base of the slide when she stepped off the base with her left foot (A). Her left foot contacted the playground surface, and she lost her balance and fell forward (B). She impacted her anterior torso and bilateral anterior legs, as well as her face on the playground surface (C). Her final position was prone on the playground surface (D).

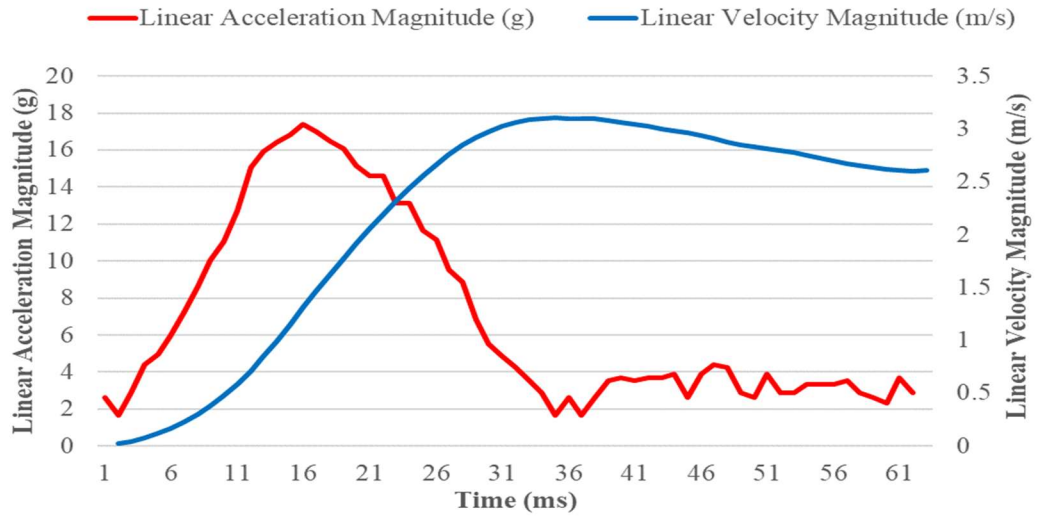


FIGURE 113 – Linear acceleration magnitude (g) and linear velocity magnitude (m/s) from SIM G output for fall 238

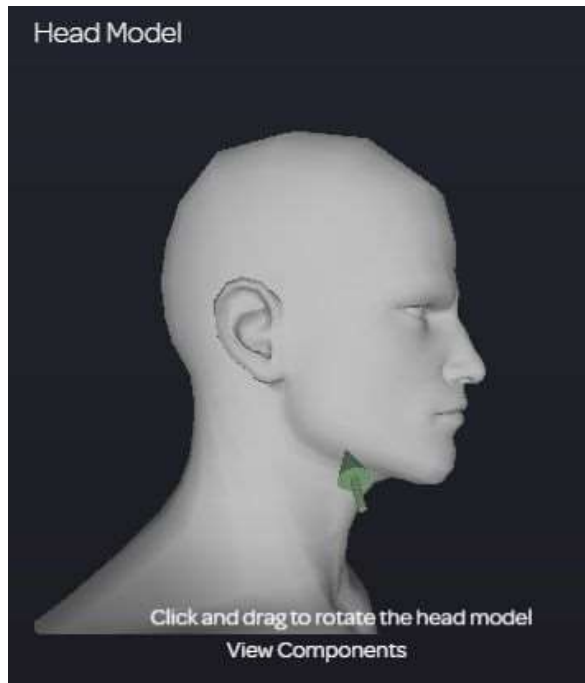


FIGURE 114 – Head impact location image generated from SIM G activation



TABLE 67

RESULTS FOR FALL 238 LUMPED MASS PHYSICS-BASED MODEL

BIOMECHANICAL MEASURE		PHYSICS-BASED MODEL OUTCOMES				PERCENT ERROR			
Outcome	SIM G	METHOD A	METHOD B	METHOD C	METHOD D	METHOD A	METHOD B	METHOD C	METHOD D
Linear Acceleration (g)	18	18	28	28	23	0%	56%	56%	27%
Change in Linear Velocity (m/s)	3.1	3.7	3.7	5.7	3.7	19%	19%	84%	18%
Angular Acceleration (rad/s <sup>2</sup> )	1281	989	1536	1536	1254	23%	20%	20%	2%
Angular Velocity (rad/s)	17.5	20.2	20.1	20.1	20.1	15%	15%	15%	15%
Impact Force (N)		373	573	365	468				

TABLE 68

RESULTS FOR FALL 238 SINGLE ROD PHYSICS-BASED MODEL

BIOMECHANICAL MEASURE		PHYSICS-BASED MODEL OUTCOMES				PERCENT ERROR			
Outcome	SIM G	METHOD A	METHOD B	METHOD C	METHOD D	METHOD A	METHOD B	METHOD C	METHOD D
Linear Acceleration (g)	18	13	50	49	40	31%	172%	170%	120%
Change in Linear Velocity (m/s)	3.1	2.5	6.4	9.9	6.3	19%	106%	218%	104%
Angular Acceleration (rad/s <sup>2</sup> )	1281	680	2683	2661	2173	47%	109%	108%	70%
Angular Velocity (rad/s)	17.5	13.9	35.1	34.8	34.8	21%	100%	99%	99%
Impact Force (N)		257	1001	632	811				

TABLE 69

RESULTS FOR FALL 238 INVERTED PENDULUM PHYSICS-BASED MODEL

BIOMECHANICAL MEASURE Outcome	SIM G	PHYSICS-BASED MODEL OUTCOMES				PERCENT ERROR			
		METHOD A	METHOD B	METHOD C	METHOD D	METHOD A	METHOD B	METHOD C	METHOD D
Linear Acceleration (g)	18	18	29	28	23	0%	57%	56%	27%
Change in Linear Velocity (m/s)	3.1	3.7	3.7	5.7	3.7	19%	19%	84%	18%
Angular Acceleration (rad/s <sup>2</sup> )	1281	989	1549	1536	1254	23%	21%	20%	2%
Angular Velocity (rad/s)	17.5	20.2	20.2	20.1	20.1	15%	16%	15%	15%
Impact Force (N)		373	578	365	468				

3. Childcare center fall 241

The results for all four methods for fall 241 are detailed below (Table 70, TABLE 71, TABLE 72). In fall 241, subject 5 (female) impacted her face on carpeted flooring (FIGURE 115). The SIM G was triggered and a graph was produced (FIGURE 116). A head impact location image was generated (FIGURE 117).



FIGURE 115 – Subject 5 was bending at the knees on the bottom step of the butterfly ramp (A). She projected forward (as if to jump) and fell forward (B). She contacted the palms of both hands on the carpeted flooring (C), and paused before falling straight to the carpeted flooring, where she impacted her face (D). She was in a supine final position at the end of the fall (E).

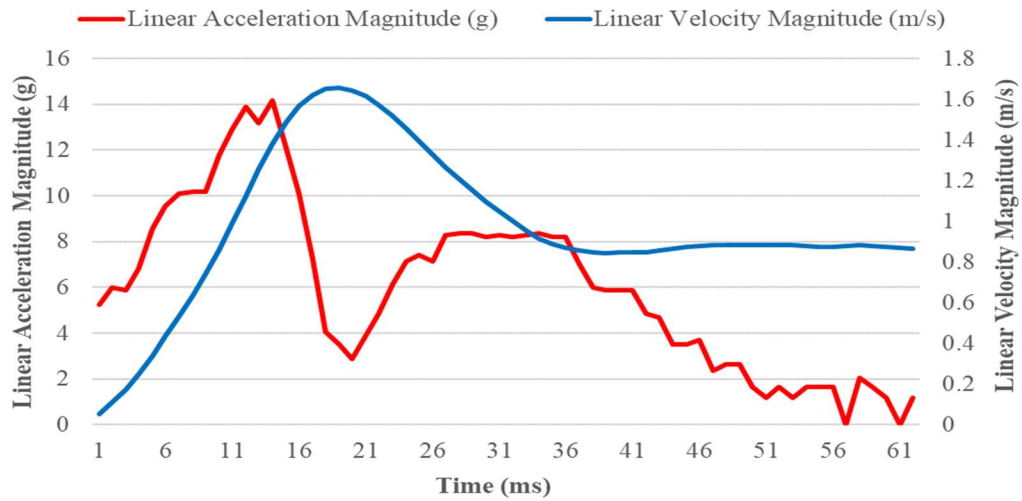


FIGURE 116 – Linear acceleration magnitude (g) and linear velocity magnitude (m/s) from SIM G output for fall 241

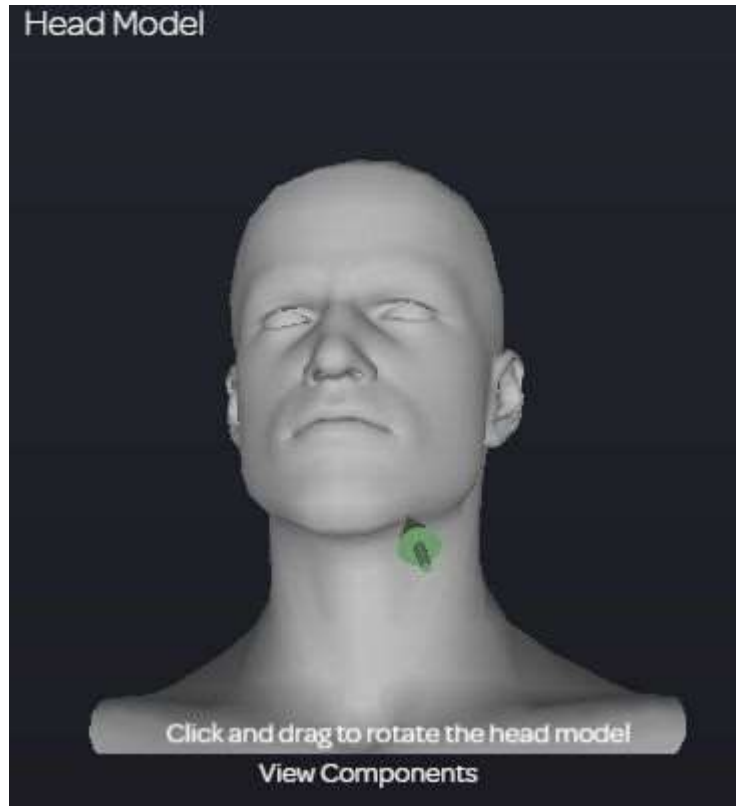


FIGURE 117 – Head impact location image generated from SIM G activation

TABLE 70

RESULTS FOR FALL 241 LUMPED MASS PHYSICS-BASED MODEL

BIOMECHANICAL MEASURE		PHYSICS-BASED MODEL OUTCOMES				PERCENT ERROR			
Outcome	SIM G	METHOD A	METHOD B	METHOD C	METHOD D	METHOD A	METHOD B	METHOD C	METHOD D
Linear Acceleration (g)	14	19	27	27	24	36%	92%	92%	73%
Change in Linear Velocity (m/s)	1.7	2.0	2.0	2.8	2.0	18%	18%	68%	19%
Angular Acceleration (rad/s <sup>2</sup> )	1151	964	1364	1364	1228	16%	19%	18%	7%
Angular Velocity (rad/s)	9.5	10.4	10.4	10.4	10.4	10%	10%	10%	10%
Impact Force (N)		575	822	524	741				

TABLE 71

RESULTS FOR FALL 241 SINGLE ROD PHYSICS-BASED MODEL

BIOMECHANICAL MEASURE		PHYSICS-BASED MODEL OUTCOMES				PERCENT ERROR			
Outcome	SIM G	METHOD A	METHOD B	METHOD C	METHOD D	METHOD A	METHOD B	METHOD C	METHOD D
Linear Acceleration (g)	14	13	46	46	42	8%	232%	232%	199%
Change in Linear Velocity (m/s)	1.7	1.4	3.5	4.9	3.5	18%	106%	190%	105%
Angular Acceleration (rad/s <sup>2</sup> )	1151	657	2362	2362	2128	43%	105%	105%	85%
Angular Velocity (rad/s)	9.5	7.1	18.1	18.1	18.1	25%	90%	90%	90%
Impact Force (N)		392	1425	907	1283				

TABLE 72

RESULTS FOR FALL 241 INVERTED PENDULUM PHYSICS-BASED MODEL

BIOMECHANICAL MEASURE		PHYSICS-BASED MODEL OUTCOMES				PERCENT ERROR			
Outcome	SIM G	METHOD A	METHOD B	METHOD C	METHOD D	METHOD A	METHOD B	METHOD C	METHOD D
Linear Acceleration (g)	14	19	27	27	24	36%	92%	92%	73%
Change in Linear Velocity (m/s)	1.7	2.0	2.0	2.8	2.0	18%	18%	68%	19%
Angular Acceleration (rad/s <sup>2</sup> )	1151	964	1364	1364	1228	16%	18%	18%	7%
Angular Velocity (rad/s)	9.5	10.4	10.4	10.4	10.4	10%	10%	10%	10%
Impact Force (N)		575	822	524	741				

4. Childcare center fall 321

The results for all four methods for fall 321 are detailed below (Table 73, TABLE 74, TABLE 75). In fall 321, subject 4 (male) tripped and fell forward, impacting his face on the classroom drywall/bulletin board edge (FIGURE 118).The SIM G was triggered and a graph was produced (FIGURE 119). A head impact location image was generated (FIGURE 120).



FIGURE 118 – The yellow arrow indicates subject 4, who was initially walking in the classroom on the carpeted surface (A). He tripped and fell forward (B/C). He contacted his righthand palm on the carpeted floor; he then continued to fall forward, and he impacted his face on the wall/edge of the bulletin board on the wall (D). His final position was on his hands and bilateral knees on the carpeted flooring (E).

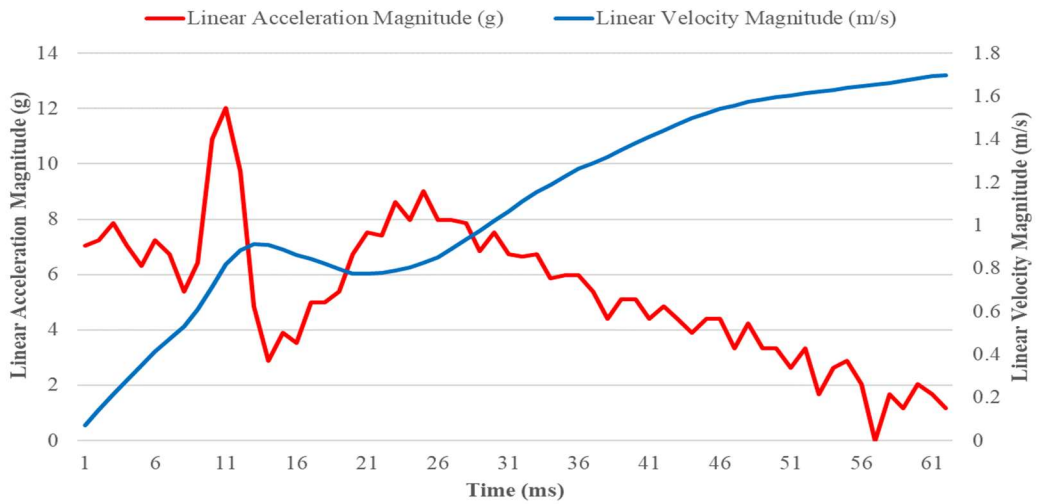


FIGURE 119 – Linear acceleration magnitude (g) and linear velocity magnitude (m/s) from SIM G output for fall 321

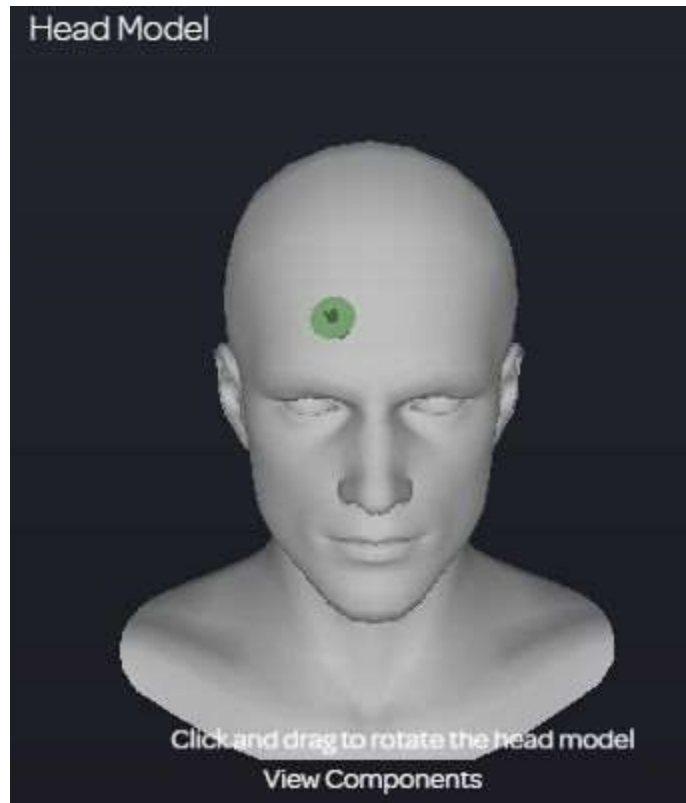


FIGURE 120 – Head impact location image generated from SIM G activation

TABLE 73

RESULTS FOR FALL 321 LUMPED MASS PHYSICS-BASED MODEL

BIOMECHANICAL MEASURE Outcome	PHYSICS-BASED MODEL OUTCOMES				PERCENT ERROR				
	SIM G	METHOD A	METHOD B	METHOD C	METHOD D	METHOD A	METHOD B	METHOD C	METHOD D
Linear Acceleration (g)	12	18	22	22	22	47%	85%	85%	87%
Change in Linear Velocity (m/s)	1.7	2.4	2.4	3.1	2.4	41%	41%	80%	43%
Angular Acceleration (rad/s <sup>2</sup> )	599	887	1119	1119	1131	48%	87%	87%	89%
Angular Velocity (rad/s)	11.9	12.4	12.4	12.4	12.4	4%	5%	5%	5%
Impact Force (N)		488	622	396	629				

TABLE 74

RESULTS FOR FALL 321 SINGLE ROD PHYSICS-BASED MODEL

BIOMECHANICAL MEASURE		PHYSICS-BASED MODEL OUTCOMES				PERCENT ERROR			
Outcome	SIM G	METHOD A	METHOD B	METHOD C	METHOD D	METHOD A	METHOD B	METHOD C	METHOD D
Linear Acceleration (g)	12	12	39	39	39	0%	221%	221%	225%
Change in Linear Velocity (m/s)	1.7	1.7	4.2	5.3	4.2	0%	147%	211%	147%
Angular Acceleration (rad/s <sup>2</sup> )	599	605	1938	1938	1959	1%	223%	223%	227%
Angular Velocity (rad/s)	11.9	8.5	21.5	21.5	21.5	29%	81%	81%	81%
Impact Force (N)		333	1077	686	1089				

TABLE 75

RESULTS FOR FALL 321 INVERTED PENDULUM PHYSICS-BASED MODEL

BIOMECHANICAL MEASURE		PHYSICS-BASED MODEL OUTCOMES				PERCENT ERROR			
Outcome	SIM G	METHOD A	METHOD B	METHOD C	METHOD D	METHOD A	METHOD B	METHOD C	METHOD D
Linear Acceleration (g)	12	18	22	22	22	47%	85%	85%	87%
Change in Linear Velocity (m/s)	1.7	2.4	2.4	3.1	2.4	41%	41%	80%	43%
Angular Acceleration (rad/s <sup>2</sup> )	599	887	1119	1119	1131	48%	87%	87%	89%
Angular Velocity (rad/s)	11.9	12.4	12.4	12.4	12.4	4%	5%	5%	5%
Impact Force (N)		488	622	396	629				

5. Childcare center fall 516

The results for all four methods for fall 516 are detailed below (Table 76, TABLE 77, TABLE 78). In fall 516, subject 15 (male) was on his buttocks and fell rearward, impacting his occiput on the carpeted floor (FIGURE 121).The SIM G was triggered and a graph was produced (FIGURE 122). A head impact location image was not generated for this fall.





FIGURE 121 – Subject 15 was initially walking and stepped with his left foot onto a toy ball, which caused him to slip rearward (A). He fell rearward and impacted his buttocks on the carpeted flooring with his torso approximately 45° to the horizontal (B/C). He then fell rearward and impacted his posterior torso and occiput on the carpeted flooring (D). He was in a final supine position at the end of the fall.

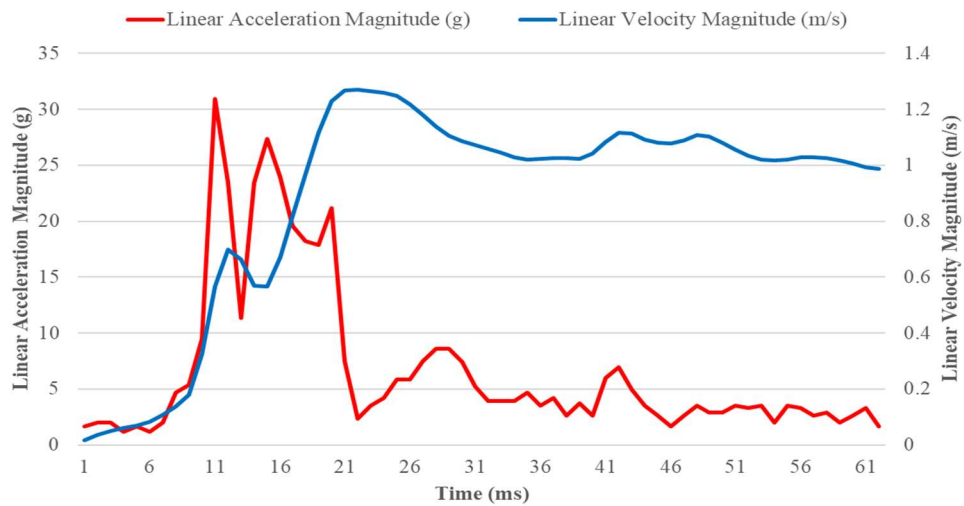


FIGURE 122 – Linear acceleration magnitude (g) and linear velocity magnitude (m/s) from SIM G output for fall 516

TABLE 76

RESULTS FOR FALL 516 LUMPED MASS PHYSICS-BASED MODEL

BIOMECHANICAL MEASURE		PHYSICS-BASED MODEL OUTCOMES				PERCENT ERROR			
Outcome	SIM G	METHOD A	METHOD B	METHOD C	METHOD D	METHOD A	METHOD B	METHOD C	METHOD D
Linear Acceleration (g)	31	29	41	41	38	5%	34%	34%	21%
Change in Linear Velocity (m/s)	1.3	2.8	2.8	3.9	2.8	112%	115%	199%	112%
Angular Acceleration (rad/s <sup>2</sup> )	2336	1926	2709	2709	2453	18%	16%	16%	5%
Angular Velocity (rad/s)	8.5	18.4	18.4	18.4	18.4	117%	116%	116%	116%
Impact Force (N)		828	1178	751	1067				

TABLE 77

RESULTS FOR FALL 516 SINGLE ROD PHYSICS-BASED MODEL

BIOMECHANICAL MEASURE		PHYSICS-BASED MODEL OUTCOMES				PERCENT ERROR			
Outcome	SIM G	METHOD A	METHOD B	METHOD C	METHOD D	METHOD A	METHOD B	METHOD C	METHOD D
Linear Acceleration (g)	31	20	72	72	65	35%	131%	131%	110%
Change in Linear Velocity (m/s)	1.3	1.9	4.8	6.7	4.8	45%	269%	417%	268%
Angular Acceleration (rad/s <sup>2</sup> )	2336	1313	4690	4692	4248	44%	101%	101%	82%
Angular Velocity (rad/s)	8.5	12.5	31.8	31.9	31.9	48%	275%	275%	275%
Impact Force (N)		564	2040	1300	1848				

TABLE 78

RESULTS FOR FALL 516 INVERTED PENDULUM PHYSICS-BASED MODEL

BIOMECHANICAL MEASURE		PHYSICS-BASED MODEL OUTCOMES				PERCENT ERROR			
Outcome	SIM G	METHOD A	METHOD B	METHOD C	METHOD D	METHOD A	METHOD B	METHOD C	METHOD D
Linear Acceleration (g)	31	29	41	41	38	5%	34%	34%	21%
Change in Linear Velocity (m/s)	1.3	2.8	2.8	3.9	2.8	115%	115%	199%	112%
Angular Acceleration (rad/s <sup>2</sup> )	2336	1926	2709	2709	2453	18%	16%	16%	5%
Angular Velocity (rad/s)	8.5	18.4	18.4	18.4	18.4	117%	116%	116%	116%
Impact Force (N)		828	1178	751	1067				

6. Childcare center fall 545

The results for all four methods for fall 545 are detailed below (Table 79, TABLE 80, TABLE 81). In fall 545, subject 21 (male) was walking, and he tripped and fell forward, impacting his face/superior head on the side of a wooden bookshelf (FIGURE 123). The SIM G was triggered and a graph was produced (FIGURE 124). A head impact location image was generated (FIGURE 125).



FIGURE 123 – The yellow arrow indicates subject 21, who was initially walking on the carpeted flooring (A). He tripped over an object and fell forward (B). He impacted his bilateral knees and the palms of both hands on the floor, and impacted his superior head/face on the side of a wooden bookshelf (C/D). He then dropped to his anterior torso, and he was in a final prone position at the end of the fall (E).

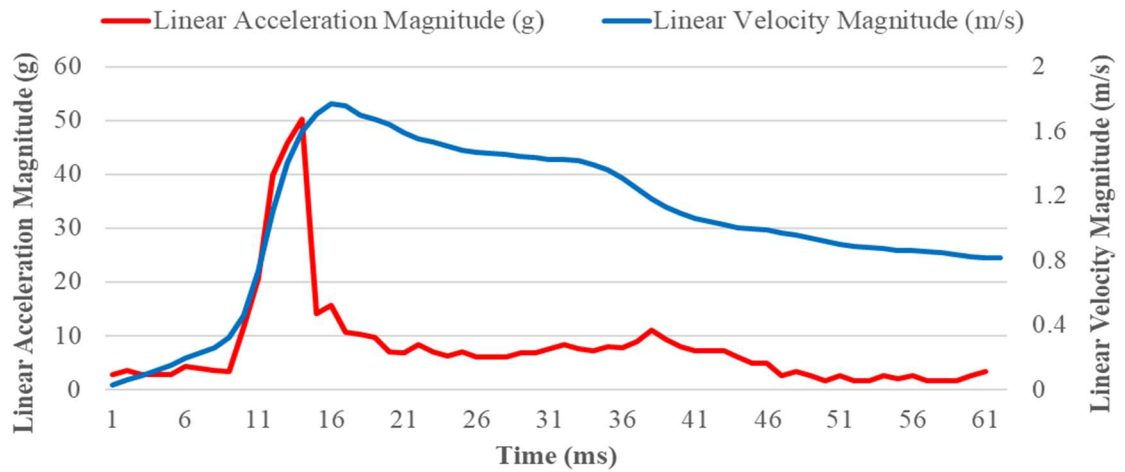


FIGURE 124 – Linear acceleration magnitude (g) and linear velocity magnitude (m/s) from SIM G output for fall 545

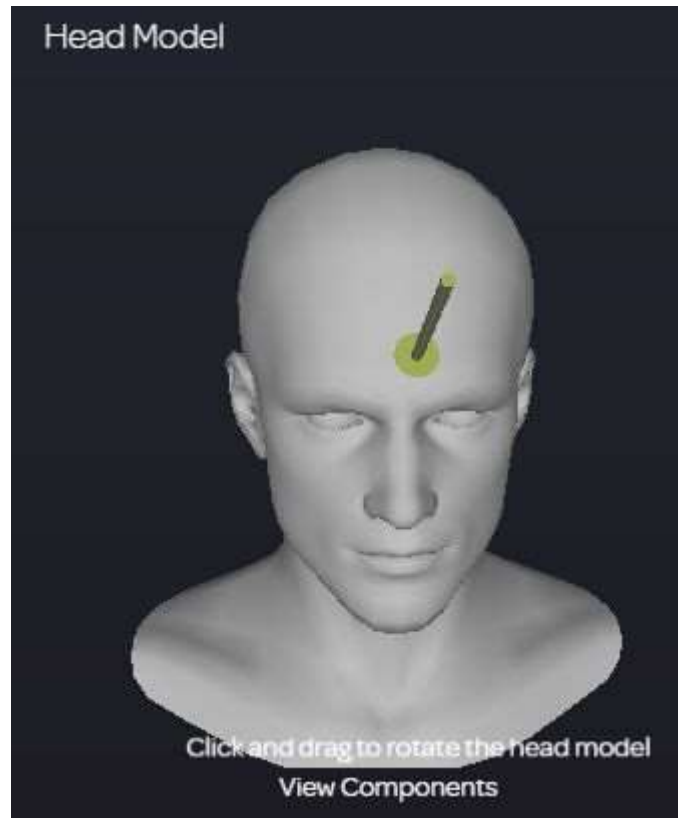


FIGURE 125 – Head impact location image generated from SIM G activation

TABLE 79

RESULTS FOR FALL 545 LUMPED MASS PHYSICS-BASED MODEL

BIOMECHANICAL MEASURE		PHYSICS-BASED MODEL OUTCOMES				PERCENT ERROR			
Outcome	SIM G	METHOD A	METHOD B	METHOD C	METHOD D	METHOD A	METHOD B	METHOD C	METHOD D
Linear Acceleration (g)	50	47	66	66	60	6%	32%	32%	20%
Change in Linear Velocity (m/s)	1.8	3.2	3.2	4.5	3.2	78%	78%	152%	80%
Angular Acceleration (rad/s <sup>2</sup> )	5388	2430	3404	3404	3097	55%	37%	37%	43%
Angular Velocity (rad/s)	13.3	17.0	17.0	17.0	17.0	28%	28%	28%	28%
Impact Force (N)		1393	1973	1256	1795				

TABLE 80

RESULTS FOR FALL 545 SINGLE ROD PHYSICS-BASED MODEL

BIOMECHANICAL MEASURE		PHYSICS-BASED MODEL OUTCOMES				PERCENT ERROR			
Outcome	SIM G	METHOD A	METHOD B	METHOD C	METHOD D	METHOD A	METHOD B	METHOD C	METHOD D
Linear Acceleration (g)	50	32	114	114	104	36%	128%	128%	108%
Change in Linear Velocity (m/s)	1.8	2.2	5.6	7.8	5.6	22%	211%	336%	211%
Angular Acceleration (rad/s <sup>2</sup> )	5388	1655	5889	5896	5365	69%	9%	9%	0%
Angular Velocity (rad/s)	13.3	11.6	29.5	29.5	29.5	13%	122%	122%	122%
Impact Force (N)		949	3413	2176	3109				

TABLE 81

RESULTS FOR FALL 545 INVERTED PENDULUM PHYSICS-BASED MODEL

BIOMECHANICAL MEASURE		PHYSICS-BASED MODEL OUTCOMES				PERCENT ERROR			
Outcome	SIM G	METHOD A	METHOD B	METHOD C	METHOD D	METHOD A	METHOD B	METHOD C	METHOD D
Linear Acceleration (g)	50	47	66	66	60	6%	32%	32%	20%
Change in Linear Velocity (m/s)	1.8	3.2	3.2	4.5	3.2	78%	78%	152%	80%
Angular Acceleration (rad/s <sup>2</sup> )	5388	2430	3400	3404	3097	55%	37%	37%	43%
Angular Velocity (rad/s)	13.3	17.0	17.0	17.0	17.0	28%	28%	28%	28%
Impact Force (N)		1393	1973	1256	1795				

7. Childcare center fall 676 (1)

Fall 676 involved two separate falls and head impacts. The results for all four methods for fall 676 (1) are detailed below (Table 82, TABLE 83, TABLE 84). In fall 676 (1), subject 21 (male) was standing on the playground surface and fell straight down, impacting his chin on the top of the tall mushroom (FIGURE 126). The SIM G was

triggered and a graph was produced (FIGURE 127). A head impact location image was generated (FIGURE 128).



FIGURE 126 – In fall 676 (1), subject 21 was initially standing upright at the base of the tall mushroom on the playground surface (A). Subject 21 was leaning to his right and lost his balance, and he fell straight down [feet-first dynamics] (B). He impacted his inferior (caudal) chin on the top of the tall mushroom surface (C). He landed on his buttocks with his torso about 90° to the horizontal (D), which completed the first part of this two-part fall.

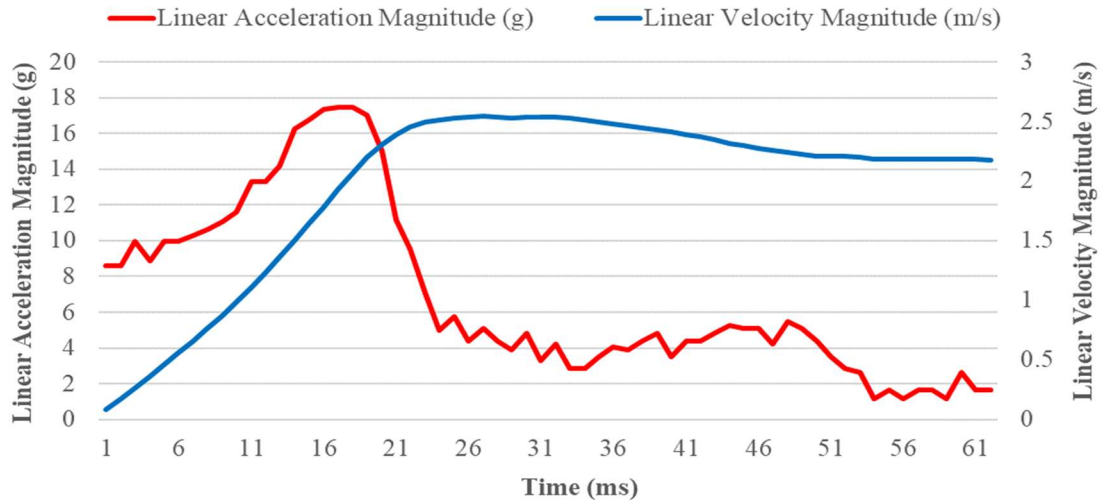


FIGURE 127 – Linear acceleration magnitude (g) and linear velocity magnitude (m/s) from SIM G output for fall 676 (1)



FIGURE 128 – Head impact location image generated from SIM G activation

TABLE 82

RESULTS FOR FALL 676 (1) LUMPED MASS PHYSICS-BASED MODEL

BIOMECHANICAL MEASURE	PHYSICS-BASED MODEL OUTCOMES					PERCENT ERROR			
	Outcome	SIM G	METHOD A	METHOD B	METHOD C	METHOD D	METHOD A	METHOD B	METHOD C
Linear Acceleration (g)	18	18	28	28	23	0%	54%	54%	27%
Change in Linear Velocity (m/s)	2.5	2.2	2.2	3.5	2.2	12%	12%	39%	10%
Angular Acceleration (rad/s <sup>2</sup> )	1159	930	1432	1432	1184	20%	24%	24%	2%
Angular Velocity (rad/s)	14.8	11.8	11.8	11.8	11.8	20%	20%	20%	20%
Impact Force (N)		533	830	528	686				



TABLE 83

RESULTS FOR FALL 676 (1) SINGLE ROD PHYSICS-BASED MODEL

BIOMECHANICAL MEASURE		PHYSICS-BASED MODEL OUTCOMES				PERCENT ERROR			
Outcome	SIM G	METHOD A	METHOD B	METHOD C	METHOD D	METHOD A	METHOD B	METHOD C	METHOD D
Linear Acceleration (g)	18	12	48	48	40	32%	167%	167%	121%
Change in Linear Velocity (m/s)	2.5	1.5	3.9	6.0	3.9	40%	56%	140%	56%
Angular Acceleration (rad/s <sup>2</sup> )	1159	634	2480	2479	2051	45%	114%	114%	77%
Angular Velocity (rad/s)	14.8	8.1	20.5	20.5	20.5	45%	39%	39%	39%
Impact Force (N)		363	1437	915	1189				

TABLE 84

RESULTS FOR FALL 676 (1) INVERTED PENDULUM PHYSICS-BASED MODEL

BIOMECHANICAL MEASURE		PHYSICS-BASED MODEL OUTCOMES				PERCENT ERROR			
Outcome	SIM G	METHOD A	METHOD B	METHOD C	METHOD D	METHOD A	METHOD B	METHOD C	METHOD D
Linear Acceleration (g)	18	18	28	28	23	0%	54%	54%	27%
Change in Linear Velocity (m/s)	2.5	2.2	2.3	3.5	2.2	12%	8%	39%	10%
Angular Acceleration (rad/s <sup>2</sup> )	1159	930	1432	1432	1184	20%	24%	24%	2%
Angular Velocity (rad/s)	14.8	11.8	11.8	11.8	11.8	20%	20%	20%	20%
Impact Force (N)		533	830	528	686				

8. Childcare center fall 676 (2)

The results for all four methods for fall 676 (2) are detailed below (Table 85, TABLE 86, TABLE 87). In fall 676 (2), subject 21 (male) was on his buttocks (after fall 676 (1)), and he fell rearward and impacted his occiput on the playground surface (FIGURE 129). The SIM G was triggered and a graph was produced (FIGURE 130). A head impact location image was generated (FIGURE 131).

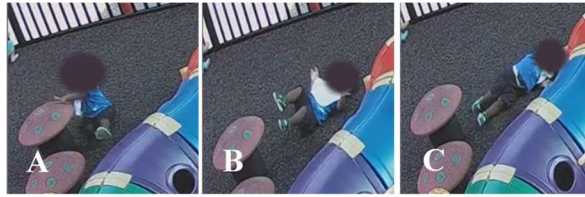


FIGURE 129 – Subject 21 was on his buttocks on the playground surface after his first fall (A). He continued to fall, rotating about his torso and falling rearward (B). He impacted his occiput on the playground surface (B). His final position was supine on the playground surface (C).

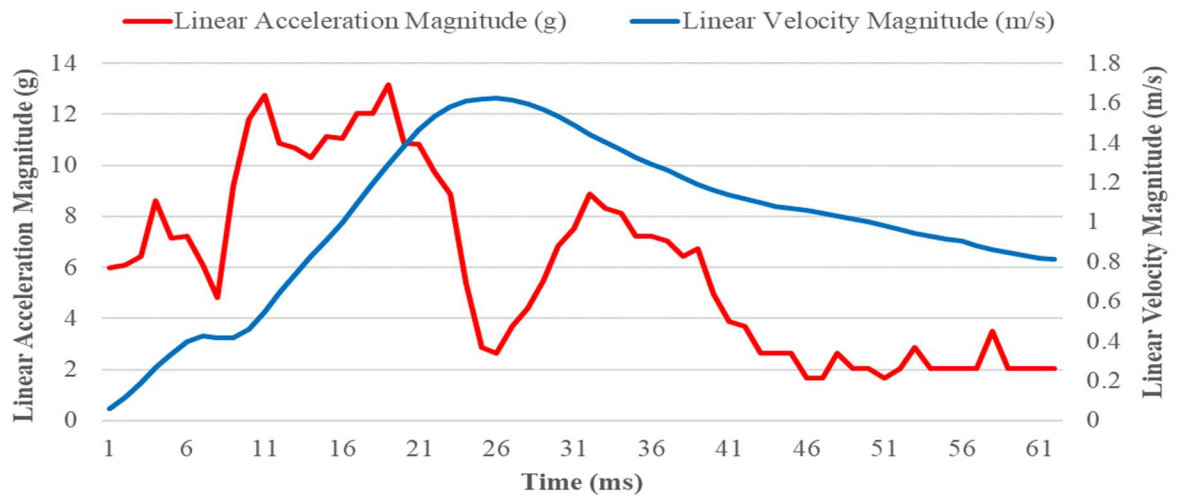


FIGURE 130 – Linear acceleration magnitude (g) and linear velocity magnitude (m/s) from SIM G output for fall 676 (2)

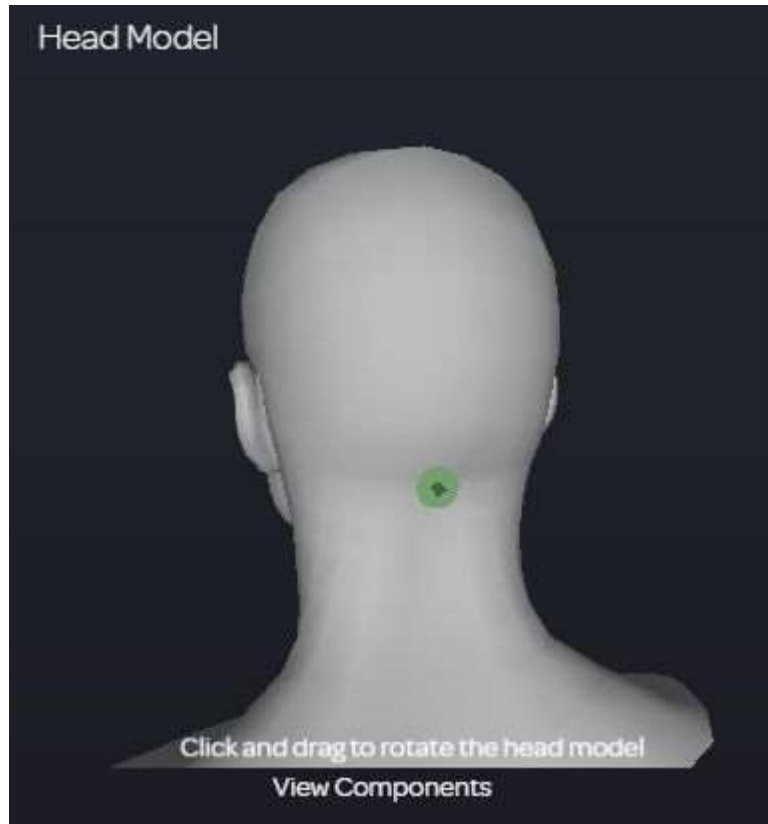


FIGURE 131 – Head impact location image generated from SIM G activation

TABLE 85

RESULTS FOR FALL 676 (2) LUMPED MASS PHYSICS-BASED MODEL

BIOMECHANICAL MEASURE	SIM G	PHYSICS-BASED MODEL OUTCOMES				PERCENT ERROR			
		METHOD A	METHOD B	METHOD C	METHOD D	METHOD A	METHOD B	METHOD C	METHOD D
Linear Acceleration (g)	13	25	39	39	31	89%	197%	197%	141%
Change in Linear Velocity (m/s)	1.6	2.8	2.8	4.3	2.8	75%	75%	171%	73%
Angular Acceleration (rad/s <sup>2</sup> )	1684	1270	1992	1992	1618	25%	18%	18%	4%
Angular Velocity (rad/s)	12.3	14.6	14.6	14.6	14.6	18%	18%	18%	18%
Impact Force (N)		728	1155	735	937				

TABLE 86

RESULTS FOR FALL 676 (2) SINGLE ROD PHYSICS-BASED MODEL

BIOMECHANICAL MEASURE		PHYSICS-BASED MODEL OUTCOMES				PERCENT ERROR			
Outcome	SIM G	METHOD A	METHOD B	METHOD C	METHOD D	METHOD A	METHOD B	METHOD C	METHOD D
Linear Acceleration (g)	13	17	67	67	54	29%	414%	414%	317%
Change in Linear Velocity (m/s)	1.6	1.9	4.8	7.5	4.8	19%	200%	370%	199%
Angular Acceleration (rad/s <sup>2</sup> )	1684	865	3450	3451	2802	49%	105%	105%	66%
Angular Velocity (rad/s)	12.3	9.9	25.2	25.2	25.2	19%	105%	105%	105%
Impact Force (N)		496	1999	1274	1624				

TABLE 87

RESULTS FOR FALL 676 (2) INVERTED PENDULUM PHYSICS-BASED MODEL

BIOMECHANICAL MEASURE		PHYSICS-BASED MODEL OUTCOMES				PERCENT ERROR			
Outcome	SIM G	METHOD A	METHOD B	METHOD C	METHOD D	METHOD A	METHOD B	METHOD C	METHOD D
Linear Acceleration (g)	13	25	39	39	31	89%	197%	197%	141%
Change in Linear Velocity (m/s)	1.6	2.8	2.8	4.3	2.8	75%	75%	171%	73%
Angular Acceleration (rad/s <sup>2</sup> )	1684	1270	1992	1992	1618	25%	18%	18%	4%
Angular Velocity (rad/s)	12.3	14.6	14.6	14.6	14.6	18%	18%	18%	18%
Impact Force (N)		728	1154	735	937				

## XII. VITA

DANIELLE KRISTINE CORY

### EDUCATION

M. Eng. in Bioengineering  
University of Louisville, J.B. Speed School of Engineering, Louisville, KY  
8/17 – Expected 05/21

B.S. in Bioengineering  
University of Louisville, J.B. Speed School of Engineering, Louisville, KY  
8/13 – 5/17

### EXPERIENCE

Research Assistant  
iRAP Lab, University of Louisville, Louisville, KY  
6/17– Present

- 11/19 – Present: Abstracted and redacted medical records from the Pediatric Forensics Team at Norton Women and Children’s Hospital; Input details of confirmed abusive and accidental childhood cases into a database in FileMaker Pro
- 6/17 – 8/17: Worked with Mimics software to apply measurements to CT scan/dcom images of fetal femur bone specimens

Production Co-op  
SCHOTT North America, Louisville, KY  
1/17 – 8/19

- Assisted with process improvement projects on two different flat glass finishing lines.
  - Performed and analyzed time studies to implement process improvement efforts on the Pyran flat glass finishing line, including material flow
- Implemented a 5S cleaning and preventative maintenance program throughout the entire production plant; performed bimonthly audits to ensure compliance
- Researched and purchased equipment for improvement of plant interior, including better lighting; better glass manipulators; communication equipment; packaging material

University of Louisville – Bioengineering Artificial Organs Course  
Graduate Project: Development of DYL Artificial Arm  
Spring 2018

- Worked with two other graduate bioengineering students to develop myoelectronically-controlled prosthesis
- Designed a bionic prosthetic arm for a person with an upper-extremity amputation; arm had 6 degrees of freedom

Engineering Fundamentals Grader  
J.B. Speed School of Engineering Fundamentals Department, Louisville, KY  
1/15 – 5/18

- Graded exams, homework, and quizzes for various mathematical courses in Speed School, including Calculus II, Calculus III, and Differential Equations

Quality Control Intern  
Isopure Corporation, Simpsonville, KY  
5/16 – 8/16

- Created various work instructions, receiving instructions, and installation instructions for water purification systems used in kidney dialysis centers
- Tested and recorded data for new automatic bag-opening equipment
- Learned about FDA regulations and compliance for Class II medical devices, including performing a Risk Analysis

R&D Intern  
enmodes, Aachen, DE  
8/15 – 12/15

- Used Matlab and Simulink to develop a PBPK computer model
- Validated the clearance and metabolic rates of 11 medications against know mouse model data

## CONFERENCES

Graduate Student Regional Research Conference 2020

- Presented “Characterization of Video-Recorded Falls Involving Children in a Childcare Setting” (February 2020)

The Ohio State University Injury Biomechanics Symposium

- 2020: Accepted for poster presentation of “Characterization of Video-Recorded Falls Involving Children in a Childcare Setting” [Conference canceled due to Covid-19]
- 2021: Accepted for poster presentation of “Characterization of Video-Recorded Falls Involving Children in a Childcare Setting”

## CERTIFICATIONS

Green Belt: Lean  
Issued by IISE, 5/18

Green Belt: Six Sigma  
Issued by IISE, 8/17

## VOLUNTEER ACTIVITIES

Associate Board Member, Gilda's Club Kentuckiana  
11/19 – Present

- Member of Wigs on Tap committee; Co-Chair Over the Edge committee
- Guest Speaker: Wigs on Tap 2019; Gilda's Night 2019; helped to raise over \$500,000 in donations

Volunteer, Kentucky Humane Society  
2/17 – Present

- Cleaned dog and cat areas; took dogs on walks; helped socialize all animals at the shelter.